The Role of Nitric Oxide Synthase Inhibitors on Macrophage Function

A thesis submitted for the degree of

Doctor of Philosophy

from Kingston University with collaboration at Imperial College London

Blerina Ahmetaj-Shala

DECLARATION

I, Blerina Ahmetaj-Shala, confirm that the work presented in this thesis is entirely my own. I confirm that any information that has been derived from any other sources has been indicated.

September 2013

DEDICATION

This thesis is dedicated to my parents, Shaban and Fetije Ahmetaj, who have been the best parents I could wish for and have provided me with a great foundation in life.

It is also dedicated to my husband, Fisnik, who is a great friend as well as a wonderful partner.

ACKNOWLEDGEMENTS

The plan to do a PhD has been one of the best decisions I have made so far. Not only have I learnt new and fascinating laboratory skills, but by working with a variety of inspirational and dedicated people, I have broadened my understanding of the whole scientific field. I would not be where I am if it were not for a few people who stuck by and supported me throughout this wonderful (yet sometimes stressful) experience.

Fran not only has enriched me with her excellent knowledge of science but has been an excellent role model and friend. I am indebted to her and am extremely grateful for the continuous support she has provided.

Nick has been a great mentor, an excellent support to me in conferences and has always been there to help with corrections.

Working with James and the nitric oxide signalling group at the MRC in Imperial College London has taught me how to think critically and allowed me to understand the importance of working with primary cells and using recent, novel experimental techniques. I have spent most of my time here and have been welcomed greatly by the whole group.

Phillip Miller-Tate recommended me for a PhD after completing my Master's project with him and I am very appreciative of the help and support he has given me during my whole time at university.

I am especially thankful for all the help, encouragement and endless love that my family have provided for me. My parents have always encouraged me to pursue my dreams and have instilled the importance of education into me since an early age – without them I would not be where I am.

Last but not least, I would like to thank my husband who has continuously motivated me (emotionally and physically by staying up all night with me while I wrote this thesis) and encouraged me to always aim as high as possible. After this we can have our belated honeymoon!

ABSTRACT

Asymmetrically methylated forms of arginine (asymmetric dimethylarginine, ADMA and L-N-monomethylarginine, L-NMMA) are competitive inhibitors of all three isoforms of nitric oxide synthase (NOS). These molecules are produced endogenously in all cells by a process that involves protein arginine methyltransferase (PRMT)-catalysed methylation of certain arginine residues in proteins and the subsequent proteolysis of these methylated proteins. Free methylarginines accumulate in the cytosol where they are actively metabolized to citrulline and methylamines by the enzyme dimethylarginine dimethylaminohydrolase (DDAH1 and 2). ADMA and L-NMMA have been shown to be elevated in patients with cardiovascular and renal disease, however, their role in immune cells and in particular macrophages is yet to be confirmed. The aim of this project was to determine the effect of increased ADMA, both endogenous and exogenous, on macrophage function.

U937-derived macrophages (a human monocytic cell line) and primary peritoneal macrophages extracted from wild type ($DDAH2^{+/+}$), global DDAH2 knock-out ($DDAH2^{-/-}$) and macrophage-specific DDAH2 knock-out ($DDAH2^{flox/flox}$ LysM-Cre) mice were used. Their NO production, motility, phagocytosis, chemotaxis, and cytokine levels was determined using the Griess assay, real-time imaging, a fluorescently labelled E-coli phagocytosis assay, a transwell migration assay and RNA-sequencing respectively.

Here we show that, in contrast to endothelial cells, DDAH2 is the only DDAH isoform expressed in primary murine macrophages basally or following cytokine stimulation of the cells. Results showed that DDAH2 metabolises methylarginines in macrophages through a VEGF-independent mechanism and significantly attenuates cytokine-stimulated NO synthesis. Both the pharmacological addition of ADMA and genetic deletion of DDAH2 in macrophages results in impaired macrophage function (as assessed by motility, phagocytosis and cytokine production). These data identify DDAH2 as a key regulator of macrophage NO synthesis and demonstrate the potential therapeutic utility of DDAH2-selective inhibitors.

TABLE OF CONTENTS

PRESENTATIONS AND PUBLICATIONS

Oral Presentations

6th International Symposium on ADMA

Title: "DDAH2 regulates macrophage motility"

Imperial College London, UK

August 2012

Physiological Society Meeting 2012

Title: "The role of DDAH2 on macrophage motility"

Winner of Pfizer Prize

Edinburgh, Scotland

June 2012

Kingston University Postgraduate Research Day 2012

Title: "The role of the ADMA/DDAH pathway on macrophage motility"

1st Prize Winner

Kingston University, UK

May 2012

Kingston University Postgraduate Research Day 2011

Title: "The role of the ADMA/DDAH pathway on macrophage motility"

1st Prize Winner

Kingston University, UK

May 2011

Poster Presentations

Physiological Society/ Kingston University Research Day
Kingston University, UK
January 2012

St. George's University of London, Graduate School Research Day
St. Georges Hospital, London
December 2011

Physiological Society Meeting 2011
Oxford University, UK
July 2011

5th International Symposium on ADMA
Runner-up of Young Investigator Award
Chicago, Illinois
November 2011

Kingston University Postgraduate Research Day 2010
1st Prize Winner
Kingston University, UK
May 2010

St. George's University of London, Graduate School Research Day
St. Georges Hospital, UK
December 2010

Abstracts

The hemodynamic effects of deletion of DDAH2 in conscious mice
Wang Z, Caplin B, Delahaye D, Dowsett L, Ahmetaj-Shala B, Leiper J
American Heart Association (Texas, USA, 2013)

Ddah2 (dimethylarginine dimethylaminohydrolase 2) is essential for a complete inflammatory response in a folate model of acute kidney injury
Tomlinson J, Ahmetaj B, Leiper J
Renal pathology, Experimental Pathology (Hong Kong, 2013)

DDAH2 regulates primary macrophage motility and phagocytosis
Ahmetaj B, Leiper J, Freestone N, Arrigoni F
ProcPhysiolSoc (Scotland, 2012)

Macrophage apoptosis and loss of motility is induced by ADMA
Ahmetaj B, Leiper J, Freestone N, Arrigoni F
ProcPhysiolSoc (UK, 2012)

Publications

1. Wang Z, Kelly P, Nandi M, Torondel B, Caplin B, Delayhe M, Dowsett L, **Ahmetaj-Shala B***, Leiper J. Genetic Knock-out of DDAH2 Attenuates Vascular Nitric Oxide Signalling: Characterisation of DDAH2-/- mice. (2013, In preparation).

2. James Leiper, Francesca Arrigoni and **Blerina Ahmetaj***. The Therapeutic Potential of Dimethylarginine Dimethylaminohydrolase-Mediated Regulation of Nitric Oxide Synthesis. Translational Vascular Medicine. 2012. Part 2. 61-88.

3. Arrigoni F, **Ahmetaj B***, Leiper J. The biology and therapeutic potential of the DDAH/ADMA pathway. Curr Pharm Des. 2010; 16 (37):4089-102.

LIST OF FIGURES

Chapter 1

Chapter 3

Chapter 4

Chapter 5

Chapter 6

Appendix

TABLES

Chapter 1

Chapter 2

Chapter 3

Chapter 5

Chapter 6

Appendix

LIST OF ABBREVIATIONS AND ACRONYMS

Main abbreviations

ADMA - asymmetric N^G, N^G- dimethyl-L-arginine
DDAH - N^G, N^G-dimethylarginine dimethylaminohydrolase
DDAH1$^{-/-}$- DDAH1 homozygous knockout mouse
DDAH1$^{+/-}$- DDAH1 heterozygous knockout mouse
DDAH1$^{+/+}$- DDAH1 homozygous wild-type mouse
DDAH2$^{-/-}$- DDAH2 homozygous knockout mouse
DDAH2$^{+/-}$- DDAH2 heterozygous knockout mouse
DDAH2$^{+/+}$- DDAH2 homozygous wild-type mouse
DDAH2$^{flox/flox}$–DDAH2 LysM-Cre floxed mouse
DDAH2$^{flox/flox}$ LyM-Cre – DDAH2 macrophage specific LysM-Cre knock-out mouse
EDRF - endothelium derived relaxing factor
eNOS- endothelial NOS (NOS3)
eNOS$^{-/-}$- homozygous knockout eNOS mouse
iNOS- inducible NOS (NOS2)
L-NAME - nitro-L-arginine methyl ester
L-NMMA - N^G-monomethyl-L-arginine
nNOS - neuronal NOS (NOS1)
NO - nitric oxide
NO_2^- - Nitrite
NO_3^- - Nitrate
NOS - nitric oxide synthase
NOx- nitrate + nitrite
NS- not significantly different
pMacs- primary peritoneal macrophages
PRMTs- protein arginine methyltransferases
SDMA - symmetric N^G, $N^{G'}$-dimethyl-L-arginine
SEM- standard error of the mean

Other abbreviations

ACE – Angiotensin converting enzyme
Ach – Acetylcholine
BH_4–Tetrahydrobiopterin
bp– Base pair
CAT –Cationic amino acid transporter
COX 1 or 2 –Cyclooxygenase 1 or 2
CPM – Counts per million

DMA – Dimethylarginine
DMSO – Dimethylsulphoxide
DNA – deoxyribonucleic acid
FBS – Fetal bovine serum
HEPES – 4-(2-hydroxyethyl)-1-piperazineethanesulfonic acid
IC_{50}–The half maximal inhibitory concentration of a substance
IFN-γ – Interferon-gamma
IL-1 – Interleukin-1
IL-10 – interleukin 10
IL-1β – Interleukin 1-beta
IL-4 – Interleukin-4
IL-6 – Interleukin-6
IL-8 – Interleukin-8
IRF-1 – Interferon regulatory factor 1
kDa– kiloDaltons
K_m – Michaelis-Menten constant; the substrate concentration at which the reaction velocity is half maximal
LPS – Lipopolysaccharide
MCP-1 – Monocyte chemoattractant protein-1
MIP-1α – Macrophage inflammatory protein-1 alpha
MIP-2 – Macrophage inflammatory protein-2
MTT – 3-(4,5-Dimethylthiazol-2-Yl)-2,5-Diphenyltetrazolium Bromide
NADPH – Nicotinamide adenine dinucleotide phosphate
NF-κB– Nuclear factor-kappa B
PBS - Phosphate buffered saline
PCR- Polymerase chain reaction
PMA - Phorbol-12-myristate-13-acetate
PRR – Pattern recognition receptor
RT-qPCR – quantitative reverse-transcription PCR
RNA – Ribonucleic acid
RPMI 1640 – Roswell Park Memorial Institute medium 1640
RXR – Retinoid X receptor
SNP – Sodium nitroprusside
TLR – Toll like receptor
TNF-α –Tumor necrosis factor- alpha
U937 –Human myeloblastic leukaemia cell line
VEGF – Vascular endothelial growth factor
XO – Xanthine oxidase
α-Tubulin – alpha-Tubulin (also TubA2)
β-Actin– beta-Actin

CHAPTER 1

The effect of nitric oxide on macrophages

1.1 The immune system

The immune system has a complex yet central role in finding and fighting infection and pathogens. In order to function properly it relies heavily on white blood cells (leukocytes) to combat infection and foreign particles, such as bacteria, viruses, fungi and parasites. There are several different types of white blood cell each of which serves a distinct role. These cells are paramount in the fight against invading pathogens in the immune response and a failure of any one of these components results in dysregulation of the immune system, which can be categorised into innate immunity or adaptive immunity.

1.1.1 Innate immunity

Innate immunity involves genes which are inherited and includes both external and internal defences. This immunity type is the first line of the defence mechanism and includes physical barriers such as the skin, chemicals in the blood, and specific immune cells (Janeway and Medzhitov, 2002). In order to activate this immune response, various chemical properties must be present on the antigen, that when introduced into the human body induces an immune response.

The defences in innate immunity are constitutively expressed meaning that they are ready to be activated upon infection. This system reacts to a variety of organisms, is not antigen specific (meaning that it reacts to all invading pathogens) and does not have memory. The circulating cells involved in this type of defence include granulocytes such as; basophils, eosinophils, Natural Killer T cells (NK T cells) and other immune cells such as; neutrophils, macrophages, dendritic cells and mast cells (Medzhitov and Janeway, 1997). Epithelial cells can also participate in this immune response by providing a physical barrier against harmful environmental agents.

1.1.2 Adaptive immunity

A more complex, yet equally important defence is adaptive immunity. This response involves the antigen becoming processed and recognised before it is attacked. Memory cells are critical in this process as they aid in the recognition of previously encountered antigens thus ensuring the immune response works faster and more efficiently if the same antigen is encountered again.

There are similarities in both innate and adaptive immunity, in that they both function to protect against invading organisms and they both rely heavily on the ability of the immune system to distinguish between self and non-self-molecules. The main difference between the two immune types, however, are that adaptive immunity requires some time to react to the invading pathogen and is antigen specific meaning that it reacts only to the organism that induced it. The components of the adaptive immune response include B and T cells and NK T cells (which are also part of the innate response) (Fig. 1.1).

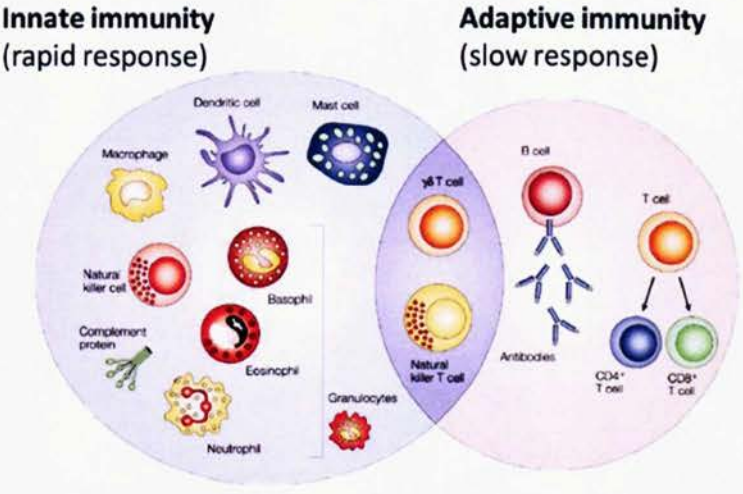

Fig.1.1: Cell types involved in innate and adaptive immunity.

The innate immune system is one with a rapid response which involves cells such as macrophages, granulocytes, dendritic cells, mast cells and various T cells in the fight against invading pathogens. Alternatively, adaptive immunity involves B cells and T cells which are critical to producing antibodies. (Image adapted from Dranoff, 2004).

1.2 Circulating cells and innate immunity

The innate immune system consists of granulocytes, mast cells, dendritic cells, macrophages and NK T cells, which all have unique functions involved in fighting disease. Their specific roles are highlighted in Table 1.1.

Cell type	Function	Mechanism of action	Ability to proliferate
Granulocytes			
Neutrophils	Fast acting cells involved in trapping and killing pathogens outside of the wall.	Release net of fibres called neutrophil extracellular trap (NET). Also release superoxide to kill pathogens.	Short half-life (4-10 hours) and unable to proliferate
Eosinophils	Movement to inflamed areas, modulating inflammatory responses , antibacterial activity and participating in immediate allergic reactions.	Release cytotoxic granule proteins such as major basic protein (MCP), eosinophil peroxidase (EPO) and eosinophil-derived endotoxin (EDN) to perforate target cell membranes.	Remain in circulation for 8-12 hours and in tissues for 8-12 days without stimulation. Some proliferative ability.
Basophils	Critical in attracting neutrophils and eosinophils to the site of inflammation.	Contain granules filled with histamine, a chemical involved in allergic reactions that increases blood flow to damaged tissues, which when activated is released.	Half-life of a few days and little proliferative capability
Mast cells	Specialised cells - can amplify or suppress the innate or acquired immune response.	Rapidly release histamine, heparin, and various hormonal mediators and chemokines.	Generally long-lived. Some tissue mast cells can proliferate after appropriate stimulation
Dendritic cells	Antigen presentation and activation of T cells, inducing and maintaining immune tolerance and maintain immune memory in tandem with B cells.	Produce various cytokines such as interleuikin-12 (IL-12) which signals naïve T cells.	Highly proliferative
Natural killer T cells	Recognize and kill abnormal cells. Also, regulate B and T cell function.	Distinguish between infected cells and tumours from normal and uninfected cells by recognizing MHC Class I levels. Regulate B and T cell function by releasing a number of cytokines	Highly proliferative
Macrophages	Critical for both the induction and resolution of immune responses in particular migration to inflamed site, phagocytosis of pathogens or necrotic cells and upregulation of pro-inflammatory cytokines.	Express a range of scavenger receptors which aid the removal of necrotic tissues, aged red blood cells and toxic molecules from the circulation.	Generally not proliferative in quiescent conditions but have been shown to be proliferative in inflamed states.

Table 1.1: The role of circulating cells in innate immunity

The involvement of granulocytes, mast cells, dendritic cells, NK T cells and macrophages in the innate immune response.

1.3 Defects and disease

Although the immune response is an organized system with clear functions, complications do occur. These failures fall into three broad categories: immunodeficiency, autoimmunity and hypersensitivity.

Immunodeficiencies occur when one or more of the components of the immune system are inactive resulting in a weakened response to pathogens. In developing countries, the major cause of immunodeficiency is malnutrition with nutrients such as; copper, zinc, vitamin A, C and E and folic acid, all known to reduce immune responses.

Autoimmune disorders are another aspect of immune dysfunction and occur when there is an over-reactive immune response. In this case, the immune system does not properly distinguish between self and non-self, and attacks part of the body. Examples of autoimmune disorders include auto-immune deficiency syndrome (AIDS), rheumatoid arthritis (RA) and multiple sclerosis (MS).

Hypersensitivity is an immune response that damages the body's own tissues. It is divided into four classes (Type I-IV) based on the mechanisms involved and the time course of the hypersensitive reaction. Asthma is an inflammatory disease which is characterized by inflammation and hypersensitivity. It is one of the most common conditions in western society and in parallel with other immune-mediated disorders; its prevalence has increased in the past few decades.

1.4 Mechanisms of activation

The different methods of activation in the immune system are highly dependent on a wide range of mechanisms and are important for the functioning of a healthy immune system. These include the recognition of pathogens via pattern recognition receptors (PRRs), the activation of important downstream signalling mechanisms via toll-like receptors (TLRs)

and both the activation of the inflammatory response and the recruitment of immune cells via cytokine production.

1.4.1 PAMPs and PRRs

Innate immune cells are able to recognise highly conserved pathogen-associated microbial patterns (PAMPs), such as; bacterial and viral nucleic acids, the bacterial protein flagellin (which produces filaments), components of the peptidoglycan bacterial cell wall, lipopolysaccharide (LPS) from Gram-negative bacteria, fungal β-glucan and α-mannan cell wall components. It does this via pattern recognition receptors (PRRs), which are germline encoded receptors (Bianchi, 2007; Seneviratne *et al.*, 2012). PRRs can also recognise endogenous molecules termed damage associated molecular patterns (DAMPs) which are released from damaged/injured cells and include ATP, the cytokine IL-1α and uric acid (Bianchi, 2007). It is therefore DAMPs and PAMPs which trigger innate immune responses.

There are two main types of PRRs: cytosolic receptors which consist of; RIG-I-like receptors (RLRs) and NOD receptors (NLRs), and transmembrane receptors which consist of; C-type lectin receptors (CLRs) and Toll-like receptors (TLRs). RLRs are important in antiviral innate immune responses such as recognising single-stranded RNA (ssRNA) or double-stranded RNA (dsRNA) whereas NLRs promote transcription of pro-inflammatory mediators via NF-κB. TLRs and NLRs both recognise bacterial peptidoglycan components and therefore promote pro-inflammatory cytokine production (Brodsky and Monack, 2009). CLRs recognise carbohydrates on pathogens which can lead to the production of pro-inflammatory cytokines or inhibition of TLR-mediated immune complexes (Takeuchi and Akira, 2010).

1.4.2 Toll like receptors

One of the most recognised PRRs are TLRs. Their name is derived from their similarity to the protein coded by the Toll gene identified in Drosophila in 1985 by Christiane Nusslein-Volhard. The roles of TLRs include the; recruitment of leukocytes to infected cells, uptake of microorganisms by phagocytic cells, activation of dendritic cells, stimulation of B and T-cell mediated immune responses and the maintenance of homeostasis by regulating tissue repair and regeneration.

At least 13 TLRs have been discovered so far, each one being highly specific for various endogenous and exogenous ligands. TLRs can be divided into two categories: 1) cell membrane TLRs (TLR1, TLR2, TLR4, TLR5, TLR6 and TLR11) for detecting LPS and lipoproteins and 2) nucleic-acid sensing TLRs (TLR3, TLR7, TLR8 and TLR9), which localise to intracellular vesicles including endosomes, lysosomes and endoplasmic reticulum and are involved in recognising viral RNA and bacterial DNA (Kawai and Akira, 2010; Cole *et al.*, 2010) (Fig. 1. 2).

TLRs have several distinct signalling pathways which are dependent on the recruitment of two adaptor proteins (myeloid differentiation primary-response protein 88 (MyD88) and TIR domain-containing adaptor inducing IFN-β (TRIF) (Fig. 1.2). MyD88-dependent signalling pathway occurs in all TLRs except TLR3 and results in the phosphorylation of IκB. Phosphorylated IκB is degraded by the ubiquitin proteasome system freeing NF-κB to translocate to the nucleus and mediate transcription of inflammatory genes. This pathway also activates Mitogen-activated protein kinase (MAPKs) resulting in the formation of activated protein-1 (AP-1), a transcription factor complex that controls many cytokine encoding genes. The TRIF-dependent signalling pathway results in IRF3 and NF-κB activation thus 'switching on' the immune response (Alexopoulou *et al.*, 2001).

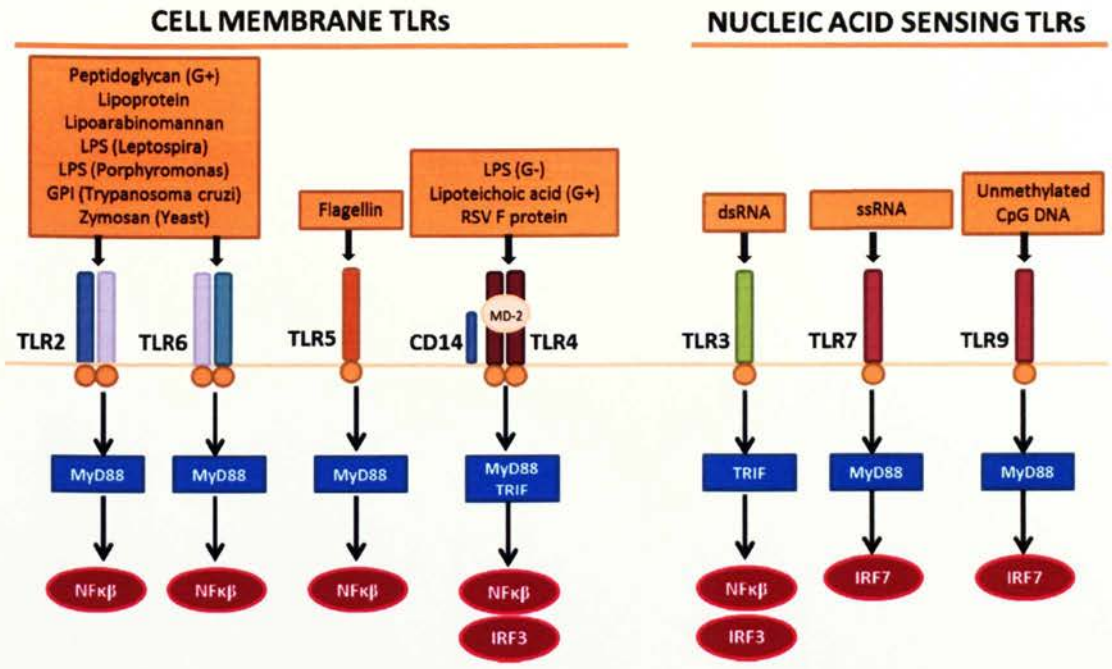

Fig. 1.2: Ligand specificities and signalling outcomes of TLRs

TLRs recognise a variety of PAMPs. TLR2 recognises a broad range of structurally unrelated ligands and functions in combination with several (but not all) other TLRs, including TLR1 and TLR6. TLR3 is involved in recognition of dsRNA. The recognition of LPS by TLR4 is aided by two accessory proteins: CD14 and MD-2. TLR5 is specific for bacterial flagellin, whereas TLR9 is a receptor for unmethylated CpG motifs, which are abundant in bacterial DNA. (G+, Gram-positive; G-, Gram-negative; GPI, glycophosphoinositol; RSV, respiratory syncytial virus).

1.4.3 Cytokines

Upon the activation of NF-κB, IRF3 and/or IRF7 there is an induction of the immune response which includes the initiation and upregulation of cytokine genes. Cytokines are important and diverse soluble proteins and peptides that can regulate many cell signalling pathways under both normal and pathophysiological conditions. They are pleiotropic in that they affect the activity of multiple cell types and produce various effects depending on the cell releasing them, timing and context (Ozaki and Leonard, 2002).

Generally, cytokines are present in very low concentrations, however, upon inflammatory stimulation can significantly increase e.g. interleukin-6 (IL-6) is present in picomolar concentrations but increases up to 1,000 fold following infection. Pro-inflammatory cytokines are involved in cellular inflammatory pathways and macrophage activation and include the following interleukins (ILs); IL-1, IL-6, IL-12, IL-18. Other pro-inflammatory cytokines include tumour necrosis factor-α (TNF-α), Interferon-γ (IFN-γ), monocyte inhibitory factor (MIF) and macrophage- colony stimulating factor (M-CSF). Cytokines which suppress the inflammatory response (anti-inflammatory cytokines) include IL-10, IL-1 and transforming growth factor-beta (TGF-β). The over expression of pro-inflammatory cytokines compared to anti-inflammatory cytokines results in inflammation (Fig. 1.3).

The main vascular effects of cytokines are to induce cell proliferation and differentiation, vascular growth, and migration. Cytokines that encourage cell proliferation and differentiation include; IL-2,which stimulates proliferation of antigen-activated B and T cells; IL-4, IL-5, and IL-6,which stimulate proliferation and differentiation of B cells; IFN-γ, which activates macrophages; and IL-3, IL-7 and GM-CSF, which stimulate hematopoiesis (development of immature blood cells to mature blood cells).

Cytokines are also involved in other cellular mechanisms. For instance, TNF-α has been shown to induce apoptosis, programmed cell death characterized by a series of morphological and biochemical malfunctions (Miller, 1999), in many cell types by activating caspase-8 and caspase-3 (Muzio *et al.*, 1998). TNF-α has also been shown to induce the production of reactive oxygen species (ROS). ROS are produced at areas of inflammation and injury. At low concentrations ROS helps to regulate cell activity such as cell growth, however, at high concentrations, it can lead to cellular stress and death resulting in vascular disease (Sprague and Khalil, 2009). Consequently, the overproduction of ROS increases cytokine production resulting in a vicious cycle of inflammation (Griendling *et al.*, 2000).

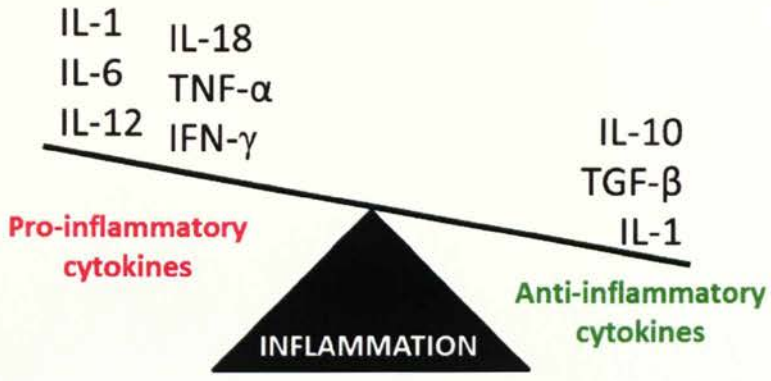

Fig. 1.3: Pro- versus anti-inflammatory cytokines

Increased pro-inflammatory cytokines such as IL-1, IL-6, IL-12, IL-18, TNF-α and IFN-γ compared to anti-inflammatory cytokines such as IL-10, TGF-β and IL-1 leads to inflammation.

1.5 The importance of macrophages

These large phagocytic cells were initially named by the Russian Nobel Prize winner Metchnikoff in 1908, whose studies and pioneering work in phagocytosis demonstrated that they were present in all vertebrates and invertebrates. Macrophages, like T cells, are critical for both the induction and resolution of immune responses. This suggests that although macrophages are protective, they can display pathogenic activity too.

Macrophage activation is critical to the inflammatory response as it prepares them for phagocytosis (engulfment of pathogens and foreign particles) and it releases various cytokines therefore initiating the innate response. Before the above can occur, monocytes, highly plastic cells which originate from $CD34^+$ myeloid progenitor cells in the bone marrow, must differentiate to macrophages. As they do this, the phenotypes and proteins that they express change. Monocytes initially have small and granular organelles with equally small intracellular lysosomes, phagosomes and nucleus. Following differentiation into macrophages, they become larger in size with large intracellular subunits. Similarly, their irregularity in shape and membrane

ruffles, combined with their extensive network of pseudopodia helps provide adherence and directional movement in order to quickly and efficiently reach their target. There they are able to carry out various critical functions that are paramount in the immune response.

1.5.1 Functions

1.5.1.1 Extravasation

Transendothelial motility is critical to macrophage function as they must be able to migrate to specific areas during infection and respond to chemotactic stimuli. Leukocyte extravasation (migration of monocytes from the bloodstream, across the endothelium and into the underlying tissue) is an important process required during; inflammation, lymphocyte recirculation, and migration of monocytes out of the circulation system to become macrophages. Transendothelial migration is dependent on adhesion molecules present on both the leukocyte and corresponding ligands on the endothelial cell.

Transendothelial migration occurs via four stages: 1) leukocyte rolling on endothelial cells enabling them to detect changes in signals 2)production of chemokines which triggers the activation of integrins3) tight adhesion to endothelial cells and 3) transmigration of leukocytes through the endothelium (Fig. 1.4) (Carlos and Harlan, 1994).

More specific chemokines which almost immediately stimulate integrin-dependent arrest of leukocytes include stromal cell-derived factor-1α and -1β (SDF-1α and SDF-1β) and macrophage inflammatory protein-3β (MIP-3β) (Campbell *et al.*, 1998). The ligands for the integrin's include; the receptor for the Ig superfamily, intracellular adhesion molecule-1 and -2 (ICAM-1 and ICAM-2) and vascular cell adhesion protein-1 (VCAM-1).The increased activity of integrin's and the upregulation of ligands during inflammation results in increased monocyte adhesion on endothelial cells (Hosokawa *et al.*, 2006).

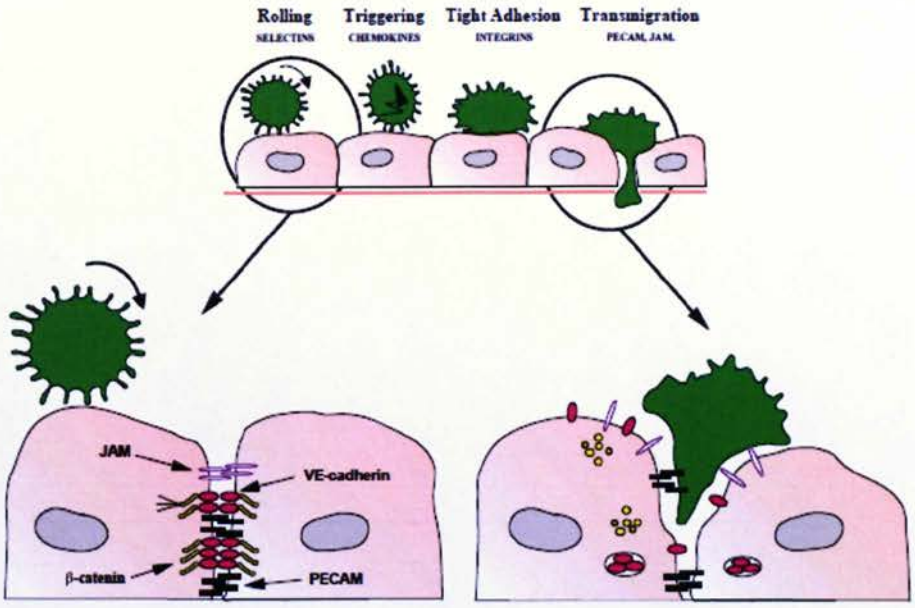

Fig. 1.4: Leukocyte transmigration through endothelium.

Under quiescent conditions, endothelial junctions are closed, and this integrity is controlled by homotypic binding of VE-cadherin (linked to the cytoskeleton via β-catenin), platelet/endothelial cell adhesion molecule 1 (PECAM-1) and junctional adhesion molecules (JAM). During the adhesion cascade, monocytes may trigger the dissociation of the VE-cadherin-β-catenin complex and may lead to interactions between opposing endothelial cells leading to loss of tight junctions. At the same time, PECAM-1 may serve as a scaffold to 'walk' the cell through the migration. Also the presence of inflammatory cytokines increases the gaps in the cells thus aiding transendothelial migration. (Image taken from Johnson-Leger, 2000).

1.5.1.2 Motility

Cell motility is particularly important for cells involved in immune functions and wound healing. The general method of motility is similar in most cells (Fig. 1.5). In macrophages, the initial step required is cell polarisation of the leading edge which is driven by actin-polarisation of an extension. This then provides traction from the adhesion of the extended edge to the extracellular matrix proteins. In order for the cell to physically move forward, the trailing edge must first detach from the surface and then move forward by acto-myosin contractility.

One of the major mechanisms required for the recruitment of macrophages to the site of inflammation is cytoskeletal rearrangement and actin polarisation (Etienne-Manneville and Hall, 2002). Actin polymerisation provides the driving force for the initial extension of the cell front. Through contraction and relaxation, it can also provide the mechanical force that is required to move the cell body forward changing the cell morphology.

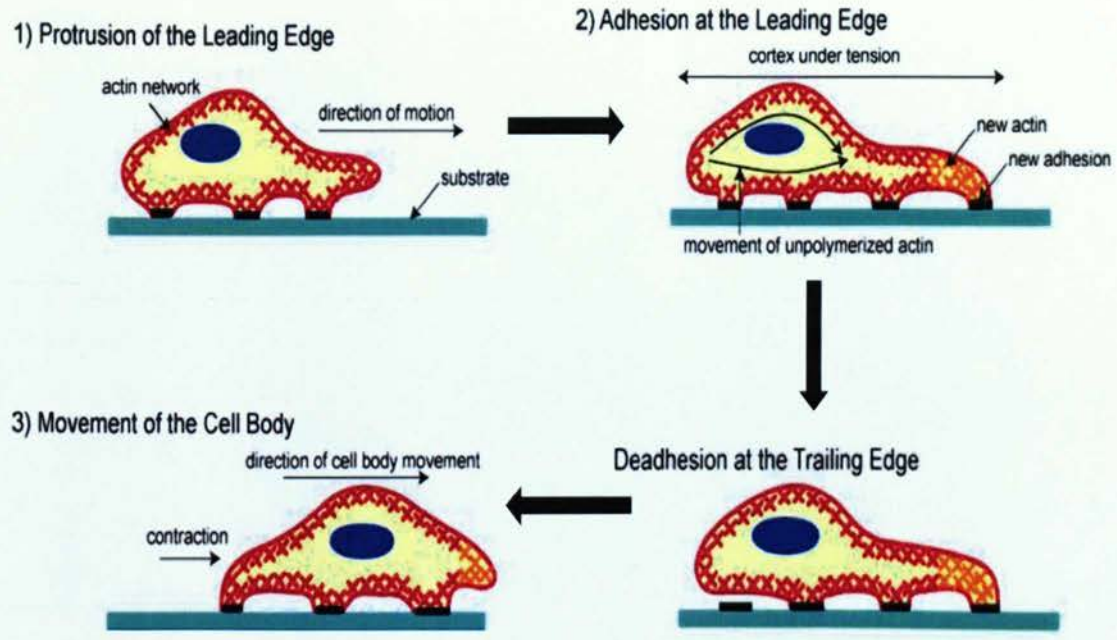

Fig. 1.5: Schematic representation of the process of cell movement.

Cells distinguish their direction of movement and extend a protrusion in this direction by actin polymerisation at the leading edge. Following this, they adhere to the leading edge of the surface on which they are moving and detach at the cell body and rear. Finally, the whole cell body is pulled forward by contractile forces generated in the cell body and rear of the cell and the cell moves in the intended direction. (Image taken from Ananthakrishnan *et al.*, 2007).

1.5.1.3 Phagocytosis

The mechanism of phagocytosis is essential for the uptake and degradation of infectious agents and senescent cells (>0.5μm) and is involved in the; immune response, inflammation, development and tissue remodelling (Aderem and Underhill, 1999). The innate immune system has developed various receptors to differentiate between self and non-self agents. As described previously, the presence of PAMPs allows PRRs to recognise pathogens and enables macrophages to carry out phagocytosis. Integrin and scavenger receptors can recognise bacterial components and mannose receptors (MR) can recognise mannans (Stahl and Ezekowitz, 1998). Furthermore, fragment crystallisable receptors (FcR's), which are proteins found on the surface of phagocytic cells, contribute to the protective functions of the immune system. They bind to components attached to the pathogens and thus stimulate phagocytosis (Daeron, 1997). The pathogen is then transported to the cytoplasm to form the phagolysosome and release ROS to induce cell death (Fig. 1.6).

In addition to this, phagocytosis is dependent on an actin mechanism and usually independent of clathrin, a protein that plays a major role in the formation of coated vesicles. Hackam *et al.* showed that phagocytosis is affected by GTPases and in particular Rho. They found that the microinjection of the Rho-specific inhibitor C3 exotoxin in the J774 mouse macrophage cell line inhibits phagocytosis by preventing receptor clustering which is fundamental for efficient particle binding and internalisation (Hackam *et al.*, 1997). The other two GTPase molecules, Rac1 and Cdc42 do not affect particle binding like Rho but in RAW 264.7 cells (a murine macrophage cell line) their inhibition was shown to reduce phagocytosis by preventing the accumulation of F-actin in the phagocytic cup (Cox *et al.*, 1997).

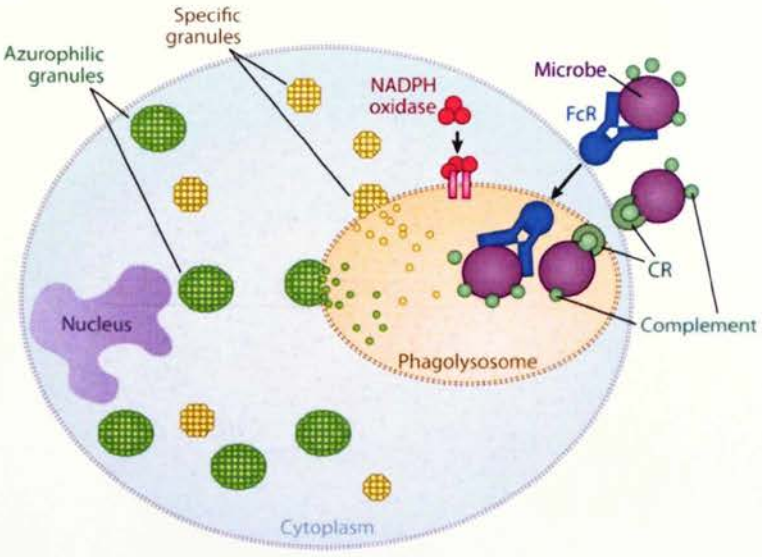

Fig. 1.6: Mechanism of phagocytic cell destruction of bacteria.

Neutrophils and macrophages are responsible for the clearance of pathogens from the body. Complement fragments bind to components on a bacterium. The bacterium is then transported to the cytoplasm where fusion of the phagosome cytoplasmic granules such as specific granules (yellow) and azurophilic granules (green) form the phagolysosome. (Image taken from Stearns-Kurosawa *et al.*, 2011)

1.5.2 Pathways to activation

In quiescent conditions macrophages are highly efficient in destroying cellular debris and apoptotic cells. They do this via their highly degradative phagosomal compartment (Russell *et al.*, 2009). Similarly, they produce low levels of inflammatory cytokines and are not very motile. In stimulated conditions, macrophages are classified according to the way they are activated. The classical or M1 pathway is so called when the macrophage is induced by IFN-γ alone or in conjunction with microbial stimuli such as LPS or different cytokines such as TNF-α or GM-CSF (Dalton *et al.*, 1993) (Fig. 1.6). M1 macrophages are critical in inflammation and move into tissue from blood. They are specifically important for bacterial killing, proteolysis (Woollard and

Geissmann, 2010) and controlling resistance against tumours and intracellular parasites (Mosser, 2003). They release IL-1, IL-6, TNF-α and effector molecules such as ROS, which act as an inflammatory signal to surrounding immune cells and initiates the inflammatory cascade.

The non-classical or M2 pathway involves macrophages that are derived from monocytes patrolling the vasculature (Woollard and Geissmann, 2010). M2 macrophages, unlike M1, are induced only by exposure to IL-4, IL-10 and IL-1 and glucocorticoid or hormones such as vitamin D3 (Gordon, 2003) (Fig. 1.7). Both macrophage subtypes are involved in phagocytosis and are known to mediate the formation of foam cells in response to lipids.

In vitro, the exact signalling requirements of immune cells to achieve optimum activation are reliant on several factors including; species (mouse or human), the tissue source and differentiation site (bone marrow, peritoneal cavity, monocytes) and stimulation conditions (quiescent cells or inflammatory cells). What is known and has been extensively reported is that experimentally in order for macrophages to reach their full cytotoxic capability; they must be stimulated with two consecutive stimuli as described below (Adams and Hamilton, 1987). The sequence of exposure to the different signals is fundamental to the activation process and to induce the synthesis of important biochemical molecules such as nitric oxide (NO). Initially, IFN-γ was used as a primary trigger for macrophage activation (Svedersky *et al.*, 1984; Pace *et al.*, 1983) followed by low LPS levels to provide a second 'trigger' (Adams and Hamilton, 1987; Lorsbach and Russell, 1992). More recently, studies have shown that IL-2 (Cox *et al.*, 1990) and TNF-α (Green *et al.*, 1990), which is produced endogenously in stimulated macrophages, have both been found to be another critical second trigger for IFN-γ primed cells. *In vivo*, settings do not always reproduce those *in vitro* in particular in the immune response. Macrophages obtained from sites of inflammation *in vivo* have often been exposed to a wide variety of signals including proteases, antibodies and immune complexes and therefore may already be partially activated.

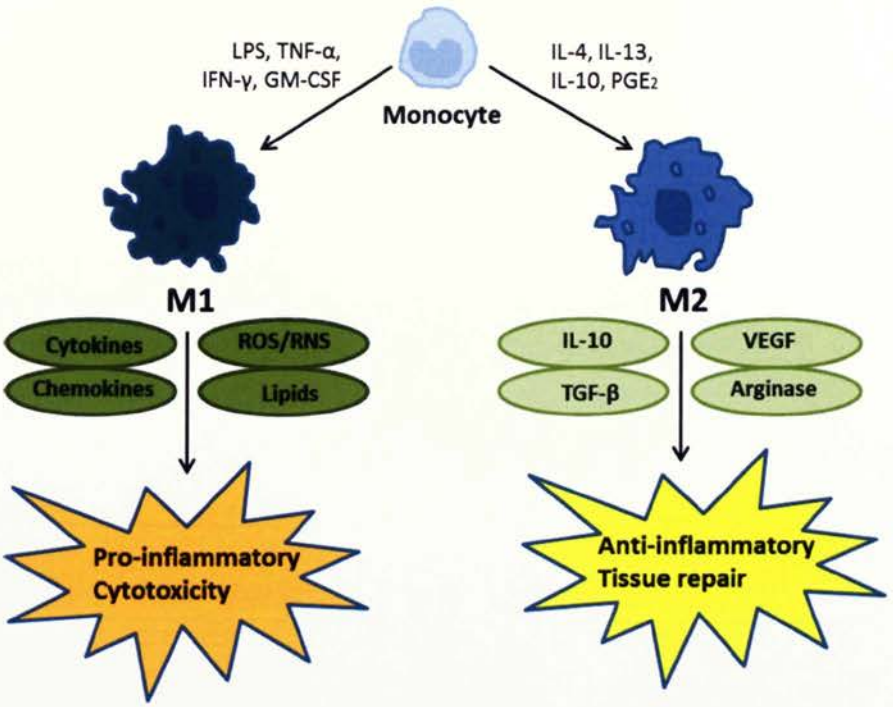

Fig. 1.7: Difference between M1 and M2 macrophages

Monocytes are activated by LPS, TNF-α, IFN-γ or GM-CSF to produce M1 macrophages (classically activated) or IL-4, IL-13, IL-10 or PGE_2 to produce M2 macrophages (alternatively activated). M1 macrophages lead to pro-inflammatory cytotoxicity by activating cytokines, chemokines, ROS/RNS and/or lipids. M2 macrophages are anti-inflammatory and important in tissue repair and produce IL-10, VEGF, TGF-β and arginase.

1.5.3 Molecular mechanisms underlying actions

1.5.3.1 NF-κB

NF-κB is a rapidly acting transcription factor consisting of five members; RelA (p65), RelB, c-rel, p105/p50 (NF-κB1) and p100/p52 (NF-κB2) (Bonizzi and Karin, 2004; Karin and Ben-Neriah, 2000). NF-κB is involved in regulating the immune response to infection and facilitates the transcription of many genes, including; pro-inflammatory cytokines, chemokines and anti-apoptotic proteins (Karin and Ben-Neriah, 2000).

In unstimulated cells, NF-κB is located in the cytoplasm bound to a member of the inhibitor of kappa B (IκB) family of proteins. The classical NF-κB activation pathway is activated by TLRs, IL-1 receptors (IL-1R) or TNF-receptors (TNFR), which results in the phosphorylation of IκB by the IκK complex and in turn induces its ubiquitination and proteasome degradation. NF-κB is then able to translocate freely to the nucleus where it facilitates the transcription of many genes and activates cell survival, inflammation and the innate immune response. NF-κB can also turn on the expression of IκB thus forming a negative feedback loop.

The alternative NF-κB activation pathway is triggered by the activation of various TNF receptor family members including; CD40, lymphotoxin beta receptor (LTβR) or B-cell activating factor belonging to the TNF-family receptor (BAFF-R). These induce kinase (NIK) and an IκK-α homodimer, which leads to p100 processing and the translocation of p52 dimers into the nucleus. Activation of the alternative pathway regulates the adaptive immune system and the development of lymphoid organs.

1.5.3.2 PPARs

The discovery of peroxisome proliferator-activated receptor gamma (PPAR-γ) in macrophages in the 1990's has led to immense interest into the effects of PPAR-γ ligands on inflammatory gene expression. PPAR-γ, abundantly present in fat cells, is a member of the nuclear hormone receptor family and is usually characterized as a regulator of adipogenesis. Although expressed at lower levels in macrophages, PPAR-γ is known to inhibit inflammatory genes such TNF-α, IL-6, IL-1β, MMP-9 and scavenger receptor A (Ricote *et al.*, 1998).

Ligands for PPAR-γ include modified fatty acids, the prostaglandin D2 metabolite and the thiazolidinedione (TZD) class of insulin-sensitising agents which are used to treat type II diabetes. The activation of PPAR-γ is known to be by the exposure of macrophages to oxLDL. This exposure induces PPAR-γ mRNA expression and activates ligands (Nagy *et al.*, 1998). For this reason

PPAR-γ has been shown to be a central switch in regulating the inflammatory potential of macrophages in adipose tissue and atherosclerotic plaques (Charo, 2007).

Recent studies have documented that PPAR-γ has important anti-inflammatory effects *in vivo*. The selective deletion of PPAR-γ in macrophages is known to increase insulin resistance and increase the progression of atherosclerosis (Chawla *et al.*, 2001; Babaev *et al.*, 2005). PPAR-γ selective deletion in macrophages also compromises the uptake and degradation of OxLDL, mainly explained by a reduction in CD36 expression, a scavenger receptor mediating the uptake of oxLDL. This could explain the increased expression of PPAR-γ found in macrophage foam cells in humans (Marx *et al.*, 2002). Overall, these studies have highlighted PPAR-γ to be a critical regulator of the inflammatory potential of tissue macrophages.

1.5.3.3 MAP kinase

Mitogen-activated protein kinases (MAPKs) include more than a dozen proteins belonging to three families; extracellular signal-regulated kinases (ERKs), p38 MAPKs, and c-Jun N-terminal kinase/stress-activated protein kinases (JNK/SAPKs). These three families are activated in macrophages by a variety of stimuli including LPS, phorbol ester (PMA) and TNF-α.

MAPKs have been implicated in the proliferation, differentiation and activation of macrophages and are therefore particularly important during infection. This response depends on the way that the cells are being activated and the maturation state of the macrophages. For example, stimulation of monocytes with LPS causes phosphorylation of MAPKs, inhibits proliferation and causes activation. However, stimulation of bone-marrow derived macrophages (BMM) with M-CSF causes phosphorylation of MAPKs and proliferation (Rao, 2001). A permanently activated MAPK-kinase cascade results in continuously activated proliferation which is an important feature of a tumor cell.

1.5.3.4 GTPases

Actin filaments and cytoskeletal organisation are regulated by Rho GTPases. These small GTPases cycle between the active GTP-bound state and the inactive GDP-bound state and are essential for the regulation of; phagocytosis, proliferation, cell survival, gene transcription, microtubule dynamics and vesicular transport pathways (Etienne-Manneville and Hall, 2002). Most of the research to date regarding motility has focused on the three ubiquitously expressed GTPases: Rho, Rac and cdc42. Rho controls stress fibre formation, contractile activity and cell assembly and maturation. Rac1 is associated predominantly with actin assembly and adhesion in the lamellipodium. Cdc42 generally controls the polarity of the cell and the formation of filopodia and focal adhesions (Ridley, 2001; Nobes and Hall, 1995).

Many reports have suggested that cdc42 is more important for gradient sensing and polarisation than cell locomotion (Allen *et al.*, 1998). Inhibition of cdc42 in macrophages resulted in cells that were still motile in response to CSF-1 but migrated randomly, rather than up the concentration gradient (Jones *et al.*, 1998). Macrophages from Rac1/2$^{-/-}$ animals were different morphologically - they did not form membrane ruffles, normal lamellipodia or podosomes, however, this was not found to be important in motility (Wheeler *et al.*, 2006).

Interestingly, TNF-α production from macrophages has been shown to affect Rho kinase. GTPases are involved in TNF-α-mediated microfilament cytoskeletal rearrangement and apoptosis in bovine pulmonary endothelial cells (Petrache *et al.*, 2003). The Rho inhibitor Y-27632 inhibits TNF-α induced stimulation, E-selectin expression, and endothelial permeability (Nwariaku *et al.*, 2003). One proposed method of action is that TNF-α may activate sphingosine kinase, leading to sphingosine-1-phosphate (S1P) formation and signalling and subsequent Rho activation (Chen *et al.*, 2004).

1.5.4 Macrophage role in diseases

1.5.4.1 Vascular inflammation and atherosclerosis

Cardiovascular disease is one the world's leading diseases from which an estimated number of 16.7 million people die annually (based on 2003 World Health Organisation statistics) (Baigent *et al.*, 2000). In North America, it is the leading cause of death and disability (Baigent *et al.*, 2000). The development and progression of atherosclerosis occurs as a result of continuous endothelial dysfunction (Ross, 1993; Anderson *et al.*, 1995;Vanhoutte, 1997). It is characterized by the formation of atherosclerotic plaques that contain; lipids, calcified regions, inflamed smooth muscle cells, endothelial cells and immune cells (Woollard *et al.*, 2010). Risk factors for the development of atherosclerosis include; hypertension, ageing, smoking, diabetes and hypercholesterolemia (Brunner *et al.*, 2005).

In 1980, Ross showed that the development of atherosclerosis was dependent on endothelial dysfunction and later described the inflammation hypothesis; "the response to injury occurs in the form of inflammation therefore atherosclerosis is an inflammatory disease" (Ross, 1980; Ross, 1999). It is now accepted that both classically and alternatively activated macrophages are key to the pathogenesis of atherosclerosis and their accumulation has been directly associated with atherosclerotic plaque progression and rupture (Woollard and Geissmann, 2010). Monocytes are recruited into the intima by inflammatory signals (increased chemokines and adhesion molecules on endothelial cells) where they differentiate into macrophages and engulf oxy-LDL resulting in foam cell formation.

1.5.4.2 Rheumatoid arthritis

Rheumatoid Arthritis (RA) is an autoimmune chronic inflammatory disease, characterised by macrophage and lymphocyte infiltration, proliferation of synovial fibroblasts and joint destruction. Symptoms of RA include pain, stiffness, warmth and redness in joints. Macrophages play a pivotal role in the

pathogenesis of RA as they produce a variety of pro-inflammatory cytokines and chemokines thus increasing inflammation and contributing to joint destruction. As a result, macrophages are attractive therapeutic targets for the therapy in the treatment of RA for a number of reasons. Firstly, increased macrophage infiltration has been correlated with increased progression of joint destruction (Mulherin *et al.*, 1996) and the majority of conventional anti-rheumatic therapies involve downregulation of the function of the mononuclear phagocyte system (Hahn *et al.*, 1993; Yanni *et al.*, 1994; Bondeson, 1997). Secondly, the most highly effective conventional therapies for RA have been those that target cytokines produced predominantly by macrophages such as TNF-α, IL-1 and GM-CSF (Feldmann *et al.*, 1999) or that target macrophage subcellular compartments (Burmester *et al.*, 1997).

1.5.4.3 Sepsis

One of the most common causes of admission to intensive care is septicemia or sepsis. Sepsis is associated with increased production of pro-inflammatory and anti-inflammatory cytokines most probably by resident macrophages (Cavaillon *et al.*, 2003). The addition of LPS has been found to regulate as many as 1,055 genes in murine macrophages (25% of which correspond to cytokines or chemokines) (Hashimoto *et al.*, 2003). It is the overproduction of the cytokines and chemokines released by macrophages combined with the increase in cell apoptosis and necrosis which augments sepsis severity, rapidly drops blood pressure and in severe cases results in multiple organ failure. Anticoagulants are often used in patients with severe sepsis and high risk of death however, they have little impact on mortality if given alone. There are multiple new therapies currently being evaluated which include the use of biomarkers to direct appropriate therapy to individuals (Stearns-Kurosawa *et al.*, 2011).

1.6 Nitric oxide as a key signalling molecule

NO, a potentially toxic molecule has been implicated in a wide range of biological functions. At room temperature and pressure NO is a colourless gas (boiling point, -151.7°C with a maximum solubility in water similar to that of pure oxygen (2-3mM)). It has a short biological half-life of 5-10 seconds and its lipophilic non-polar structure ensures it is able to freely diffuse through plasma membranes and lipoproteins. This means that its signalling action is not restricted to the cell of origin, but neighbouring cells can also feel its effect. Once NO is formed, it can be converted to nitrites (NO_2^-) and nitrates (NO_3^-) by oxygen and water. It can also react with superoxide (which is produced from multiple sources including; electron leak from the mitochondria, NADPH oxidase, xanthine oxidase (XO) and uncoupling of NO synthases (NOS)) to form peroxynitrite ($ONOO^-$) and hydrogen peroxide (H_2O_2).

One of the most unique chemical features of NO is that it possesses a free radical species due to its unpaired electron in the outer electrical orbit (Fig. 1.8). Since this is an unfavourable state, free-radicals are typically very reactive. Despite this, NO does not display the typical normal reactivity of most other free radicals. One example is that it does not have a tendency to dimerise meaning that at standard temperature and pressure it tends to remain in the monomeric form. This is attributed to the fact that overall bonding does not increase when two NO molecules interact. These diverse chemical and physical properties of NO highlight the many targets of action that this molecule may have in different cells and tissues.

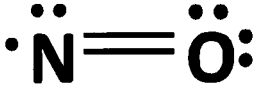

Fig. 1.8: Chemical structure of one molecule of nitric oxide

Nitric oxide is formed by the bonding of nitrogen and oxygen atoms as indicated by The Lewis dot structure. The lone pair of electrons on the nitrogen gives rise to the molecule exhibiting free radical properties. Bond length measurements have shown that the bond order of N-O is 2.5.

1.6.1 Discovery

The initial discovery of the role of NO in biology was in 1980 by Furchgott and Zawadski. They found that the relaxation of rabbit aortic rings was dependent on an unknown factor arising from the endothelium – endothelium derived relaxing factor (EDRF) (Furchgott and Zawadzki, 1980). More specifically their studies revealed that when blood vessels nurtured in an organ bath were chemically stimulated, the muscles relaxed. If the inner layer of cells of an artery or vein (endothelium) were absent, then the muscles of the blood vessel lost this ability to make the vessel expand. This result provoked curiosity and a wide range of scientific experiments were carried out to help determine the exact biological agent responsible for these effects.

In the late 80's, Salvador Moncada, Louis Ignarro and Ferid Murad independently made some ground-breaking findings regarding the exact identity of EDRF (for which Ignarro, Murad and Furchgott won the Nobel Prize in 1998). Firstly, they found that endothelial cells were able to produce NO (Palmer *et al.*, 1987; Ignarro *et al.*, 1987) and they subsequently showed that NO was produced directly from the amino acid L-arginine (Moncada *et al.*, 1989; Vallance *et al.*, 1989). These findings were determined by culturing vascular endothelial cells on microcarrier beads and perfusing them *in vitro* with either uniformly labelled arginine or guanidine labelled arginine. By connecting the effluent directly to a mass spectrometer they were able to measure the formation of 15N-labelled NO. When endothelial cells were stimulated with bradykinin, there was a release of 15N-labelled NO. Also, the amounts of NO generated from both types of arginine were similar leading to the conclusion that NO was specifically made from the guanidine nitrogen atoms of the amino acid (Palmer and Moncada, 1989).

Shortly after this it was discovered that molecular oxygen was an important part of NO synthesis. Experiments showed that molecular oxygen was introduced in the formation of N-hydroxy L-arginine, which is an intermediate in NO synthesis and in the formation of L-citrulline, which is the co-product of the generation of NO (Moncada, 1991).

1.6.2 Physiological and pathophysiological role

Studies investigating the role of NO have increased significantly since its discovery mainly due to its involvement in a range of regulatory mechanisms. It is known that a reduction in NO *in vivo* and *in vitro* can lead to changes in vascular function therefore NO production must be controlled.

In the cardiovascular system NO is crucial for the maintenance of; vascular tone, anti-thrombotic events, leukocyte adhesion, control of smooth muscle cell proliferation, endothelial cell motility, and endothelial cell survival and proliferation (Cooke, 2003; Murohara, 2002; Goligorsky *et al.*, 1999). NO is also found to be involved in the inhibition of anti-angiogenic factors (Cooke, 2003) and the promotion and expression of VEGF and pro-angiogenic factors (Olsson *et al.*, 2006; Murohara, 2002).

In physiological conditions, NO rapidly diffuses and interacts with the NO receptor soluble guanylate cyclase (sGC). Here it reversibly binds to the sGC heme group leading to activation of sGC and an increase in intracellular cyclic guanylate monophosphate (cGMP) concentrations (Ignarro *et al.*, 1986; Moncada and Higgs, 1993). cGMP is an important molecule as it activates Protein Kinase G (PKG) (Clementi, 1998), which lowers intracellular Ca^{2+} in smooth muscle leading to a decrease in vascular tone due to dephosphorylation of myosin light chains (Eardley, 1997). cGMP is rapidly hydrolysed by phosphodiesterases and their inhibitors are a useful tool which can increase NO signalling (Eardley, 1997).

At the same time, NO can go on to form the stable end products, NO_2^- and NO_3^- and it is often these which are used to measure total NO production via the Griess reaction (Schmidt and Walter, 1994). Under conditions of low oxygen tension, they can be reduced to the free radical NO• (a reactive oxygen species) and eventually form $ONOO^-$ if reacted with O_2^-. $ONOO^-$ is known for its role in cellular damage and cell death (Stamler *et al.*, 1992). In macrophages, O_2- production is critical for host defence as it contributes to the killing of invading microbes following their phagocytosis and also causes tissue damage in inflammation when released (Xia and Zweier, 1997).

In the immune system, NO production promotes cytotoxicity, which is important for the immune defence against invading pathogens, and acts as a signalling molecule for the wider immune response (Liew, 1995; MacMicking *et al.*, 1997). These antimicrobial and cytotoxic NO properties are due to the production of hydrogen peroxide, superoxide, cysteine, and glutathione in macrophages. Despite the biological relevance of NO in immunity, the overproduction of NO can lead to an overactive immune response, a sharp drop in blood pressure and in diseases such as sepsis, may even contribute to death.

1.6.3 Roles in macrophages

Macrophage NO production is dependent on their activation by stimuli such as bacterial endotoxin or pro-inflammatory cytokines. In quiescent conditions, macrophages maintain their role as 'patrolling cells' and produce low levels of NO, which are important in cellular communication and self-defence. During inflammation, they release excessive amounts of NO and its downstream products including $ONOO^-$ and O_2^-, which are important in the damage and killing of microorganisms (Hibbs *et al.*, 1988; Marletta *et al.*, 1988). Although macrophage NO appears to be critical for their phagocytic function, extremely high levels of NO in macrophages have been found to induce apoptosis and necrosis (Sarih *et al.*, 1993) and has also been implicated in various autoimmune reactions such inflammatory arthritis and asthma (Barnes and Liew, 1995; Schmidt and Walter, 1994). This suggests that macrophage produced NO must be modulated.

In macrophages, NO has also been associated with affecting another critical function – their motility, however, the specific pathways involved in this have yet to be discovered. The NO_2^- production, motility and F-actin expression of alveolar macrophages were increased following the addition of IFN-γ, suggesting a potential role for NO in macrophage motility which is in part mediated by F-actin (Fukushima *et al.*, 1994). Also, the addition of an NO donor to macrophages already expressing low NO_2^- levels and impaired motility increased NO production and restored their motility (Jain *et al.*, 1995).

In 2009, Zhou suggested a mechanism for this effect –that NO promotes macrophage migration via the hypoxia inducible factor-1α (HIF-1α) which is stimulated by the GTPases cdc42 and Rac1 (Zhou *et al.*, 2009).

1.6.4 Synthesis

The classical pathway involved in the synthesis of NO (and the by-product citrulline) is via the amino acid L-arginine and the enzyme nitric oxide synthase (NOS) (Fig. 1. 9) (Hibbs *et al.*, 1987a; Hibbs *et al.*, 1987b; Palmer *et al.*, 1987; Palmer *et al.*, 1988). In mammals there are three types of NOS isoforms: nNOS (neuronal NOS, NOS 1), iNOS (inducible NOS; NOS 2), eNOS (endothelial NOS, NOS 3) (Fig. 1.9). These are coded by different genes (Leiper *et al.*, 1999; Tran *et al.*, 2000), which were named in accordance to their general anatomical localisation; in neuronal cells, following appropriate induction in most cells and in the endothelium respectively. For optimal NOS activity a number of co-factors are required including NADPH, BH_4, the substrate L-arginine and, depending on the isoform, Ca^{2+}. Glutathione (GSH) can sustain enzyme activity and/or influence the reaction product. The constitutively expressed NOS isoforms, eNOS and nNOS, are Ca^{2+}-dependent enzymes whereas iNOS is Ca^{2+}-independent as it binds tightly to calmodulin in the absence of Ca^{2+} (Fig. 1.9).

It is now known that iNOS is expressed predominantly in immune cells such as macrophages, Kupffer cells and neutrophils, and in endothelial and smooth muscle cells. The activation of iNOS in these cells results in the overproduction of NO, which can also feedback negatively to inhibit NOS activity by s-nitrosation of the enzyme (Assreuy *et al.*, 1993; Yasinka *et al.*, 2004). There are two main mechanisms that result in iNOS activation. Firstly, IFN-γ can activate Janus kinase (JAK)-1 and JAK-2, which phosphorylate and activate signal transducers and activators of transcription (STAT)1. In turn, the activated STAT1 translocates into the nucleus and increases Interferon Regulatory Factor 1 (IRF-1) levels. This leads to induction of iNOS and a subsequent increase in NO (Chong *et al.*, 2002).

Secondly, the activation of NF-κB by LPS, IFN-γ and TNF-α results in the translocation of free NF-κB from the cytosol to the nucleus and induction of iNOS expression (Aktan, 2004; Marks-Konczalik *et al.*, 1998; Huang *et al.*, 1998). As well as affecting iNOS expression, NF-κB is also known to induce adhesion molecules such as VCAM-1 and cyclooxygenase-2 (COX-2), which is involved in the production of prostaglandins, prostacyclin and thromboxane and is also associated with inflammation and pain (Xia *et al.*, 2001).

It is important to bear in mind, however, that there are several other possible reaction routes that may result in NO production independently of the L-arginine: NO pathway *in vivo*, in particular during hypoxia. These include; acidotic degradation of tissue NO_2^- to NO (Zweier *et al.*, 1995; Duncan *et al.*, 1995), reaction between arginine and H_2O_2 to form NO (Nagase *et al.*, 1997) and the reduction of NO_2^- to NO catalysed by microbial NO_2^- reductase (Payne *et al.*, 1997). Zhang *et al.*, 1998 have found that both purified XO and XO-containing tissue can generate NO by reducing NO_2^- in the presence of NADPH. This NO_2^- reductase activity of XO may act as a supplement to the activity of NOS to redistribute blood flow to ischemic tissues when NOS activity is absent (Zhang *et al.*, 1998). Interestingly, XO is also found in macrophages, at elevated levels upon inflammatory stimuli suggesting that this may be another mechanism involved in the overproduction of NO during inflammation.

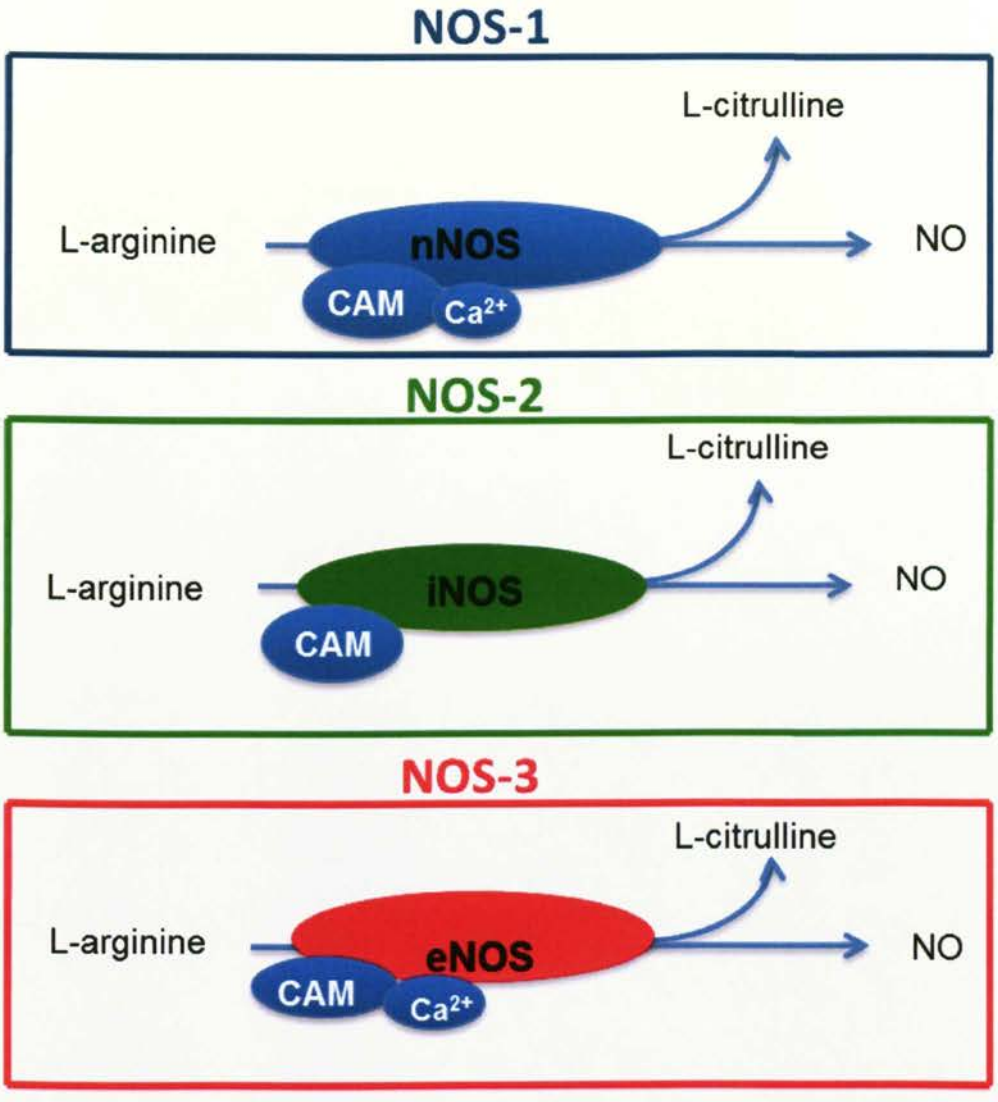

Fig. 1.9: The NO-signalling pathway.

NOS converts L-arginine to citrulline, dimethylarginine and nitric oxide. This reaction requires the cofactors BH_4, NADPH, and O_2. O_2^- and hydrogen peroxide (H_2O_2) are typically generated by NOS to some degree as well as $ONOO^-$, which is associated with cellular damage and death. NOS can be regulated by Ca^{2+}/ calmodulin and other associated proteins. eNOS and nNOS are both constitutive isoforms which are permanently active yet produce lower levels of NO compared to iNOS, which is Ca^{2+}-independent and induced by an inflammatory stimulus such as LPS and cytokines. NO elicits various effects including activation of sGC to produce cGMP thus affecting proteins kinases, phosphodiesterases and ion channels. Only eNOS leads to the production of superoxide.

1.6.5 Regulation

It is important that NO levels are regulated as unphysiologically high levels of NO have been found to result in DNA damage, apoptosis and mutation in many different cell types (Sarih *et al.*, 1993; Li and Wogan, 2005). NO regulation occurs by the methylarginines, asymmetric dimethylarginine (ADMA) and N^G-monomethyl-L-arginine (L-NMMA), which compete with the substrate L-arginine for binding to the active site of NOS enzymes (Vallance *et al.*, 1992) (Fig. 1.10). The inhibition of NOS causes a reduction in subsequent NO_2^- and NO_3^- production.

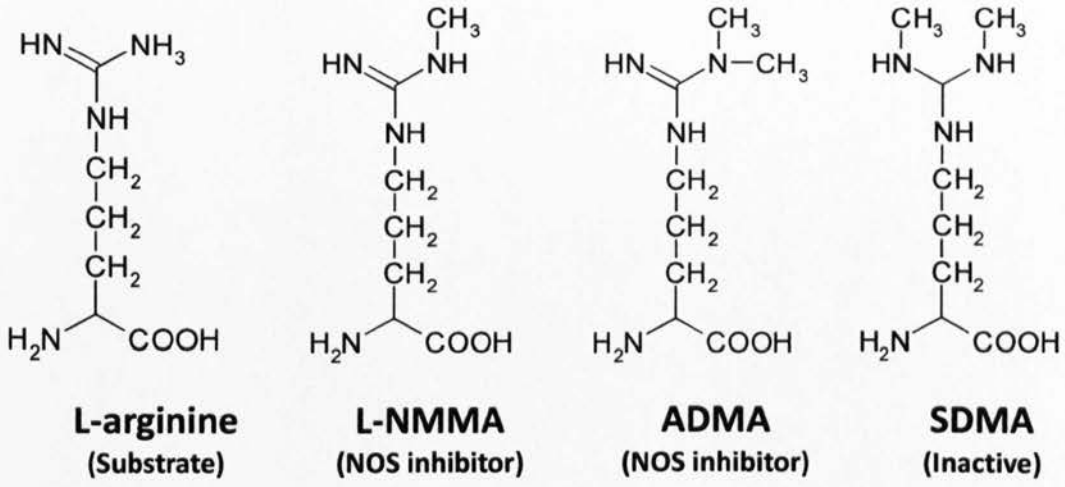

Fig. 1.10: Structures of L-arginine, ADMA, L-NMMA and SDMA.

The methylarginines ADMA and L-NMMA are both inhibitors of NOS whereas SDMA is not. ADMA, L-NMMA and SDMA are structurally very similar to L-arginine; however, lack the additional methyl group/s.

Methylated arginines are formed from the post-translational modification of arginine residues in proteins by Protein Methyl-Transferases (PRMTs) (Clarke, 1993;Paik and Kim, 1968). This ubiquitously expressed family of enzymes are involved in various important cellular processes including; signal transduction, RNA splicing, DNA repair and gene regulation (Paik *et al.*, 2007). More importantly, they initially catalyse monomethylation to produce L-NMMA (McBride and Silver, 2001), and subsequently add a second methyl

group to the arginine to produce ADMA or SDMA – they can never generate ADMA and SDMA together.

There are at least nine different PRMTs in mammals, however, although three of them share sequence homology with the PRMT family, they are not enzymatically active (Bedford and Richard, 2005; Bedford and Clarke, 2009). The six active PRMTs have been categorised into two groups based on their ability to produce ADMA (Type I enzymes; PRMT 1, 3, 4, 6 and 8) or SDMA (Type II enzymes; PRMT 5).

Methylated protein-arginine residues are present in the nucleus, cytoplasm and organelles therefore they have the ability to methylate a wide range of protein substrates. PRMT activity is regulated by gene expression, posttranslational modification and protein binding and by many other factors including cellular stress (Chen *et al.*, 2009; Osanai *et al.*, 2003; Sasser *et al.*, 2010). To date, there is no evidence to suggest that ADMA can be made from the methylation of free arginines (Leiper and Vallance, 2006; Vallance and Leiper, 2004) and the proteolysis of methylated arginines appears to be the only source of ADMA (Bedford and Richard, 2005). Although much research has gone into determining the effects of proteolysis on methylarginines, important fundamental questions relating to methylated arginines remain unanswered including whether protein turnover itself is the most important influence on ADMA concentration *in vivo* (Vallance and Leiper, 2004) or what the basic rate of ADMA creation is, either basally or in response to a specific stimulus.

1.7 Asymmetric dimethylarginine

L-NMMA and ADMA both inhibit the NOS isoforms with an EC_{50} of approximately 2-7μM depending on the prevailing substrate concentration (Vallance and Leiper, 2004). Similarly the K_m of the NOS isoforms for L-arginine is 2-19μM (Cardounel and Zweier, 2002; Cardounel *et al.*, 2005;Lowenstein *et al.*, 1992). L-arginine concentrations can affect the inhibition of NOS by ADMA /L-NMMA (in particular exogenous addition) as high concentrations of L-arginine will compete with methylarginines for transport into and out of the cell.

The majority of work on the inhibition of NOS by ADMA wasn't recognised until the early 1990's. In the cardiovascular system, exogenous L-NMMA addition was shown to inhibit NO production which resulted in the increase of vascular tone, systemic vascular resistance and blood pressure (Vallance *et al.*, 1989;Stamler, 1994). In the immune system, L-NMMA was used as an *in vitro* pharmacological tool to inhibit the release of NO derived from L-arginine in macrophages and to investigate the physiological roles of NO *in vivo* (Hibbs *et al.*, 1987a;Hibbs *et al.*, 1987b;Hibbs *et al.*, 1988).

In 1992, Vallance and colleagues found that ADMA, but not SDMA, had similar effects on NOS as L-NMMA. They showed that exogenously occurring ADMA can inhibit NOS *in vitro*, *in vivo*, in animal models, humans and macrophage extracts (Vallance *et al.*, 1992). This inhibition under normal physiological conditions, only involved however, a low percentage of NOS activity. For eNOS, the K_m of the enzyme for arginine is 3.14μmol/L whereas the Ki of ADMA on eNOS is 0.9μmol/L and for L-NMMA is 1.1μmol/L. This means that the percentage inhibition for eNOS activity is only 10% (Cardounel *et al.*, 2007). However, under pathophysiological conditions, plasma concentrations of ADMA can increase 3-9 fold meaning that cellular NO output can be inhibited by 30 - 70% (Vallance and Leiper, 2004; Schnabel *et al.*, 2005; Tanaka *et al.*, 2005).

The movement of methylated arginines into and out of the cell is aided by the cationic amino acid transport family (CAT) via an anti-porter mechanism

(Broer *et al.*, 2000). There are two main types of CAT transporters (CAT 1 and 2) and these are able to transport arginine, lysine ornithine and methylarginines into cells. L-arginine has a lower affinity for both CAT 1 and 2 transporters (Closs *et al.*, 1997; Bogle *et al.*, 2007) than ADMA (Cardounel *et al.*, 2007). L-NMMA, ADMA and SDMA all appear to be handled in a similar manner and compete with each other and arginine for transport. In endothelial cells the intracellular concentration of L-NMMA may exceed the extracellular concentration by about 5-fold suggesting that the transporter system concentrates methylarginines within cells rather than outside. The surrounding arginine concentrations are much higher than methylarginine concentrations meaning that it is difficult to fully understand the effect of competition between methylated and non-methylated arginines at these transporters. However, it is known that the transporter system is inducible and can be regulated by certain pro-inflammatory cytokines such as TNF-α and IL-1β (Malandro *et al.*, 1996). To reverse the inhibition of NOS activity by L-NMMA or ADMA, L-arginine can be added but this must be in excess as the stoichiometry in the biological systems is not 1:1 (Leiper and Vallance, 1999).

It is very clear that L-NMMA and ADMA both reduce NO levels by competitive inhibition of NOS and that L-NMMA, ADMA and SDMA all compete with arginine for uptake by CAT transporters. These methylarginines may then have the potential to disrupt transport of arginine and other cationic amino acids, however, little is known about this.

1.7.1 Clearance of methylarginines

Free methylarginines are cleared from the plasma by hepatic metabolism or renal excretion (Tran *et al.*, 2003). Hepatocytes are cells which make up most of the liver and have the ability to remove large amounts of amino acids such as ADMA and arginine (Nijveldt *et al.*, 2003) from the hepatic circulation. This may explain why elevated levels of ADMA, SDMA and arginine are seen in liver failure (Kimoto *et al.*, 1993; Nijveldt *et al.*, 2003; Mookerjee *et al.*, 2007).

The kidney has a more complex role in methylarginine clearance. Approximately 60% of SDMA and 20% of ADMA are metabolized by the kidney while the rest is removed by metabolic degradation or enzymatic metabolism (described later). ADMA can also be both generated and metabolised by the kidney as ADMA is taken up from the circulation via CAT transporters (Teerlink *et al.*, 2009).

In kidney failure, there is reduced NO production and elevated ADMA levels (Baylis, 2006). SDMA is also increased, which suggests increased expression of PRMTs (Matsaguma *et al.*, 2006), and is associated with elevated levels of creatinine, a marker for kidney dysfunction (Kielstein *et al.*, 2006). In early stage renal failure, ADMA concentrations are only slightly elevated; however, this is correlated with an increase in significant cardiovascular event rates. High concentrations of ADMA lead to a reduction in plasma flow and further progression of kidney damage which increases ADMA to pathophysiological levels (Fliser *et al.*, 2005; Vallance *et al.*, 1992) and promotes the progression of cardiovascular dysfunction (Baylis, 2006). Furthermore, induced chronic NOS inhibition in experimental conditions leads to chronic renal disease (Zatz and Baylis, 1998).

1.7.2 Asymmetric dimethylarginine and disease

Elevated plasma ADMA levels have been associated with various diseases including pulmonary hypertension, stroke, renal failure and diabetes (Table 1.2). High-performance liquid chromatography (HPLC) has shown that plasma ADMA and SDMA levels in normal (50-75 years old) individuals lie in the range of 0.43μmol/L – 0.56μmol/L and 0.38μmol/L – 0.73μmol/L respectively. The highest elevated levels of plasma methylarginines have been seen in patients with chronic renal disease with median ADMA and SDMA concentrations of 1.08μmol/L and 2.42μmol/L respectively. Vallance *et al* first showed an 8-fold increase in plasma ADMA in a cohort of patients with end-stage renal failure on dialysis compared with healthy controls (Vallance *et al.*, 1992).

Similar effects are seen in cardiovascular diseases, which show increased plasma ADMA to be positively correlated and predictive of cardiovascular events and/or mortality (Nijveldt *et al.*, 2003). Although there is overwhelming evidence that ADMA is involved in disease, understanding the biology of the endogenous methylarginines is required in order to describe the potential mechanistic pathways and to develop useful models to address any casual role in disease (Caplin *et al.*, 2013; Arrigoni *et al.*, 2010).

System	Examples were increased ADMA in disease is detrimental	References
Cardiovascular	**Atherosclerosis**	**Schulze *et al.*, 2006**
	Hypertension	**Pullamsetti *et al.*, 2005**
	Peripheral vascular disease	**Böger *et al.*, 1997**
	Stroke	**Yoo *et al.*, 2001**
	Pre-eclampsia	**Pettersson *et al.*, 1998**
Metabolic	**Diabetes mellitus**	**Eid *et al.*, 2003** **Altinova *et al.*, 2007**
	Obesity	**McLaughlin *et al.*, 2006**
Neuronal	**Alzheimer's disease**	**Selley *et al.*, 2003** **Arlt *et al.*, 2008**
Others	**Renal failure**	**Vallance *et al.*, 1992** **Aucella *et al.*, 2009**
	Septic shock	**O'Dwyer *et al.*, 2006**
	Liver disease	**Mookerjee *et al.*, 2007**
	Sickle cell disease	**Schnog *et al.*, 2005**
System	Examples where increased ADMA in disease can be beneficial	References
Cardiovascular	**Combats the increased iNOS in myocytes**	**Usui *et al.*, 1998**
Other	**Prevents sepsis related hypotension**	**Leiper *et al.*, 2007;** **Nandi *et al.*, 2012**

Table. 1.2: Negative and positive effects of increased ADMA in disease

High ADMA levels have shown to contribute in the pathogenesis of various cardiovascular, metabolic and neuronal diseases. In contrast, there are examples were increased ADMA in cardiovascular disease and sepsis have been shown to be beneficial.

1.8 Dimethylarginine dimethylaminohydrolase

The intracellular pool sizes of the methylarginines ADMA and L-NMMA, but not SDMA can be controlled through metabolism of alanine to produce methyl valeric acids. To date, the predominant hydrolysis of ADMA and L-NMMA to citrulline and dimethylamine occurs in most cells by dimethylarginine dimethylaminohydrolase (DDAH) (Hasegawa *et al.*, 2006; Murray-Rust *et al.*, 2001) and also in the kidney by Alanine-Glyoxylate Aminotransferase 2 (AGXT2) (Ogawa *et al.*, 1987).

In most cells, DDAH is responsible for the majority of methylarginine metabolism. DDAH (Mw= 37kDa) was first discovered by Ogawa and colleagues in 1989 who showed that unlike ADMA, DDAH is selectively expressed in tissues and cells and catalyses the breakdown of L-NMMA and ADMA to L-citrulline and mono- or di- methylamine (Ogawa *et al.*, 1989). The overall architecture of human DDAH is known to resemble that of the P. aeruginosa DDAH (Murray-Rust *et al.*, 2001), with the active site at the centre of a pentene fold formed by five ββαβ motifs arranged around a pseudo–five-fold axis. The human DDAH-1 residues Cys273, His172 and Asp126 form a catalytic triad that interacts with the reaction product citrulline.

In 1999, Vallance and Leiper determined that there were two different isoforms of DDAH (DDAH1 and DDAH2) (Leiper *et al.*, 1999) and that certain tissues which are found to express NOS also express DDAH. There is a large overlapping pattern for the two isoforms as confirmed from RNA and western blotting performed on human and mouse tissues (Leiper and Vallance, 1999;Tran *et al.*, 2000).

Interestingly, some tissues express higher levels of one of the isoforms than others. DDAH1 is found predominately in neural tissue (cerebellum and cerebrum) whereas DDAH2 is predominantly found in immune tissue (monocytes, macrophages, neutrophils as well as the thymus, spleen and lymph nodes). Other key organs include the heart, which expresses mainly DDAH2 and the kidney and liver, which have equal levels of DDAH1 and 2. Interestingly, functional homologues of DDAH were also found in several

microbial species which do not have any NOS expression suggesting a function of DDAH other than NOS regulation, however, this has yet to be addressed fully (Santa Maria *et al.*, 1999).

DDAH metabolises ~80% of ADMA (MacAllister *et al.*, 1996) yet the regulatory mechanism of this is not fully understood. Leiper and colleagues showed that *in vitro* NO donors reversibly inhibit recombinant DDAH and mammalian cytosolic DDAH extracts and that heterologous expressed human DDAH2 was s-nitrosylated in endothelial cells after cytokine-induced expression of iNOS. This suggests that in conditions of high NO production, DDAH activity is diminished by s-nitrosylation leading to a build-up of ADMA and inhibition of NOS (Leiper *et al.*, 2002).

There is yet no information regarding the specific cofactors required for the catalytic reaction of DDAH, however, there is evidence about its function. DDAH catalyses the breakdown of one molecule of ADMA to one molecule of L-citrulline and one molecule of dimethylamine. For purified DDAH, the optimum temperature is 55°C (Ogawa *et al.*, 1989) and maximum pH activity is between pH 5.2-6.5 (Ogawa *et al.*, 1987; Ogawa *et al.*, 1989). At 37°C and between pH 5.0-8.5, the enzyme is stable for at least 1 hour. The K_m of DDAH1 for L-NMMA is 360μM whereas for DDAH2 it is 510μM (Ogawa *et al.*, 1989). These concentrations are much higher than intracellular methylarginine concentrations and the reason for this is not yet understood. A study by Cox and colleagues showed that 72 hours following the intravenous injection of small interfering RNA (siRNA) target to DDAH1, there was a 30-40% reduction in DDAH1 expression in the liver, kidneys and blood vessels of rats. This was complemented by an increase in 20-30% of ADMA concentrations (Cox *et al.*, 1990). Such results show that intracellular concentrations of ADMA are very sensitive to changes in DDAH activity or expression. In endothelial cells pharmacological inhibition of DDAH activity leads to ADMA accumulation demonstrating that the enzyme is central to determining local levels of methylarginines in cells and tissues (MacAllister *et al.*, 1996).

DDAH2 has also been implicated in having a significant effect on the function of immune cells. This is due to the proximity of the location of the DDAH2

gene to the major histocompatibility complex III (MHCIII) region (involved in inflammation) – both are in the region of chromosome 6 (Ribas *et al.*, 1999). This specific area of interest is highly gene dense and is associated with a wide range of diseases including; rheumatoid arthritis, and insulin-dependent diabetes. The presence of DDAH2 in the genomic region of MHC III and the expression of DDAH2 in immune cells, suggests a potential role for DDAH2 in immune-related diseases and infection.

Furthermore the location of the DDAH2 gene close to genes that affect the immune and inflammatory responses make DDAH2 a candidate for sepsis (Tran *et al.*, 2003). O'Dwyer *et al* showed that in 47 ICU patients with severe sepsis, plasma ADMA and IL-6 levels were elevated compared to control (O'Dwyer *et al.*, 2006). They also suggested that ADMA levels may be regulated via a genetic component and that a polymorphism at position -449 in the DDAH2 gene may be functional and could be used as a marker for the susceptibility to, and the severity of, an inflammatory response following an infective insult (O'Dwyer *et al.*, 2006).

Although DDAH is the only isoform expressed in immune cells, it is important to recognise the role of AGXT in methylarginine metabolism. AGXT2 catalyses the conversion of glyoxylate to glycine using alanine as the amino donor (Takada *et al.*, 1982). AGXT2 can also utilise ADMA as an amino donor leading to the formation of α-keto- δ-(N,N-dimethylguanidino) valeric acid (DMGV) (Ogawa *et al.*, 1990). AGXT2 metabolises 16% of ADMA and SDMA levels *in vivo* (Ogawa *et al.*, 1987; Rodionov *et al.*, 2010) and may be involved in mediating blood pressure (Caplin *et al.*, 2012; Kittel *et al.*, 2013).

Overall the data suggests that macrophage function is important to the development and onset of various immune diseases, and that macrophage function may be modulated by NO. What is already known is that macrophages produce high levels of NO upon stimulation and that they only express DDAH2 but as yet no work has demonstrated the effect of DDAH2 on macrophage methylarginine metabolism. There is also no evidence about the effect of DDAH2 on general macrophage function and how it may contribute to the diseases mentioned above (Fig. 1.11).

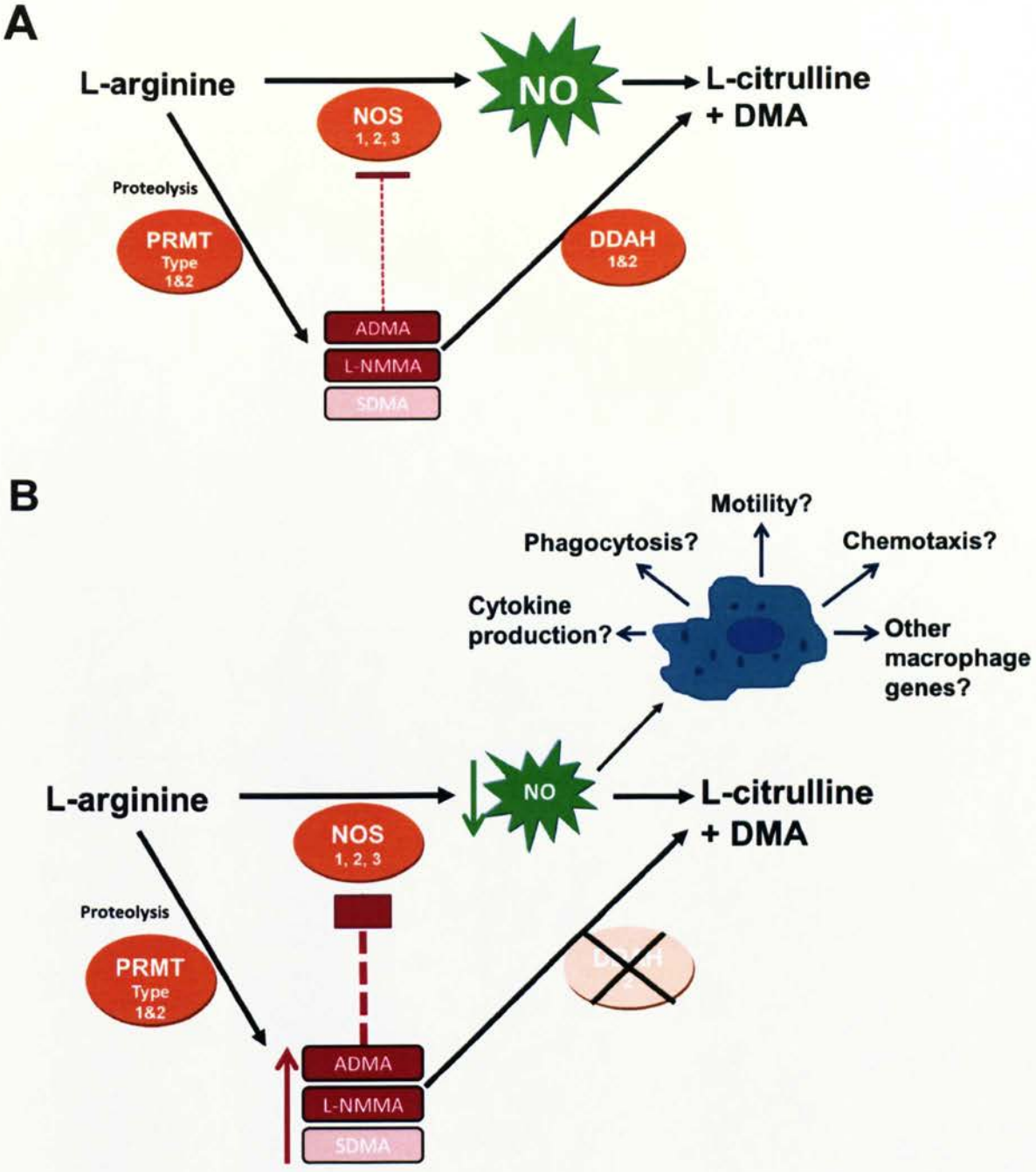

Fig. 1.11: The ADMA/DDAH/NOS pathway.

(A) ADMA and L-NMMA, but not SDMA, are competitive inhibitors of all NOS isoforms and are metabolised by the enzyme DDAH1 or 2. NO production can be controlled by modulating the synthesis of NOS inhibitors via PRMTS or their metabolism by DDAH. (B) Disruption of DDAH2 (the only DDAH isoform present in macrophages) is thought to increase intracellular methylarginines and inhibit NO production; however, the effect of this on various macrophage functions is yet to be confirmed.

1.9 Overall hypothesis and specific aims

We hypothesise that DDAH2, not DDAH1, regulates NO production in macrophages through the control of ADMA and L-NMMA. Thus, generating a genetic knockout of DDAH2 will lead to increased ADMA concentrations and decreased NO bioavailability *in vivo*. Any changes in macrophage function will therefore be related to NO and/or intracellular changes in NOS inhibitors.

Chapter 3: To determine the effects of NOS inhibitors on the monocytic human cell line U937 and how this affects monocyte/macrophage function.

Chapter 4: To investigate the effect of global DDAH2 deletion on primary murine macrophages and how an increase in intracellular NOS inhibitors affect macrophage function.

Chapter 5: To create a novel DDAH2 macrophage-specific knock-out mouse and investigate whether results are similar to those in global DDAH2 knock-out animals.

Chapter 6: To elucidate the effect of specific macrophage DDAH2 deletion on different genes using RNA-sequencing.

CHAPTER 2

General Methods

2.1 Animal subjects

All animal experiments were carried out under a Home Office License and were conducted according to the Animals Scientific Procedures Act of 1986. Mice were maintained on a 12 hour day/night light cycle and had continuous access to food and water. Prior to experiments the animals were matched according to their sex and age unless otherwise stated.

To anaesthetise the animals, 5% isoflourine was used until the animals were unconscious. They were then maintained under 2% anaesthetic and plasma was obtained from cardiac puncture. All animals were then sacrificed by cervical dislocation unless otherwise indicated and peritoneal cells were obtained and used immediately. Tissue was collected under aseptic conditions and placed directly into liquid nitrogen.

For the characterisation of macrophages in Chapter 4, 5, and 6 both male and female littermates were used and were not matched for age. Tissues and cell lysates were collected from these animals and were either stored at -80°C immediately or plated accordingly.

2.2 Generation and genotyping of DDAH2 transgenic mice

DDAH2 transgenic mice were purchased from the Texas Institute for Genetic Medicine (TIGM, Houston, Texas, USA). The DDAH2 gene was knocked out by the insertion of a long terminal repeat into the first exon of the gene using a retroviral vector (for more information see http://www.tigm.org/technologies.html, and Zambrowicz *et al.*, 2003; Zambrowicz *et al.*, 1998). The $DDAH2^{flox/flox}$ LysM-Cre specific deletion involved the addition of the specific Cre between the two *Lox*P sites which then allows deletion of the *Lox*P flanked sequence. The targeted deletion is exon 2-5 and results in specific DDAH2 deletion in macrophages only. DNA

samples were collected at two time points to confirm genotype: at weaning and at the time of death. DNA was isolated using the DNeasy Tissue Column (Qiagen). Endpoint PCR was used to amplify the gene for DDAH2 and $DDAH2^{flox/flox}$ LysM-Cre. All primer sequences for DDAH2 were provided by TIGM whereas LysM-Cre primers were designed by our lab. Primer sequences are described in equivalent chapters. The breeding, genotyping and maintenance of all mice and their colonies were carried out by our group animal technician Matthew Delahaye.

2.3 Cell lines and culture

The human myeloblastic leukaemia cell line U937 (a kind gift from Dr James Leiper, Imperial College, UK) was grown in Roswell Park Memorial Institute medium-1640 (RPMI 1640) (Gibco Life Technologies, UK) supplemented with 10% heat-activated fetal calf serum gold (FCS), 100U/ml penicillin (PAA Laboratories, UK), 100 µg/ml streptomycin (PAA Laboratories, UK), and 2mM L-glutamine (PAA Laboratories, UK). Supplemented media was stored at 4°C for up to two weeks, after which time the L-glutamine was replenished. Cells were cultured under a humidified atmosphere of 5% CO_2 at 37°C, and cell density was maintained between $1x10^5$ and $2x10^6$ viable cells/mL. Cell viability was assessed by trypan blue exclusion dye with viability being greater than 95% before use.

U937 cells are suspension cultures but were differentiated to macrophages (Garcia, 1999) by the addition of 20ng/mL phorbol-12-myristate-13-acetate (PMA) (Calbiochem, UK). PMA is a protein kinase C (PKC) activator that changes the lipid phase of the membrane, increases membrane fluidity and changes surface morphology and adhesion. Monocytes differentiated into macrophages after 72 hours incubation. This was verified by increased attachment of cells to the flask, and changes in cell morphology including; enlargement in size, a smaller nucleus, a larger cytoplasm filled with vacuoles and increased membrane ruffles.

2.4 Isolation and culture of murine primary peritoneal macrophages

Peritoneal macrophages were isolated and cultured based upon the protocol described in Methods in Enzymology (Packer, 1996). The peritoneal cavity was filled with 5mL cold PBS (Invitrogen, UK) and gently agitated for 10-15 seconds to rinse the cavity. 5 mL of PBS was recovered and kept on ice. The peritoneal washout was then spun for 10 minutes at 1000xg, at 4°C to sediment the cells. Cells were suspended in DMEM (Dulbecco's Modified Eagles Medium) cell culture media, 10% fetal bovine serum (FBS), penicillin and streptomycin and L-glutamine without phenol red (Invitrogen, UK). The total cell number was counted using a haemocytometer (approximately 2 x 10^6 cells were retrieved from each animal). Generally, cells were plated at 5 x10^5 per well into 24-well plates or the equivalent density if other tissue culture plates were used. Cells were incubated for 2-3 hours at 37°C and 5% CO_2 to allow macrophages to adhere to the wells. Once the cells had adhered, media was removed and cells were gently washed with PBS to remove any non-adherent macrophages. The desired media was then added to the culture and cells were allowed to grow overnight to stabilise. The phenotype of the cells was confirmed by flow cytometry.

For motility and other macrophage culture time course experiments, cells were stimulated with or without media containing a pro-inflammatory cocktail of 10ug/mL Tumor Necrosis Factor-α (TNF-α) (R&D Systems, UK), 100units/mL Interferon-γ (IFN-γ) (R&D Systems, UK), and 5ug/mL Lipopolysaccharide (LPS) (*Salmonella typhosa*) (Sigma Aldrich, UK). Reagents used to test nitrite production included; ADMA (Calbiochem, UK), SDMA (Calbiochem, UK), and L-NMMA (Calbiochem, UK). Media was collected for nitrite quantification and LC-MS/MS analysis while cell lysates were collected for western blotting or LC-MS/MS analysis.

2.5 Flow cytometry analysis

To determine whether the cells grown from the peritoneal washout were indeed macrophages, flow cytometry was carried out. Primary macrophages were isolated and plated in 6 well plates at a density of 5 x 10^5/ well. Cells were allowed to adhere and then washed 3 times with PBS followed by supplement of fresh media for 24 hours. Cells were washed again with PBS (3 times) and trypsin (an endopeptidase that cleaves lysine and arginine) was added to detach the cells. It was noticed that macrophages, in particular those which had genetically been modified to not include the DDAH2 gene, were extremely adherent, therefore trypsin and gentle cell scraping was required to remove the cells. The acquired cells were spun at 1000 x g for 5 minutes, the supernatant was discarded, and lysis buffer added to cell pellet and incubated for 5 minutes at RT. Cells were spun again and suspended in 1mL of FACS buffer (PBS, 5% FBS and sodium azide (0.01%)).

Cells were counted and sample aliquots of 2-5 x 10^6 cells were prepared for antibody staining. Samples were spun at 16,000xg for 5mins and resuspended in 100µl flow buffer. A fluorescence antibody was added at an optimised concentration and incubated on a shaking plate in the dark for 30 minutes at 4°C. Cells were washed once in FACS buffer (remembering to change tips between each sample), and resuspended in 500µl FACS buffer. Samples were read by flow cytometry. The antibody used was the murine macrophage specific marker F4-80 (BD Biosciences) at 1:2000 dilution.

2.6 RNA extraction

For quantitative real time PCR analysis RNA was extracted from cells using the RNeasy plus universal mini kit (Qiagen, Venlo, Netherlands) following the manufacturers protocol. Adherent macrophages were scraped from culture and the samples were homogenised mechanically with 5mM stainless steel

beads using a Tissuelyser II (Qiagen) set at 25Hz for 5 minutes. Qiagengenomic DNA (gDNA; the natural genetic material) eliminator was added post homogenisation to remove any gDNA contamination.

RNA was extracted with the addition of chloroform to the trizol, separation of phases was allowed to start before centrifugation at 12,000xg for 15 minutes at 4°C. The clear upper aqueous phase containing the RNA was removed and added to an equal volume of 70% ethanol. The RNA was cleaned up using the filter columns and buffers provided in the kit before being eluted from the filter membrane with RNAse free water. Concentrations of RNA were determined by absorbance by a Nanodrop Spectrophotometer (Thermo Scientific, MA, USA) and the quality determined by the ratio of absorbance between 260nM-280nM. RNA was then taken forward for cDNA (product of reverse transcription) generation and RT-qPCR analysis.

2.7 Reverse-Transcription quantitative PCR

To quantify mRNA expression in extracted samples two-step real time PCR was used. Before mRNA expression can be quantified it must first be converted to cDNA. This was completed using the iScript cDNA synthesis kit (Bio-Rad, CA, USA) following the manufacturer's instructions and the cycling conditions shown below (Table 2.1).

Reverse transcription	30 min at 42°C
RTase inactivation	5 min at 85°C

Table 2.1: PCR-cycling conditions

The PCR cycling conditions for 1 cycle were based upon the above manufacturers conditions (Bio-Rad, CA, USA).

Qualitative real-time PCR in contrast to end-point PCR above is able to detect subtle differences in mRNA expression as it visualises the quantity of product at the end of each PCR cycle before conditions become saturated. This is achieved by the binding of a fluorophore (Sybr green) to double stranded DNA and the amount of emission quantified. A Sybr green ready mix (iTAQ fast Sybr green supermix, Bio-Rad) containing fluorophore, polymerase, dNTP's and ROX (a fluorescent dye used to normalise any pipetting errors) was used following the manufacturers protocol. cDNA (10ng)was added to the ready mix and primers (10μM) (for a full list of primers see Appendix and equivalent Chapters). Plates were run on Applied Biosytems (CA, USA) 7900HT fast machine using the following cycling protocol.

Initial step	95°C 10minutes
Thermal cycling x 40	
Denaturation	95°C 15 seconds
Annealing	60°C 15 seconds

Fig. 2.2: Thermal cycling protocol for RT-qPCR

The main steps of the thermal profile for the PCR program include 95°C for 10 minutes, 40 repeats of RNA amplification at 95°C (15 seconds), 60°C and an annealing at 60°C (15 seconds).

2.8 Cell and tissue homogenate preparations

Cell and tissue homogenates intended for protein blotting were prepared in RIPA (radio-immunoprecipitation) buffer (Roche, France) supplemented with a protease inhibitor (PI) cocktail (Roche). Cultured cells were collected using cell scraping and tissues were harvested from animals and frozen in liquid nitrogen. Sections of frozen tissue were cut and weighed, and PBS

(phosphate buffered saline) supplemented with a PI cocktail (as proteases interfere with the protein), was added. Magnetic ball-beads were added to the samples (to help break down and extract the protein since there are strong and have a high degree of structure) and centrifuged for 15 minutes at 14,000xg. Samples obtained were used for western blotting.

2.9 Western blotting and antibodies

Western blotting, first developed by Towbin *et al.* (1979) is used to determine relative amounts of a specific protein in cells or tissues. The process involves the separation of proteins by gel electrophoresis before transferring them to a membrane and probing with a specific primary antibody. The addition of a secondary antibody enables the signal to be amplified and detected by either chemiluminescence or infrared.

Following protein quantification using a Nano-Drop machine, the protein lysates were suspended in 4x Laemlli Sample Buffer (Bio-Rad, UK), which contains glycerol to help the protein sink to the bottom of the gel and a blue dye to see how far the protein has travelled. The samples were heated at high temperature to help denature the protein by breaking cysteine bonds in protein tertiary structures. Protein samples and a pre-stained protein ladder marker (Precision Blue All-Blue Ladder, Bio-Rad, UK) were then electrophoresed in a 7-15% acrylamide resolving gel, depending on the proteins of interest, for up to 90minutes between 90-150V.

The following recipe was used for the preparation of the standard percentage resolving gel (12%) that was used for the detection of low molecular weight proteins: 3mL acrylamide/Bis (40%; 37.5:1); 4.35mL dH_2O; 2.5mL Tris-HCl (1.5M; pH8.8); 100µL SDS (10%); 5µL TEMED; 50µL APS (10%) (all from Bio-Rad). The resolving gel has a basic pH of 8.8 and a high acrylamide concentration which makes the gels narrow pores and separates the protein more by size. A 4% standard stacking gel (10mL) was made as follows; 1mL

acrylamide/Bis (37.5:1); 6.32mL dH_2O; 2.52mL Tris-HCl (0.5M; pH6.8); 100µL SDS (10%); 10µL TEMED; 50µL APS (10%) (all Bio-Rad, UK). The stacking gel has an acidic pH of 6.8 and less acrylamide which makes the gels more porous and allows only poor separation of protein but forms thin bands.

Wet transfer was performed onto a Hybond-P Immunoblot-PVDF membrane (Millipore, UK). The blot was then blocked in buffer containing PBS plus 0.1% Tween-20 (v: v) (PBS and Tween = PBS-T) and 5% milk powder or BSA (w: v), for 1 hour on a rocking platform. The primary antibody was incubated at the necessary concentration overnight at 4°C on a rocking platform. The secondary antibody (Infra-red conjugate for Licor detection) was incubated at room temperature on a rocking platform for 1 hour. Blots were washed in excess PBS-T 3x 5 minutes after primary and secondary antibody incubation. For antibodies and dilutions see Appendix.

2.10 Nitric oxide assay

NO_2^-, a stable end product of NO and a product of nitrate reduction, was measured using the Griess method. Cells ($5x10^5$) were plated in a 24 well plate and incubated with the appropriate drugs for various time points (6, 24 and 48 hours). The supernatant (100µL) was removed and 50µL of this was incubated with an equal volume (50µL) of Griess Reagent A (1% w/v sulphanilamide in 5% phosphoric acid) and B (0.1% N-(*1-naphthyl*) ethylenediamine dihydrochloride, NED) (Promega, UK) at room temperature in 96 well plates. The mixture was incubated for 10 minutes at room temperature to allow the colour to develop and the absorbance was measured at 550nm in a microplate reader (V Max, Molecular Devices). The concentration of samples was determined using a sodium nitrite (Sigma Aldrich, UK) standard curve (1 - 100µM) made up in culture media (see Appendix), only correlation coefficients (R^2) which were at least >0.98 were used for analysis. For peritoneal macrophage NO production, NO_2^- alone was measured using a 50µL sample plated in triplicate. The limitation for this technique is that it only

allows measurement of NO_2^- and not NO_3^- in the samples, it has a limit of detection of 2.5μM and is not very sensitive for plasma and serum.

2.11 Cell proliferation assay

2.11.1 MTT assay

This assay was first described by Mosmann in 1983 and has been used for numerous studies on: chemosensitivity, cytotoxicity testing (Mosmann, 1983) (Romijn *et al.*, 1988), cytokine production (Naha *et al.*, 2010), cell stimulation in immunology (Niks *et al.*, 1990), and radio sensitivity (Price *et al.*, 1990). The assay is based on the conversion of the yellow tetrazolium salt, 3-(4,5-dimethylthiazol-2-yl)-2,5-diphenyltetrasolium bromide (MTT) to the coloured formazan product by NADPH mitochondrial enzymes in viable cells. Only active mitochondrial enzymes are able to cleave the tetrazolium ring, reducing the MTT dye yielding purple formazan crystals. The number of viable cells is proportional to the concentration of MTT formazan formed which can be monitored by measuring the absorbance.

In the initial procedure by Mossman 1983, MTT was dissolved in PBS (5mg/mL), filtered carefully to remove insoluble residues, and added directly to the assay plates. However, experiments in subsequent years have since shown that dissolving the formazan crystals in DMSO gives rise to a better absorbance (Sladowski *et al.*, 1993) therefore this was carried out in our experiments.

The number of viable cells was determined by the addition of 20μL of the tetrazolium salt MTT; 3-(4,5-Dimethylthiazol-2-Yl)-2,5-Diphenyltetrazolium Bromide (Sigma Aldrich, UK), to 1 x 10^5 cells plated in triplicate in a 96 well plate. MTT dye (yellow in colour) is converted into purple formazan crystals by mitochondrial dehydrogenase enzymes in the presence of an electron coupling reagent. Cells were incubated for 3 hours at 37°C in the dark, after which it was removed and 100μL dimethylsulphoxide (DMSO) was added in

order to reveal the formazan crystals. The amount of formazan produced was measured spectrophotometrically at 540nm (BioTek ELx808). The more viable cells present, the higher the amount of formazan that is produced. Values obtained were subtracted from a background reference value of media only.

2.11.2 BrDU assay

The principle of this assay is the detection of the pyrimidine analogue 5-bromo-2'deoxyuridine (BrdU) which is incorporated in place of the thymidine into newly synthesised DNA of proliferating cells. Incorporated BrDU is detected using a fluorescent anti-BrdU antibody and the signal measured using a spectrophotometer.

The BrdU Proliferation Assay kit was obtained from Calbiochem, UK. Briefly, 100µL of cells were seeded at 100,000 cells/ well in triplicate in a 96 well plate and primary macrophages allowed to adhere overnight. Cells were then either left untreated or treated with an inflammatory cocktail. A working stock of BrdU was prepared by diluting the BrdU Label 1:2000 into fresh tissue culture media. The BrdU label was added after 4 hours incubation with or without an inflammatory cocktail to each well (20µL) for a total of 20 hours in a tissue culture incubator. The contents were then removed again by inverting over the sink and tapping on paper towels and 200µL of Fixing/Denaturing solution added to each well for 30 minutes. The contents were then removed again using the previous method and an anti-BrdU antibody (1x) added to each well (100µL) for 1 hour at RT. Cells were washed three times with 1X Wash Buffer and blotted on paper towels during each wash. Peroxidase Goat Anti-Mouse IgG HRP conjugate (Calbiochem, UK) was added to each well (100µL) for 30 minutes at RT. After incubation, cells were washed again three times using the 1X wash buffer and flooded with distilled water. The well contents were removed as previously described on a paper towel. Flouorogenic Substrate Working Stock solution (100µL) was added for 30 minutes at RT followed by Stop Solution (100µL). Fluorescence was measured within 30 minutes of

adding the Stop Solution at excitation ~325nm and emission ~420nm. Wells in triplicate with media only were used as a control.

2.12 Motility assay

Macrophage motility was observed over a total period of 12 or 16 hours using real-time live microscopy unless otherwise indicated. Generally, cells were plated in 6 well plates (1 x 10^6) (Corning, UK) and, if using the human monocytic cell line U937, were differentiated into macrophages using 50nM PMA (Calbiochem, UK) for a period of 3 days after which the media was substituted with normal media for one day.

U937 differentiated macrophages were treated with the appropriate compounds 4 hours prior to recording. In previous work by Wojciak-Stothard, 2007, NO inhibitors were added 4 hours prior to the videos being captured on the microscope. In those particular experiments a time interval of 1 hour/ frame was used, as endothelial cell motility is relatively slow. Human macrophages however move at a faster rate than endothelial cells therefore the time interval/ frame was reduced to 10 minutes.

For each experimental condition 3 - 5 random fields of vision were selected and saved (total of 30 fields of vision in a 6 well plate) (Leica SP5II confocal microscope). The z-plane was altered in every experiment to try and obtain the best quality image by focusing in on the cells. Images were obtained in sequence and could be viewed as a movie or as individual frames (total 72 frames in 12 hours).

2.12.1 Maintaining the temperature and CO_2 levels

The 6 well plates containing macrophages which had been treated with various compounds were viewed using a Leica SP5 II confocal microscope.

To ensure that the cells were not affected in anyway by changes in temperature or pressure, a chamber was used to maintain the temperature at 37°C and CO_2 levels at 5%. After the experiment was completed the pH of the media was checked using pH litmus paper to make certain that the temperature and CO_2 conditions had not changed throughout the experiment. If any changes in pH were observed the experiment was not used in this analysis.

2.12.2 Microscope settings

Before beginning the recordings appropriate settings needed to be applied to the microscope. The settings were made in the first experiment and were applied to all future experiments in order to make sure that this did not affect the images produced in any way. The scan mode settings selected were based on an X, Y, T scale where X and Y are co-ordinates and T is the duration/ time of the experiment. This setting is used because the cells are being tracked over a period of time unlike the standard 'XY' settings used when taking an individual image using a confocal microscope. The plates used were made from plastic and a x10 lens was used to obtain images. Bright-field settings were selected as the cells had not been stained with any fluorochromes.

2.12.3 Manual Tracking Program

After 12 hours of tracking, the images obtained were opened in an Image J program (developed by National Institutes of Health) and a manual plugin was used to track the cells. The parameters were altered to correspond with the settings on the microscope. The time interval was set to 10 min/ frame and the x/y calibration was calculated to determine the pixel measurement. Depending on the magnification of the lens and the type of instrument used, the pixel measurement will change, therefore it is important to alter this individually in

all experiments. Five cells were randomly selected per each field of vision (25 cells per well/ 75 cells per experiment) and their motility individually tracked.

The distance and velocity obtained were exported to a Microsoft Excel file. X and Y results refer to the direction of movement and the distance and velocity of motility is based on the movement of each cell at a specific time point.

Motility was presented as both the total distance travelled and the average motility per cell per minute, where n is equal to the total number of frames (in this case 72):

$$\textbf{\textit{Average motility/ min}}\ (x) = \frac{\textit{Total cell motility per min}}{n}$$

The total distance travelled by a cell to an end point was determined by the following equation:

Total distance travelled (y) = Sum of distances obtained at each time interval

2.13 Chemotaxis migration

The migration of cells through a barrier is an alternative way to measure chemotaxis. Monocytes ($5x10^4$ cells) were placed on the top of a 3.0μM polycarbonate transwell (Corning, Fisher, UK) and were allowed to freely migrate into the lower chamber for 4 hours (time was selected based on the results of a previous experiment whereby monocytes were allowed to migrate freely for 1, 2, 4 and 24 hours, see Chapter 3). Images at x 200 magnification of three random fields were taken using a phase-contrast microscope.

For transendothelial migration, human umbilical vein endothelial cells (HUVECs) ($8x10^4$ cells) were cultured on gelatine treated polycarbonate transwells for 2-3 days. Independently, monocytes ($5x10^4$ cells) were treated

with the pro-inflammatory cocktail for 4 hours or left untreated in media alone. Untreated and treated monocytes were added to the upper compartment of individual transwells and were allowed to migrate through the endothelium monolayer for 4 hours. Again, images at x200 magnification were taken using a phase contract microscope.

2.14 Phagocytosis assay

Cells (1×10^5) were plated in triplicate in 96 well plates (Nunc, UK) and treated for either 4 or 24 hours. Cell media was removed and fluorescein-labelled *Escherichia coli* (K-12 strain) Bio-Particles® dissolved in Hanks balanced salt solution (HBSS) (both Invitrogen, UK) were added (100µL) for 2 hours. Following incubation, all contents in the wells were removed and trypan blue (100µL) added immediately in order to quench the extracellular probe. The fluorescence emitted at 480nm excitation – 520nm emission was measured using a fluorescent microplate reader. Values obtained were subtracted from a background reference value of media only.

2.15 LC-MS/MS measurements

The identification and concentration of methylarginines in cell media, cell and tissue extract and plasma were carried out using Liquid chromatography-Mass Spectrometry (LC-MS/MS). The principle of LC-MS/MS is easily described in four stages; (1) Ionisation – molecules in the sample are vaporised (by heating) and converted to ions by bombarding them with an electron beam (2) Acceleration – positive ions from the ionisation stage are accelerated towards a negative plate (speed of acceleration depends on the mass) (3) Deflection – ions are deflected by a magnetic field (extent of deflection depends on the

mass) (4) Detection – ions of increasing mass reach the detectors and a spectrum is provided on the computer.

Before the samples can be analysed by LC-MS/MS they must be extracted appropriately. Cell lysates were collected from cells plated for measuring nitrite production. Cells plated in 24 well plates at $5x10^5$ cells/well were collected by adding lysis buffer (MPER - Mammalian Protein Extraction Reagent buffer) (Invitrogen, UK) and protease inhibitor (Invitrogen, UK)) and gentle cell scraping. Lysates were spun at 16,000xg at 4°C for 10 minutes. The supernatant was collected (50µL) and an internal standard solution containing 7-deuterated ADMA (D7-ADMA; 100µM) was added to allow calculation of extraction efficiency. The methylarginines were then extracted with 5x volume of methanol: supernatant (to remove any proteins). Samples were centrifuged at 16,000xg for 10 minutes and the supernatant collected. The supernatants were then spun on a speed-vacuum or heated on a heat-block to remove the excess methanol. A mobile phase containing 0.1% formic acid (50µL) was added to the residue and the contents transferred to a 96 well plate.

High pressure liquid chromatography (HPLC) allows the separation of components of samples based upon their binding affinity to a silica based column. The HPLC system (Agilent) injected 10µL of sample on to a Hypercarb chromatography column (Thermo Scientific). This is a porous, graphite column that separates highly polar molecules with similar structure, is pH stable and is not prone to chemical attack. Samples were eluted off the column using a mobile phase of 0.1% formic acid, 1% acetonitrile with a gradient increasing to 50% acetonitrile between 5 and 10 minutes of a 15 minute run per a sample. A mobile phase consisting of 1% formic acid, 50% acetonitrile was used to wash the column clean preparing it for the next sample with no carryover of contamination.

The eluted samples were passed into the Agilent 6400 series triple quadruple LC-MS/MS were they are vaporised and ionized. The MS parameters for detection were as follows: ADMA, mass-to-charge ratio *(m/z)*: 203.3 to 46.0,

collision energy (CE; energy required to fragment the molecular ions): 12; SDMA, *m/z*: 203.3 to 70.2, CE: 24; monomethylarginine, *m/z:* 189.3 to 70.2, CE: 24; L-arginine, *m/z*: 175.2 to 60.1, CE: 8; d7-ADMA, *m/z*: 210.0 to 46.0, CE: 24.

The data was acquired and analysed using Agilent's Masshunter Qualitative analysis programme. Chromatograms (see Appendix) were acquired and the data extracted using the multiple reactions monitoring (MRM) method. The amount of each methylarginine in the sample was determined by the total ion count within the relevant peak and the actual concentrations were determined by running a standard curve within the sample run (see Appendix).

2.16 RNA sequencing

The Illumina TruSeq RNA-Seq library preparation kit was used to determine entire changes in the RNA sequence and this work was carried out with the kind assistance of the post-doc in our lab, Dr Lucy Colman. Peritoneal macrophages from DDAH2$^{flox/flox}$ and DDAH2$^{flox/flox}$ LysM-Cre isolated from male mice were left untreated or treated with LPS (5μg/mL) for 6 hours. RNA was collected using the RNA*later* buffer and purified using the RNA extraction kit and spin columns (Qiagen, UK). The Illumina TruSeq^{TM} RNA sample preparation kit (Low-Throughput protocol- less than 48 samples) was used according to manufacturer's instructions. Briefly, 0.5μg of total RNA (with technical replicate) from mouse treated macrophage samples was used for poly-A mRNA selection using streptavidin-coated magnetic beads. This protocol uses two rounds of enrichment for poly-A mRNA followed by thermal mRNA fragmentation. mRNA was then fragmented before the sheared RNA is reverse -transcribed to cDNA. The double-stranded cDNA is then synthesized, end-repaired and adenylated. Illumina adaptors were then ligated to the processed double-stranded DNA. Finally, the DNA products were amplified using primers to produce a sequence-ready library. RNA sequences were acquired from GenBank and remaining reads were mapped to the

genome using TopHat v.1.1.3. For DDAH2$^{flox/flox}$ LysM-Cre samples, the exons deleted (exon 2 - 5) were used to mask all reads to account for this deletion. This region is the functional region of DDAH2. Exons 1, 6 and 7 are non-functional and remain in the genetic make-up of the mice. Reads that uniquely map to these remaining exons were used in the analysis for differential expression. The number of aligned reads was counted across all samples. Transcript abundance was determined from the TopHat alignment using a custom pearl script and annotated transcripts from RefSeq. All gene changes were shown and the desired genes of interest were looked for.

2.17 Statistical analysis

Statistical analysis was performed using the Prism software package (Graph Pad Inc., UK). All statistical tests were specifically indicated and included either one-way ANOVA using the Bonferroni post-hoc test for paired/unpaired t-tests. Unless otherwise stated, all numbers were presented as mean ± standard error of the mean (mean ± SEM). For statistical tests, all t-tests were two-tailed and a p value of <0.05 was considered as significantly different.

CHAPTER 3

The effect of ADMA/NO on macrophage cell function in a human cell line

3.1 Introduction

Since its initial isolation in 1974 from a 37 year old Caucasian male, the U937 human leukemic monocytic cell line has gone on to form the basis of fundamental research looking at a variety of immunological-related diseases among many others. These suspended cells double every 24-48 hours (Kiley *et al.*, 1997), making them easy to culture. Since its primary extraction, the cell line has become particularly advantageous in that the addition of various stimuli such as PMA, vitamin D3, retinoic acid, TNF-α and IFN-γ causes them to differentiate into macrophages therefore making U937's a convenient model of human macrophages. Following terminal differentiation, U937 cells acquire macrophage-like cell morphology and express functional differentiation markers (Kim *et al.*, 1991; Oberg *et al.*, 1993).

There is still some controversy regarding the production of NO from human monocyte-derived macrophages. Numerous studies of cytotoxic agents have shown a lack of measureable NO production from monocyte-derived macrophages in response to various microbial pathogens such as parasites (Weinberg *et al.*, 1995; Denis, 1991; Denis, 1994). Despite this U937 cells are one of the most widely used immune cell lines. This may be because obtaining primary macrophages from humans is a difficult process which requires a lot of planning, patient background health checks and ethical approval. Although there has been research looking at U937s and motility, this research is limited in the field of NO/ADMA. More specifically, there has been no research focusing on the role of ADMA on U937 motility and phagocytosis. For this reason, this part of the study aims to provide an insight into the effect of NO on macrophage function and more importantly, how this may play an important role in the immune response.

3.2 Specific aims

This chapter reports the effects of the ADMA/DDAH/NO pathway on the motility and diapedesis of a human monocyte cell line in the presence and absence of NOS inhibitors. As explained previously, the effect of NO on monocyte/macrophage function has not been studied previously although there have been investigations looking at other cell types such as endothelial cells and sperm cells (Wojciak-Stothard *et al.*, 2007; Lewis *et al.*, 1996; Donnelly *et al.*, 1997).

The hypothesis in this chapter is that:

> ***ADMA is an important regulator of U937-macrophage derived motility and phagocytosis.***

Thus, the null hypothesis (H_0) is that:

> ***ADMA does not have any regulatory effect on U937-macrophage derived motility and phagocytosis.***

In order to accept or reject my null hypothesis, the following aims were generated:

1. **To investigate the effect of the pharmacological addition of methylarginine analogues on macrophage motility.**
   This will be carried out using real-time microscopy. The total distance and speed travelled by the cells will be determined using an Image J program.

2. **To investigate the role of methylarginine analogues in macrophage phagocytosis in quiescent and inflammatory stimulated conditions.**
   This will be determined using the addition of a fluorescent E-coli dye to the cells.

3. **To determine the effect of methylarginines analogues on macrophage diapedesis.**

   Transwell membranes will be used to determine the number of macrophages travelled through the membrane in response to treatment with methylarginines, an NO donor and a chemo-attractant at a given time interval. This will be repeated with the addition of an endothelial monolayer to the transwell insert.

4. **To investigate the effect of methylarginines on NO production in macrophages before and after inflammatory stimulation.**

   NO production, in the form of nitrite, will be measured using the Griess assay.

3.3 Human U937 monocytes can be differentiated into macrophages with PMA

The function of monocytes is to flow in the circulatory system seeking to fight or destroy pathogens and remove dead/ dying cells. Monocytes are a non-adherent cell type, which following activation, differentiate in to macrophages; an adherent cell type whose role is to enter tissues or sites of infection and target pathogens (MacMicking *et al.*, 1997).

U937 monocytes were grown as described previously in Chapter 2 and then differentiated into macrophages using PMA (Fig. 3.1). Initially U937 cells appeared round in shape with no membrane ruffles and were typically around 8-10μm in diameter. They were able to reach approximately 80% confluence within 2-3 days after which they had to be split. At x400 magnification the cells were easier to visualise, were mononuclear and fairly uniform in shape and size. These characteristics are of normal monocytic cells grown in a healthy environment (Fig. 3.1A).

Following stimulation of U937 with PMA for 3 days, there was a change in morphology (Fig. 3.1B). The cells generally increased in size to 18-20μm and became adherent. They formed membrane ruffles and although typically larger, were not as uniform in size as the monocytes were previously. Another major trait was their ability to stick together and form clumps of macrophages. The clumping together occurred in all PMA-treated macrophages irrespective of the size and shape of the plates grown in. The fact that macrophages appeared to form these clumps meant that it was difficult to obtain a confluent monolayer of cells but instead had many discrete areas with high numbers of cells. These alterations in morphology are in accordance with U937 differentiation observed by Daigneault *et al.* (Daigneault *et al.*, 2010).

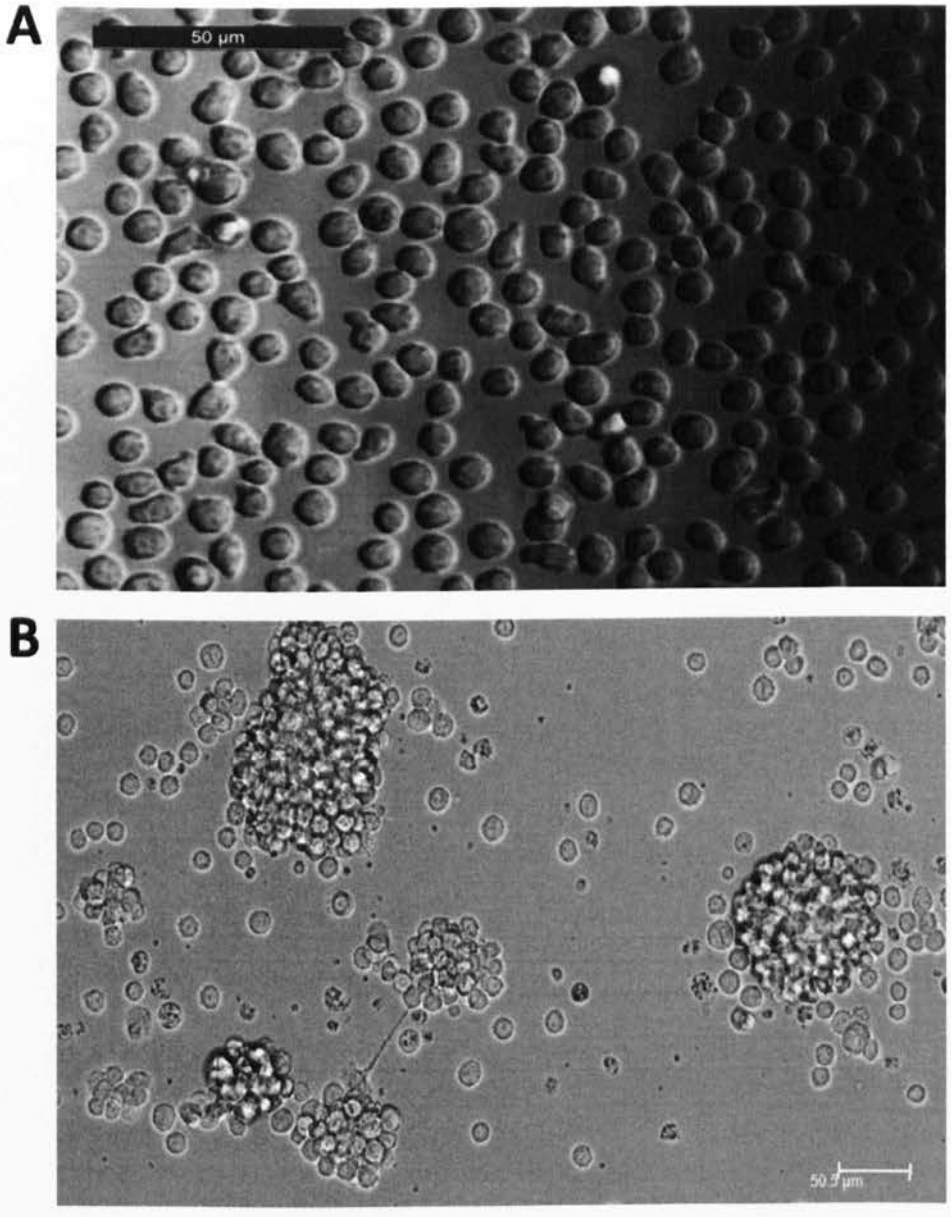

Fig. 3.1: Morphology of U937 monocytes and PMA differentiated macrophages.

U937 cells were grown as described previously in T75 flasks. Images were taken of (A) monocytes (x400) and (B) monocyte-derived macrophages at (x200) magnification using a Leica Microscope. Due to the nature of monocytes, cells were grown in a suspension and as shown here in the images were round, fairly uniform in size and mononuclear. They are separated (there is no clumping of cells together) and have a doubling time of 48-72 hours – media needed to be replaced every 3 days.

3.4 Human macrophage cell motility and phagocytosis is regulated by ADMA.

3.4.1 Speed travelled in the presence of methylarginines

To date research into NO and macrophage motility has been limited. Although NO has been shown to affect endothelial cell motility, its role on macrophages, an immune cell type where motility is fundamental to their function, has not yet been described. By carrying out the following experiments, we can determine whether NO has a direct effect on macrophage motility and if so, how we can modulate this pathway to, either increase or reduce motility. In macrophage differentiated U937 cells, motility was determined in the presence of; ADMA, SDMA and LPS, as previously described in Chapter 2.

Under control conditions, the speed of macrophages travelled was 0.45 ± 0.015μm/min. The addition of LPS (100ng/ml) significantly increased macrophage speed compared to control (0.561 ± 0.032μm/min and 0.45 ± 0.015μm/min for LPS and control respectively, where *p<0.05) (Fig. 3.2A, Fig. 3.2B and Fig. 3.3A).

Although the addition of 1μM ADMA significantly reduced macrophage speed compared to 1μM SDMA (0.36 ± 0.019μm/min and 0.53 ± 0.036μm/min respectively, where *p<0.05), the size of the difference was not enough to cause it to reach statistical significance when compared to control (0.36 ± 0.019μm/min and 0.45 ± 0.015μm/min respectively, where p>0.05). Similarly the addition of 1μM SDMA did not have any significant effect on macrophage speed compared to control (0.53 ± 0.036μm/min and 0.45 ± 0.015μm/min respectively, where p>0.05) (Fig. 3.3A).

After the addition of 10μM ADMA, macrophage speed was significantly reduced compared to control (0.29 ± 0.013μm/min and 0.45 ± 0.015μm/min respectively, where *p<0.05). However, the addition of 10μM SDMA did not have any significant effect on macrophage speed compared to control (0.37 ± 0.028μm/min and 0.45 ± 0.015μm/min respectively, where p>0.05). Despite

this significant difference between ADMA and SDMA when comparing either 10μM ADMA or SDMA to control, there was no significant difference when comparing macrophages treated with either 10μM ADMA or 10μM SDMA but there was a trend for ADMA to be less than SDMA (0.29 ± 0.013μm/min and 0.37 ± 0.028μm/min for ADMA and SDMA respectively, where $p>0.05$) (Fig. 3.3B). This suggests that at this concentration the effect on motility may not be solely NO dependent.

At 100μM, ADMA and SDMA both significantly reduced macrophage speed compared to control cells (0.262 ± 0.016μm/min, 0.370 ± 0.0.19μm/min and 0.45 ± 0.015μm/min for ADMA, SDMA and control respectively, where $*p<0.05$), with ADMA decreasing (Fig. 3.2C, Fig. 3.2D and Fig. 3.3C). The difference between motility in the presence of ADMA and SDMA suggests that macrophage motility may in part be NO dependent, however, the contribution of NO independent factors cannot be ruled out.

In addition to this, the effect of methylarginines on the percentage inhibition of speed compared to control was calculated. The data shows that the addition of 1μM ADMA results in a significant reduction in the motility as a percentage of control compared to1μM SDMA (80.6 ± 6.87% and 114 ± 6.42% respectively, where $*p<0.05$). The addition of 10μM ADMA did not significantly affect the speed compared to 10μM SDMA (65.0 ± 5.94% and 76.7 ± 10.8% respectively, where $p>0.05$). Motility remained similar to control levels following 100μM SDMA addition but was significantly reduced following 100μM ADMA (57.0 ± 3.74% and 105 ± 15.7% respectively, where $*p<0.05$) (Fig. 3.3D). These data suggest that at physiological and pathophysiological concentrations of 10 and 100μM, ADMA reduces speed. The effect of SDMA is rather more complex as at pathophysiological concentrations, SDMA it appears to reduce speed – possibly due to increased competition with L-arginine.

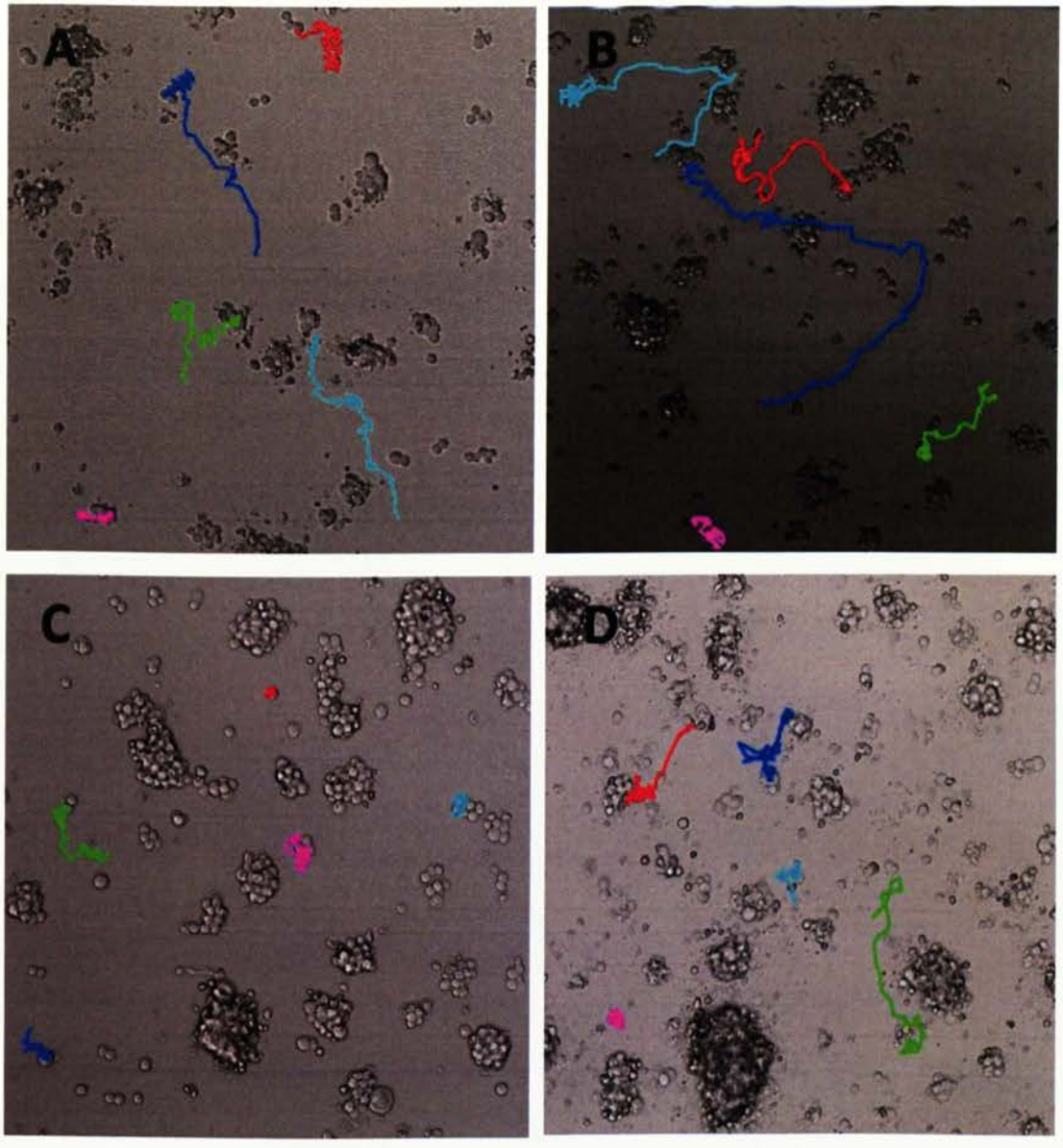

Fig. 3.2: Manual cell tracking of U937 differentiated monocytes after 12 hour recordings.

U937 monocytes were differentiated to macrophages with PMA for 3 days. Differentiated monocytes were treated for 8 hours with: (A) media only, (B) LPS (100ng/mL), (C) ADMA (100μM) and (D) SDMA (100μM). Cells were then tracked with a Leica microscope for 12 hours with images (x100 magnification) being taken at 10 minute intervals. Five random fields per condition were selected initially and after tracking, five randomly selected cells were manually tracked using an Image J manual tracking program. Different colours correspond to different cells. The images above are from one (out of five) random fields per treatment group.

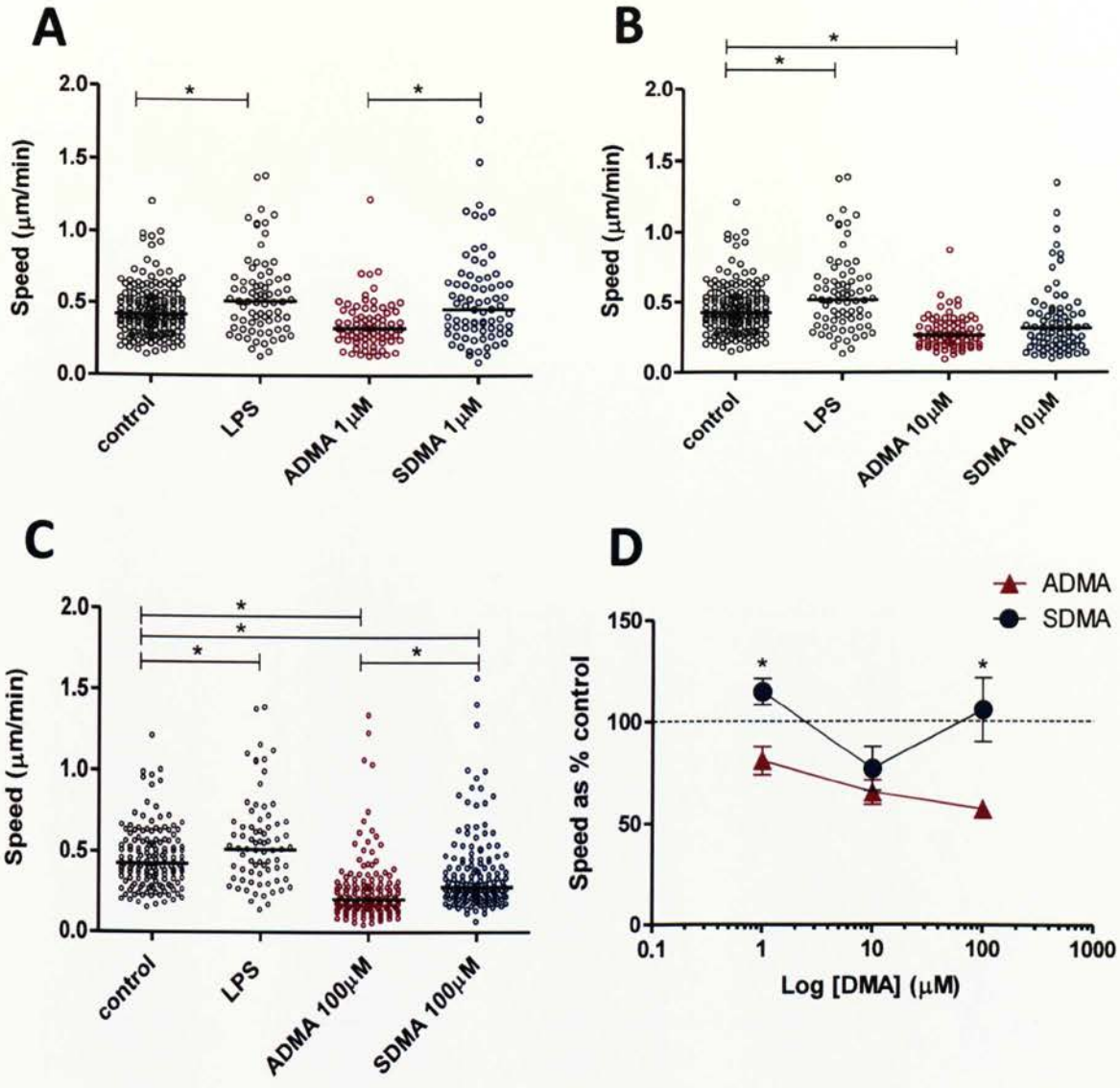

Fig. 3.3: Effects of the dimethylarginines ADMA and SDMA on macrophage speed.

Motility results after 12 hour recording of U937 differentiated monocytes containing: media only (control), LPS (100ng/ml) and (A) ADMA 1µMand SDMA 1µM, (B) ADMA 10µM and SDMA 10µM, and (C) ADMA 100µM and SDMA 100µM. (D) Dose dependent curve of ADMA and SDMA on macrophage speed. Results are indicative of n=3 (for LPS, SDMA 1 and 10µM) and n=6 (for control, ADMA 1, 10 and 100µM and SDMA 100µM) experiments and a total of 75 or 125 cells tracked per treatment. Significance was measured using a one-way ANOVA with a Bonferroni post-hoc test for images A-C (bars represent median) and a two-way ANOVA for image D.

3.4.2 Distance travelled in the presence of methylarginines

The previous results described investigated the effect of different concentrations of dimethylarginines on human macrophage speed. In the same experiment, the total distance travelled was also determined as described in the methodology.

Under control conditions the total distance that the cells travelled in 12 hours was 329 ± 11.05μm. Following the addition of LPS (100ng/ml; positive control), the total distance travelled increased compared to control but in contrast to speed was not statistically different (401 ± 22.2μm and 329 ± 11.05μm for LPS and control respectively, where $p>0.05$).

The treatment of differentiated monocytes with 1μM ADMA alone led to a non-significant reduction in total distance travelled compared to control (256.1 ± 14.12μm and 329 ± 11.05μm respectively, where $p>0.05$) (Fig. 3.4A). However, the distance travelled following the addition of 1μM ADMA was significantly lower than that of 1μM SDMA (256.1 ± 14.12μm and 381.7 ± 22.85μm for 1μM ADMA and 1μM SDMA respectively, where $*p<0.05$). There was no significant reduction in distance travelled by cells treated with 1μM SDMA compared to control (381.7 ± 22.85μm and 329 ± 11.05μm for 1μM SDMA and control respectively, where $p>0.05$).

In contrast, the addition of 10μM ADMA resulted in a significant reduction in distance travelled of cells compared to control (207 ± 9.91μm and 329 ± 11.05μm for 10μM ADMA and control respectively, where $*p<0.05$), although no significant difference between 10μM ADMA and 10μM SDMA was observed (207 ± 9.91μm and 271.8 ± 20.68μm for 10μM ADMA and 10μM SDMA respectively, where $p>0.05$) (Fig. 3.4B)

The addition of 100μM of ADMA led to a significant reduction in total distance travelled compared to control (192.2 ± 11.79μm and 329 ± 11.05μm for 100μM ADMA and control respectively, where $*p<0.05$). In addition to this, 100μM ADMA significantly reduced distance travelled compared to 100μM SDMA

(192.2 ± 11.79μm and 269 ± 14.08μm for 100μM ADMA and 100μM SDMA respectively, where *p<0.05) (Fig. 3.4C).

As the concentration of ADMA increased there was a clear reduction in the distance that macrophages have travelled in 12 hours when calculated as a percentage of control. Following the addition of SDMA, the percentage inhibition of the total distance travelled was statistically smaller when compared to ADMA (Fig. 3.4D).

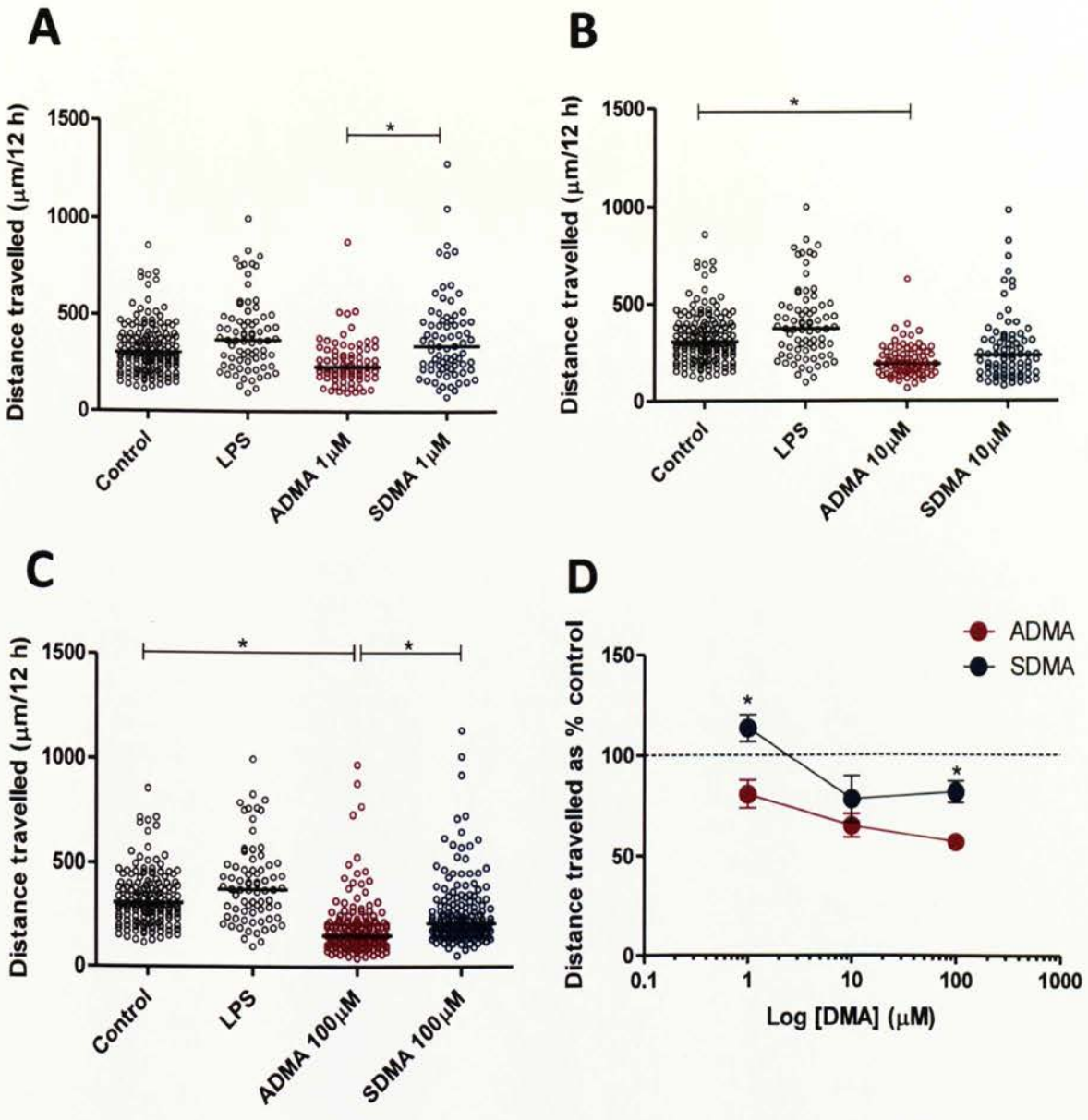

Fig. 3.4: Effects of the dimethylarginines ADMA and SDMA on macrophage distance travelled.

The distance travelled after 12 hours recording of U937 differentiated monocytes containing media only (control), LPS (100ng/ml) and (A) ADMA 1µMand SDMA 1µM, (B) ADMA 10µM and SDMA 10µM, and (C) ADMA 100µM and SDMA 100µM. (D) Dose dependent curve of ADMA and SDMA on macrophage distance travelled. Results are indicated of n=3 and n=6 experiments and a total of 75 or 125 cells tracked per treatment. Significance was measured using a one-way ANOVA with a Bonferroni post-hoc test for images A-C (bars represent median) and a two-way ANOVA for image D.

3.4.3 Phagocytosis levels in the presence of methylarginines

Phagocytosis is another important feature of macrophage function. It is a major mechanism used to remove pathogens and cell debris and therefore is a critical part of the immune system. We know that phagocytosis is an important process in immune cells and among other factors may rely on macrophage motility. For this reason exploring the effects of methylarginine addition on macrophage phagocytosis may be essential to determining the effect of NO on macrophage function. To investigate this, the effect of addition of ADMA and SDMA was determined either alone or with an inflammatory cocktail (LPS/TNF-α/IFN-γ at 5μg/mL/ 10μg/mL and 100units/mL respectively). This involved measuring the phagocytosis of an inert particle; although it is not reflective of destruction of pathogens it does model the initial stages of pathogen internalisation (Aderem and Underhill, 1999).

The motility data have shown that 10 and 100μM ADMA has both NO-specific and non-specific effects and the same seems to be true for phagocytosis. A significant reduction in phagocytosis following the addition of 10μM and 100μM ADMA, was observed when compared to control (4.45 ± 1.08a.u, 1.33 ± 0.51a.u, 1.95 ± 0.56a.u for control, ADMA 1μM and ADMA 10μM respectively, where $*p<0.05$) (Fig. 3.5). The addition of 100μM SDMA did not have any significant effect on phagocytosis levels when compared to control or 10μM and 100μM ADMA (3.17 ± 0.91a.u, 1.33 ± 0.51a.u, 1.95 ± 0.56a.u 4.45 ± 1.08a.u for 100μM SDMA, 10μM ADMA, 100μM ADMA and control respectively, where $p>0.05$).

Following the addition of an inflammatory cocktail for 24 hours, the phagocytosis levels of macrophages treated either alone or with 10μM ADMA, 100μM ADMA and 100μM SDMA did not alter significantly (5.42 ± 1.98a.u, 5.08 ± 1.78a.u, 2.57 ± 0.65a.u and 2.50 ± 0.25a.u respectively, where $p>0.05$). These data suggest that NO has specific and non-specific effects on macrophage phagocytosis and methylarginines may have a greater effect of eNOS than iNOS.

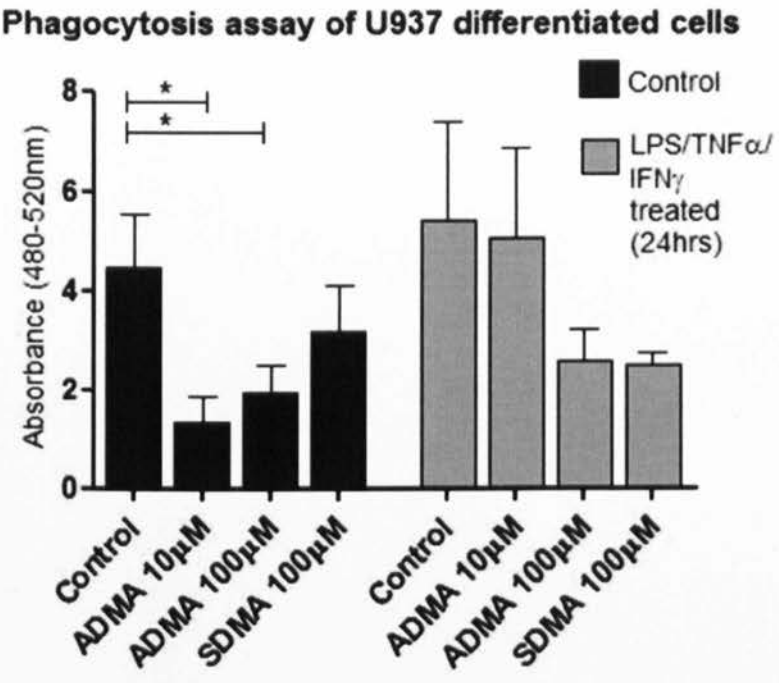

Fig. 3.5: Phagocytosis of U937 differentiated macrophages in untreated and inflammatory treated conditions.

Monocytes ($2x10^5$) plated in triplicate in a 96 well plate. They were treated with ADMA (10μM and 100μM) and SDMA (100μM) for 4 hours in cells with media only or cells which had been pre-treated with an inflammatory cocktail for 24 hours. In untreated conditions, ADMA 10 and 100μM significantly reduced phagocytosis whereas SDMA (100μM) did not. Under inflammatory treated conditions, phagocytosis levels generally increased but there was no significant difference between the data. These results suggest that in macrophages, there may be differential effects seen with iNOS and eNOS. Results are indicative of n=4 individual experiments (bars represent mean ± SEM). Significance was measured using a Mann-Whitney paired t-test and was accepted as significant when $*p<0.05$.

3.5 ADMA regulates monocyte transmigration

The aim of this series of experiments was to mimic the chemotaxis of cells *ex vivo* using transwell inserts. Transwell inserts allow cells to migrate through a micro-porous membrane from an upper compartment to a lower compartment (Fig 3.9). Micro-porous membranes can be synthesised from polyester (PET), polycarbonate (PC) or collagen coated PTFE and can vary in size depending on the cell type used (see Appendix). Additionally, cells may be grown on the membrane in order to study the migration of cells through a specific cell type i.e. the migration of monocytes through an endothelial monolayer. The initial transwell experimental study was designed to determine the ideal time to measure monocyte migration.

The migration of cells through a barrier is an important factor in chemotaxis. Briefly, $5x10^4$ monocytes were placed on the top of a 3.0μM polycarbonate transwell (Corning, UK) and allowed to freely migrate into the lower chamber containing either ADMA (1, 10, 100μM), SDMA (100μM) or stromal cell-derived factor-1 (SDF-1; a CXC-family of cytokines involved in chemotaxis of T lymphocytes and monocytes) (100ng/ml). Images (at x200 magnification) of three random fields were taken at 1, 2, 4 and 24 hours to help determine the kinetics of migration. SDF-1 is a chemokine that induces macrophage transmigration and was used as a positive control. The numbers of cells were counted in each image and statistical analysis was performed. Results expressed in Fig. 3.6 identified 4 hours as maximal for migration therefore this time point was used for subsequent experiments.

Following the addition of 1μM ADMA for 1 hour, the number of cell migrated through the transwell was 2.44 ± 0.47 monocytes migrated/ field (Table 3.1). After 2 hours, the number of cells migrated through increased significantly compared to 1 hour (10.0 ± 2.12 monocytes migrated/ field and 2.44 ± 0.47 monocytes migrated/ field respectively, where $*p<0.05$). After 4 hours, there was no significant difference in the migrated cell number when compared to 2 hours (9.31 ± 1.17 monocytes migrated/ field and 10.0 ± 2.12 monocytes migrated/ field respectively, where $p>0.05$). At 24 hours, the number of monocytes migrated through for 1μM ADMA increased significantly compared

to 4 hours (133 ± 48.0 monocytes migrated/ field and 9.31 ± 1.17 monocytes migrated/ field respectively, where *p<0.05).

After the addition of 10μM ADMA for 1 hour, the number of cell migrated were 1.11 ± 0.45 monocytes migrated/ field (Table 3.1). At 2 hours, this increased significantly compared to 1 hour (7.22 ± 1.16 monocytes migrated/ field and 1.11 ± 0.45 monocytes migrated/ field respectively, where *p<0.05). At 4 hours, there was no significant difference in the number of cells migrated when compared to 2 hours (6.47 ± 0.90 monocytes migrated/ field and 7.22 ± 1.16 monocytes migrated/ field respectively, where p>0.05). At 24 hours, the number of cells migrated increased significantly compared to 4 hours (89.6 ± 30.1 monocytes migrated/ field and 6.47 ± 0.90 monocytes migrated/ field respectively, where *p<0.05).

Following the addition of 100μM ADMA for 1 hour, the number of monocytes migrated through the transwell were 2.22 ± 0.46 monocytes migrated/ field (Table 3.1). At 2 hours, this increased significantly when compared to 1 hour (4.56 ± 1.29 monocytes migrated/ field and 2.22 ± 0.46 monocytes migrated/ field respectively, where *p<0.05). At 4 hours, there was no significant difference in migration compared to 2 hours (5.89 ± 0.79 monocytes migrated/ field and 4.56 ± 1.29 monocytes migrated/ field respectively, where p>0.05). At 24 hours, the number of monocytes migrated increased significantly compared to 4 hours (71.9 ± 36.4 monocytes migrated/ field and 5.89 ± 0.79 monocytes migrated/ field respectively, where *p<0.05).

Following the addition of SDF-1 for 1 hour, the number of monocytes migrated was 83.8 ± 19.1 monocytes migrated/ field (Table 3.1 and Fig. 3.6). At 2 hours, there was no significant difference in the number of migrated cells when compared to 1 hour (92.7 ± 12.8 monocytes migrated/ field and 83.8 ± 19.1 monocytes migrated/ field respectively, where p>0.05). After 4 hours, there was a significant increase in the number of cells migrated through compared to 4 hours (296 ± 77.4 monocytes migrated/ field and 92.7 ± 12.8 monocytes migrated/ field respectively, where *p<0.05). After 24 hours, there was no significant difference in cell migration compared to 4 hours (317 ± 53.4 monocytes migrated/ field and 296 ± 77.4 monocytes migrated/ field

respectively, where $p>0.05$) suggesting that maximal migration was reached at 4 hours.

Control	2.00 ± 0.60	9.56 ± 2.04	16.0 ± 3.45	114 ± 28.8
SDF	*83.8 ± 19.1	*92.7 ± 12.8	*296 ± 77.4	*317 ± 53.4
ADMA 1μM	2.44 ± 0.47	10.0 ± 2.12	*9.31 ± 1.17	133 ± 48.0
ADMA 10μM	1.11 ± 0.45	7.22 ± 1.16	*6.47 ± 0.90	89.6 ± 30.1
ADMA 100μM	2.22 ± 0.46	4.56 ± 1.29	*5.89 ± 0.79	71.9 ± 36.4
SDMA 100μM	1.89 ± 0.70	8.00 ± 1.09	13.9 ± 1.76	115 ± 22.1

Table 3.1: Number of monocytes migrated through a transwell membrane at different time intervals (1, 2, 4 and 24 hours).

Monocytes were added to the top chamber of a transwell membrane and treated with SDF-1 (100ng/ml), ADMA (1, 10 and 100μM) and SDMA (100μM). Cells were allowed to migrate for either 1, 2, 4 or 24 hours. The number of cells migrated through was counted by selecting 3 random fields at x200 magnification. Results are indicative of n=3 experiments and statistical significance was determined using a one-way ANOVA and Bonferroni post-hoc test compared to control and was accepted when *$p<0.05$.

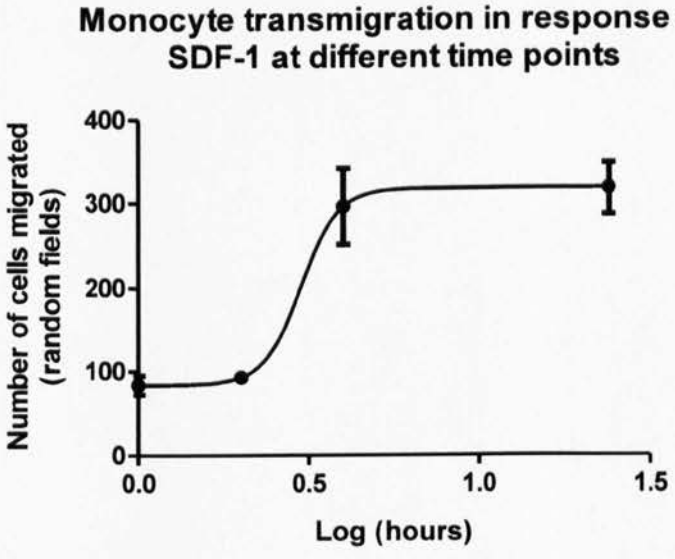

Fig. 3.6: The effect of SDF-1 on monocyte transmigration at 1, 2, 4 and 24 hours.

SDF-1 increased monocyte transmigration at 1, 2 and 4 hours. After 24 hours incubation with SDF-1 monocyte migration increased slightly but was not significantly different to 4 hours suggesting that maximal migration was achieved at 4 hours. Based on this, 4 hours was chosen as an appropriate time point to use in future experiments.

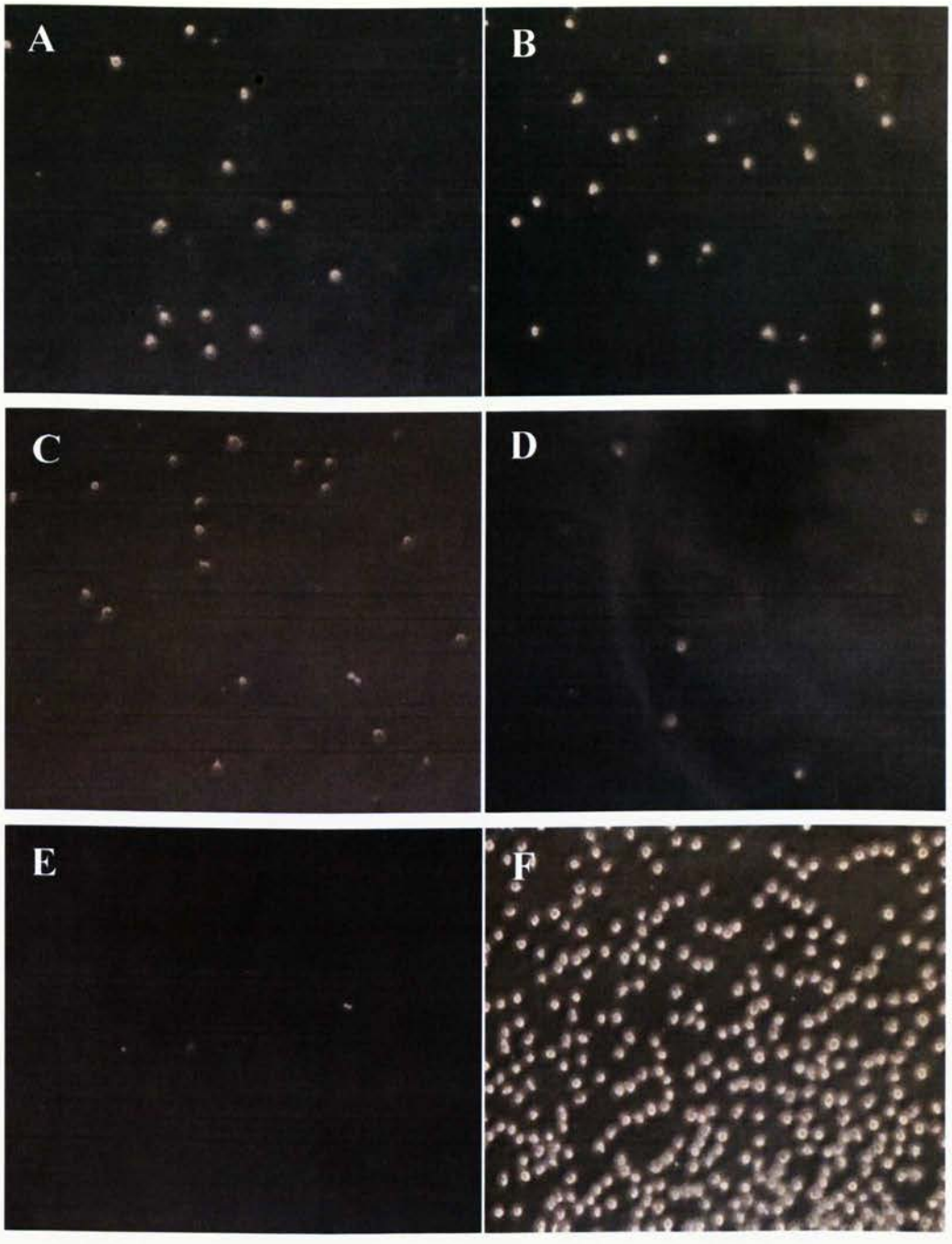

Fig. 3.7: Phase contrast images of monocytes migrated through a 3μm pore at 4 hours.

(A) Media only (control) (B) SDMA (100μM) (C) ADMA 1μM (D) ADMA 10μM (E) ADMA 100μM and (F) SDF-1 were added to the bottom of transwell inserts. Cells ($5x10^4$) were added to the upper chamber and after 4 hours incubation, the total number of cells migrated through the transwell were counted from 3 random fields using a Leica DFC 420C microscope. Phase contrast images were taken at x200 magnification in each random field.

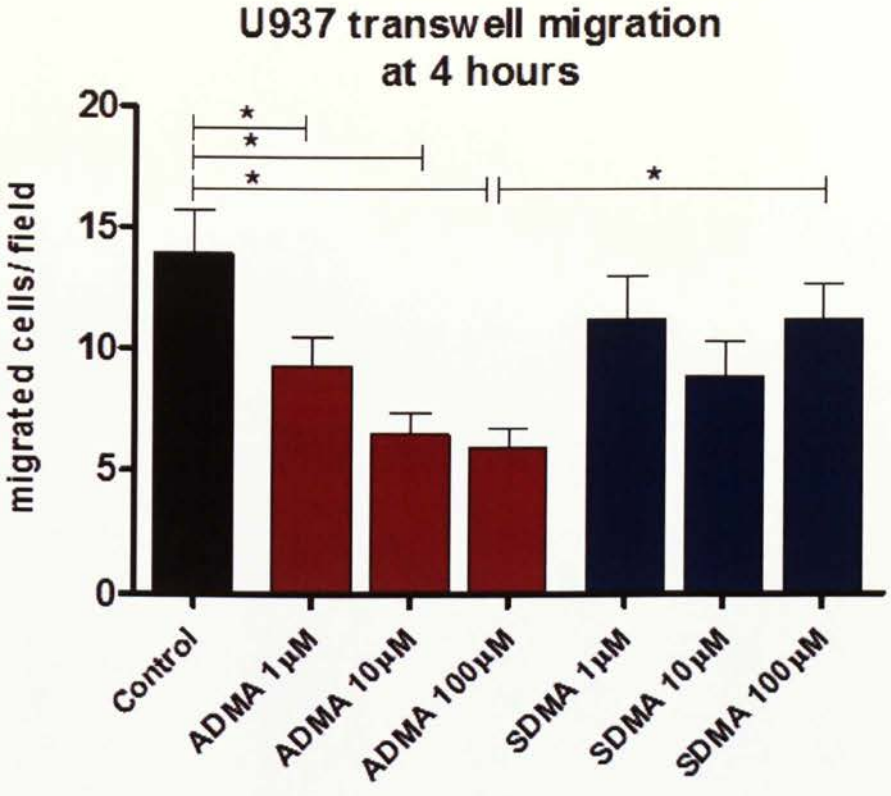

Fig. 3.8: Effect of ADMA (1, 10 and 100µM) and SDMA (1, 10, and 100µM) on U937 monocyte migration after 4 hours.

To determine the role of NO on monocyte transwell migration, ADMA (1, 10 and 100µM) and SDMA (1, 10 and 100µM) added to the lower compartment. Monocytes ($5x10^4$) in the top compartment were allowed to migrate through the transwell for 4 hours and then counted. A significant reduction in migration of monocytes was seen with ADMA 1, 10 and 100µM (*$p<0.05$) and between ADMA 100µM and SDMA 100µM (*$p>0.05$). Results are indicative of n=4 experiments (bars represent mean + SEM). A one way ANOVA comparing all means using a Bonferroni test and a Mann-Whitney t-test was carried out and significance was accepted where *$p<0.05$.

In the previous results, ADMA, but not SDMA, was shown to affect migration both in culture and through a transwell. To determine whether this effect could be reversed by increasing extracellular NO, the NO donor, sodium nitroprusside (SNP; 100μM) was added.

ADMA (10μM) and SDMA (100μM) were added either individually or in addition with SNP (100μM) (Fig. 3.9). SNP was also added alone to determine the sole effect of this on migration compared to an untreated control. SNP (100μM) significantly increased migration of cells compared to control conditions (28.3 ±3.32 monocytes migrated/ field compared and 17.3 ±2.05 monocytes migrated/ field respectively, where $*p<0.05$) (Fig 3.13). The addition of ADMA 10μM significantly reduced migration compared to control (9.21±1.38 monocytes migrated/field and 17.3 ± 2.05 monocytes migrated/ field respectively, where $*p<0.05$). This effect was reversed by the addition of SNP which significantly increased migration of ADMA treated cells (16.9 ±4.37 monocytes migrated/field and 9.21 ± 1.38 monocytes migrated/ field respectively, where $*p<0.05$). Similarly, there was no significant difference in migration following the simultaneous addition of ADMA and SNP compared to SNP addition alone (16.9 ± 4.37 monocytes migrated/ field and 28.3 ± 3.32 monocytes migrated/ field respectively, where $p>0.05$).

Conversely, SDMA (100μM) did not have any significant effect on monocyte migration compared to control (14.7 ± 2.20 monocytes migrated/field and 17.3 ± 2.05 monocytes migrated/ field respectively, where $p>0.05$) (Fig. 3.9). There was no significant difference in the number of cells following the simultaneous addition of SNP and SDMA compared to SDMA treatment alone (26.3 ± 6.92 monocytes migrated/ field and 14.7 ± 2.20 monocytes migrated/ field respectively, where $p>0.05$). Similarly there was no significant difference in monocyte migration following the simultaneous addition of SDMA and SNP compared to SNP addition alone (26.3 ± 6.92 monocytes migrated/ field and 28.3 ± 3.32 monocytes migrated/ field respectively, where $p>0.05$). This confirms that SDMA does not have any significant effect on monocyte migration.

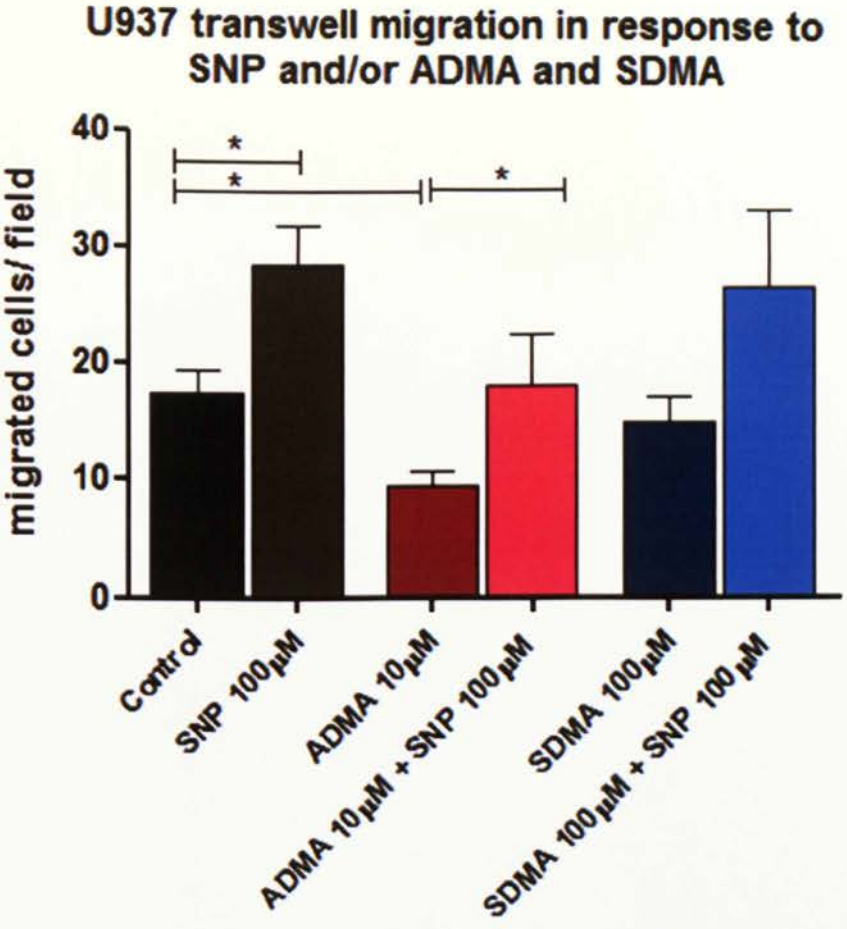

Fig. 3.9: Effect of SNP 100µM and/or ADMA (10µM) and SDMA (100µM) on U937 monocyte migration after 4 hours.

SNP (100µM), ADMA (10µM) and SDMA (100 µM) were added alone or the latter two in combination with SNP, 100µM. The addition of the NO donor (SNP, 100µM) significantly increased migration. ADMA, 10µM, significantly reduced migration compared to control and SDMA, 100µM. The addition of SNP to ADMA at 10µM significantly increased migration but to SDMA at100µM only tended to increase migration levels. These results are representative of 3 individual experiments (bars are representative of mean ± SEM). A one way ANOVA comparing all means using a Bonferroni post-test and a Mann-Whitney t-test was carried out and significance was accepted when $*p<0.05$.

3.6 ADMA regulates monocyte trans-endothelial cell migration

One of the major roles of monocytes is chemotaxis through endothelial cells. It is this critical stage which contributes to the development of atherosclerosis. The mechanism of action of monocyte infiltration is a complex one as it relies on two different cell types: monocytes (the cells that are migrating) and endothelial cells (the cells that monocytes are migrating through). NO has different effects on these cells therefore it is critical to look at monocytes and endothelial cells in parallel. This model can be replicated in culture by growing endothelial cells on the transwell inserts and once they have adhered, adding monocytes on top.

Briefly, $8x10^4$ HUVEC's were grown on a transwell insert. $5x10^4$ monocytes were added to the top chamber and the bottom chamber was treated with the following: media only, 10μM ADMA, 100μM SDMA, or the previous in the presence of an inflammatory cocktail (LPS/TNF-α/IFN-γ). Monocytes were incubated for 4 hours to allow migration through the endothelial monolayer and images taken as mentioned previously (Fig. 3.10).

The addition of an inflammatory cocktail (LPS/TNF-α/IFN-γ) into the lower chamber significantly increased monocyte migration through an endothelial monolayer compared to control (73.0 ± 20.7 monocytes migrated/ field and 24.9 ± 2.29 migrated cells/ field respectively, where $*p<0.05$). Similarly the addition of ADMA into the lower chamber significantly increased monocyte migration through the endothelial monolayer compared to control (65.3 ± 7.72 monocytes migrated/ field and 24.9 ± 2.29 monocytes migrated/ field respectively, where $*p<0.05$) (Fig. 3.11).

The co-incubation of ADMA with the inflammatory cocktail (LPS/TNF-α/IFN-γ) resulted in a further increase in cell migration compared to control cells (87.7 ± 13.0 monocytes migrated/ field and 24.9 ± 2.29 migrated cells/ field respectively, where $*p<0.05$). There was no significant difference following the simultaneous addition of ADMA and the inflammatory cocktail compared to either ADMA or inflammatory cocktail addition alone (87.7 ± 13.0 monocytes

migrated/ field, 65.3 ± 7.72 monocytes migrated/ field and 73.0 ± 20.7 monocytes migrated/ field respectively, where $p>0.05$) (Fig. 3. 11).

Finally, the addition of SDF-1 has no effect on monocyte migration through the endothelial monolayer when compared to control (28.2±6.27migrated cells/field and 24.9 ± 2.29 monocyte migrated/field respectively, where $p>0.05$). The addition of100μM ADMA in parallel also had no significant effect on monocyte migration compared to control (28.5 ±10.2 monocytes migrated/ field and 24.9 ± 2.29 monocyte migrated/ field respectively, where $p>0.05$).

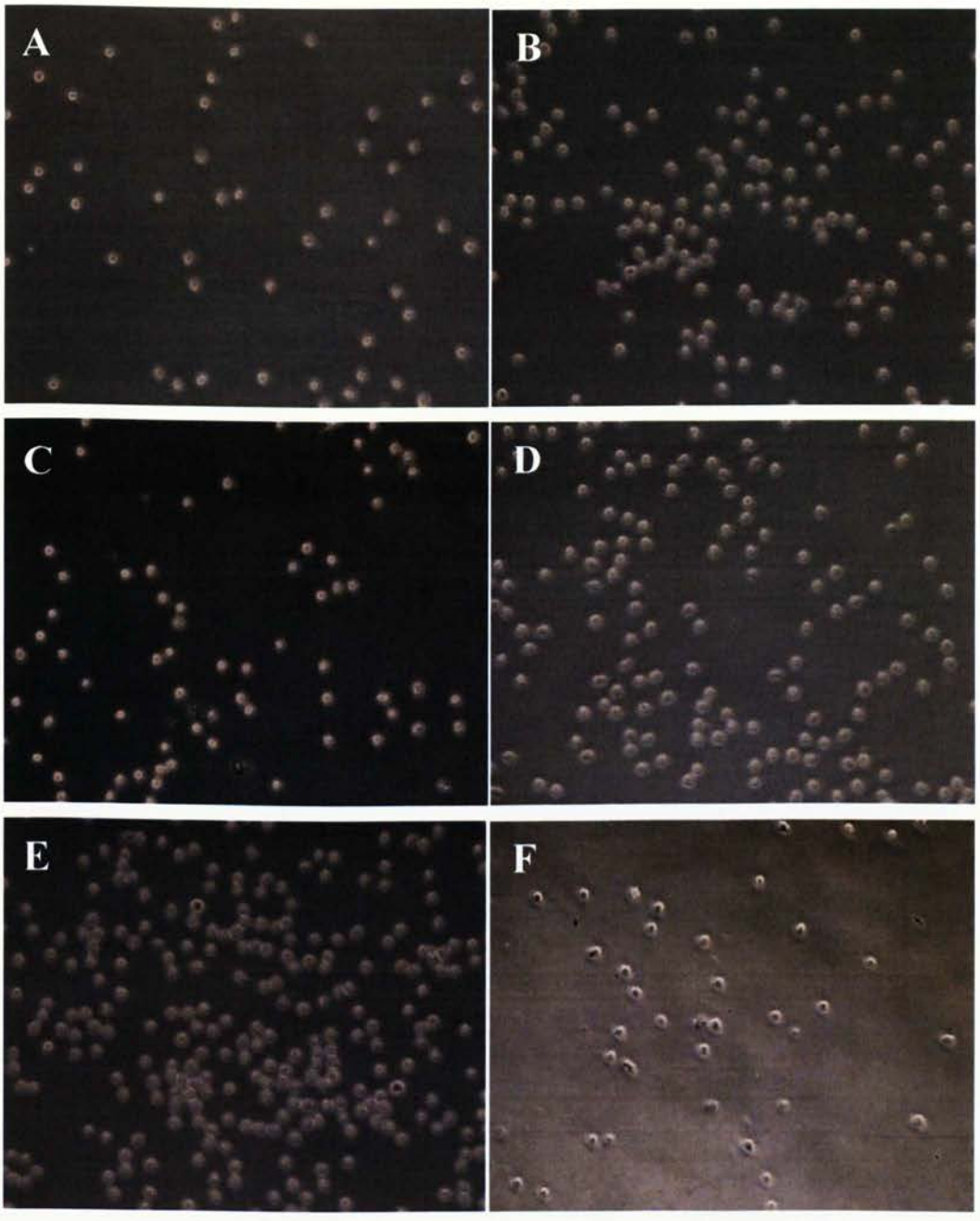

Fig. 3.10: Phase-contrast images of monocytes migrated through an endothelial cell barrier at 4 hours.

A) Control (B) ADMA (100μM) (C) SDF-1 (D) LPS/TNF-α/IFN-γ (E) LPS/TNF-α/IFN-γ and ADMA (100μM) (F) SDF-1 and ADMA (100μM) were added to the lower compartment of a transwell membrane. Monocytes ($5x10^4$) were added to the upper chamber and after 4 hours incubation, the total number of cells migrated through the transwell were counted from 3 random fields using a Leica DFC 420C microscope. Phase contrast images were taken at x200 magnification in each random field.

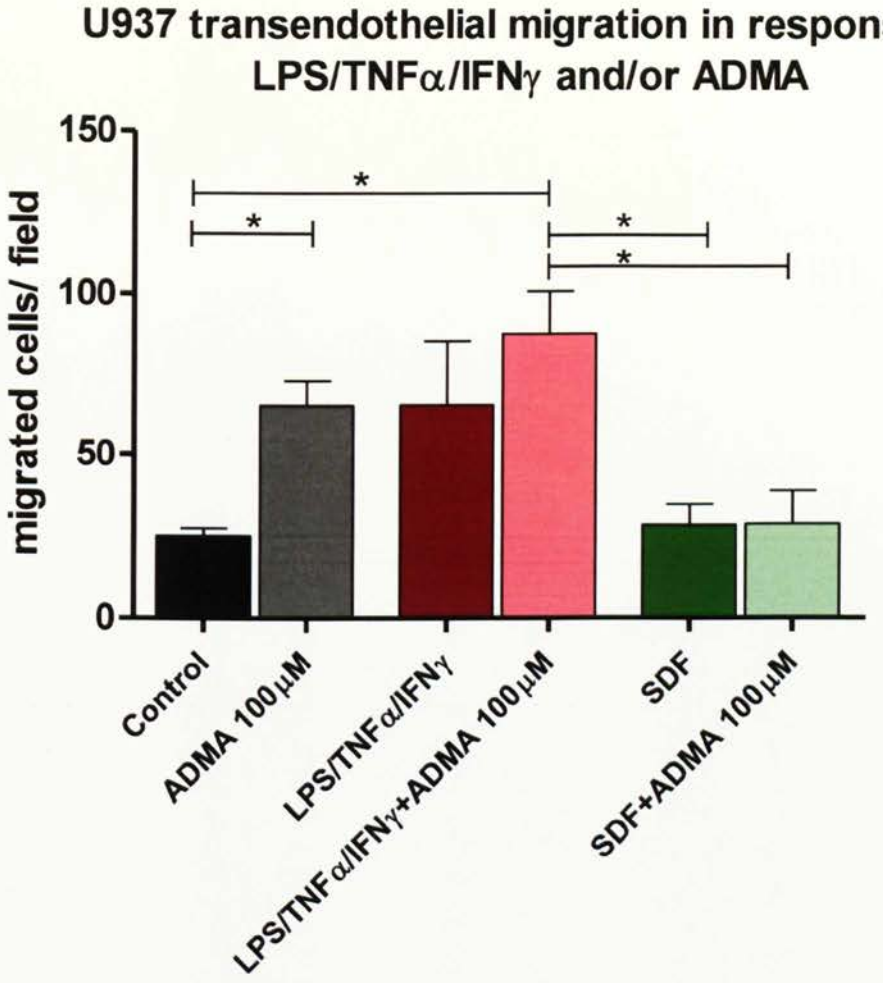

Fig. 3.11: Monocyte migration through endothelial monolayers at 4 hours.

HUVEC cells were grown on a transwell insert and allowed to adhere for 24 hours. Monocytes were treated for 4 hours with media only (control), LPS/TNFα/IFN-γ, or SDF-1 all with or without ADMA, 100μM. Monocytes were then added to the top of the transwell and allowed to migrate for 4 hours. The number of cells migrated through were counted per field. The addition of 100μM ADMA and LPS/TNFα/IFN-γ significantly increased diapedesis. It is presumable that this effect is due to ADMA and/or cytokines increasing endothelial permeability. Similarly this suggests that the net effect of increased ADMA *in vivo* is increased monocyte migration. Results of cells migrated through a 3μm pore at 4 hours are indicative of 3 experiments (bars represent mean ± SEM).

3.7 NO production in human macrophages.

Nitrite production from macrophages is critical to the activation of downstream pathways which lead to an enhanced immune response. Based on this, nitrite production from macrophage derived U937 cells was measured using the Griess assay after treatment with the methylarginines ADMA and SDMA, and/or an inflammatory cocktail (LPS at 5μg/mL and IFN-γ at 100units/mL respectively) (Fig. 3.12).

The addition of 1μM ADMA at 6, 24 and 48 hours had no significant effect on nitrite production compared to control (5.21 ± 0.056μmol; 6.39 ± 0.23μmol; 6.59 ± 0.49μmol; compared to 5.93 ± 0.56μmol; 6.66 ± 0.33μmol; and 8.03 ± 0.40μmol; for 1μM ADMA treated compared to control at 6, 24 and 48 hours respectively, where $p>0.05$). The addition of LPS/IFN-γ and 1μMADMA had no significant effect on motility compared to control (5.84 ± 0.31μmol; 6.89 ± 0.18μmol; 7.99 ± 0.64μmol; compared to 5.82 ± 0.78μmol; 6.15 ± 0.11μmol; 8.43 ± 0.92μmol; for LPS/IFN-γ/1μM ADMA treated compared to LPS treated at 6, 24 and 48 hours respectively, where $p>0.05$).

The addition of 10μM ADMA had no significant effect on nitrite production compared to control (4.98 ± 0.60μmol, 6.98 ± 0.13μmol and 8.20 ± 0.38μmol compared to 5.93 ± 0.56μmol, 6.66 ± 0.33μmol and 8.03 ± 0.40μmol for 10μM ADMA treated compared to control at 6, 24 and 48 hours respectively, where $p>0.05$). The addition of LPS/IFN-γ and 10μM similarly, although increased nitrite production time-dependently, had no significant effect on nitrite production compared to LPS/IFN-γ treated alone (5.61 ± 0.23μmol, 6.52 ± 0.08μmol, and 7.12 ± 0.71μmol compared to 5.82 ± 0.78μmol, 6.15 ± 0.11μmol, 8.43 ± 0.92μmol for LPS/IFN-γ/10μM ADMA treated and LPS/IFN-γ treated at 6, 24 and 48 hours respectively, where $p>0.05$).

Again the addition of 100μM ADMA had no significant effect on nitrite production compared to control at 6 and 24 hours (5.61 ± 0.47μmol, 6.34 ± 0.29μmol and 7.65 ± 0.24μmol compared to 5.93 ± 0.56μmol, 6.66 ± 0.33μmol and 8.03 ± 0.40μmol for 100μM ADMA treated compared to control at 6, 24 and 48 hours respectively, where $p>0.05$). Although the addition of LPS/IFN-γ and

100μM increased nitrite production time-dependently, it had no significant effect on nitrite production compared to LPS/IFN-γ treated alone at 2 and 24 hours (6.07 ± 0.34μmol and 6.25 ± 0.34μmol compared to 5.82 ± 0.78μmol and 6.15 ± 0.11μmol, for LPS/IFN-γ/100μM ADMA treated and LPS/IFN-γ treated at 6 and 24 hours respectively, where $p<0.05$). There was a significant reduction in nitrite production for the addition of 100μM ADMA to inflammatory stimulated cells compared to LPS/IFN-γ treated cells alone (6.06 ± 0.454μmol compared to 8.43 ± 0.92μmol for LPS/IFN-γ/100μM ADMA treated and LPS/IFN-γ treated alone at 48 hours respectively, where $*p<0.05$).

The addition of 100μM SDMA had no significant effect on nitrite production compared to control (5.38 ± 0.36μmol, 6.52 ± 0.11μmol and 7.38 ± 0.20μmol compared to 5.93 ± 0.56μmol, 6.66 ± 0.33μmol and 8.03 ± 0.40μmol for 100μM SDMA treated compared to control at 6, 24 and 48 hours respectively, where $p>0.05$). Although the addition of LPS/IFN-γ and 100μM SDMA increased nitrite production time-dependently, had no significant effect on nitrite production compared to LPS/IFN-γ treated alone at 2, 24 and 48 hours (6.07 ± 0.30μmol, 6.97 ± 0.28μmol, and 8.16 ± 0.58μmol compared to 5.82 ± 0.78μmol, 6.15 ± 0.11μmol, 8.43 ± 0.92μmol for LPS/IFN-γ/10μM ADMA treated and LPS/IFN-γ treated at 6, 24 and 48 hours respectively, where $p>0.05$).

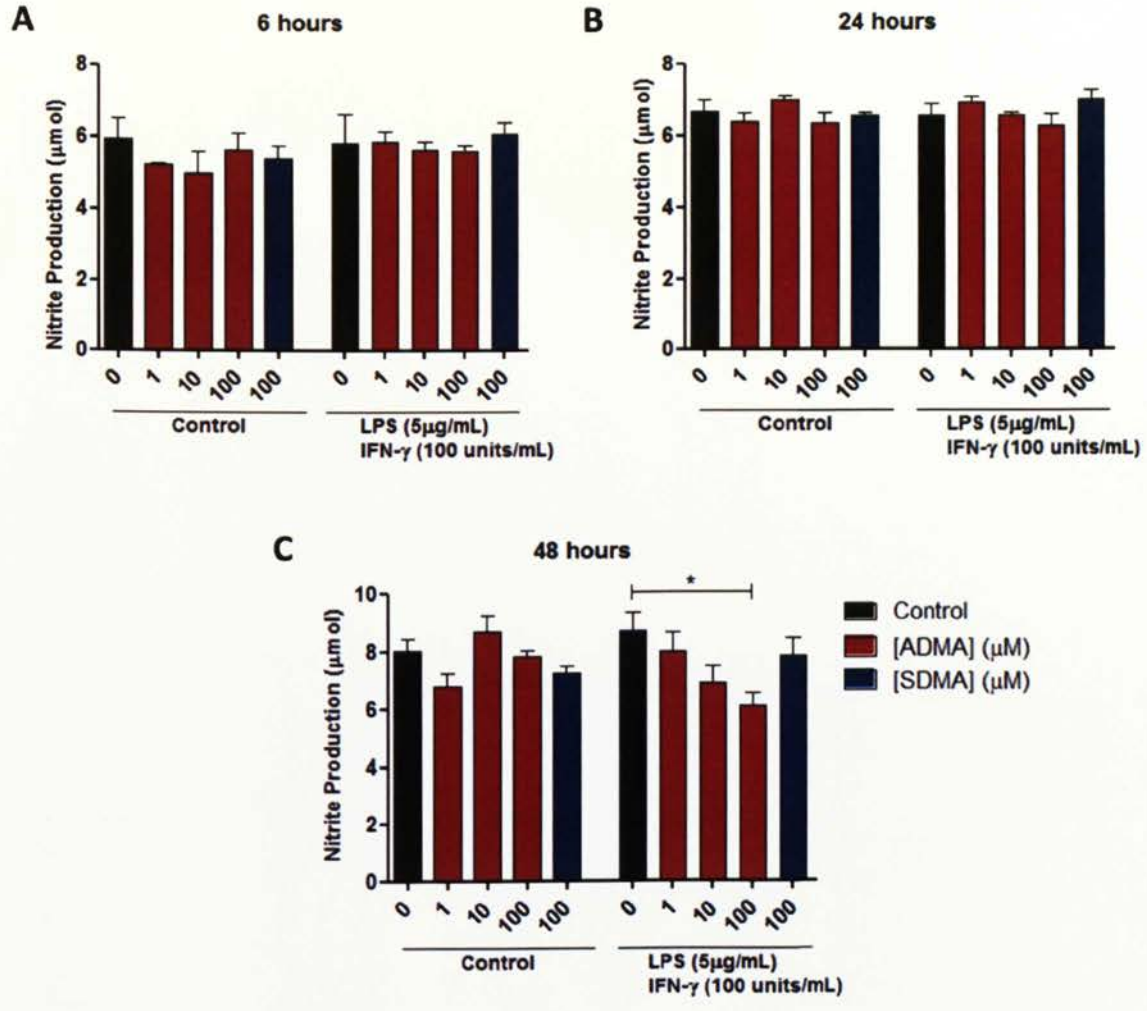

Fig. 3.12: The effects of dimethylarginines on nitrite production in human macrophages in unstimulated and LPS/IFN-γ stimulated conditions.

U937 monocytes ($1x10^5$) were plated in 96 well plates in duplicate and differentiated to macrophages for 3 days with PMA. Cells were then treated with different concentrations of ADMA (1, 3, 10 and 100µM) and SDMA (100µM) with or without an inflammatory cocktail (LPS/IFN-γ). Media was collected at (A) 6, (B) 24 and (C) 48 hours and nitrite production was measured using the Griess method described previously. Results are indicative of n=3 experiments and open bars represent quiescent conditions whereas chequered bars represent inflammatory stimulated conditions. Statistical analysis includes a one way ANOVA and a Bonferroni post-hoc test (bars represent mean ± SEM).

3.8 Discussion

This chapter highlights the effects of the exogenous addition of different concentrations of the dimethylarginines, ADMA and SDMA, on the motility, phagocytosis and chemotaxis of the monocytic human cell line, U937. Although U937 cells are a monocytic cell line by lineage, they can easily be differentiated into macrophages by the addition of PMA for 3 days. This treatment changes the usual round suspension of monocytes into adherent macrophages with membrane ruffles. PMA is a treatment widely used to differentiate U937 cells to macrophages (Daigneault *et al.*, 2010).

Physiological NO concentrations in most cells vary between 2-5μM. We found that inducing macrophages with an inflammatory cocktail had no significant effect on NO_2^- production (NO_2^- levels remained ~6-8μM). However, this failure to detect extracellular NO with the Griess assay is not definitive evidence for a lack of NO production as our data clearly implies NO-dependence.

Firstly, the real-time motility experiments show that only the addition of ADMA (concentration dependently) but not SDMA significantly reduced motility compared to control. This demonstrates that the effects seen are NOS-dependent. The findings from the chemotaxis studies corroborate this. Following the addition of different concentrations of ADMA and SDMA it was found that ADMA at 1, 10 and 100μM significantly reduced the migration of monocytes through the transwell compared to control whereas SDMA had no significant effect. Also, the effect of ADMA can be reversed by the addition of the NO donor, SNP suggesting that NO itself is critical in mediating macrophage chemotaxis. Interestingly, but not surprisingly the addition of an endothelial monolayer resulted in ADMA-induced migration presumably due to ADMA and/or cytokines increasing endothelial cell permeability.

Previous findings agree with the results seen in the motility and chemotaxis data. Maa *et al* and Zhou *et al* independently showed that the addition of either LPS or SNP significantly increased chemotaxis of primary macrophages (Maa *et al.*, 2008; Zhou *et al.*, 2009) whereas LPS mediated migration was inhibited by the addition of the iNOS specific inhibitor 1400W or genetically deleting

iNOS$^{-/-}$in mice (Maa *et al.*, 2008). This suggests that iNOS is required for macrophage migration. Similarly Wojciak-Stothard *et al* (2007) demonstrated that ADMA significantly inhibits endothelial cell motility and is therefore important in angiogenesis (Wojciak-Stothard *et al.*, 2007). Later, they showed that the effect on endothelial barrier function was a result of the modulation of Rac-1 by ADMA (Wojciak-Stothard *et al.*, 2009). This and the fact that cytokines are known to directly affect endothelial and epithelial cell permeability (Madara and Stafford, 1989; Petrache *et al.*, 2001; Ozaki *et al.*, 1999; Bruewer *et al.*, 2003) may explain the increased transendothelial monocyte migration seen with ADMA and LPS.

The phagocytosis data illustrates that this important macrophage function is controlled through NO-dependent effect in untreated conditions as the addition of ADMA, at either 10 or 100μM, but not SDMA, significantly reduced phagocytosis. Stimulating the cells with an inflammatory cocktail did not have any significant effect as did the addition of ADMA and SDMA suggesting that there may be NO-independent effects.

Interestingly, SDMA was shown to have some effect on motility and impair phagocytosis under inflammatory conditions at higher concentrations. These effects may be explained by arginine uptake and so this may also be NO dependent. Closs *et al* showed that SDMA had no effect on iNOS that was extracted from macrophages but competed for L-arginine transport (Closs *et al.*, 1997). Tojo *et al* also found that SDMA significantly reduced the L-arginine uptake from the perfused loop of Henle of the rat kidney (Tojo *et al.*, 1997). Furthermore, the reduced bioavailability of L-arginine has been shown to result in uncoupled eNOS and under these conditions, eNOS generates O_2^-, which increases oxidative stress and NO bioactivity and induces endothelial dysfunction (Mueller *et al.*, 2005). To determine whether the effects of SDMA were NO-dependent, an NO donor was added to cells in a transwell membrane treated with SDMA (100μM). Although exogenous NO increased the mean number of cells migrating through the transwell, this was not significant suggesting that SDMA has non-NO dependent effects on motility and phagocytosis.

Many studies have tried to investigate the difference between human and murine NO production. Bertholet and colleagues examined the conditions necessary for human monocytes/ macrophages to synthesis NO when expressing iNOS. To do this the U937 cell line was engineered to synthesis this gene, following infection with a retroviral expression vector containing hepatic iNOS (DFGiNOS). They reported that, in contrast to primary murine macrophages, the rate limiting co-factor for NO production of DFGiNOS U937 cells treated with LPS and IFN was BH_4 (Bertholet *et al.*, 1999). Previous work corroborated these findings thus suggesting that BH_4 may play a critical role in promoting the assembly of human iNOS into an active dimer and in NO synthesis (Tzeng *et al.*, 1995).

In vitro, normal human monocytes/ macrophages, similar to U937 cells, do not synthesis any BH_4 (Weinberg *et al.*, 1995) and the stimulation of these cells with cytokines (IFN-γ) has been shown to induce neopterin (a marker of cellular immune system activation) accumulation, but little or no BH_4 (Schoedon *et al.*, 1987). This may help to explain why there is little production of NO in this experiment following LPS/IFN treatment. *In vivo* the system may be different in that human monocytes/macrophages may obtain BH_4 from other cell types which are capable of synthesising it such as lymphocytes and endothelial cells (Schoedon *et al.*, 1995) thus this may be responsible for the higher NO levels seen *in vivo* during inflammation.

In addition to this, previous studies that have shown that measureable NO production in cells from humans *ex vivo* required prolonged exposure to cytokines and the amount of NO produced was much lower than that produced by murine cells. One reason for this may be that there is a physiological difference between monocyte-derived macrophages and tissue or resident macrophages derived from mice (Gordon and Taylor, 2005; Daems *et al.*, 1976). Tissue-derived macrophages have been exposed to many stimuli in the process of exiting the circulation such as exposure to pro-inflammatory mediators and therefore may already be activated.

The data obtained from the U937 cells line suggest that although this cell line does provide some interesting results, it may not be an ideal cell line to use

when looking at the effects of intracellular ADMA or DDAH. Obtaining primary macrophages from human patients is a difficult process which has many ethical issues thus U937 cells are more widely used. U937 cells are a transformed cell line therefore it may possibly be that looking at the effects of NO on these cells is a vague model to use.

Overall this data suggests that NO has specific and non-specific effects on macrophage motility and chemotaxis whereas the phagocytosis data shows that methylarginines may have a greater effect of eNOS than iNOS. The concentrations of methylarginines used in this chapter ranged from physiological (low micromolar) to pathophysiological (10μM and above), however, these were applied exogenously and depend on their transport into and out of the cell. This may explain why increasing exogenous SDMA concentrations (1 and 10μM) seem to have an effect on macrophage function as it may increase competition for the substrate L-arginine to enter the cells.

Also, one caveat of this chapter may be the concentrations of L-arginine in the media as this may overwhelm the quantities of the inhibitor used in some experiments. A solution to this may therefore be to investigate the effects of different L-arginine concentrations on macrophage function. Similarly, a better system may be to use an animal model where NO levels are significantly altered intracellularly. For this reason we have decided to generate a specific DDAH2 global knock-out animal. By using animal model we can determine more specifically whether the effects seen above are indeed NO and/or NOS dependent.

Conclusion

In this chapter I set out to determine whether the pharmacological inhibition of NOS, by addition of ADMA, had any effect on human macrophage (from a cell line) functions that included motility, phagocytosis and transmigration. Based on the results obtained in this chapter we can reject our null hypothesis and more specifically conclude that:

1. *ADMA, but not SDMA, significantly reduces macrophage motility and transmigration.*

2. *ADMA, but not SDMA, is a key modulator of macrophage phagocytosis.*

3. *The effects of methylarginines on macrophage motility suggest that the inhibition of NOS may not be their only function.*

CHAPTER 4

The role of DDAH2 on primary peritoneal macrophage function

4.1 Introduction

Endogenously produced methylarginines are a unique mechanism for inhibiting NO production. ADMA is a molecule that regulates NO and appears to be important in human disease. It is clear that the ADMA/DDAH pathway is unique biochemically and may be important clinically therefore it is important to study it in more detail.

There is a wealth of associative data linking ADMA to disease but currently there is no data demonstrating a causal link between ADMA and NO. The data from chapter 3 demonstrated the effect of pharmacological inhibition of NOS signalling on macrophages. These reiterated that using a pharmacological approach alone may not provide sufficient information about intracellular NOS/ADMA activity. A more comprehensive approach of acquiring direct changes in intracellular ADMA involves using genetic deletion/disruption. The use of genetic manipulation provides long-term exposure to increased ADMA levels whereas the pharmacological approach used in chapter 3 is short-term.

NO levels can be manipulated by deleting or disrupting different genes involved in its synthesis. Possible target genes that can be disrupted include eNOS/iNOS/nNOS, which are essential to NO synthesis, or DDAH1/DDAH2, which are involved in ADMA/L-NMMA metabolism. In the case of determining the effect of NO on macrophage function, iNOS/eNOS or DDAH2 can be disrupted as these are so far the specific isoforms found in macrophages.

In most cells iNOS is effectively absent under physiological conditions but in response to pro-inflammatory cytokines or LPS is expressed in many cells. Various studies looking at iNOS have shown it to have a critical immunological significance in macrophages. In 1995 both MacMicking and Wei independently showed that following bacterial inoculation, iNOS genetic knockout mice ($iNOS^{-/-}$) had reduced NO generation by peritoneal macrophages and increased bacterial titre in tissues which eventually led to an overall increase in mortality compared to $iNOS^{+/+}$ mice (MacMicking *et al.* 1995; Wei *et al.* 1995).

Interestingly, eNOS expression is not limited to endothelial cells but is also associated with macrophages. Connelly and colleagues have repeatedly shown that eNOS activity is necessary to obtain maximal iNOS expression and activity following the exposure of murine macrophages to LPS stimulation. In both *in vivo* and *in vitro* settings these data have shown eNOS expression to regulate macrophage NF-κB, iNOS protein expression and NO production following LPS activation (Connelly *et al.*, 2003). Thus, an $eNOS^{-/-}$ mouse model is expected to limit iNOS activation and therefore prevent significant NO production in macrophages. Whilst both iNOS and eNOS deletion may provide important information regarding the activation of macrophages, they do not determine the specific ADMA effects on NOS. A better approach may therefore be to inhibit or reduce the enzyme which specifically catalyses ADMA metabolism – DDAH.

DDAH1 genetically modified mice have increased vascular pathophysiology such as endothelial dysfunction, increased systemic vascular resistance and elevated systemic and pulmonary blood pressure (Leiper *et al.*, 2007). DDAH1 has also been shown to regulate trophoblast motility and invasion, which is crucial for the establishment of a successful pregnancy and may be an important regulator of preeclampsia (Ayling *et al.*, 2006). However, previous reports have shown DDAH2 to be the predominant isoform in immune tissue that includes macrophages; therefore this knockout would be the ideal model to use. If DDAH2 per se is deleted then there may be a compensatory mechanism to increase DDAH1 levels, however since macrophages only express DDAH2, then this would not be the case. For this reason global $DDAH2^{-/-}$ mice would be an appropriate model to use when determining the effect of specific intracellular ADMA changes on macrophage function.

As this project aims to study the effect of NO on macrophage function, primary murine macrophages (pMacs) extracted from the peritoneal cavity were used. The peritoneal cavity provides an easily accessible site for the harvesting of moderate numbers of resident, non-manipulated macrophages and most of our understanding of resident tissue macrophages comes from the study of these macrophages (Zhang *et al.*, 2008). Isolation of peritoneal macrophages

was first described by Hirsch in 1956 (Hirsch, 1956) and involves a single injection of cold PBS into the peritoneum followed by extraction of the suspension after gentle agitation.

With the availability of DDAH2$^{-/-}$ animals and the extraction of pMacs, this chapter should provide more insight into the regulatory role of DDAH2 in macrophage function – an area that has largely remained unexplored.

4.2 Specific Aims

The proposed mechanism is that NO is a key regulator of macrophage function, in particular in immunoregulation and survival. It is well accepted that ADMA is an endogenous inhibitor of NOS and that DDAH principally regulates ADMA concentrations *in vivo*; however little is known about the specific role of DDAH in macrophages. Although previous research involving macrophages have looked at the ADMA/NO pathway in terms of NOS depletion, to date there has been no research examining the effect of DDAH2 endogenous inhibition.

The hypothesis in this chapter is that:

> ***DDAH2 plays a regulatory role in macrophages thus DDAH2 disruption will result in a loss of primary macrophage function.***

Thus, the null hypothesis (H_0) is that:

> ***DDAH2 does not play a regulatory role in macrophages thus DDAH2 disruption will have no effect on primary macrophage function.***

In order to accept or reject my null hypothesis, the following aims were generated:

1. **Confirmation of DDAH2 gene disruption.**
   Tissues (heart, kidney and liver) will be extracted from $DDAH2^{+/+}$ and $DDAH2^{-/-}$ mice and DDAH1 and DDAH2 protein expression measured using western blotting.

2. **Determination of intracellular methylarginine concentrations.**
   The methylarginines ADMA, L-NMMA and SDMA will be measured in primary macrophage lysates using LC-MS/MS. This aims to answer the question: How does DDAH2 affect ADMA metabolism?

3. **Investigate the involvement of DDAH2 and iNOS/eNOS in macrophage NO_2^- production.**

   The Griess assay will be used to determine NO_2^- production following pro-inflammatory stimulation of macrophages extracted from $DDAH2^{+/+}$, $DDAH2^{-/-}$ and $eNOS^{-/-}$ mice. To confirm the importance of iNOS, a specific iNOS inhibitor will also be used on $DDAH2^{+/+}$ pMacs.

4. **Confirmation of the effect of pharmacological methylarginine addition on macrophage motility.**

   Motility (speed and distance travelled) will be determined in pMacs extracted from $DDAH2^{+/+}$, $DDAH2^{-/-}$ and $eNOS^{-/-}$ mice using real-time imaging.

5. **Elucidate the effect of DDAH2 depletion on primary macrophage phagocytosis.**

   Phagocytosis in $DDAH2^{+/+}$ and $DDAH2^{-/-}$ pMacs will be measured by monitoring the uptake of a fluorescently labelled E-coli bio-particle.

6. **Investigate the role of DDAH2 in macrophage cell death and/or proliferation.**

   The BrDU assay and MTT assay will be used to determine the cell viability and proliferation of pMacs from $DDAH2^{+/+}$ and $DDAH2^{-/-}$ mice.

4.3 Generation and determination of global DDAH2 deletion in mice

A specific, global DDAH2 transgenic knockout mouse was generated to determine the effect of endogenous DDAH2 inhibition on the ADMA/NO pathway in macrophages. This approach provides a direct measure of the long-term effects of global DDAH2 depletion.

The disruption of the DDAH2 gene was not found to be lethal when homozygous (Breckenridge *et al.*, 2010). The DDAH2 knockout allele was created by the Texas Institute for Genomic Medicine (TIGM) in Houston, Texas. The technology and protocol employed to generate the $DDAH2^{-/-}$ mice is described in detail elsewhere ((Zambrowicz *et al.* 2003; Zambrowicz *et al.*, 1998) and http://tigm.org/technologies.html).

Briefly, this method involved the infection of a retroviral vector containing two active parts into mouse embryonic stem cells (ES). The first part of the retrovirus (5' end) contained the following in the order of: a splice receptor sequence, an antibiotic selectable marker and a polyadenylation (pA) signal. A fusion transcript containing a 5' fragment of the target gene spliced to an antibiotic selectable marker and pA was created after insertion of this retroviral sequence into the endogenous gene. This role of the first fusion transcript is to select for ES cells with integration of the retrovirus.

The second part of the retrovirus contained, in the following order; an ES cell active promoter, a marker exon (containing termination codons in all reading frames which prevents translation), and a splice donor signal. A second fusion transcript with the marker transcript followed by the transcript sequence of the target gene where the retrovirus was inserted was created after insertion. This second fusion transcript is under control of the ES cell promoter and its role is to act as a sequence tag in order to help identify the location of the retroviral insertion. The DDAH2 gene on mouse chromosome 17 was disrupted by inserting a 5kB viral gene trap into the first exon of the gene. PCR screening was then used by TIGM to determine the genomic location of the gene trap.

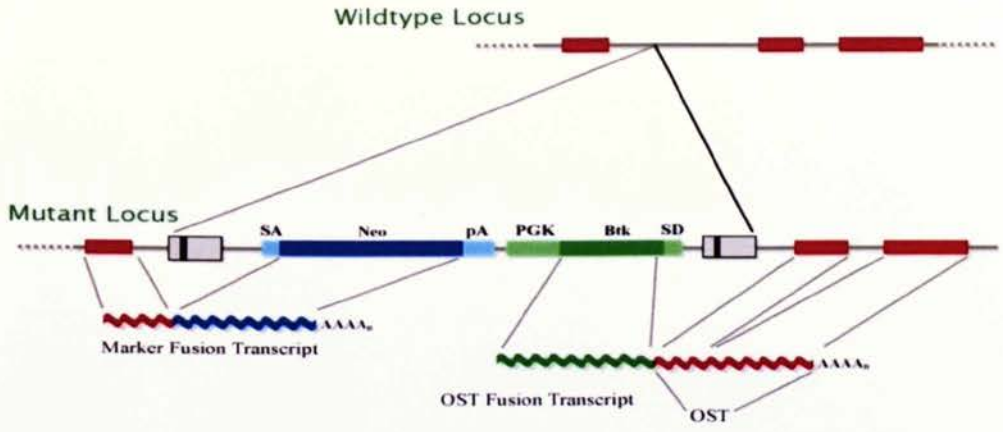

Fig. 4.1: Schematic diagram of the retroviral technique used to generate DDAH2 knockout mice.

The insertion of the viral vector into the target gene locus (Wild-type Locus) generates two fusion transcripts. The 5' fusion transcript (Marker Fusion Transcript) contains the target gene transcript, a splice acceptor sequence (SA), promoter-less selectable Neomycin (Neo) marker, and a poly-adenylation site (pA). This construct is used to screen for embryonic stem (ES) cells which have been successfully infected with the vector. The 3' fusion construct (OST Fusion Transcript) contains a promoter which is active in ES cells, in this case mouse phosphoglyceratekinase (PGK), the first exon of Brutons tyrosine kinase (Btk), and a splice donor sequence (SD) followed by sequence from the target gene. The sequence tag (OST) is used to identify the gene which has been specifically disrupted by the viral insertion. The Btk sequence contains stop codons in all reading frames to prevent translation of any viral transcripts. (Adapted from TIGM website: http://www.tigm.org/technologies.html)

Importantly, the animals generated from the DDAH2$^{-/-}$ mice were normal in that they had a normal life span and did not show any phenotypic differences compared to their wild types (DDAH2$^{+/+}$) littermates. However, there were differences in weight whereby male DDAH2$^{-/-}$ animals weighed significantly less than DDAH2$^{+/+}$ animals (27.13 ± 0.319 grams for DDAH2$^{+/+}$ (n=40), and 25.78 ± 0.389 grams for DDAH2$^{-/-}$ (n=42), unpaired t-test, ** $p<0.01$ where weights are mean ± SEM). The same trend was apparent between female DDAH2$^{-/-}$ and DDAH2$^{+/+}$ mice, however, there was no significant difference between them (all data taken from Kelly P. 2011).

The generated mice were genotyped using end-point PCR (Fig. 4.2) and protein expression of DDAH1 and DDAH2 were visualized and quantified using Licor, UK Imaging (Fig. 4.3). It is known that DDAH2 is present in various tissues and is primarily the dominant isoform found in immune cells (Tran *et al.*, 2000). The heart is known to express high levels of DDAH2 and low levels of DDAH1, whilst the kidney and liver both express high levels of DDAH1 and DDAH2 protein. More specifically, western blotting confirmed the complete absence of DDAH2 protein (37kDa) in the kidney, heart and liver of global DDAH2$^{-/-}$ mice after normalising against α-tubulin (64kDa) (Fig. 4.3). These data confirm the successful global deletion of DDAH2, whilst the western blots for the DDAH1 protein showed no evidence for any compensatory upregulation of DDAH1.

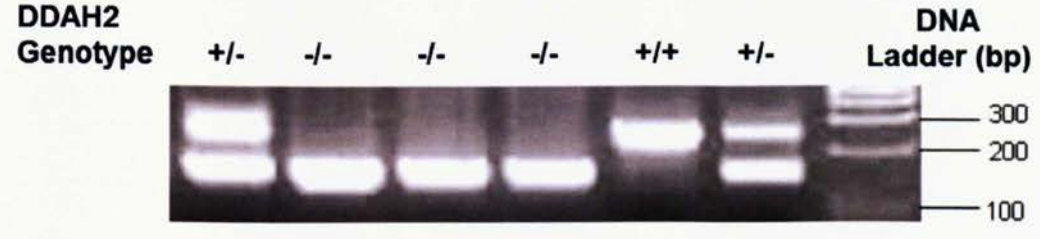

Fig. 4.2: PCR confirmation of DDAH2 gene disruption.

Genotyping using PCR gel was performed on tissue biopsies. The samples were tested for the presence of DDAH2$^{+/+}$ PCR fragments (230bp) and/or DDAH2$^{-/-}$ PCR fragments (160 bp). Data taken with permission from Kelly, P. 2011.

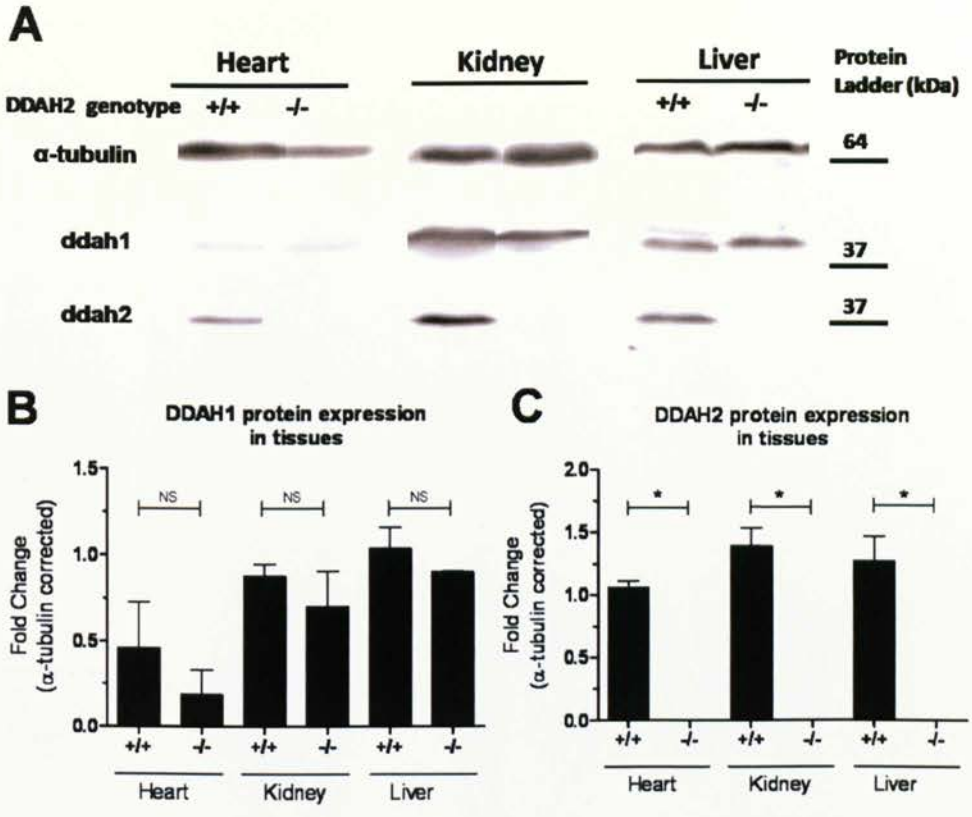

Fig. 4.3: DDAH1 and 2 levels in heart, liver and kidney (taken from western blots).

Protein expression of DDAH1 and DDAH2 in the kidney, heart and liver was determined using western blotting (A). Results for DDAH1 (B) and DDAH2 (C) were quantified using Licor Imaging. DDAH1 and 2 bands were divided separately by their α-tubulin loading controls to correct for protein levels. Fold change was calculated against the liver tissue and statistical analysis was carried our using a one-way ANOVA (n=4). (+/+ and -/- represent $DDAH2^{+/+}$ and $DDAH2^{-/-}$ respectively).

4.4 Number of primary macrophages extracted from peritoneum

The number of primary macrophages extracted each time from all animals was recorded. Macrophages were extracted using an injection of 5mL PBS into the peritoneal cavity followed by gentle agitation of the abdomen and extraction of peritoneal cells. There was no significant difference between the number of macrophages extracted from the peritoneal cavity of $DDAH2^{+/+}$ and $DDAH2^{-/-}$ animals (2.56 ± 0.202 $x10^6$ and 2.20 ± 0.146 $x10^6$ macrophages extracted respectively, where $p>0.05$) (Fig. 4.4). Flow cytometry was also used to confirm that the cells cultured from the wash-out were macrophages (see Appendix).

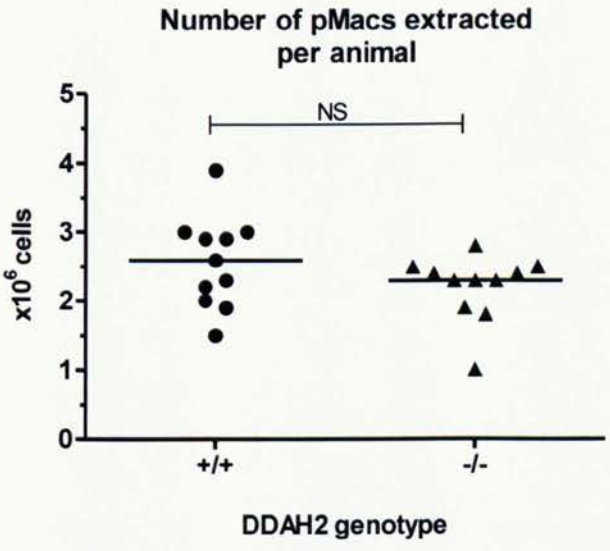

Fig. 4. 4: Number of primary macrophages extracted from $DDAH2^{+/+}$ and $DDAH2^{-/-}$ mice

Macrophages were extracted from the peritoneal cavity of $DDAH2^{+/+}$ and $DDAH2^{-/-}$ mice, stained with trypan blue and counted on a haemocytometer. There was no statistically significant difference between the animal genotype and the number of cells extracted from the peritoneum. Results are based on n=11 animals (bars represent median). Statistical significance was measured using an unpaired t-test and was accepted when $p<0.05$. Circles and triangles represent $DDAH2^{+/+}$ and $DDAH2^{-/-}$ respectively.

4.5 Intracellular ADMA and L-NMMA levels in peritoneal macrophages

ADMA, L-NMMA and SDMA levels were measured as previously described in the methodology (Chapter 2, Section 4). Briefly macrophage cell lysates were collected from $DDAH2^{+/+}$ and $DDAH2^{-/-}$ animals. D7 ADMA was added to the cell samples followed by methanol (1:5 ratio of sample: methanol). Samples were then centrifuged, the supernatant collected and spun again in a vacuum for 1 hour to remove excess methanol. A mobile phase (0.1% formic acid) was added to the samples and intracellular methylarginine concentrations measured using liquid chromatography-mass spectrometry (LC-MS).

The results show that SDMA was not present or was present in very low and undetectable levels in the samples. The intracellular concentration of ADMA significantly increased in $DDAH2^{-/-}$ macrophages compared to $DDAH2^{+/+}$ macrophages (21.0 ± 4.47μM and 5.25 ± 0.441μM for $DDAH2^{-/-}$ and $DDAH2^{+/+}$ respectively, where mean ± SEM and $*p<0.05$) (Fig. 4.5A).

L-NMMA was undetectable in $DDAH2^{+/+}$ macrophages whilst in $DDAH2^{-/-}$ macrophages it was 26.6 ± 6.94μM (Fig. 4.5B). This shows that global DDAH2 deletion significantly increases intracellular ADMA and L-NMMA concentrations in macrophages.

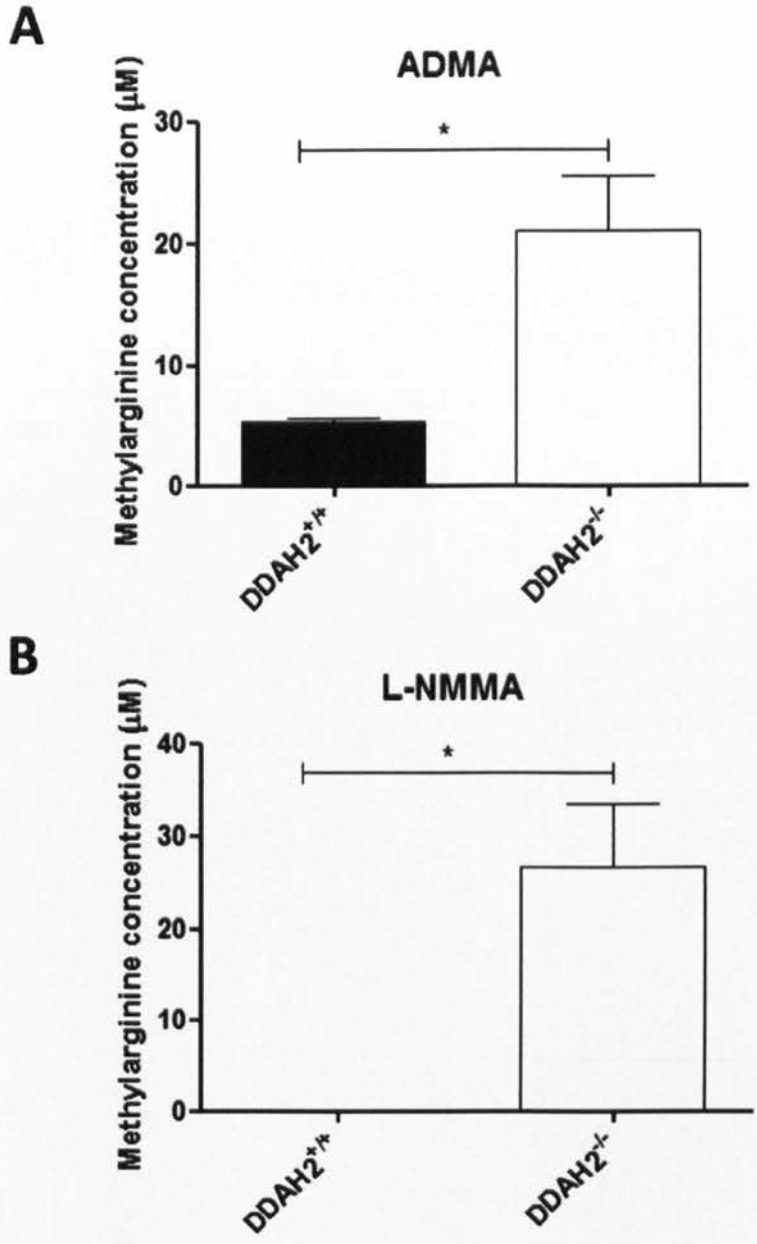

Fig. 4.5: Intracellular concentrations of ADMA and L-NMMA in DDAH2$^{+/+}$ and DDAH2$^{-/-}$ macrophage lysates.

Intracellular (A) ADMA and (B) L-NMMA levels were measured in DDAH2$^{+/+}$ and DDAH2$^{-/-}$ macrophage lysates using LC-MS/MS. Results are indicative of n=3 for both DDAH2$^{+/+}$ and DDAH2$^{-/-}$ macrophages respectively. Significance was accepted where *p<0.05 using an un-paired t-test.

4.6 DDAH, iNOS and eNOS regulate NO production in macrophages

It is widely accepted that macrophages produce NO following the induction of iNOS; however, they also express eNOS basally (Connelly *et al.*, 2003). Under constitutive conditions, macrophages produce low levels of NO, which increase significantly when activated. To determine the cumulative synthesis of NO in response to an inflammatory stimuli in macrophages the Griess assay was used. This was carried out in pMacs extracted from $DDAH2^{+/+}$ and $DDAH2^{-/-}$ (and global $DDAH1^{-/-}$ to confirm that deletion of this isoform is not relevant in macrophages).

Briefly, cells were stimulated maximally by the simultaneous addition of LPS (5μg/mL), TNF-α (10ng/mL) and IFN-γ (100units/mL) in order to produce maximal NO production. The media from the cells was extracted at 6, 24 and 48 hours. Prior to obtaining data, an assay using a NO_2^- standard curve was carried out to relate the absorbance from the spectrophotometer with the NO_2^- concentrations (see Appendix).

The initial levels of NO_2^- production in $DDAH2^{+/+}$ macrophages before the addition of inflammatory cocktail (at 0 hours) were 1.21 ± 0.29μmol (mean ± SEM) (data not shown). Following the addition of an inflammatory cytokine cocktail, NO_2^- production significantly increased over time for $DDAH2^{+/+}$ mice (4.91 ± 0.53μmol, 18.39 ± 1.83μmol, 42.63 ± 4.79μmol at 6, 24 and 48 hours respectively, where mean ± SEM and $*p<0.05$) (Fig. 4.6). This confirms that in $DDAH2^{+/+}$ mice, primary peritoneal macrophages produce high levels of NO in response to an inflammatory stimulus.

The lack of effect of global DDAH1 deletion on pMac NO production, confirms that DDAH1 is not involved in ADMA metabolism in macrophages. There was a significant increase in $DDAH1^{-/-}$ pMac NO_2^- production over the time course (8.84 ± 1.15μmol, 21.7 ± 4.35μmol, 46.1 ± 9.45μmol at 6, 24 and 48 hours respectively, where mean ± SEM and $*p<0.05$). There was no significant difference between $DDAH1^{-/-}$ and $DDAH2^{+/+}$ pMac NO_2^- production over time.

DDAH2 is important for macrophage-induced NO production. When compared to $DDAH2^{+/+}$, $DDAH2^{-/-}$ pMacs had significantly reduced NO production over time (3.15 ± 0.21µmol, 9.80 ± 1.19µmol, and 21.0 ± 2.68µmol at 6, 24 and 48 hours for $DDAH2^{-/-}$ and 4.91 ± 0.53µmol, 18.39 ± 1.83µmol, 42.63 ± 4.79µmol for $DDAH2^{+/+}$ at 6, 24 and 48 hours respectively, where mean ± SEM and $*p<0.05$) (Fig. 4.6). Although NO production was significantly reduced, it was not completely impaired.

To determine the specific effects of the inhibition or deletion of the different NOS isoforms on macrophage induced NO production, a specific iNOS inhibitor (1400W) and macrophages from $eNOS^{-/-}$ mice were compared. This aimed to validate the theory by Connelly *et al.*, 2003 that eNOS, as well as iNOS, is required for macrophage NO production.

Following the addition of 1400W with an inflammatory cocktail to pMacs, NO_2^- production was significantly reduced at all time-points (2.31 ± 0.98µmol, 2.96 ± 1.23µmol, and 3.48 ± 1.78µmol for 1400W treated compared to 4.91 ± 0.53µmol, 18.39 ± 1.83µmol, 42.63 ± 4.79µmol for $DDAH2^{+/+}$ at 6, 24 and 48 hours respectively, where mean ± SEM and $*p<0.05$). The same trend was observed in $eNOS^{-/-}$ pMacs which had significantly reduced NO production over time, compared to $DDAH2^{+/+}$(3.621 ± 1.368µmol, 2.475 ± 1.258µmol and 3.696 ± 1.294µmol for $eNOS^{-/-}$ and 4.91 ± 0.53µmol, 18.39 ± 1.83µmol, 42.63 ± 4.79µmol for $DDAH2^{+/+}$ at 6, 24 and 48 hours respectively, where mean ± SEM and $*p<0.05$). There was no significant difference in pMac NO_2^- production between $eNOS^{-/-}$ or iNOS inhibition over time (3.621 ± 1.368µmol, 2.475 ± 1.258µmol and 3.696 ± 1.294µmol for $eNOS^{-/-}$ pMacs and 2.31 ± 0.98µmol, 2.96 ± 1.23µmol, and 3.48 ± 1.78µmol for 1400W treated at 6, 24 and 48 hours respectively, where mean ± SEM and $p>0.05$) (Fig. 4.6).This would seem to confirm the hypothesis that in macrophages NO produced by eNOS and iNOS are both required.

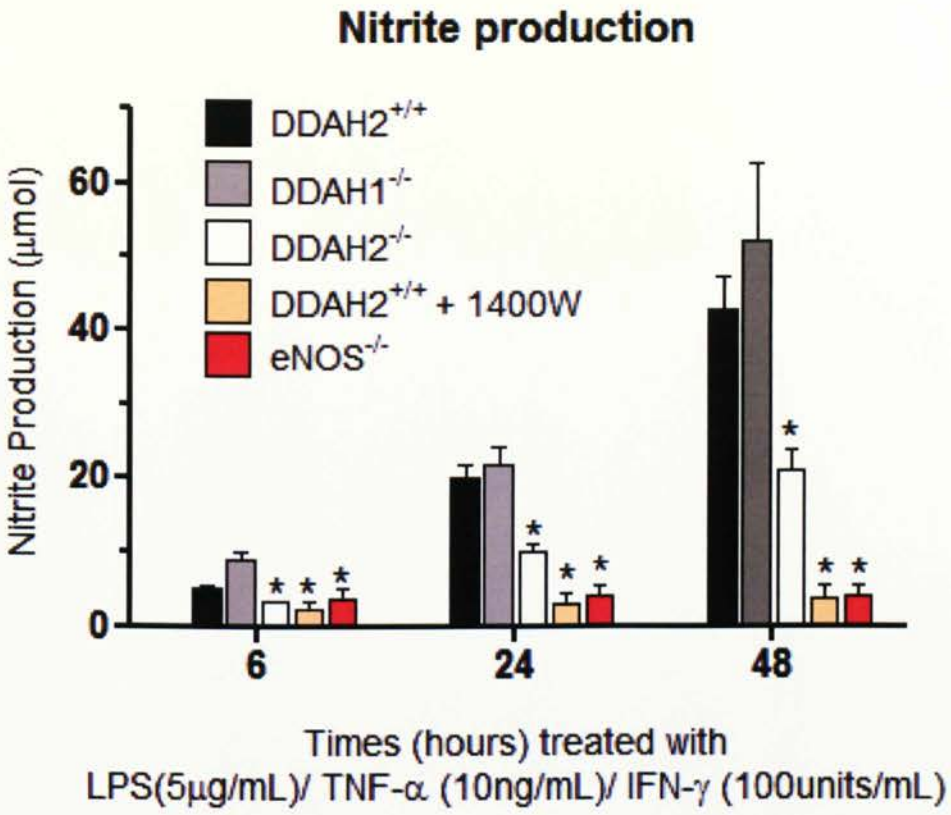

Fig. 4. 6: Time course accumulation of NO_2^- from pMacs treated with an inflammatory cytokine cocktail.

pMacs extracted from DDAH2$^{+/+}$, DDAH2$^{-/-}$, DDAH1$^{-/-}$, and eNOS$^{-/-}$ were cultured into 24 well plates (5 x10^5 cells/well) and treated with a pro-inflammatory cocktail of LPS/TNF-α/IFN-γ. Aliquots (200µL) were removed at time 6, 24, and 48 hours following cytokine treatment. NO_2^- concentration was determined using the Griess assay and a standard NO_2^- curve. The NO_2^- production of pMacs extracted from DDAH2$^{+/+}$ and DDAH1$^{-/-}$ animals increased significantly over 48 hours with no significant difference between the two genotypes. Conversely the NO_2^- production from macrophages derived from global DDAH2$^{-/-}$, eNOS$^{-/-}$ and DDAH2$^{+/+}$ treated with the iNOS inhibitor 1400W were significantly lower than DDAH2$^{+/+}$ and DDAH1$^{-/-}$ alone. Results are based on n=8 for DDAH2$^{+/+}$; n=9 for DDAH2$^{-/-}$; n=3 for DDAH1$^{-/-}$, n=3 for eNOS$^{-/-}$ and n=3 for DDAH2$^{+/+}$ with 1400W. Media only was used as a blank/reference. Significance was measured using an unpaired two-tailed t-test vs. DDAH2$^{+/+}$ mice (control) and was accepted when *p<0.05.

4.7 Pharmacological inhibition and genetic disruption of NO synthesis regulates macrophage function

4.7.1 DDAH2$^{+/+}$ primary macrophage motility

Based on the data seen in Chapter 3, we hypothesised that the pharmacological addition of ADMA and/or the genetic deletion of DDAH2 will both disrupt primary macrophage motility. DDAH2$^{+/+}$ mice were treated for 8 hours with an inflammatory cocktail (LPS/TNF-α/IFN-γ) and/or ADMA (10μM). Randomly selected fields (3) per condition were followed using real-time imaging as described in more detail in Chapter 2, section 10. Analysis was carried out using an Image-J program and the speed and distance that the cells travelled were determined (Licor, UK).

Stimulating primary macrophages with an inflammatory cocktail significantly increased macrophage speed compared to untreated cells. The addition of ADMA to inflammatory treated cells significantly reduced motility back to values similar to that of untreated cells (0.252 ± 0.0182μm/min, 0.382 ± 0.0211μm/min and 0.268 ± 0.0227μm/min for untreated, LPS/TNF-α/IFN-γ treated and co-incubation of LPS/TNF-α/IFN-γ and ADMA (10μM) respectively, where mean ± SEM and $*p<0.05$) (Fig. 4.7B). This trend agrees with that seen in human macrophages where the addition of LPS was shown to significantly increase macrophage speed (Chapter 3). This would seem to confirm that the inhibition of NOS significantly reduces primary macrophage speed.

As the distance is measured over a fixed time, then the changes in speed must be mirrored by distance. The total distance travelled by DDAH2$^{+/+}$ pMacs in untreated conditions was significantly lower compared to inflammatory cocktail treated cells (242.3 ± 17.51μm for untreated and 367.4 ± 20.22μm for LPS/TNF-α/IFN-γ treated respectively, where $*p<0.05$) (Fig. 4.7C). The addition of 10μM ADMA significantly reduced the total distance travelled back to untreated levels (242.3 ± 17.51μm for untreated and 256.9 ± 21.78μm for co-incubation of LPS/TNF-α/IFN-γ with ADMA (10μM) respectively, where

mean ± SEM and *p<0.05). These results substantiate the previous data from human macrophages and indicate that upon stimulation macrophage motility is increased and the addition of ADMA reduces motility both in resting conditions and in inflammatory conditions as shown here.

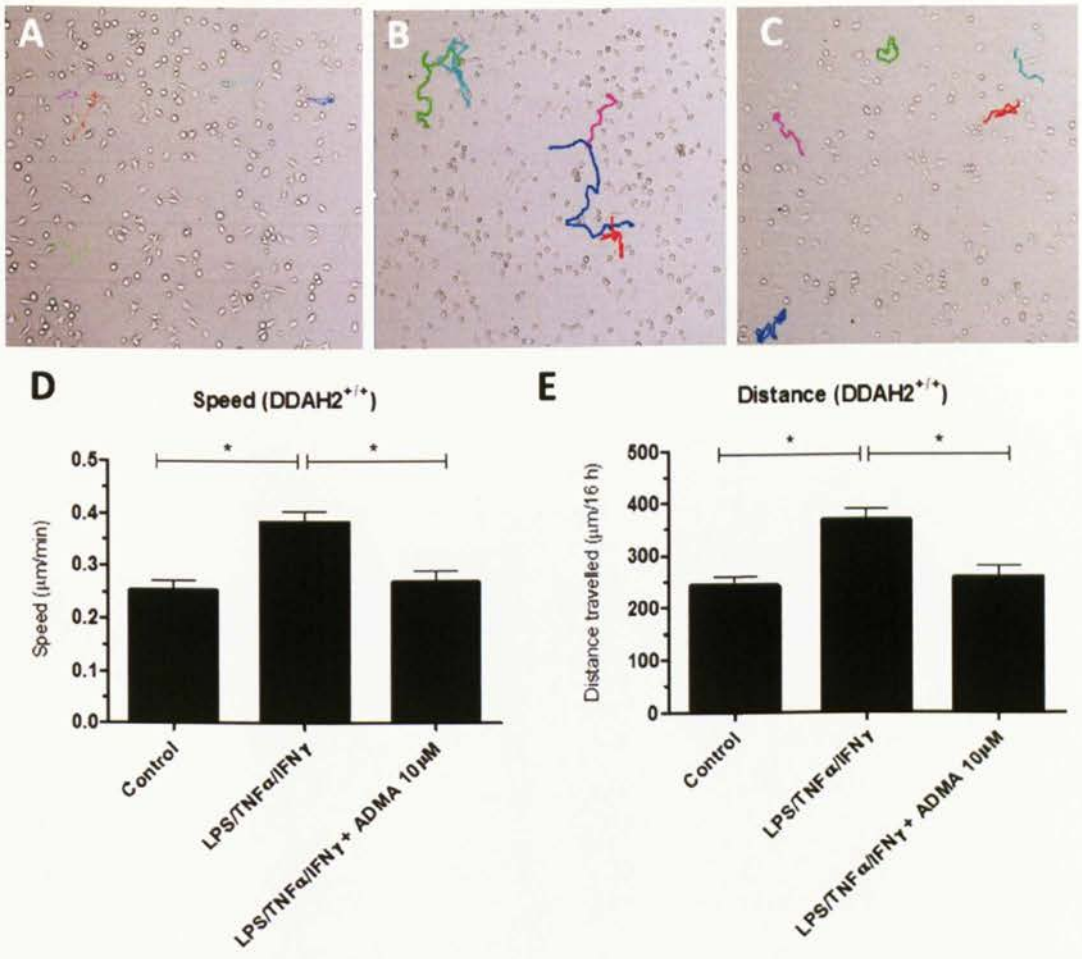

Fig. 4.7: Motility and distance travelled of pMacs obtained from DDAH2$^{+/+}$ mice.

Images (A, B and C) showing the cells tracked for DDAH2$^{+/+}$ pMac motility. There was a significant increase in speed (D) and distance travelled (E) after the inflammatory cocktail was added for a total of 24 hours. This increase in motility was significantly inhibited after the addition of ADMA (10µM). Cell motility and distance travelled was determined after 8 hours incubation with compounds followed by 16 hours real-time imaging. Images were taken at 10 minute intervals at 3-5 random fields per treatment group. Results are based on n=3 and statistical testing was carried out using a one way ANOVA. Significance was accepted when *p<0.05.

4.7.2 DDAH2$^{-/-}$ primary macrophage motility

Increasing ADMA levels pharmacologically was found to reduce primary macrophage motility however, it was important to determine whether using a genetic approach had the same effect. To determine this, DDAH2$^{-/-}$ pMacs were treated with ADMA (1, 10 and 100μM), SDMA (100μM) and SNP (100μM) and tracked as described previously.

In resting conditions, DDAH2$^{-/-}$ pMacs travelled significantly slower than DDAH2$^{+/+}$ pMacs (0.186 ± 0.0261μm/min for DDAH2$^{-/-}$ and 0.252 ± 0.0182μm/min for DDAH2$^{+/+}$, where mean ± SEM and *p<0.05) (Fig. 4.8A). DDAH2$^{-/-}$ pMac average speed was not significantly altered following the exogenous addition of 1, 10 or 100μM ADMA (0.164 ± 0.0149μm/min, 0.164 ± 0.0221μm/min and 0.161 ± 0.0190μm/min for 1, 10 and 100μM ADMA compared to 0.186 ± 0.0261μm/min for untreated conditions, where mean ± SEM and p>0.05) (Fig. 4.8A). The addition of SDMA (100μM) had no significant effect on speed when compared to control or the same concentration of ADMA (0.174 ± 0.0215μm/min for 100μM SDMA treated compared to 0.161 ± 0.0190μm/min for 10μM ADMA and 0.186 ± 0.0261μm/min for untreated, where mean ± SEM and p>0.05) (Fig. 4.8A). Interestingly the addition of SNP (100μM) showed a tendency to increase pMac speed; however, this effect was not significant when compared to control (0.218 ± 0.0229μm/min for 100μM SNP and 0.186 ± 0.0261μm/minor control, where mean ± SEM, and p>0.05).

The data for the total distance travelled by pMacs mimicked the data observed for speed. The total distance travelled by DDAH2$^{-/-}$ pMacs in untreated conditions was significantly reduced compared to DDAH2$^{+/+}$ (143 ± 14.1μm for DDAH2$^{-/-}$ and 242 ± 17.5μm for DDAH2$^{+/+}$, where mean ± SEM, and p>0.05) (Fig. 4.8B). The addition of 1, 10 and 100μM ADMA did not have any significant effect on the total distance travelled (172 ± 15.7μm, 173 ± 23.3μm and 160 ± 18.6μm respectively compared to 143 ± 14.1μm for untreated conditions, where mean ± SEM and p>0.05) (Fig. 4.8B). SDMA (100μM) also had no significant effect when compared to control and ADMA (100μM) (183 ±

22.6μm for 100μM SDMA compared to 160 ± 18.6μm for 100μM ADMA and 143 ± 14.1μm for untreated conditions, where mean ± SEM and $p>0.05$). The addition of SNP (100μM) significantly increased the distance travelled compared to control (199 ± 14.0μm compared to 143 ± 14.1μm for untreated conditions, where mean ± SEM and $*p<0.05$) (Fig. 4.8B).

The data above confirms the hypothesis that in quiescent conditions the genetic disruption of global DDAH2 significantly impairs primary macrophage motility and that further pharmacological addition of ADMA or SDMA does not alter this effect. To confirm this same hypothesis under inflammatory conditions, the same experiment was conducted but with the co-incubation of an inflammatory stimulus (LPS/TNF-α/IFN-γ).

The average speed of $DDAH2^{-/-}$ pMacs following the addition of an inflammatory cocktail was significantly reduced compared to $DDAH2^{+/+}$ pMacs (0.227 ± 0.0149μm/min for $DDAH2^{-/-}$ and 0.383 ± 0.0211μm for $DDAH2^{+/+}$, where mean ± SEM and $*p<0.05$) (Fig. 4.8C). The addition of 1, 10 and 100μM ADMA did not have any significant effect on the average speed travelled compared to control (0.208 ± 0.0204μm/min, 0.209 ± 0.0208μm/min and 0.218 ± 0.0213μm/min for 1, 10 and 100μM ADMA respectively, where mean ± SEM, and $p>0.05$) (Fig. 4.8C). Similarly the addition of 100μM SDMA had no significant effect on control or 100μM ADMA treated cells (0.269 ± 0.0304μm/min, 0.227 ± 0.0149μm/min and 0.218 ± 0.0213μm/min for 100μM SDMA, control and 100μM ADMA respectively, where mean ± SEM, and $p>0.05$). SNP had no significant effect on the speed travelled compared to control (0.203 ± 0.0242μm/min for 100μM SNP and 0.227 ± 0.0149μm/min for control for mean ± SEM, and $p>0.05$) (Fig. 4.8C).

When looking at the distance travelled, the results showed that the total distance travelled by inflammatory stimulated $DDAH2^{-/-}$ macrophages travelled significantly less than $DDAH2^{+/+}$ (239 ± 15.6μm for $DDAH2^{-/-}$ and 367 ± 20.2μm for $DDAH2^{+/+}$, where mean ± SEM and $*p<0.05$) (Fig. 4.8D). Following the addition of 1, 10 and 100μM ADMA in inflammatory stimulated conditions, there was no significant difference compared to control (219 ± 21.9μm, 220 ± 21.9μm and 229 ± 22.4μm for 1, 10 and 100μM ADMA respectively compared

to 239 ± 15.6μm for untreated, where mean ± SEM and $p>0.05$) (Fig. 4.8D). The addition of 100μM SDMA did not significantly alter motility compared to control or 100μM ADMA (268 ± 28.6μm, 239 ± 15.6μm and 229 ± 22.4μm for 100μM SDMA, control and 100μM ADMA respectively, where mean ± SEM, and $p>0.05$). Similarly the addition of SNP had no significant effect on the distance travelled compared to control (213 ± 25.4μm for 100μM SNP compared to 239 ± 15.6μm for untreated, where mean ± SEM and $p>0.05$) (Fig. 4.8D).

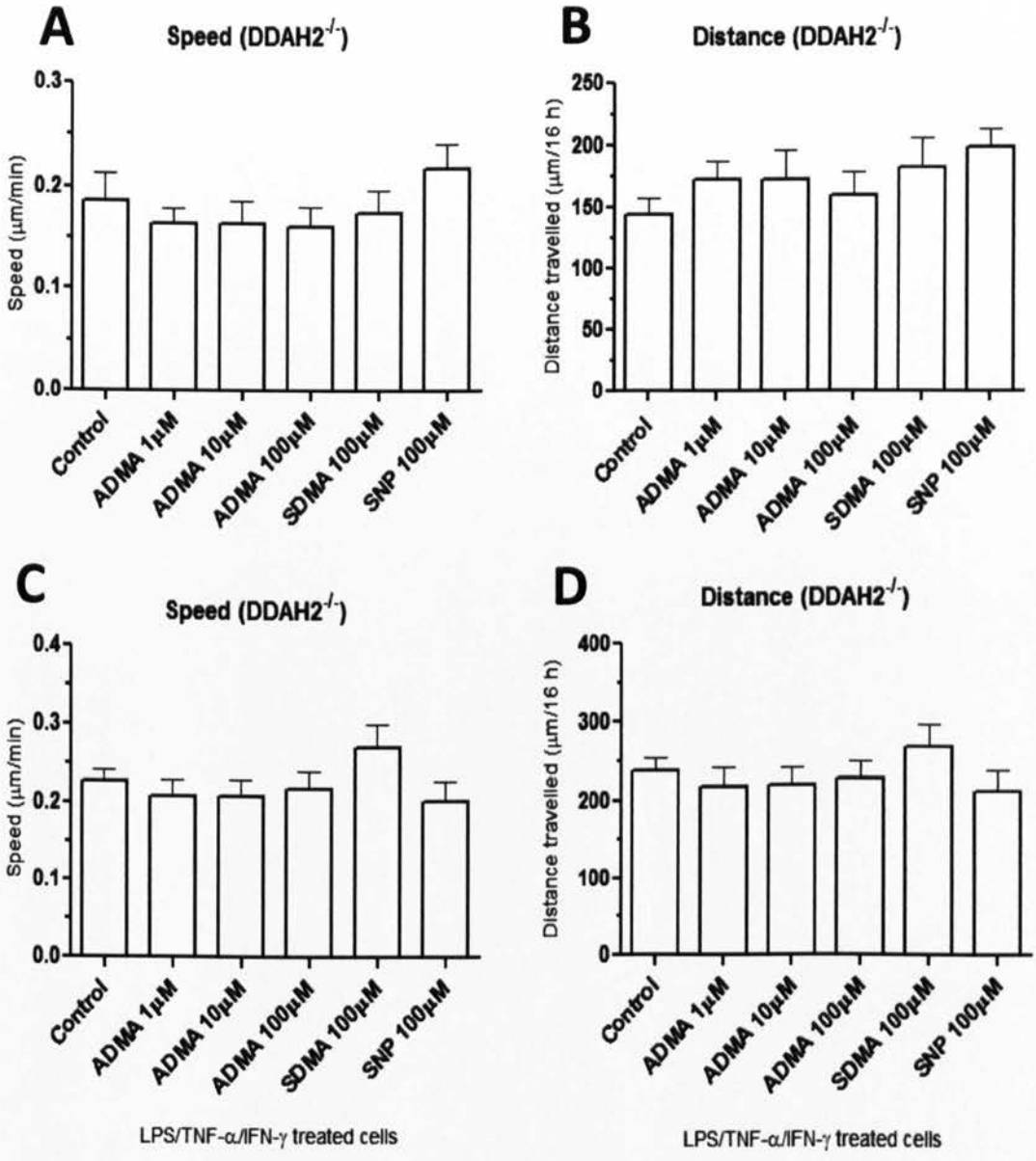

Fig. 4.8: Motility of primary macrophages obtained from DDAH2$^{-/-}$ mice under untreated or inflammatory treated conditions.

pMacs from DDAH2$^{-/-}$ were treated with ADMA (1, 10 or 100µM), SDMA (100µM) or SNP (100µM) under untreated (A and B) or inflammatory treated (C and D) conditions. The speed (A and C) and distance travelled (B and D) were determined for both cases. Results are representative of n=45 cells and 3 individual experiments. Significance was measured using a one-way ANOVA and a Bonferroni post-hoc test, where mean ± SEM and *p<0.05.

4.7.3 eNOS$^{-/-}$ primary macrophage motility

The results from the Griess assay suggested that eNOS may be required for macrophage NO production during inflammation. pMacs were extracted from eNOS$^{-/-}$ mice and their motility following inflammatory conditions was tracked as previously described. The motility of cells in quiescent conditions was not observed since even following maximal inflammatory stimulus eNOS$^{-/-}$ pMacs produced significantly similar levels of NO compared to DDAH2$^{+/+}$ macrophages in untreated conditions.

Following an inflammatory stimulus with LPS, TNF-α/IFN-γ, eNOS$^{-/-}$ pMacs travelled at significantly slower speed than DDAH2$^{+/+}$ pMacs under the same conditions (0.249 ± 0.0104μm/min for eNOS$^{-/-}$ compared to 0.383 ± 0.0211μm/min for DDAH2$^{+/+}$, where mean ± SEM and $*p<0.05$) (Fig. 4.9B). The exogenous addition of the 1 and 10μM ADMA and 500μM L-NAME had no significant effect on pMac speed compared to control (0.251 ± 0.0158μm/min, 0.236 ± 0.0140μm/min, and 0.228 ± 0.0104μm/min for 1μM, 10μM and 500μM respectively compared to 0.249 ± 0.0104μm/min for control, where mean ± SEM and $p>0.05$) (Fig. 4.9B). The addition of 10μM SDMA did not have any significant effect compared to the 10μM ADMA or control conditions (0.257 ± 0.0140μm/min for 10μM SDMA compared to 0.236 ± 0.0140μm/min for 10μM ADMA and 0.249 ± 0.0104μm/min for control, where mean ± SEM and $p>0.05$).

The total distance travelled by global eNOS$^{-/-}$ pMacs in response to an inflammatory stimulus mimicked the speed data. There was a reduction in total distance travelled by eNOS$^{-/-}$ pMacs compared to DDAH2$^{+/+}$ in control conditions (237.5 ± 10.23μm for eNOS$^{-/-}$ and 242.3 ± 17.51μm for DDAH2$^{+/+}$, where mean ± SEM and $*p<0.05$) (Fig. 4.9C). There was no significant difference in the distance travelled after the addition of 1 and 10μM ADMA or 500μM L-NAME compared to control (235 ± 13.7μm, 226 ± 13.6μm and 215 ± 9.44μm for 1 and 10μM ADMA and 500μM L-NAME respectively compared to 237.5 ± 10.23μm for control, where mean ± SEM and $p>0.05$). This is in

accordance with the suggestion that eNOS is not only critical to NO production, but also important for macrophage motility.

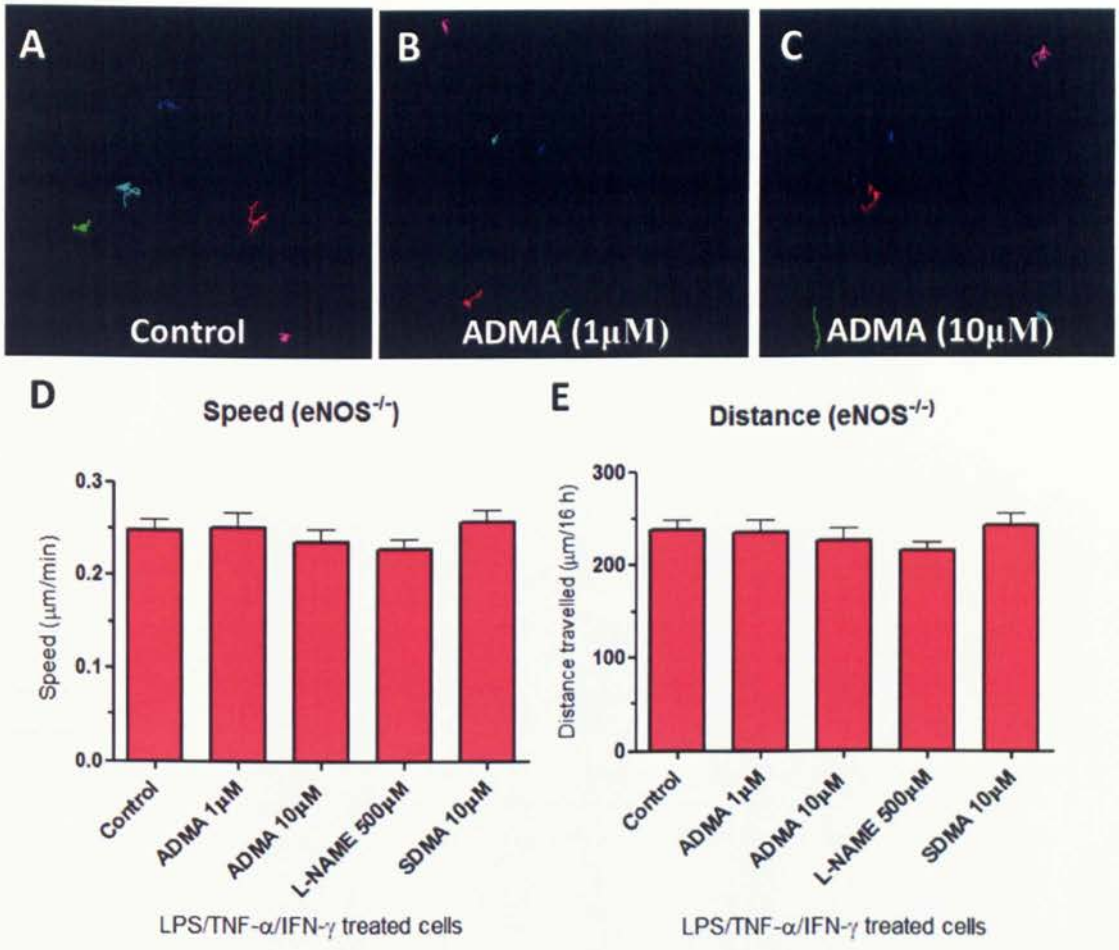

Fig. 4.9: Motility of primary macrophages obtained from eNOS$^{-/-}$ mice.

pMacs from eNOS$^{-/-}$ mice were treated with ADMA (1 or 10μM), L-NAME (500μM) or SDMA (10μM) under inflammatory conditions and their speed and distance travelled determined (D and E). Images of pMacs tracked following the treatment of control (A) ADMA 1μM (B) and ADMA 10μM (C) are shown. Results are representative of n=45 cells and 3 individual experiments. Significance was measured using a one-way ANOVA and a Bonferroni post-hoc test, where mean ± SEM and $*p<0.05$.

4.8 The effect of DDAH2 disruption on primary macrophage phagocytosis

Phagocytosis is dependent on cell motility, the ability of immune cells to recognise foreign pathogens and the ability to engulf them. This function was measured by monitoring the uptake of a fluorescent E-coli bio-particle - an established protocol previously used (Taylor *et al.,* 2010; Wheeler *et al.*, 2008). The aim of this part of the study was to determine whether DDAH2 regulates macrophage phagocytosis, and if so, how this corresponds with the previous findings in this chapter.

Under quiescent conditions, $DDAH2^{-/-}$ pMacs had lower levels of phagocytosis compared to $DDAH2^{+/+}$ (1.44 ± 0.51a.u for $DDAH2^{-/-}$ untreated pMacs and 3.01 ± 0.45a.u for $DDAH2^{+/+}$ untreated pMacs, where mean ± SEM and $*p<0.05$) (Fig. 4.10). Upon stimulation with an inflammatory cocktail, phagocytosis of $DDAH2^{+/+}$ pMacs increased significantly compared to $DDAH2^{-/-}$ under inflammatory stimulation conditions and $DDAH2^{+/+}$ in control conditions (5.73 ± 0.70a.u for inflammatory stimulated $DDAH2^{+/+}$ pMacs compared to 2.34 ± 0.45a.u for $DDAH2^{-/-}$ pMacs and 3.01 ± 0.45a.u for $DDAH2^{+/+}$ untreated pMacs, where mean ± SEM and $*p<0.05$) (Fig. 4.10). Unlike $DDAH2^{+/+}$ pMacs, in $DDAH2^{-/-}$ there was no significant difference between untreated and inflammatory stimulated $DDAH2^{-/-}$ pMacs (1.44 ± 0.51a.u for $DDAH2^{-/-}$ untreated pMacs and 2.34 ± 0.45a.u for $DDAH2^{-/-}$ in inflammatory stimulated conditions, where mean ± SEM and $p>0.05$). These data suggest that DDAH2 is important in regulating macrophage phagocytosis in both untreated and inflammatory conditions.

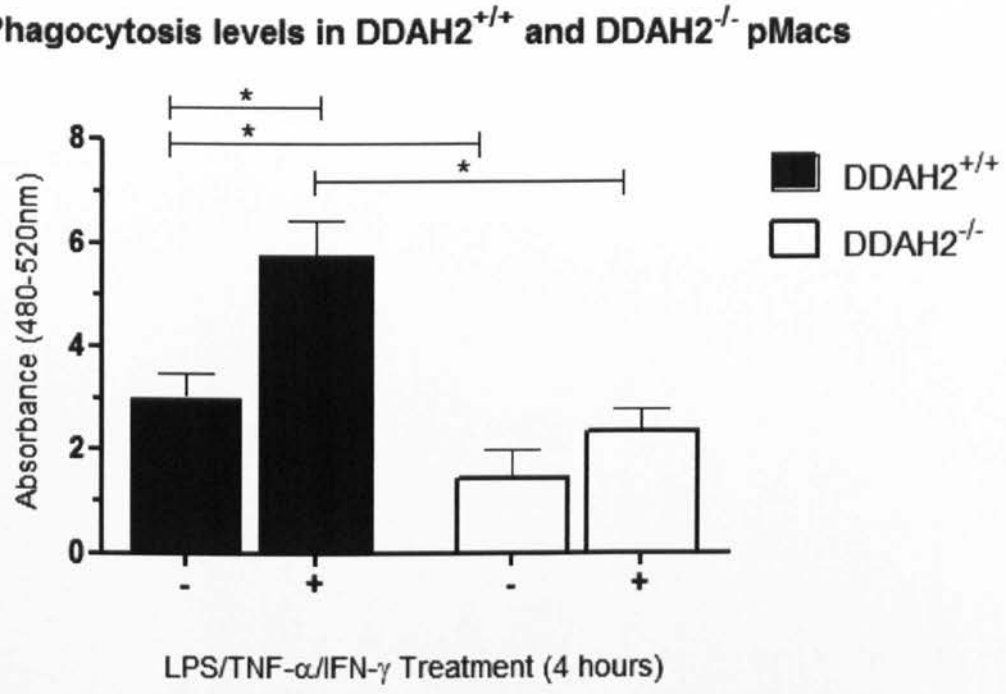

Fig. 4. 10: Phagocytosis of DDAH2$^{+/+}$ and DDAH2$^{-/-}$ pMacs in unstimulated or inflammatory stimulated conditions.

pMacs ($2x10^5$) from DDAH2$^{+/+}$ and DDAH2$^{-/-}$ were cultured in triplicate in a 96 well plate and treated with either an inflammatory cocktail (+) or left untreated (-) for 4 hours. Following treatment, the media was removed and cells were incubated with a fluorescent E-coli bio-particle for 2 hours followed by trypan blue for 1 minute. The absorbance at 480-520nm was measured using a spectrophotometer. Data is presented in response to a reference sample of media only (blank). Results correspond to n=4 experiments. Statistical significance was determined using a two-tailed statistical test (Mann-Whitney) and one-way ANOVA for analysis with a Bonferroni post-hoc test, where mean ± SEM and *p<0.05.

4.9 The effect of DDAH2 on macrophage proliferation

The BrdU assay was used to determine the effect of DDAH2 deletion on macrophage proliferation. The results from Fig. 4.11 demonstrated that in quiescent and inflammatory stimulated conditions there was no significant difference in proliferation between $DDAH2^{+/+}$ and $DDAH2^{-/-}$ pMacs. The absorbance of $DDAH2^{+/+}$ in resting and inflammatory cocktail stimulated conditions was 2.29 ± 0.214a.u and 2.51 ± 0.783a.u respectively whereas the absorbance for $DDAH2^{-/-}$ was 1.836 ± 267a.u and 1.649 ± 0.137a.u for resting and inflammatory stimulated conditions (where mean ± SEM, and $p>0.05$). This suggests that any differences seen in assays that are highly dependent on cell number, such as the phagocytosis assay, was not due to differences in the quantity of cells but was in fact a true representation of the data.

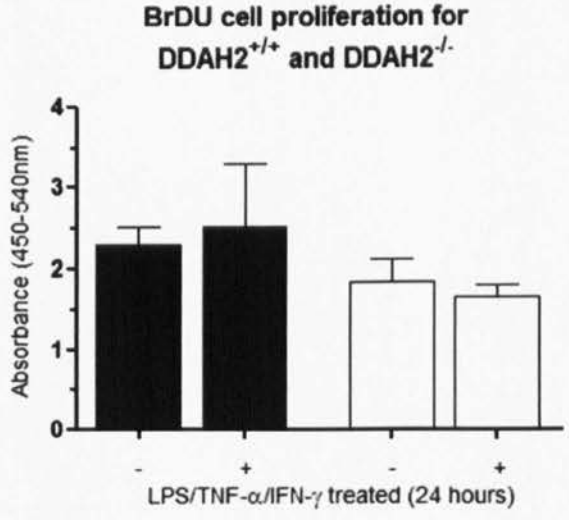

Fig. 4.11: BrDU cell proliferation assay comparing $DDAH2^{+/+}$ and $DDAH2^{-/-}$ macrophages.

pMacs ($1x10^5$) from $DDAH2^{+/+}$ and $DDAH2^{-/-}$ were plated in triplicate in 96 wells were treated with media only (-) or with an inflammatory control (+) for 24 hours. Data is representative of n=3 experiments and shows no significant difference ($p>0.05$) between the data using a one way ANOVA and a Bonferroni post-hoc test. Data is presented as mean ± SEM. (Black bars represent $DDAH2^{+/+}$ and white bars $DDAH2^{-/-}$).

4.10 Discussion

It is widely accepted that ADMA is an endogenous inhibitor of NOS and that elevated human plasma concentrations are associated with and predictive of increased cardiovascular risk (Vallance and Leiper, 2004; Schnabel *et al.*, 2005). Although it has been shown that the heterozygous knock-out of DDAH1 results in increased ADMA levels and reduction in NO signalling, which in turn causes vascular pathology (Leiper *et al.*, 2007), there is yet no clear understanding of how DDAH2 might effect ADMA levels in macrophages. To test this, we generated global DDAH2$^{-/-}$ mice and extracted primary peritoneal macrophages in order to carry out various functional assays.

The results from this chapter confirm the successful generation of a global DDAH2$^{-/-}$ mouse model. Western blotting confirmed the absence of DDAH2 in the heart, kidney and liver of DDAH2$^{-/-}$ mice compared to DDAH2$^{+/+}$ mice and showed that genetic knock-out of DDAH2 led to no compensatory increase in DDAH1 protein expression (Tran *et al.*, 2000). DDAH1 protein expression in the heart is very low in comparison with DDAH2 yet in accordance with previous studies (Jacobi *et al.*, 2005) it was picked up in this study, thus confirming the specificity of the DDAH antibodies.

To examine the effect of DDAH2 knockout on the concentration of free methylarginines, we analysed cultured pMacs using LS-MS/MS. We were able to quantify all three free methylarginines (ADMA, L-NMMA and SDMA) in pMacs. This analysis revealed for the first time significantly elevated ADMA and L-NMMA levels in pMacs from DDAH2$^{-/-}$ compared to DDAH2$^{+/+}$, whilst SDMA levels were undetectable. Although methylarginine levels in the plasma and specific tissue were not measured, significant research has demonstrated the effects of DDAH (1 and 2) on these. In accordance with our findings that SDMA was not present or was present in very low but undetectable concentrations in pMacs, previous research in plasma and tissue homogenates has also shown very little SDMA present and DDAH2 was not

found to affect these concentrations (Leiper *et al.*, 2007; Cardounel and Zweier, 2002).

It has been previously reported that significant concentrations of L-NMMA are present in plasma and tissue (Paik *et al.*, 2007; McDermott, 1976; Cardounel and Zweier, 2002). In a study yet to published by our lab (Wang *et al.*, In Press), L-NMMA levels were found to be significantly elevated in heart lysates and plasma of $DDAH2^{-/-}$ mice, whilst ADMA levels were elevated in the heart but no change was detected in the plasma. These findings implicate DDAH2 as a critical determinant of L-NMMA concentrations *in vivo* and since both L-NMMA and ADMA are approximately equally potent inhibitors of eNOS (Cardounel and Zweier, 2002), highlight the significant inhibitory effect that a DDAH2 knockout may have on eNOS function. This is particularly important if eNOS is thought to be necessary for macrophage induced NO production (Connelly *et al.*, 2003).

Various reports have suggested DDAH1 and not DDAH2, to be responsible for the majority of DDAH activity under basal conditions. In contrast to $DDAH2^{-/-}$, both $DDAH1^{+/-}$ and endothelial-specific $DDAH1^{-/-}$ mice had significantly elevated ADMA concentrations in the plasma, lung and brain (Leiper *et al.*, 2007; Hu *et al.*, 2009). Similarly transiently knocking out DDAH1 using siRNA was found to increase plasma ADMA concentrations in rats whilst the same DDAH2 knockout did not have an effect (Wang *et al.*, 2007).

The Griess assay was used to determine NO_2^- (a stable by-product of NO) production from pMacs in response to an inflammatory stimulus. Although the disruption of DDAH2 did not totally abolish NO_2^- production, $DDAH2^{-/-}$ pMacs had significantly reduced NO_2^- levels over time compared to $DDAH2^{+/+}$ (approximately 50% less).

Our data also suggests eNOS to be critical in macrophage-produced NO. Compared to pMacs from $DDAH2^{+/+}$ and $DDAH2^{-/-}$ mice, $eNOS^{-/-}$ pMacs produced significantly less NO in response to an inflammatory stimulus. The essential role for eNOS in the activation and production of NO by

macrophages has been closely examined by others. Previous studies have revealed that eNOS acts in a pro-inflammatory manner in immune cells by facilitating iNOS expression in response to endotoxin, whereby a 50% reduction in iNOS expression and activity was observed in $eNOS^{-/-}$ bone marrow-derived macrophages compared to their WT controls (Connelly *et al.*, 2003). Similarly, iNOS expression was reduced in the lung, liver, heart and aorta of $eNOS^{-/-}$ following LPS stimulation compared to WT mice (Connelly *et al.*, 2003). The enzymatic action of macrophage iNOS is more than to generate NO: NADPH and L-arginine are consumed, BH_4 is oxidised and citrulline is generated (MacMicking *et al.*, 1997). In quiescent macrophage conditions, where there is low iNOS activity, DDAH and iNOS inhibition will have little effect on NO production and other pathway-associated co-factors.

Although eNOS appears to be critical to macrophage induced NO production by enhancing iNOS expression and activity, iNOS is still the predominant isoform in macrophages and is also important in endotoxin-induced NO production. The pharmacological inhibition of iNOS using 1400W confirms this, whereby NO production from pMacs from $DDAH2^{+/+}$ mice following inflammatory stimulus was completely abolished following iNOS inhibition. Similarly, $iNOS^{-/-}$ mice have very low survival rates following infection with *L. Monocytogens* and *M.* tuberculosis (MacMicking *et al.*, 1995) highlighting the importance of iNOS in host protection following infection. This shows that generally disrupting NOS, rather than DDAH2, has a more severe effect on macrophage activation. This may be explained by the fact that inhibiting NOS prevents any NO production whereas inhibiting DDAH2 increases methylarginines and therefore competition for the substrate, L-arginine.

Moreover, NO production has also been shown to affect endothelial (Wojciak-Stothard *et al.*, 2007) and trophoblast (Ayling *et al.*, 2006) motility. In our studies, real-time imagining was used to determine the effects of DDAH2 deletion on macrophage motility. Manual cell tracking was used to investigate the motility (total distance travelled and the speed) over a given time. $DDAH2^{+/+}$ significantly increased following inflammatory stimulation and

ADMA significantly reversed this effect. Our data has revealed for the first time that DDAH2 regulates pMac motility since DDAH2$^{-/-}$ pMacs had impaired motility in both quiescent and inflammatory stimulated conditions compared to DDAH2$^{+/+}$. These data compliment previous results seen with ADMA and/or DDAH1 expression on motility. In trophoblasts, DDAH1 was found to regulate their invasion and motility through NO effects (Ayling *et al.*, 2006) whilst pharmacological addition of ADMA in endothelial cells reduced NO levels and motility (Wojciak-Stothard *et al.*, 2007).

Another possible action of altered DDAH expression may be through the effects of the production of growth factors such as vascular endothelium growth factor (VEGF), because increased DDAH expression has been shown to increase tumour and endothelial VEGF production (Kostourou *et al.*, 2002; Smith *et al.*, 2003). Hasegawa *et al* showed DDAH2 overexpression increases endothelial VEGF production, proliferation and migration via the transcription factor SP-1 and independent of ADMA (Hasegawa *et al.*, 2006). Although VEGF has been shown to affect macrophage motility (Berse *et al.*, 1992), in our hands, the disruption of DDAH2 had no significant effect on macrophage VEGF expression when compared to DDAH2$^{+/+}$ confirming that VEGF expression is not DDAH2 dependent (see Appendix) (Wang *et al.*, In publication).

All of the above data indicate that DDAH2 plays an important role in macrophage function and that DDAH2 disruption results in an inhibition in macrophage inflammatory-stimulated NO production, motility and phagocytosis. This could help explain the results observed by our group in sepsis mice. Global DDAH2$^{-/-}$mice had significantly faster deterioration times and higher mortality rates compared to DDAH2$^{+/+}$ following Caecum Ligation Puncture (CLP) (an inducer of sepsis). This was correlated with an increased bacterial titre in blood and the peritoneal washout (Fig. 4.12). These data depict the complexity of diseases such as sepsis because DDAH1 inhibition by compound L-257 has been suggested to be a putative therapeutic option by stabilising blood pressure and increasing cardiac output (Nandi *et al.*,

2012). However, we know that DDAH1 is not present in immune cells therefore this inhibitor does not work directly through the inhibition of DDAH2 in immune cells such as macrophages.

A promising solution would be to design and develop a selective DDAH2 inhibitor as a therapeutic target in diseases which are mediated in part by macrophages. Such an inhibitor may help reduce the progression of arthritis or atherosclerosis by inhibiting further macrophage infiltration, motility and phagocytosis in the plaque or fibrous cap. Various well-known pharmaceutical agents, such as; ACE-inhibitors, statins and NSAID's have already been shown to be effective in reducing ADMA levels by modulating DDAH and/or PRMT activity or expression (Arrigoni *et al.*, 2010).

DDAH2 is predominantly expressed in immune cells; however, it is also expressed in many tissues. Although the data obtained here seem to show interesting and novel correlations between DDAH2 and macrophages, the limitation that these effects seen (in particular the sepsis data) can be due to a DDAH2 deletion in other tissues or cells cannot be ruled out. Using a global $DDAH2^{-/-}$ mouse model uses a genetic approach to test long-term exposure of increased ADMA levels in all cells and tissues that express this gene. Since we are only interested in determining the effect of DDAH2 on macrophages, a far better approach would be to target DDAH in these cells specifically rather than globally.

Conclusion

DDAH2 has been shown to be important in macrophage function. In this chapter I set out to ascertain whether the global DDAH2$^{-/-}$ disruption has any effect on macrophage motility and phagocytosis. We can reject our null hypothesis and conclude that:

1. *DDAH2 metabolises the intracellular methylarginines ADMA and L-NMMA in pMacs.*

2. *eNOS and iNOS are pro-inflammatory mediators of pMac NO-production.*

3. *DDAH2 is a critical regulator of pMac motility and phagocytosis both basally and in inflammatory conditions, and may explain the increased mortality rates seen in DDAH2$^{-/-}$ mice compared to DDAH2$^{+/+}$ mice in a sepsis model.*

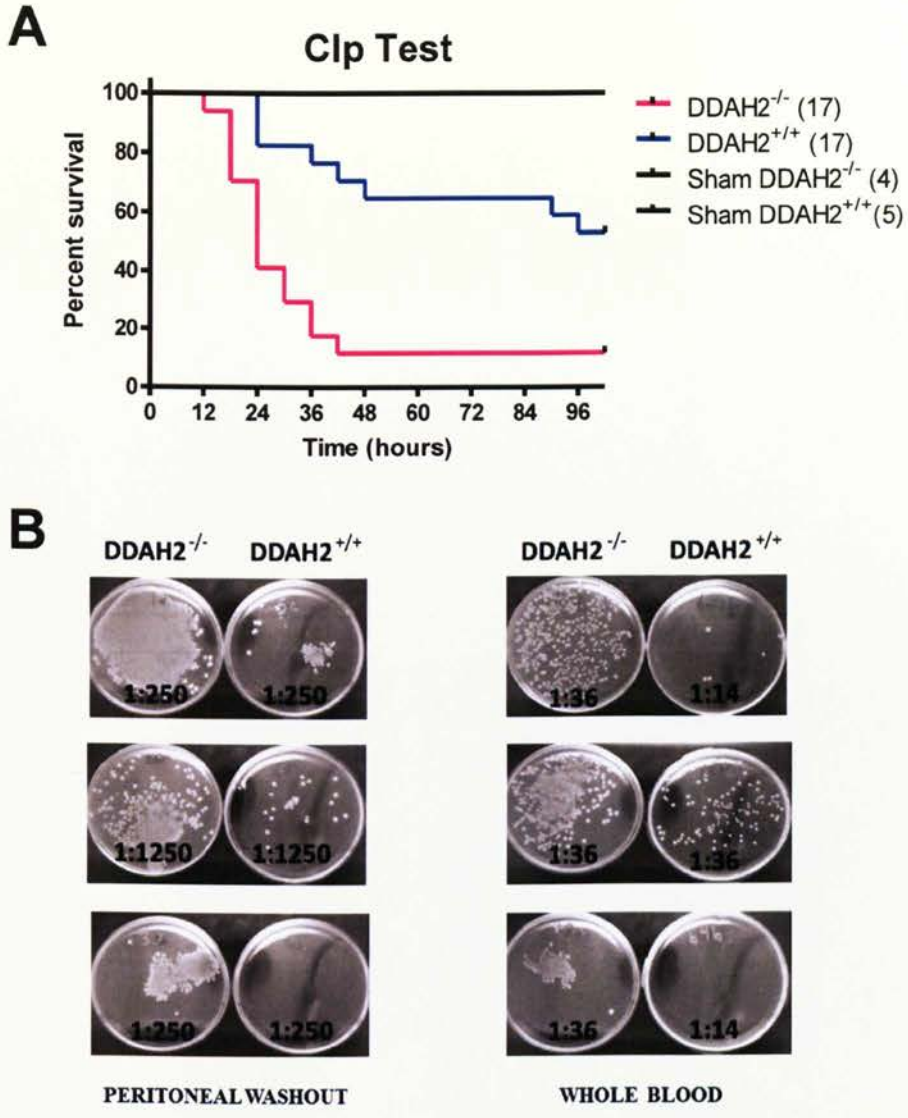

Fig. 4.12: Combined data of percentage survival and bacterial titre in DDAH2$^{+/+}$ and DDAH2$^{-/-}$ animals after CLP.

(A) The percentage survival was measured over a period of 96 hours for DDAH2$^{+/+}$ and DDAH2$^{-/-}$ mice following CLP. Sham-operated animals without any CLP where used as a negative control for both phenotypes. (B) The peritoneum was washed with PBS and whole blood was obtained following cardiac puncture 6 hours after CLP. The overall data represents a significant reduction in DDAH2$^{-/-}$ animal survival and increased bacterial titre in the blood and peritoneal washout compared to DDAH2$^{+/+}$ mice suggesting that DDAH2 disruption leads to increased death in a sepsis model. Black line represents Sham (without CLP, n=5 and n=4 for DDAH2$^{+/+}$ and DDAH2$^{-/-}$ respectively), blue line represents DDAH2$^{+/+}$ (n=17) and pink line represents DDAH2$^{-/-}$ (n=17). (Data taken with permission from Kelly, P., 2011).

CHAPTER 5

Creation and characterisation of a macrophage specific DDAH2 knock-out mouse

5.1 Introduction

The process of synthesising NOS inhibitors occurs in all cells irrespective if they express NOS. ADMA can inhibit all isoforms of NOS, and ADMA made in one cell can inhibit NO synthesis in adjacent cells (Fickling *et al.*, 1999). So far we have shown that pharmacological manipulation of ADMA and the global genetic deletion of DDAH2 regulate macrophage function.

The results presented in Chapter 4 relied heavily on the use of pMacs extracted from global DDAH2$^{-/-}$ mice. DDAH2 is known to be associated predominantly with tissues that express eNOS (Vallance and Leiper, 2004; Gray *et al.*, 2009; Palm *et al.*, 2007; Wojciak-Stothard *et al.*, 2007, Zakezewicz and Eickelberg, 2009; Birdsey *et al.*, 2000; Smith *et al.*, 2003; Tran *et al.*, 2003; Tanaka *et al.*, 2005) and decreased DDAH expression/activity is evident in disease states associated with endothelial dysfunction. Wang *et al.* showed that *in vivo* DDAH2 gene silencing significantly inhibited vascular endothelium-dependent relaxation response to acetylcholine without affecting plasma ADMA levels (Wang *et al.*, 2007). These findings were supported by later reports demonstrating that down-regulation of DDAH2 in response to hyperhomocesterinemia was not associated with increased plasma ADMA levels (Dayal *et al.*, 2008).

These results are particularly important because endothelial cells and macrophages are both important NO producing cells. More specifically, endothelial cells are critical for the induction of macrophage differentiation and activation (He *et al.*, 2012). Similarly we know that eNOS is dependent on ADMA concentrations thus increased inhibition of eNOS by increased endogenous ADMA due to the global disruption of DDAH2 may lead to reduced macrophage-synthesised NO.

In order to confirm the effects seen in the previous experiments with DDAH2$^{-/-}$ pMacs, a macrophage-specific DDAH2 knock-out model was generated for the first time. Like the global DDAH2$^{-/-}$, this genetic approach is a measure of increased ADMA levels but in this case this occurs only in macrophages. As described previously, pMacs will be extracted from the peritoneal cavity and

the same protocols will be followed. This method of genetic manipulation aims to validate, more specifically, the role of DDAH2 as a regulator of macrophage function through an ADMA dependent or independent mechanism.

5.2 Specific Aims

To date, we have determined the functional effects of the pharmacological manipulation of exogenous NO levels in human macrophages and have used a genetic approach to investigate whether there is a similar effect following DDAH2 disruption. The genetic data, in particular, provides information regarding the effect of global DDAH2 deletion, thus the main aim of this chapter was to determine the effects of a novel DDAH2 macrophage specific mouse model on macrophage function.

The hypothesis in this chapter is that:

> ***DDAH2, through an ADMA dependent mechanism, is a key regulator of macrophage function.***

Thus, the null hypothesis (H_0) is that:

> ***DDAH2 is not a key regulator of macrophage function.***

In order to accept or reject my null hypothesis, the following aims were generated:

1. **Confirmation of specific macrophage DDAH2 disruption.**
   RT-qPCR, PCR and western blotting will be used to confirm the specific deletion of DDAH2 in macrophages.

2. **Determination of intracellular methylarginine concentrations.**
   The methylarginines ADMA, L-NMMA and SDMA will be measured in primary macrophage lysates using LC-MS/MS.

3. **Investigate the effect of DDAH2 on macrophage NO_2^- production**.
   The Griess assay will be used to determine NO_2^- production following pro-inflammatory stimulation of macrophages extracted from $DDAH2^{flox/flox}$ LysM-Cre, $DDAH2^{+/+}$ and $DDAH2^{-/-}$ mice.

4. **Confirmation of the specific effect of DDAH2 and pharmacological methylarginine addition on macrophage motility.**
   Motility (speed and distance travelled) will be determined in pMacs extracted from DDAH2$^{flox/flox}$ LysM-Cre, DDAH2$^{+/+}$ and DDAH2$^{-/-}$ mice using real-time imaging.

5. **Elucidate the specific effect of DDAH2 depletion on primary macrophage phagocytosis.**
   Phagocytosis in DDAH2$^{flox/flox}$ LysM-Cre, DDAH2$^{+/+}$ and DDAH2$^{-/-}$ pMacs will be measured by monitoring the uptake of a fluorescently labelled E-coli bio-particle.

6. **Investigate the specific role of DDAH2 in macrophage proliferation.**
   The BrDU assay will be used to determine the cell viability and proliferation of macrophage extracted from DDAH2$^{+/+}$ and DDAH2$^{-/-}$mice.

7. **Examine the effects of specific macrophage DDAH2 deletion on intracellular cytokine production following stimulation with an inflammatory cocktail.**
   RT-qPCR was used to determine intracellular expressions of iNOS, TNF-α, IL-1β and IL-6 in untreated or inflammatory stimulated pMacs extracted from DDAH2$^{flox/flox}$ LysM-Cre, DDAH2$^{+/+}$ and DDAH2$^{-/-}$ mice.

5.3 Generation of DDAH2$^{flox/flox}$ LysM-Cre mice

Lysosomes are membrane-bound organelles that are present in animal cells and contain acid hydrolases. Their role is to receive and degrade macromolecules from the secretory, endocytic, autophagic and phagocytic membrane-trafficking pathways (Luzio *et al.*, 2007). Mice express two types of lysozyme genes; LysM, which is the predominant protein in most cells including alveolar macrophages (Klockars, 1974) and LysP (Markart *et al.*, 2004).

In 1999, Clausen and Forster developed a highly specific LysM-Cre strain that is 83-90% efficient in the deletion of the LoxP-flanked target genes in macrophages (and 100% in granulocytes but no deletion in T and B cells) (Clausen *et al.*, 1999). To date the LysM-Cre method is the most efficient method of specific deletion of target genes in macrophages so this method was used. More specifically, the Cre deletion recombination is added between the two *Lox*P sites which then allow deletion of the *Lox*P flanked sequence. A stop codon is inserted before the end of the second *Lox*P site. After breeding, a Cre *Lox*P mouse is produced where the original selected gene function is disrupted and a transporter gene is transcribed instead. The gene lacks Cre recombinase so the original gene function is untouched (see Fig. 5. 1 and Fig. 5. 2). LysM-Cre mice are available from the Jackson Laboratories (Bar Habor, ME, USA) and have been used extensively in conditional gene-targeting studies, with more than 200 citations by 2010.

In the previous chapter DDAH2 was disrupted ubiquitously therefore for this chapter it was decided that the target gene, DDAH2, should be deleted in only the macrophage specific promoter. The aim of generating such a knock-out was to help ascertain the specific effect of DDAH2 deletion on macrophage function irrespective of DDAH2 function in other cells. The DDAH2$^{flox/flox}$ LysM-Cre mice generated are a novel mouse model designed to succinctly investigate the role of macrophages in the ADMA-DDAH pathway

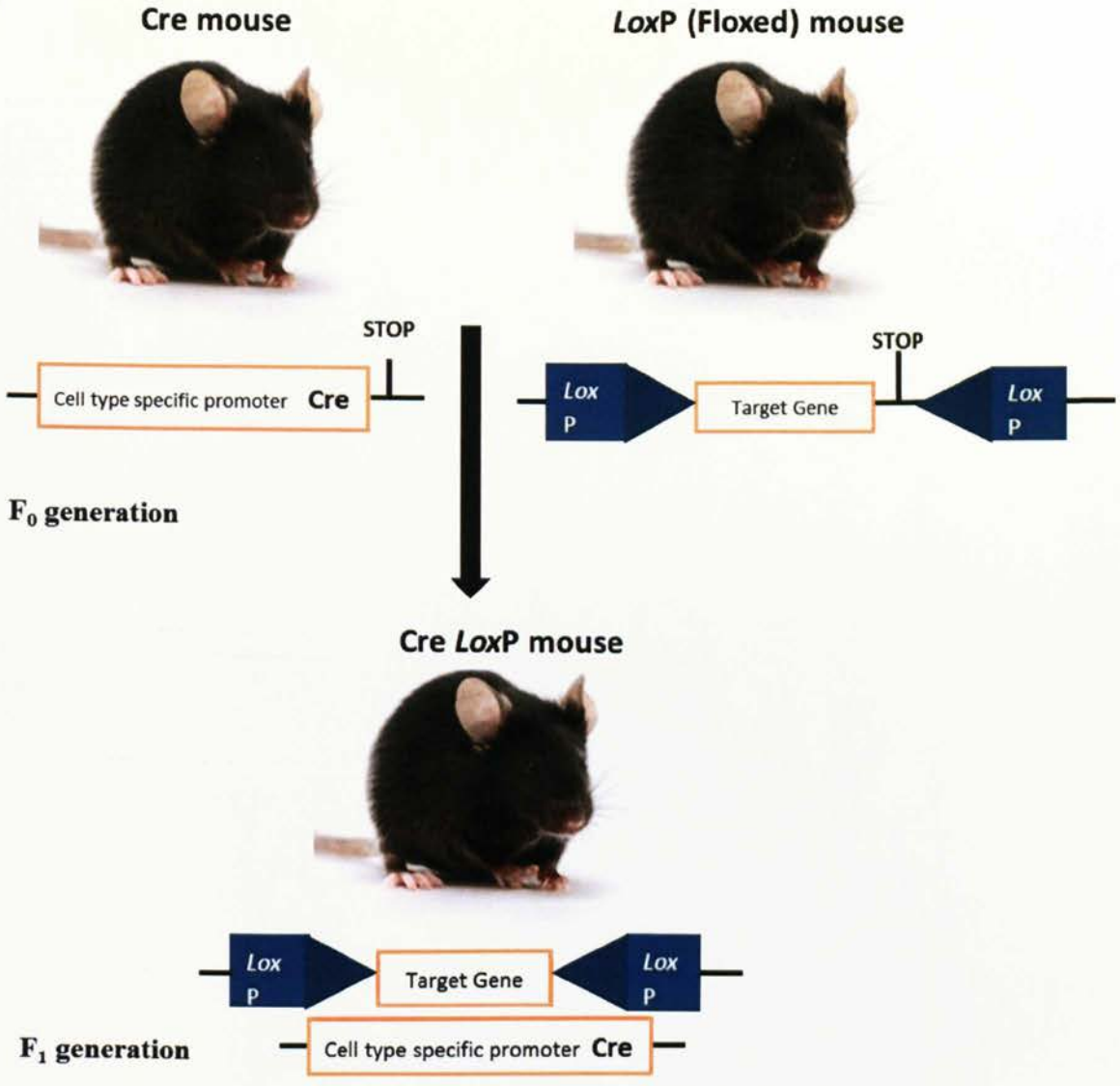

Fig. 5.1: A model experiment using the Cre-Lox system

In this model the function of a target gene is disrupted by a conditional knock-out. This is performed with a tissue specific promoter (macrophages) driving the expression of the Cre-recombinase. In next generation animals, the original gene function is disrupted and a reporter gene is transcribed instead producing animals with the targeted gene deletion at a specific cell type. In this case DDAH2 is the target gene and macrophages are selected as the cell type-specific promoter. The breeding and maintenance of colonies was carried out by Matthew Delahaye.

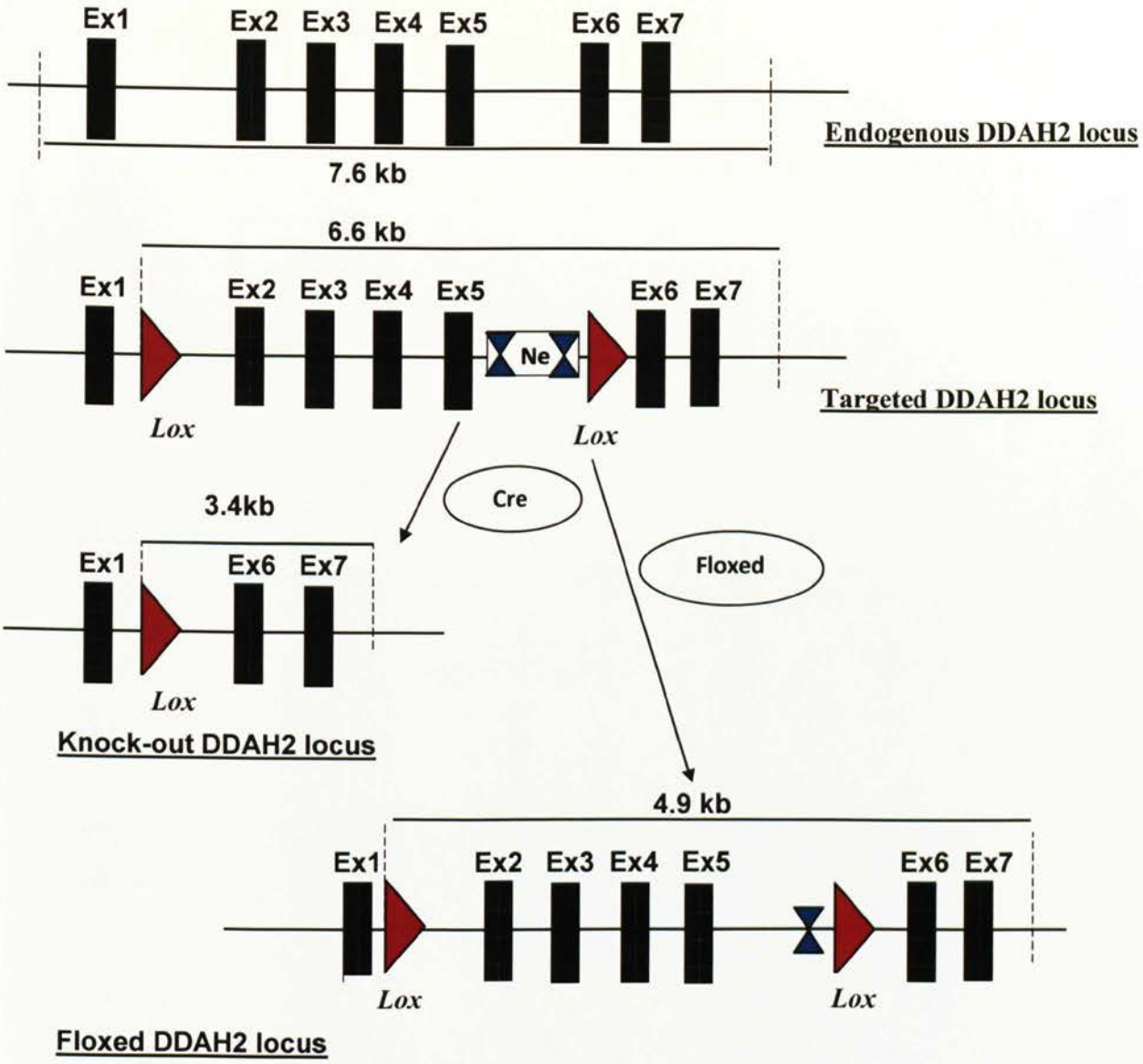

Fig. 5.2: Cre and Loxed-mediated excision of the targeted DDAH2 locus.

A schematic representation of the wild type, targeted, floxed and knock-out DDAH2 alleles with the relevant restriction sites. The targeted DDAH2 locus area is between exon 2-5 (3.2 kb). Following addition of a neomycin cassette at the *Lox*P sites, the DDAH2 locus size is reduced to 3.4 kb in the DDAH2$^{flox/flox}$ LysM-Cre and 4.9 kb in the floxed allele. DDAH2$^{flox/flox}$ animals are used as WT controls to the DDAH2-specific knock-out animals as they have undergone the same *Lox*P insertions.

Due to the fact that the LysM-Cre method of DDAH2 deletion in only macrophages is different to the global DDAH2$^{-/-}$ animals generated previously, the primers used to determine RNA levels were different. In addition, the fragmented allele sizes were different between the different animals and their corresponding wild-types. The expected fragment size in Cre and floxed southern blot analysis and the primers used for determining the LysM-Cre deletion are shown in Table 5.1 and Table 5.2.

Wild-type	7618 bp
Targeted	6635 bp
Floxed-excised	4961 bp
Cre-excised	3385 bp

Table 5.1: Expected fragmented sizes in Cre and floxed Southern blot analysis.

The estimated fragment size for the Floxed and Cre-excised alleles is reduced after the insertion of the specific *Lox*P.

LysM	Forward primer, PCR	CTCAAAAGCCCGAGCTATCC
	Reverse primer, PCR	CATCTGGGAGGGTCAGAGAG
LysM	Forward, RT- qPCR	TCAACGGTACCGGTCTCAG
	Reverse, RT-qPCR	CATCTGGGAGGGTCAGAGAG
Pol-2	Forward, RT-qPCR	CCGCTCATGAAATGCTCCTT
	Reverse, RT-qPCR	CGGGTCACTCTCCCCATGT

Table 5.2: Primer sequences for DDAH2$^{flox/flox}$ LysM-Cre mouse genotyping PCR.

PCR primers used to genotype DDAH2$^{flox/flox}$ LysM-Cre are shown above. Polymerase 2 was used as a standard housekeeper control in RT-qPCR experiments and when compared with β-actin, another often used common housekeeper gene, smaller changes in RNA levels were seen. Two different primers LysM primers were used for standard end-point PCR and RT-qPCR.

5.4 DNA, RNA and protein expression of macrophages and tissues from DDAH2$^{flox/flox}$ LysM-Cre.

The results showed that when comparing wild type animals with DDAH2$^{-/-}$, different size bands are seen (DDAH2$^{+/+}$, 230bp and DDAH2$^{-/-}$, 160bp). When comparing macrophages from DDAH2$^{flox/flox}$ and DDAH2$^{flox/flox}$ LysM-Cre the Cre is apparent in the DDAH2$^{flox/flox}$ LysM-Cre mice whereas in the DDAH2$^{flox/flox}$ there is no Lys M-Cre (Fig. 5.3A). In terms of RNA quantification, RT-qPCR data shows that DDAH2 levels in DDAH2$^{flox/flox}$ LysM-Cre were significantly lower compared to DDAH2$^{flox/flox}$ macrophages and proved the deletion of DDAH2 in LysM animals (Fig. 5.3C). RNA expression of DDAH2 was not measured in DDAH2$^{-/-}$ mice as they have an insertion into the DNA sequence therefore DDAH2 will still be present in RNA (as is seen for DDAH2$^{+/+}$) but will not be functionally active.

The tissue protein expression revealed that DDAH1 was present in the heart, kidney and liver in all the samples irrespective of the genotype (Fig. 5.3D). The low levels of DDAH1 protein expression (37kDa) in the heart of all the three genotypes confirmed that DDAH1 is not highly expressed in this tissue. Contrary to this, both the kidney and liver had high levels of DDAH1 expression; however, there was no significant difference between the genotypes. These data also showed no evidence for compensatory upregulation of DDAH1 in these tissues following deletion of DDAH2 (Fig. 5.3E).

The protein expression of DDAH2 (37kDa) showed that it was present in the heart, kidney and liver of DDAH2$^{+/+}$ and DDAH2$^{flox/flox}$ LysM-Cremice but not in DDAH2$^{-/-}$ mice (Fig. 5.3D and Fig. 5.3F). These data confirmed the successful deletion of DDAH2 in macrophages only in DDAH2$^{flox/flox}$ LysM-Cre without any compensatory increase of DDAH1 or DDAH2 in other tissue. Furthermore, DDAH2 was found to be the only DDAH protein present in human macrophages (Fig. 5.3B).

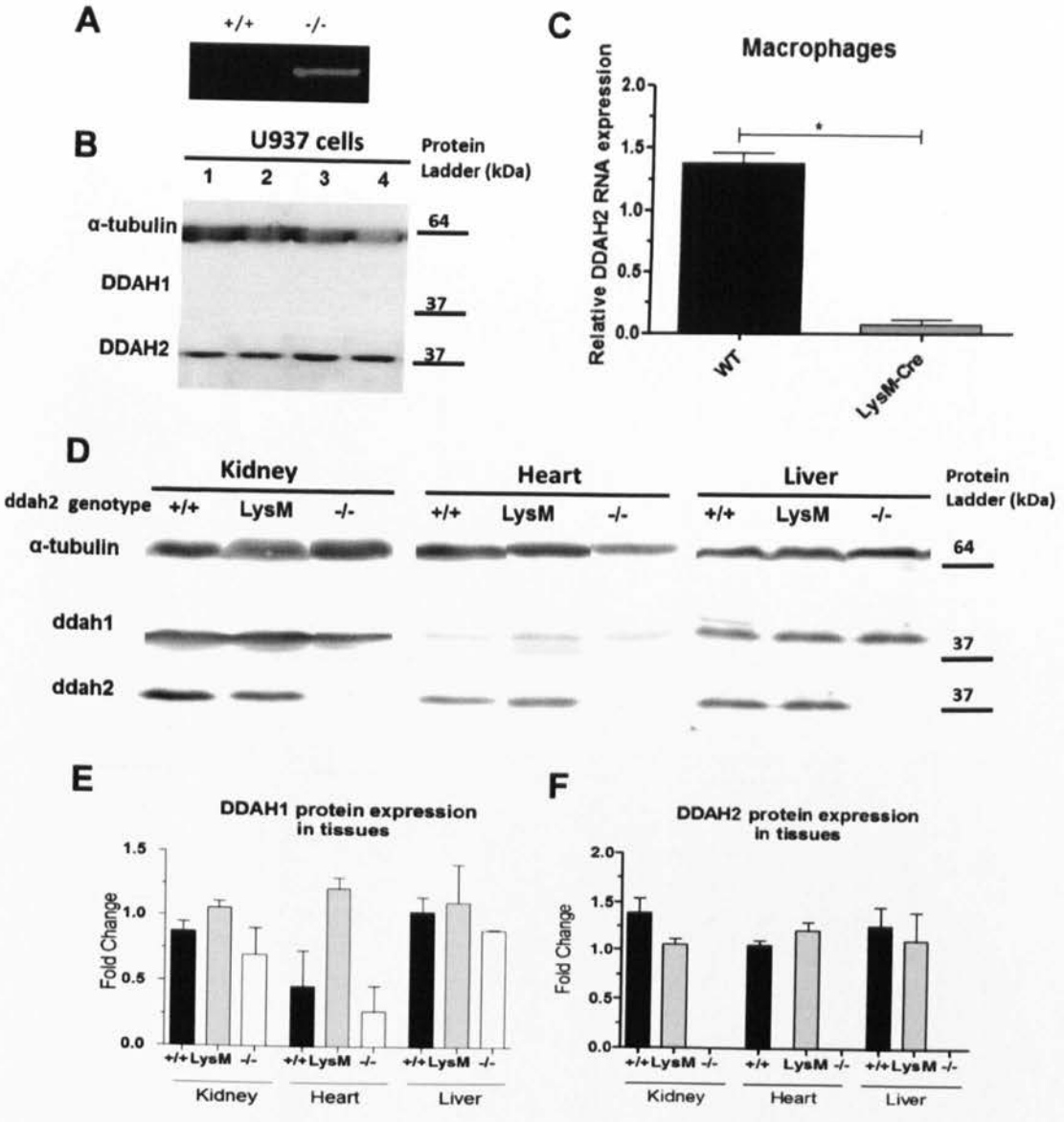

Fig. 5.3: RNA and protein expression of pMacs and tissues of DDAH2$^{+/+}$, DDAH2$^{flox/flox}$ LysM-Cre and DDAH2$^{-/-}$ mice and U937 cells.

(A) Genotyping for DDAH2$^{flox/flox}$ and DDAH2$^{flox/flox}$ LysM-Cre mice was carried out using PCR. (B) DDAH1/2 protein expression in U937 cells. (C) DDAH2 RNA expression of pMacs from DDAH2$^{flox/flox}$ and DDAH2$^{flox/flox}$ LysM-Cre mice was determined using RT-qPCR. (D) Protein expression of DDAH1/2 in the kidney, heart and liver were determined using western blotting. (E) Results for DDAH1 (37kDa) (F) and DDAH2 (37kDa) were quantified using Licor-Imaging normalised against their α-tubulin (64kDa) controls. Fold change was calculated against the liver tissue and statistical analysis was carried our using a one-way ANOVA (n=4). (+/+, LysM and -/- represent DDAH2$^{+/+}$, DDAH2$^{flox/flox}$ LysM-Cre and DDAH2$^{-/-}$ respectively).

5.5 Intracellular ADMA and L-NMMA levels in primary peritoneal macrophages

The ADMA, L-NMMA and SDMA levels were measured as previously described in the methodology. Briefly macrophage cell lysates were collected from $DDAH2^{+/+}$ and $DDAH2^{flox/flox}$ LysM-Cre mice. D7 ADMA, an internal standard used for the quantification of ADMA, L-NMMA and SDMA, was added to the cell samples followed by methanol. Samples were centrifuged, the supernatant collected and spun again in a vacuum for 1 hour to remove excess methanol. A mobile phase (0.1% formic acid) was added to the samples and intracellular methylarginine concentrations measured using liquid chromatography-mass spectrometry (LC-MS/MS).

The data shows that SDMA was not present in any of the samples. The data from Fig. 5.4A shows that the deletion of DDAH2 in macrophages resulted in a significant increase in ADMA levels (5.25 ± 0.441μM and 16.78 ± 3.95μM for $DDAH2^{+/+}$ and $DDAH2^{flox/flox}$ LysM-Cre pMacs, where mean ± SEM and $*p<0.05$). Similarly, in $DDAH2^{flox/flox}$ LysM-Cre pMacs there were also significantly increased L-NMMA concentrations compared to $DDAH2^{+/+}$ pMacs, which had undetectable levels of L-NMMA in the same conditions (31.87 ± 6.483, where mean ± SEM and $*p<0.05$) (Fig. 5.4B). These data confirm that DDAH2 is a critical regulator of methylarginine concentrations in pMacs.

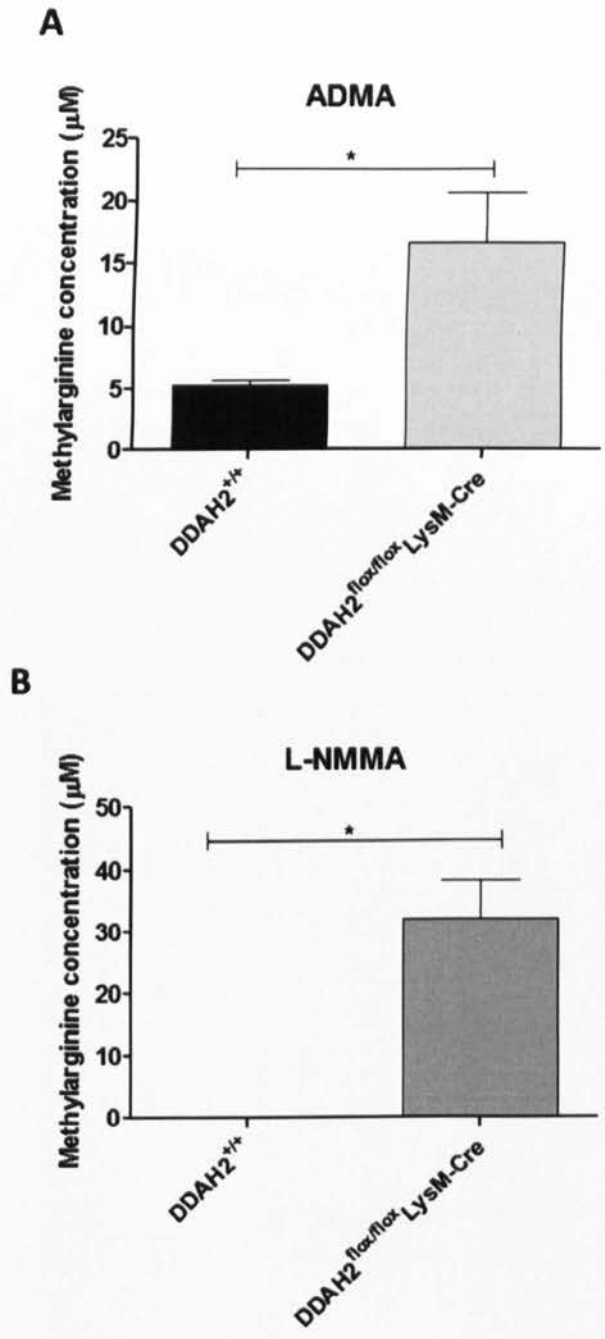

Fig. 5.4: Intracellular concentrations of the methylarginines ADMA and L-NMMA in DDAH2$^{+/+}$ and DDAH2$^{flox/flox}$ LysM-Cre macrophage lysates.

Intracellular (A) ADMA and (B) L-NMMA levels were measured in DDAH2$^{+/+}$ and DDAH2$^{flox/flox}$ LysM-Cre macrophages using LC-MS/MS. Results are indicative of n=3 and significance was determined using an unpaired t-test, where mean ±SEM and *p<0.05. Black bars represent DDAH2$^{+/+}$ and grey bars represent DDAH2$^{flox/flox}$ LysM-Cre pMacs.

5.6 DDAH2 in macrophages regulates their NO production

Briefly, pMacs extracted from DDAH2$^{+/+}$, DDAH2$^{-/-}$ and DDAH2$^{flox/flox}$ LysM-Cre were stimulated maximally by the simultaneous addition of LPS (5µg/mL), TNF-α (10ng/mL) and IFN-γ (100units/mL) to produce maximal NO production.

The addition of an inflammatory cytokine cocktail to DDAH2$^{+/+}$pMacs increased NO_2^- production significantly over a time course of 48 hours (4.91 ± 0.53µmol, 18.4 ± 1.83µmol, 42.6 ± 4.79µmol at 6, 24 and 48 hours respectively, where *p<0.05) (Fig. 5.5). This confirmed that pMacs from DDAH2$^{+/+}$ produced high levels of NO in response to inflammation.

In contrast to DDAH2$^{+/+}$ pMacs, pMacs extracted from DDAH2$^{-/-}$mice had significantly reduced NO_2^- levels over all time points (3.15 ±0.21µmol, 9.80 ± 1.19µmol, and 21.0 ± 2.68µmol at 6, 24 and 48 hours for DDAH2$^{-/-}$ pMacs respectively, compared to 4.91 ± 0.53µmol, 18.4 ± 1.83µmol, 42.6 ± 4.79µmol at 6, 24 and 48 hours for DDAH2$^{+/+}$respectively, where *p<0.05) (Fig. 5.5). Despite this, DDAH2$^{-/-}$ pMacs produced a significant increase in NO_2^- over the time course implying that they can produce NO upon inflammatory stimulation, albeit to a lesser extent than macrophages extracted from DDAH2$^{+/+}$.

More importantly, there was no significant difference in NO_2^- production over time from DDAH2$^{flox/flox}$ LysM-Cre pMacs compared to DDAH2$^{-/-}$ pMacs (3.95 ± 0.31µmol, 10.1 ± 1.60µmol, and 22.1 ± 4.50µmol at 6, 24 and 48 hours for DDAH2$^{flox/flox}$ LysM-Cre pMacs respectively compared to 3.15 ± 0.21µmol, 9.80 ± 1.19µmol, and 21.0 ± 2.68µmol at 6, 24 and 48 hours for DDAH2$^{-/-}$ pMacs respectively, where *p<0.05) (Fig. 5.5). However, like with DDAH2$^{-/-}$ pMacs, there was a significant reduction inNO_2^- compared to DDAH2$^{+/+}$ (3.95 ± 0.31µmol, 10.1 ± 1.60µmol, and 22.1 ± 4.50µmol at 6, 24 and 48 hours for DDAH2$^{flox/flox}$ LysM-Cre pMacs respectively compared to 4.91 ± 0.53µmol, 18.4 ± 1.83µmol, 42.6 ± 4.79µmol at 6, 24 and 48 hours for

DDAH2$^{+/+}$respectively, where *p<0.05). This demonstrated that DDAH2$^{flox/flox}$ LysM-Cre pMacs exhibit the same effects as DDAH2$^{-/-}$ pMacs on NO_2^- production in response to inflammation.

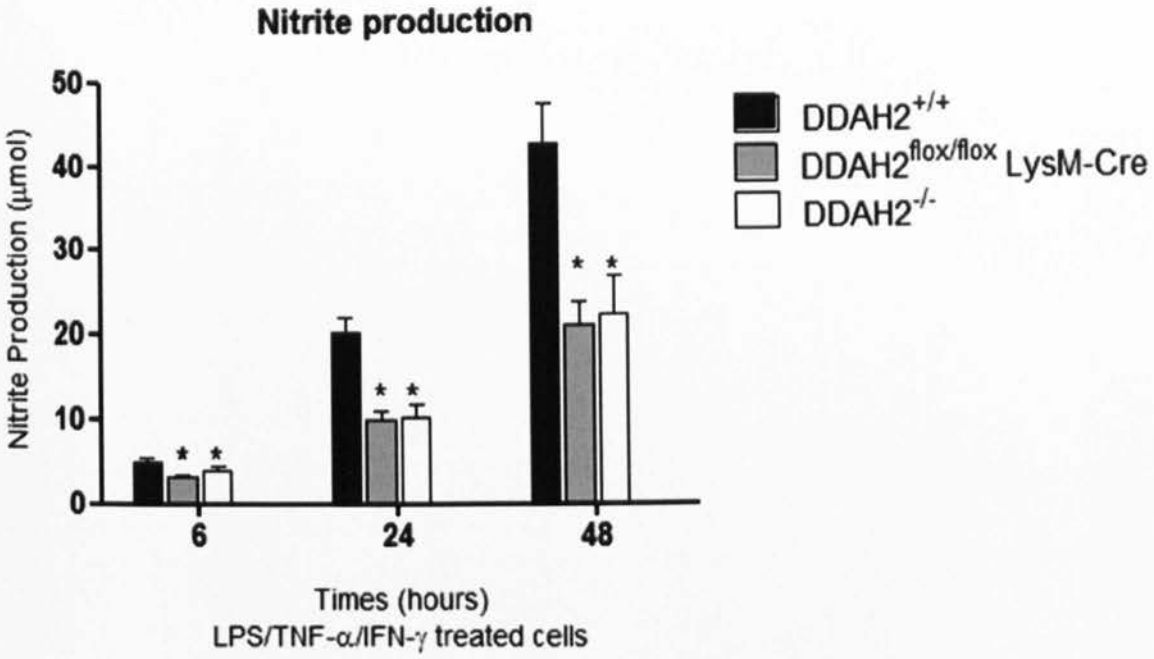

Fig. 5.5: Time course accumulation of NO_2^- from macrophages treated with an inflammatory cytokine cocktail.

pMacs extracted from DDAH2$^{+/+}$, DDAH2flox$^{/flox}$ LysM-Cre and DDAH2$^{-/-}$ were cultured into 24 well plates ($5x10^5$ cells/well) and treated with a pro-inflammatory cocktail of LPS/TNF-α/IFN-γ. Aliquots (200µL) were removed at time 6, 24, and 48 hours following cytokine treatment. NO_2^- concentration was determined using the Griess assay and normalised using a standard NO_2^- curve. Results were based on an n=8 for DDAH2$^{+/+}$; n=9 forDDAH2$^{flox/flox}$ LysM-Cre, n=9 for DDAH2$^{-/-}$. Media only was used as a blank/reference. Significance was measured using a two-tailed t-test of the knock-out groups versus DDAH2$^{+/+}$ macrophages and was accepted when *p<0.05.

5.7 Genetic disruption of DDAH2 regulates primary macrophage motility

Previous chapters have shown that the pharmacological addition of NOS inhibitors and the global genetic disruption of DDAH2 regulates pMac motility. To determine whether this response is also seen with DDAH2$^{flox/flox}$ LysM-Cre mice, pMacs were extracted as previously and treated with the NOS inhibitor ADMA (1, 10 and 100μM), SDMA (100μM) and SNP (100μM) to test whether NO can reverse any of the effects seen.

Under resting conditions, pMacs fromDDAH2$^{flox/flox}$ LysM-Cre mice moved at 0.186 ± 0.026μm/min (Fig. 5.6A and Fig. 5.8A). Following the addition of 1μM ADMA the speed at which macrophages move tended to reduce but was not significantly different from control (0.164 ± 0.149μm/min and 0.186 ± 0.026μm/min for 1μM ADMA and control respectively, where mean ± SEM and p>0.05) (Fig. 5.6B). Increasing the concentration of ADMA further to 10μM and 100μM reduced average speed compared to control, however, again there was no significant difference (0.121 ± 0.022μm/min and 0.104 ± 0.019μm/min for 10μM and 100μMrespectively compared to 0.186 ± 0.026μm/min for control, where mean ± SEM and p>0.05) (Fig. 5.6C and D). The addition of SDMA (100μM) showed similar trends to ADMA as it did not appear to change the speed travelled compared to either control or the same concentration of ADMA (0.174 ± 0.0215μm/min for SDMA compared to 0.186 ± 0.026μm/min and 0.104 ± 0.019μm/min for control and 100μM ADMA respectively, where mean ± SEM and p>0.05) (Fig. 5.6E). Again there was no significant effect on DDAH2$^{flox/flox}$ LysM-Cre pMac motility compared to control following the addition of 100μM SNP (0.218 ± 0.022μm/min for 100μM SNP compared to 0.186 ± 0.026μm/min for control, where mean ± SEM and p>0.05) (Fig. 5.6F).

The results for the total distance travelled agreed with the data for speed. In resting conditions, pMacs travelled a total distance of 143 ± 14.1μm (Fig. 5.8B). The addition of 1, 10 or 100μM ADMA did not have any significant effect on the distance travelled compared to control (172 ± 15.7μm, 172.6 ±

23.3μm, 159.8 ± 18.6μm compared to 143 ± 14.1μm for 1, 10 and 100μM ADMA compared to control respectively, where mean ± SEM and $p>0.05$). Similarly the addition of 100μM SDMA did not effect DDAH2$^{flox/flox}$ LysM-CrepMac distance travelled compared to control of the same concentration of ADMA (183.1 ± 22.59μm for 100μM SDMA compared to 159.8 ± 18.6μm for 100μM ADMA respectively, where mean ± SEM and $p>0.05$). In contrast, by adding SNP (100μM) macrophages moved significantly further than control (229 ± 24.1μm compared to 143 ± 14.1μm for 100μM SNP compared to control respectively, where mean ± SEM and $p>0.05$).

The data above suggests that under quiescent conditions the specific genetic disruption of DDAH2 in macrophages significantly impairs primary macrophage motility and that further pharmacological addition of ADMA or SDMA does not appear to have any further effect. To confirm this same hypothesis under inflammatory conditions, the same experiment was conducted but with the co-incubation of an inflammatory stimulus (LPS/TNF-α/IFN-γ).

In response to an inflammatory cocktail, DDAH2$^{flox/flox}$ LysM-Cre pMacs increased in speed, however, this was no significant (0.186 ± 0.026μm/min and 0.227 ± 0.0149μm/min for resting and inflammatory treated pMacs respectively, where mean ± SEM and $p>0.05$) (Fig. 5.7A and Fig. 5.8C).The addition of 1, 10 or 100μM ADMA did not alter the speed compared to control in inflammatory conditions (0.208 ± 0.0208μm/min, 0.209 ± 0.0208μm/min, and 0.217 ± 0.0215μm/min for 1, 10 and 100μM ADMA respectively compared to 0.227 ± 0.0149μm/min for control, where mean ± SEM and $p>0.05$) (Fig. 5.7B, C and D). Similarly, the addition of 100μM SDMA did not have any significant effect on the speed compared to control or the same concentration of ADMA (0.269 ± 0.304μm/min for 100μM SDMA compared to 0.227 ± 0.0149μm/min and 0.217 ± 0.0215μm/min for control and 100μM ADMA, where mean ± SEM and $p>0.05$) (Fig. 5.7E). The addition of SNP did not significantly affect the speed of inflammatory-induced pMacs compared to control (0.203 ± 0.0242μm/min and 0.227 ± 0.0149μm/min for 100μM SNP and control respectively, where mean ± SEM and $p>0.05$) (Fig. 5.7F).

Similar effects were seen with the data for the total distance travelled. The addition of 1, 10 and 100μM ADMA had no significant effect on the total distance travelled by $DDAH2^{flox/flox}$ LysM-Cre pMacs compared to control (219 ± 21.8μm, 220 ± 21.9μm, 229 ± 22.4μmfor 1, 10 and 100μM ADMA compared to 239 ± 15.6μm for control, where mean ± SEM and $p<0.05$) (Fig. 5.8D). Also, the addition of 100μM SDMA had no significant effect on distance travelled compared to control and the same concentration of ADMA (0.269 ± 0.03μm for 100μM SDMA compared to 239 ± 15.6μm and 239 ± 15.6μmμm for control and 100μM ADMA respectively, where mean ± SEM and $p>0.05$). The addition of SNP was also found to have no significant effect on the distance travelled compared to control (213 ± 25.4μm compared to 239 ± 15.6μm for 100μM SNP and control respectively, where mean ± SEM and $p>0.05$).

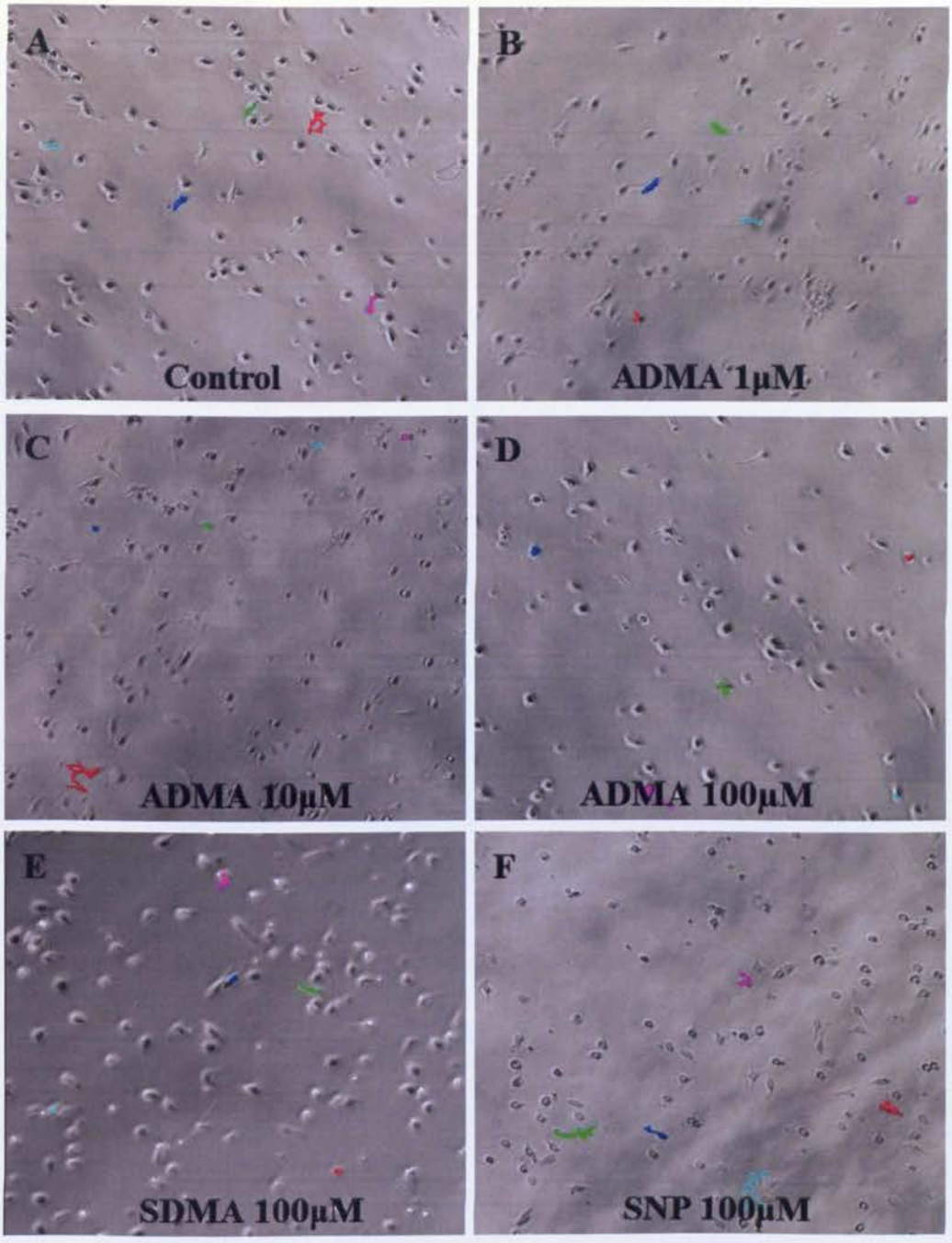

Fig. 5.6: Cell trajectories of macrophages extracted from DDAH2$^{flox/flox}$ LysM-Cre in untreated conditions.

Primary macrophages were treated with either ADMA (1, 10, 100μM), SDMA (100μM) or SNP (100μM) (A-F respectively) for a total of 24 hours and tracked for 16 hours (with 10 minute intervals between frames). Cell tracking was carried out using an Image J manual tracking program. Different colours correspond to different randomly selected cells tracked. Results are indicative of 3 individual experiments where number of cells tracked = 75.

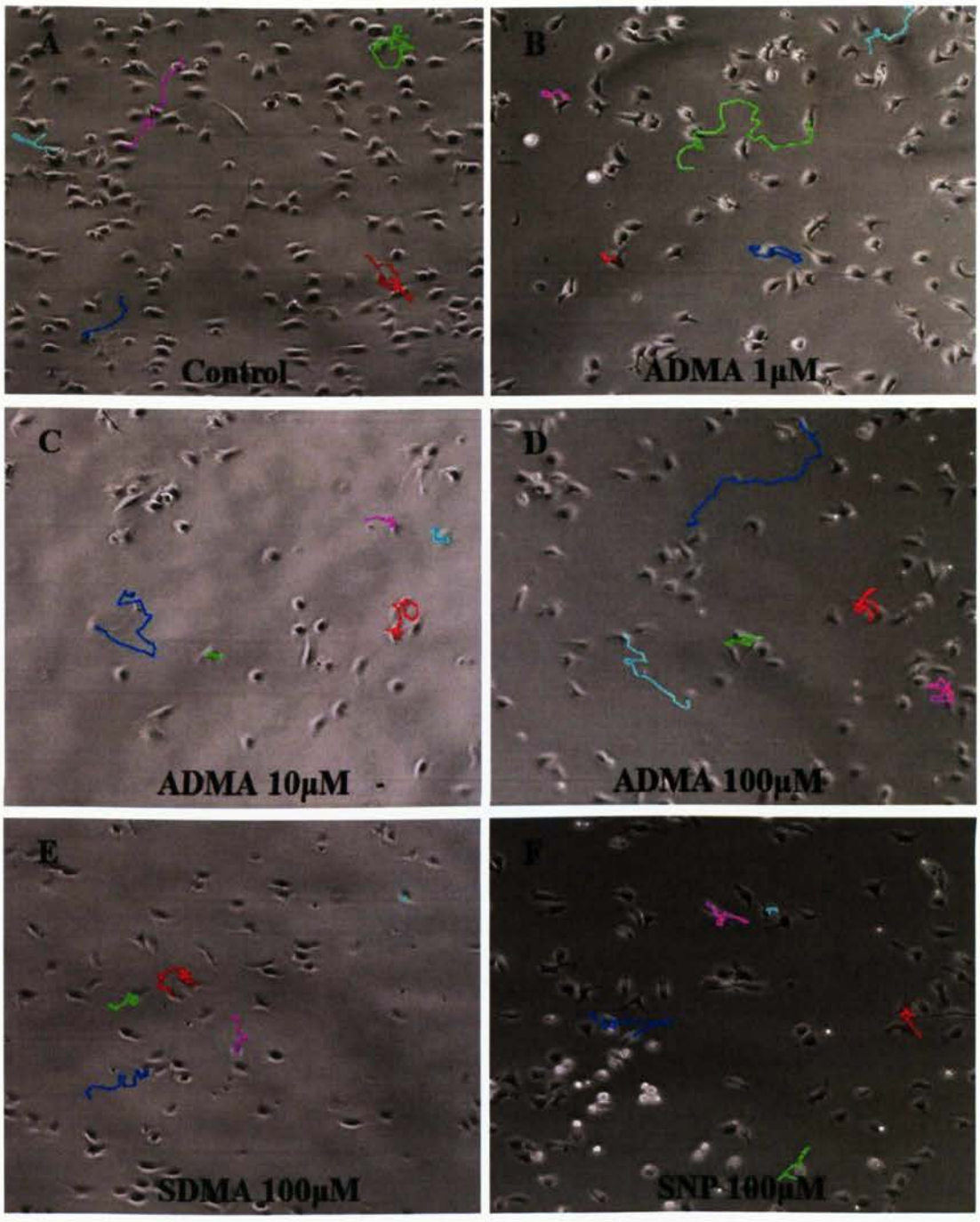

Fig. 5.7: Cell trajectories of macrophages extracted from DDAH2$^{flox/flox}$ LysM-Cre mice in inflammatory-stimulated conditions.

Macrophages were treated with an inflammatory cocktail and the following: media only, ADMA 1, 10, 100μM, SDMA 100μM and SNP 100μM (A-F respectively) for 24 hours and tracked for 16 hours (with 10 minute intervals between frames).Cell tracking was carried out using an Image J manual tracking program. Results are indicative of 3 individual experiments where number of cells tracked = 75.

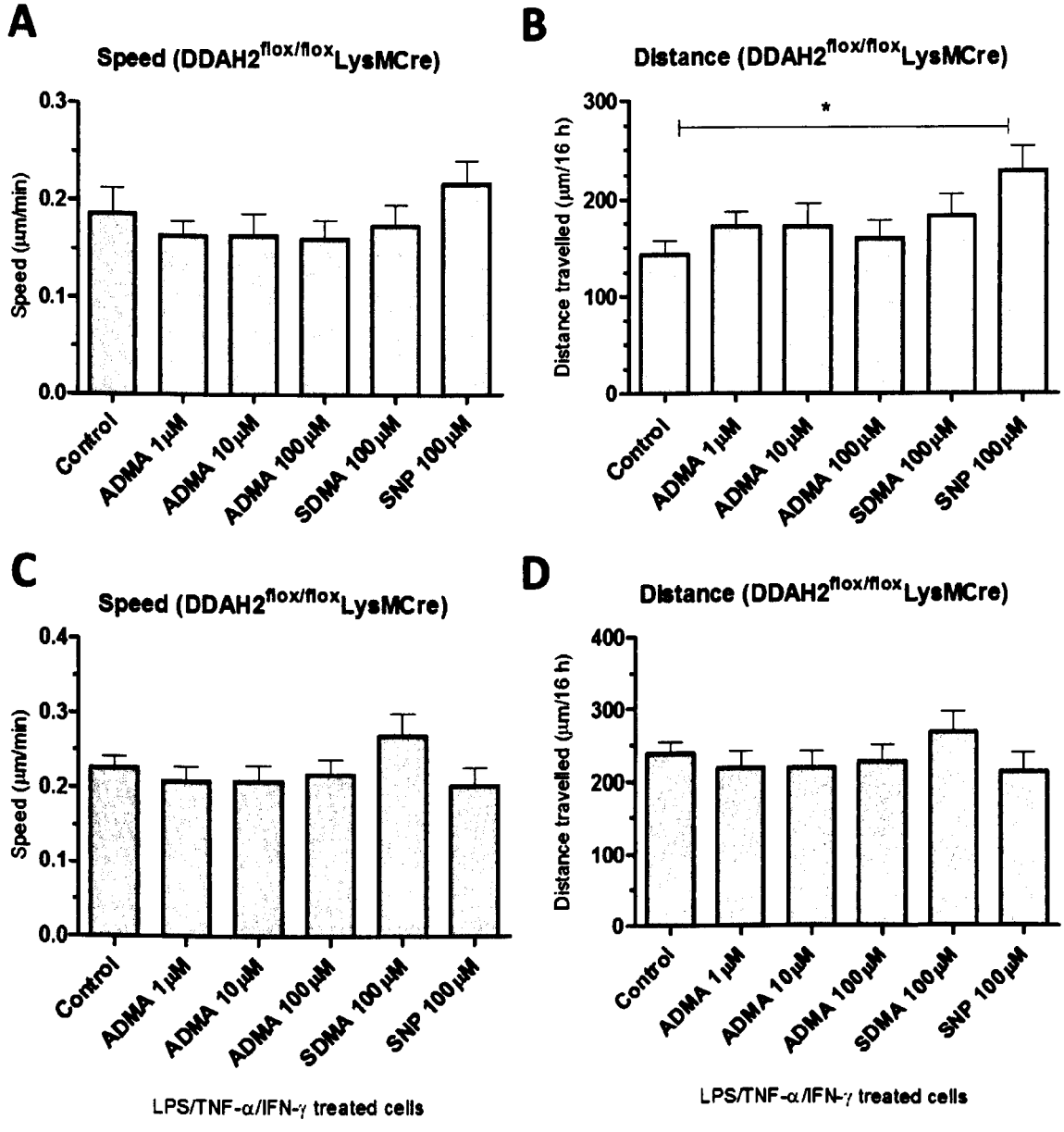

Fig. 5.8: Motility of primary macrophages obtained from DDAH2$^{flox/flox}$ LysM-Cre.

The speed and distance travelled of pMacs under untreated conditions (A-B) and inflammatory stimulated conditions (C-D). Statistical significance was determined using a one-way ANOVA and a Bonferroni post-hoc test. Results are indicative of n=3 individual experiments, where mean ± SEM and *p<0.05.

5.8 The motility differences between DDAH2$^{+/+}$, DDAH2$^{-/-}$ and DDAH2$^{flox/flox}$ LysM-Cre macrophages

One aim of this chapter was to compare the effects of two different models of genetic DDAH2 disruption on macrophage motility. In order to do this, the data acquired from the experiments conducted thus far were gathered and analysed.

Under non-inflammatory conditions the addition of 10μM ADMA on DDAH2$^{+/+}$ pMacs significantly reduced their speed compared to control (0.163 ± 0.021μm/min compared to 0.252 ± 0.018μm/min for 10μM ADMA and control respectively, where mean ± SEM and *p<0.05) (Fig. 5.9A). Their speed increased significantly compared to control following the addition of an inflammatory cocktail (0.382 ± 0.021μm/min compared to 0.252 ± 0.018μm/min for inflammatory treated and untreated DDAH2$^{+/+}$ pMacs respectively, where *p<0.05). Co-incubation with 10μM ADMA significantly reversed this effect back to control levels (0.262 ± 0.114μM and 0.252 ± 0.018μm/min for 10μM ADMA with inflammatory cocktail and control respectively, where mean ± SEM and p>0.05) (Fig. 5.9A).This clearly showed that the exogenous addition of ADMA either to untreated or inflammatory treated macrophages significantly reduced cell speed.

In contrast, DDAH2$^{flox/flox}$ LysM-Creand DDAH2$^{-/-}$ pMacs behaved differently. The addition of 10μM ADMA to resting macrophages had no significant effect on the speed compared to control (0.164 ± 0.022μm/min and 0.1869 ± 0.026μm/min for 10μM ADMA and control DDAH2$^{flox/flox}$ LysM-Cre pMacs respectively, and, 0.140 ± 0.0160 μm/min and 0.158 ± 0.0228μm/min for 10μM ADMA and control DDAH2$^{-/-}$ pMacs respectively, where mean ± SEM and p>0.05) (Fig. 5.9A). The addition of an inflammatory cocktail did not significantly increase the speed travelled compared to its genotypes control, but was significantly different to DDAH2$^{+/+}$ inflammatory treated pMac speed (0.227 ± 0.014μm/min and 0.1869 ± 0.026μm/min for inflammatory treated

and untreated DDAH2$^{flox/flox}$ LysM-Cre pMacs, 0.190 ± 0.0121μm/min and 0.157 ± 0.0228μm/min for inflammatory treated and untreated DDAH2$^{-/-}$pMacs compared to 0.382 ± 0.021μm/min and 0.252 ± 0.0182μm/min for DDAH2$^{+/+}$ inflammatory treated and control pMacs) (Fig. 5.9A). The addition of 10μM ADMA to inflammatory treated cells had no significant effect on DDAH2$^{flox/flox}$ LysM-Cre or DDAH2$^{-/-}$pMac speed (0.268 ± 0.0227μm/min, 0.214 ± 0.0207μm/min and 0.203 ± 0.0199μm/min for DDAH2$^{+/+}$, DDAH2$^{flox/flox}$ LysM-Cre and DDAH2$^{-/-}$ pMacs respectively, where mean ± SEM and $p>0.05$). These data suggest that the exogenous addition of a NOS inhibitor does not significantly affect pMacs which already have lower than average NO levels (Fig. 5.5) and significantly increased ADMA (Fig. 5.4).

The total distance travelled was also determined. In DDAH2$^{+/+}$ the distance travelled was significantly reduced following the addition of 10μM ADMA and significantly increased following the addition of an inflammatory cocktail (250.3 ± 16.5μm in control conditions compared to 169.9 ± 10.55μm and 371.6 ± 20.96μm following 10μM ADMA or inflammatory cocktail addition, where mean ± SEM and $*p<0.05$) (Fig. 5.9B). Upon treatment with an inflammatory cocktail and ADMA (10μM) the total distance travelled was reduced and this was not significantly different to control (256.9 ± 21.78μm compared to 250.3 ± 16.5μm for inflammatory cocktail with 10μM ADMA and control respectively, where mean ± SEM and $p>0.05$).

Compared to DDAH2$^{+/+}$, pMacs from DDAH2$^{flox/flox}$ LysM-Creand DDAH2$^{-/-}$ and significantly reduced distances in control and inflammatory conditions (250.3 ± 16.5μm for DDAH2$^{+/+}$ control compared to 143.4 ± 14.08μm and 134.0 ± 13.05μm for DDAH2$^{flox/flox}$ LysM-Cre and DDAH2$^{-/-}$ respectively, where mean ± SEM and $*p<0.05$) (Fig. 5.9B).

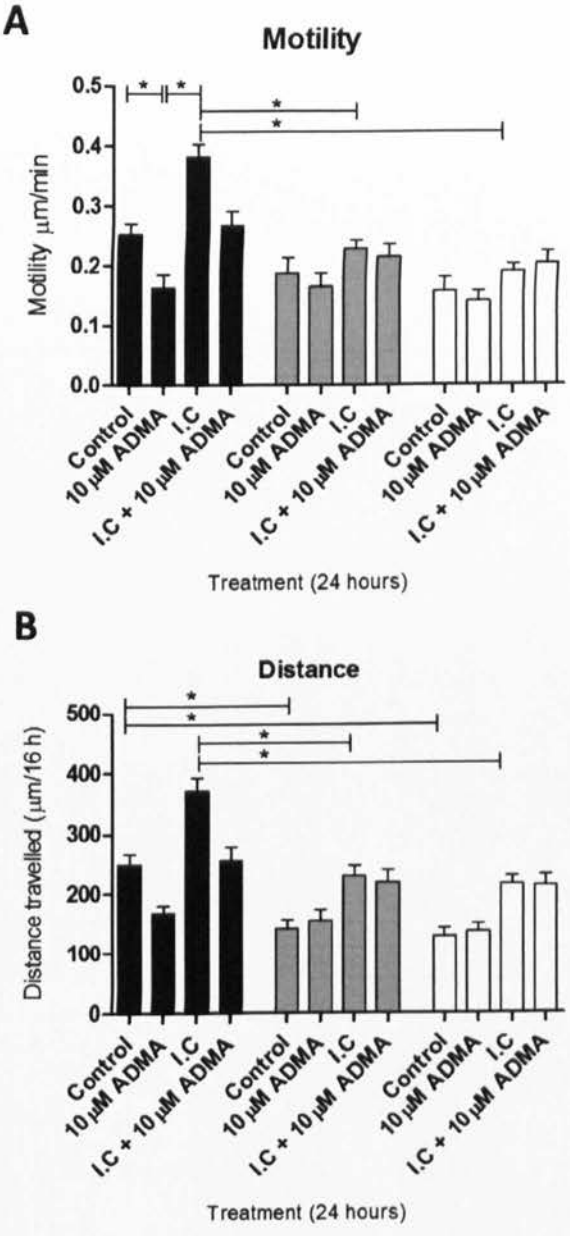

Fig. 5.9: Summary of the speed and distance travelled of macrophages extracted from DDAH2$^{+/+}$, DDAH2$^{flox/flox}$ LysM-Cre and DDAH2$^{-/-}$ mice.

The speed and total distance travelled by pMacs, extracted from DDAH2$^{+/+}$, DDAH2$^{flox/flox}$ LysM-Cre and DDAH2$^{-/-}$ was determined using an Image J program. A one-way ANOVA and Bonferroni post-hoc test was used to determine statistical significance. Results are based on n=3 experiments (n=75 individual cells tracked) and are shown as mean ± SEM. I.C refers to the addition of an inflammatory cocktail (LPS/TNF-α/IFN-γ). Black bars represent DDAH2$^{+/+}$, grey bars DDAH2$^{flox/flox}$ LysM-Cre and white bars DDAH2$^{-/-}$pMacs.

5.9 Macrophage phagocytosis is regulated by DDAH2

We have already shown in the previous chapters that the global deletion of DDAH2 results in a significant reduction in pMac phagocytosis. To determine whether this effect occurs specifically as a result of DDAH2 deletion in macrophages, the previous experiments were repeated in $DDAH2^{flox/flox}$ LysM-Cre.

In resting conditions, the specific deletion of DDAH2 in macrophages resulted in a slight, yet non-significant reduction in pMac phagocytosis compared to $DDAH2^{+/+}$ (2.50 ± 0.52a.u and 3.02 ± 0.45a.ufor $DDAH2^{flox/flox}$ LysM-Creand $DDAH2^{+/+}$ in untreated conditions respectively, where mean ± SEM and $p>0.05$) (Fig. 5.10). Interestingly, global $DDAH2^{-/-}$ pMacs had a significant reduction in phagocytosis compared to $DDAH2^{+/+}$ but was not significantly different from $DDAH2^{flox/flox}$ LysM-Cre (1.45 ± 0.52a.u for $DDAH2^{-/-}$ compared to 3.02 ± 0.45a.u and 2.50 ± 0.52a.u for $DDAH2^{+/+}$ and $DDAH2^{flox/flox}$ LysM-Cre in untreated conditions respectively, where mean ± SEM and $*p<0.05$ or $p>0.05$) (Fig. 5.10).

The stimulation of $DDAH2^{+/+}$ pMacs with an inflammatory cocktail resulted in a significant increase in phagocytosis compared to control conditions (3.02 ± 0.45a.u and 5.73 ± 0.71a.u for $DDAH2^{+/+}$ untreated and inflammatory stimulated pMacs respectively, where mean ± SEM and $*p<0.05$) (Fig. 5.10).In contrast, the stimulation of pMacs from $DDAH2^{flox/flox}$ LysM-Cre and $DDAH2^{-/-}$ had no significant effect on phagocytosis compared to their genotype controls (2.50 ± 0.52a.u and 3.02 ± 0.45 for $DDAH2^{flox/flox}$ LysM-Cre untreated and inflammatory treated pMacs respectively and 1.45 ± 0.52a.u and 2.3 ± 0.45a.u for $DDAH2^{-/-}$ untreated and inflammatory treated pMacs respectively, where mean ± SEM and $p>0.05$) (Fig. 5.10). There was no significant difference between$DDAH2^{flox/flox}$ LysM-Cre and $DDAH2^{-/-}$ pMac phagocytosis levels under inflammatory conditions (3.02 ± 0.45 and 2.3 ± 0.45a.u for $DDAH2^{flox/flox}$ LysM-Cre and $DDAH2^{-/-}$ respectively, where mean ± SEM and $p>0.05$).

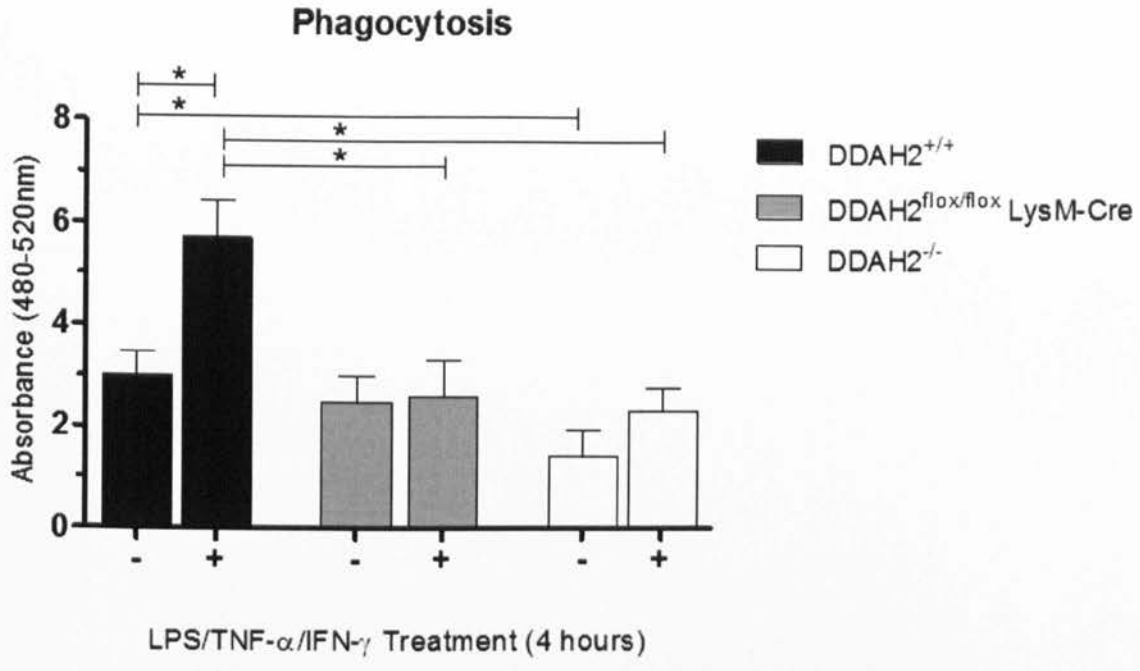

Fig. 5.10: Phagocytosis levels of DDAH2^{++-}, DDAH2$^{flox/flox}$ LysM-Cre and DDAH2$^{-/-}$ in untreated or inflammatory-treated pMacs.

pMacs ($2x10^5$) from DDAH2$^{+/+}$, DDAH2$^{flox/flox}$ LysM-Cre and DDAH2$^{-/-}$ were cultured in triplicate in a 96 well plate and treated with either an inflammatory cocktail (+) or left untreated (-) for 4 hours. Following treatment, the media was removed and cells were incubated with a fluorescent E-coli bio-particle for 2 hours followed by trypan blue for 1 minute. The absorbance at 480-520nm was measured using a spectrophotometer. Data is presented in response to a reference sample of media only (blank). Results correspond to n=4 experiments and use a two-tailed statistical test to assess significance and one-way ANOVA for analysis. Bars represent mean ± SEM and *p<0.05.

5.10 Macrophage cell proliferation is not regulated by DDAH2

The data in Chapter 4 has shown that pMac cell proliferation is not altered following the global deletion of DDAH2 (Fig. 4.11B). This experiment was also carried out in DDAH2$^{flox/flox}$ LysM-Cre to confirm whether this is also true in this genetic knock-out model. There was no significant difference in the cell proliferation of DDAH2$^{+/+}$ macrophages in untreated and inflammatory treated conditions (2.28 ± 0.214a.u and 2.51 ± 0.783a.u for untreated and inflammatory treated respectively, where mean ± SEM and p>0.05) (Fig. 5.11). Similarly, there was no significant difference betweenDDAH2$^{flox/flox}$ LysM-Cre and DDAH2$^{+/+}$ pMacs in untreated and inflammatory treated conditions (1.94 ± 0.417a.u and 2.08 ± 0.187a.u for untreated and inflammatory treatedDDAH2$^{flox/flox}$ LysM-Cre pMacs and 1.83 ± 0.137a.u and 1.64 ± 0.137a.u for untreated and inflammatory treated DDAH2$^{-/-}$ pMacs, where mean ± SEM and p>0.05) (Fig. 5.11).

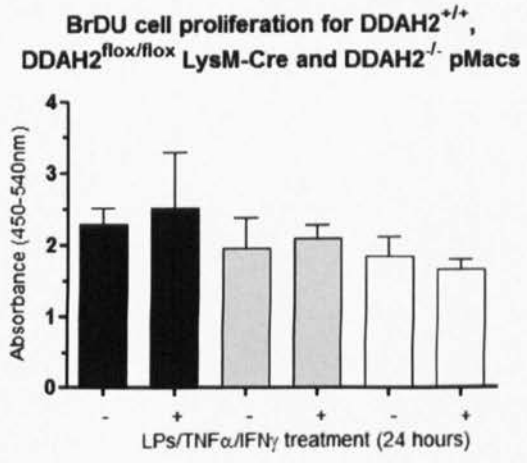

Fig. 5.11: Cell proliferation measured by BrDU incorporation in DDAH2$^{+/+}$, DDAH2$^{flox/flox}$ LysM-Cre and DDAH2$^{-/-}$ pMacs.

pMacs (1x10^5) from DDAH2$^{+/+}$, DDAH2$^{flo/flox}$ LysM-Cre and DDAH2$^{-/-}$ mice were plated in triplicate in 96 wells were treated with media only (-) or with an inflammatory control (+) for 24 hours. Data is representative of n=3 experiments and shows no significant difference (p>0.05) between the data using a one way ANOVA and a Bonferroni post-hoc test. Data is presented as mean ± SEM. (Black bars represent DDAH2$^{+/+}$, grey bars DDAH2$^{flox/flox}$ LysM-Cre and white bars DDAH2$^{-/-}$).

5.11 DDAH2 in macrophages is a key regulator of intracellular TNF-α gene expression

Cytokines are critical for the activation of macrophages and other immune cells. To investigate whether DDAH2 has an effect on macrophage cytokine levels, the intracellular gene expression of the cytokines TNF-α, IL-1β and IL-6 and iNOS were measured using RT-qPCR. RNA from pMacs extracted from 4 male $DDAH2^{flox/flox}$ and 4 male $DDAH2^{flox/flox}$ LysM-Cre animals (6 weeks of age) was collected and purified as described in Chapter 2. Samples were analysed against a polymerase 2 housekeeper gene.

There was no significant different in iNOS expression between $DDAH2^{flox/flox}$ and $DDAH2^{flox/flox}$ LysM-Crein resting conditions (0.66 ± 0.64 a.u and 0.012 ± 0.0047a.u for $DDAH2^{flox/flox}$ and $DDAH2^{flox/flox}$ LysM-Cre pMacs, where mean ± SEM and $p>0.05$) (Fig. 5.12A). Upon LPS (10μg/mL) stimulation for 6 hours iNOS expression increased for both genotypes, however, there was no significant difference between the two (1.565 ± 0.617a.u and 1.49 ± 0.65a.u for $DDAH2^{flox/flox}$ and $DDAH2^{flox/flox}$ LysM-Cre respectively, where mean ± SEM and $p>0.05$) (Fig. 5.12A).

IL-1β expression was not significantly altered between $DDAH2^{flox/flox}$ and $DDAH2^{flox/flox}$ LysM-Crein resting conditions (0.0299 ± 0.083a.u and 0.038 ± 0.0048a.u for $DDAH2^{flox/flox}$ and $DDAH2^{flox/flox}$ LysM-Cre respectively, where mean ± SEM and $p>0.05$) (Fig. 5.12B). Upon stimulation, there was a significant increase in IL-1β in $DDAH2^{flox/flox}$ and $DDAH2^{flox/flox}$ LysM-Crebut there was no significant difference between the two genotypes (1.786 ± 0.467a.u and 0.896 ± 0.095a.u for $DDAH2^{flox/flox}$ and $DDAH2^{flox/flox}$ LysM-Crerespectively, where mean ± SEM and $*p<0.05$) (Fig. 5.12C).

Under resting conditions, TNF-α expression was significantly reduced in $DDAH2^{flox/flox}$ LysM-Crecompared to $DDAH2^{flox/flox}$ (0.229 ± 0.078a.u and 0.043 ± 0.016a.u for $DDAH2^{flox/flox}$ and $DDAH2^{flox/flox}$ LysM-Cre respectively, where mean ± SEM and $*p<0.05$ (Fig. 5. 12C). Following LPS stimulation for 6 hours there was a significant increase in TNF-α in $DDAH2^{flox/flox}$ compared to resting

conditions whereas there was no significant difference in DDAH2$^{flox/flox}$ LysM-Cre compared to resting conditions There was a significant difference between DDAH2$^{flox/flox}$ LysM-Cre and DDAH2$^{flox/flox}$ TNF-α expression in LPS stimulated conditions (2.67 ± 0.90a.u for DDAH2$^{flox/flox}$ compared to 0.234 ± 0.095 for DDAH2$^{flox/flox}$ LysM-Cre, where mean ± SEM and *p<0.05).

IL-6 was minimally expressed in both genotypes prior to LPS stimulation. Following the addition of LPS, IL-6 levels increased for both genotypes although there was no significant difference between the two (1.332 ± 0.342a.u and 1.887 ± 0.551a.u for DDAH2$^{flox/flox}$and DDAH2$^{flox/flox}$ LysM-Cre respectively, where mean ± SEM and p>0.05).

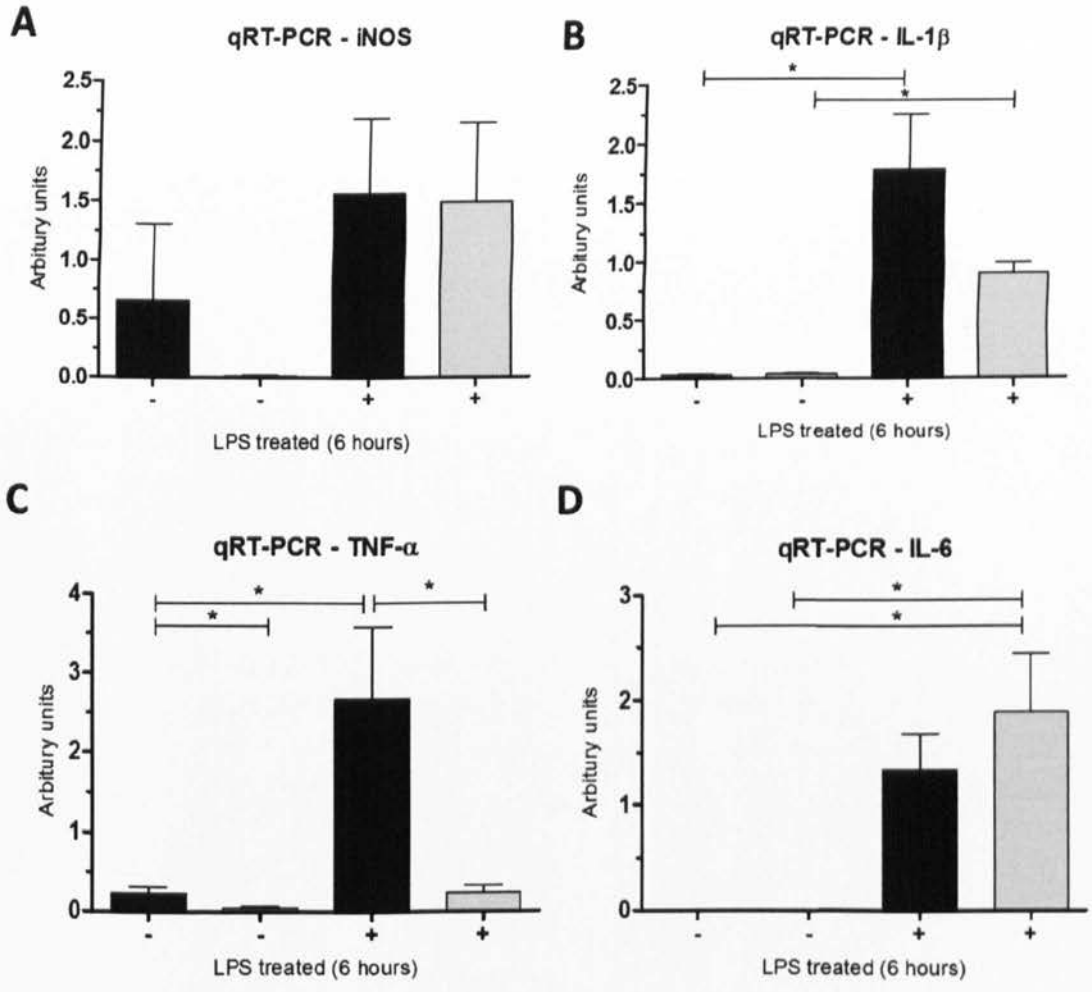

Fig. 5.12: iNOS, IL-1β, TNF-α and IL-6 expression in macrophages fromDDAH2$^{flox/flox}$ and DDAH2$^{flox/flox}$ LysM-Cre animals.

pMacs extracted from DDAH2$^{flox/flox}$ and DDAH2$^{flox/flox}$ LysM-Cre were either left untreated (-) or treated (+) with LPS (10μg/ml) for a period of 4 hours. Cell lysates were collected and the RNA was extracted as explained previously in Chapter 2. RT-qPCR was carried out to determine iNOS (A), IL-1β (B), TNFα (C) and IL-6 (D) expression in macrophages. Polymerase-2 was used as a standard control. Results portrayed are indicative of n=5 and statistical significance was determined using a two-tailed t-test where mean ± SEM and *p<0.05. Black bars represent DDAH2$^{flox/flox}$ and grey bars represent DDAH2$^{flox/flox}$ LysM-Cre.

5.12 Discussion

Macrophages are critical to the immune response and using pMacs derived from global DDAH2$^{-/-}$ we have previously shown DDAH2 to be an important regulator of their function. The main aim of this chapter was to exclude the effect of DDAH2 in other cell types and determine whether the same DDAH2-associated responses are observed in macrophages from DDAH2$^{flox/flox}$ LysM-Cre mice.

The data obtained confirmed the successful deletion of DDAH2 in only pMacs and showed that a DDAH2 deletion resulted in a significant increase in intracellular methylarginines ADMA and L-NMMA. Since this is a novel mouse model, there is no comparable data describing the effect of specific macrophage DDAH2 deletion on methylarginine concentrations, however, the results are in accordance with previous increases in methylarginine concentrations following global DDAH2 deletion. In our DDAH2$^{flox/flox}$ LysM-Cre and DDAH2$^{+/+}$ there were very low and undetectable levels of SDMA, however, L-NMMA and ADMA levels were elevated agreeing with the effect of DDAH2 on other cells and tissues (McDermott, 1976). Corresponding with this, DDAH2$^{flox/flox}$ LysM-Cre pMacs produced lower NO_2^- levels following activation with an inflammatory cocktail.

DDAH2 is also an important regulator of macrophage motility as demonstrated by the real-time imaging data. Macrophage-specific deletion of DDAH2 resulted in a significant reduction in the motility following inflammatory stimulation compared to DDAH2$^{+/+}$. In the context of endothelial cells, DDAH1 deletion and the pharmacological addition of ADMA have already been known to affect their motility (Wojciak-Stothard *et al.*, 2007). This ADMA mechanistic effect was found to be through reduced NO resulting in decreased RhoA phosphorylation on Ser188, which facilitates its membrane localisation and activation. RhoA activation and Rho kinase increase cell adhesion and slow down the turnover of focal adhesions thus preventing motility (Wojciak-Stothard *et al.*, 2007). These data suggests that DDAH can improve cell movement in endothelial cells by inhibiting the effects of ADMA and restoring

angiogenic responses. In cultured HUVECs, L-NAME was shown to induce the formation of stress fibres and large focal adhesions and inhibits cell motility (Goligorsky *et al.*, 1999). DDAH2 deletion in macrophages significantly inhibited motility, increased intracellular NOS inhibitors and reduced NO production and phagocytosis levels.

The results from the gene expression studies reveal a significant reduction in TNF-α, an important pro-inflammatory cytokine which orchestrates the release of many other cytokines, expression in both untreated and inflammatory stimulated conditions. This rapidly released cytokine is one of the most important molecules in initiating the immune response and one of the most abundant mediators in inflamed tissues. The results shown here suggest that the deletion of DDAH2 significantly reduces TNF-α production and thus may prove to be beneficial in providing an appropriate and not over-induced inflammatory response (Maini *et al.*, 1995). NO has been shown to increase in other cell types. In HUVECs, TNF-α has been found to reduce eNOS m-RNA expression by shortening its half-life and this has been suggested to contribute to the impaired endothelium-dependent relaxation associated with atherosclerosis (Yoshizumi *et al.*, 1993). The addition of an NO donor also increases TNF-α mRNA expression in human neutrophils suggesting that NO released by endothelial and vascular smooth muscle cells may exert paracrine effects of human neutrophils and augment inflammatory response in sepsis (Van Devort *et al.*, 1994).

Overall these results demonstrate DDAH2 to be a key regulator of macrophage function in particular under inflammatory conditions. The differences in intracellular TNF-α gene expression suggests that this may be one of many macrophage genes altered by DDAH2 and that a more wide-ranging analysis of such genes using cutting edge technology such as transcriptomics may provide a novel insight into the reasoning behind the functional differences seen in DDAH2 knock-out animals.

Conclusion

In this chapter we set out to generate a novel DDAH2$^{flox/flox}$ LysM-Cre mouse model and determine whether the functional difference seen in the global DDAH2$^{-/-}$ pMacs correlate with the data obtained from the DDAH2$^{flox/flox}$ LysM-Cre pMacs. Based on the results obtained in this chapter we can reject our null hypothesis and more specifically conclude that:

1. *DDAH2 macrophage specific deletion, via increased intracellular ADMA and L-NMMA, impairs macrophage NO production, motility and phagocytosis.*

2. *In inflammatory conditions, DDAH2 is a key regulator of macrophage TNF-α expression.*

CHAPTER 6

RNA-Sequencing: A novel tool for determining the regulatory effects of DDAH2

6.1 Introduction

Transcriptomics is *"the complete set of transcripts in a cell, and their quantity for a specific developmental stage or physiological condition"* (Wang, 2009). The key aims of transcriptomics are to catalogue all species of transcript (mRNAs, non-coding RNAs and small RNAs), to determine the transcriptional structure of genes (splicing patterns, start and end sites) and to quantify any changes in expression levels of each transcript during various conditions or developmental stage. RNA-sequencing (RNA-Seq), a modern transcriptomics technique, involves converting RNA to a library of cDNA fragments with adapters attached to one or both ends. Each fragment is then sequenced in a high-throughput manner to obtain short single-end or pair-end sequences. Although RNA-Seq is under active development, it has already been used successfully in mouse and human cells (Nagalakshmi *et al.*, 2008; Mortazavi *et al.*, 2008; Marioni *et al.*, 2008).

There are several advantages to using RNA-Seq compared to more traditional microarrays. Firstly, RNA-Seq is not limited to detecting transcripts that correspond to existing genomic sequences and is very useful when studying more complex transcriptomics such as non-model organisms with genetic sequences which have yet to be determined. Secondly, the technique is very sensitive and there is very limited, if any, background interference. There is also no upper limit for quantification meaning that a large dynamic range of expression levels can be detected (Wang *et al.*, 2009). Finally, the amount of RNA sample required for RNA-Seq is very small as there are no cloning steps required. Overall the technique is a novel, high-throughput procedure with high levels of reproducibility for both technical and biological samples (Cloonan *et al.*, 2008; Nagalakshmi *et al.*, 2008).

The studies in Chapter 5 show DDAH2 to be an important regulator of macrophage function including motility, phagocytosis and TNF-α production. The gene expression of TNF-α and other cytokines was measured using RT-qPCR. The disadvantage we have with this approach is that it requires more sample and you only test for the primers/cytokines you are interested in and

therefore may miss key genes which are significantly altered that you are not aware of. There has yet to be RNA-Seq carried out on DDAH animals so combined with the novel DDAH2$^{flox/flox}$ LysM-Cre model this study will help further investigate the correlation between DDAH2 and other immune system pathways and may help provide a novel insight into its mechanisms of action and possible therapeutic potential.

6.2 Specific Aims

The previous data show macrophage motility and phagocytosis to be regulated by DDAH2 but does not highlight any of the key mechanisms involved. RNA-sequencing is a novel, high-throughput procedure that allows you to determine gene expression levels, map the gene and exon boundaries and determine extensive transcript complexity such as splicing events. The main aim of this chapter was to use RNA-sequencing to investigate the key pathways and any specific genes associated with deleting DDAH2 in macrophages specifically.

The hypothesis for this chapter is that:

> ***DDAH2 is a key regulator of many immune system responses by directly altering the expression of cytokine, motility and cell activation genes, and is a key regulator of immune cell function.***

Thus, the null hypothesis is that:

> ***DDAH2 is not key regulator of immune system responses and does not directly alter the expression of cytokine, motility and cell activation genes.***

In order to accept or reject my null hypothesis, the following aims were generated:

1. **Successfully generate RNA libraries.**
   Extract RNA from DDAH2$^{flox/flox}$ and DDAH2$^{flox/flox}$ LysM-Cre pMacs in untreated and inflammatory treated conditions and create RNA expression profiles and libraries.

2. **Investigate the pathways altered by the deletion of DDAH2 in macrophages.**
   Comparing DDAH2$^{flox/flox}$ and DDAH2$^{flox/flox}$ LysM-Cre mice in untreated and inflammatory treated conditions, determine the key pathways altered in both genotypes.

3. **Determine the effect of macrophage DDAH2 on ADMA/NO pathway related genes.**

   Using the obtained RNA-sequencing data, investigate the differences in important genes associated with the ADMA/NO pathway that are significantly altered between treatments and genotypes.

4. **Determine the effect of macrophage DDAH2 on cytokine related genes.**

   Using the obtained RNA-sequencing data, investigate the differences in important cytokines such as TNF-α and different interleukins that are significantly altered between treatments and genotypes.

5. **Determine the effect of macrophage DDAH2 on motility related genes.**

   Using the obtained RNA-sequencing data, investigate the differences in important motility-related genes that are significantly altered between treatments and genotypes.

6. **Determine the effect of macrophage DDAH2 on cell activation and the immune system responses.**

   Using the obtained RNA-sequencing data, investigate the differences in important cell activation and immune system responses that are significantly altered between treatments and genotypes.

6.3 Generation of RNA libraries and results analysis

6.3.1 Extraction of RNA from primary macrophages

The extraction of RNA, preparation of RNA-seq libraries and sequencing was carried out with the help of the senior postdoctoral researcher, Dr Lucy Coleman. All RNA sequencing experiments were carried out as described by the manufacturer's protocol (TruSeq® RNA Sample preparation v2 Guide, Illumina). Briefly 0.1-4µg total RNA was purified and fragmented to mRNA. The pMacs used were collected from $DDAH2^{flox/flox}$ and $DDAH2^{flox/flox}$ LysM-Cre animals (n=5 each). Only male mice aged 6 weeks were used for this study to exclude any hormonal changes that may affect the results obtained. Samples were either left untreated or treated with LPS (10µg/mL) for 6 hours prior to collection. RNA was extracted from treated and untreated cells using Qiagen RNAeasy kit (Qiagen, UK).

6.3.2 Preparation of RNA-Seq libraries

In order to prepare the libraries we used the Illumina TruSeq™ RNA-Seq library preparation kit (Low-Throughput protocol- less than 48 samples). This replaces the purification steps with solid-phase reversible immobilisation (SPRI) magnetic beads reaction clean-up methodology. RNA-Seq provides direct sequencing information of all polyadenylated mRNAs and is not limited by probe design; RNA-Seq data has inherently less noise and higher specificity, and, importantly, provides quantitative information on mRNA transcript number. Briefly, 0.5µg of total RNA (with technical replicate) from mouse treated macrophage samples was used for poly-A mRNA selection using streptavidin-coated magnetic beads. This protocol uses two rounds of enrichment for poly-A mRNA followed by thermal mRNA fragmentation. mRNA was then fragmented before the sheared RNA is reverse -transcribed to cDNA. The double-stranded cDNA was synthesized, end-repaired and

adenylated. Illumina adaptors, which are unique index sequences, are then ligated to the processed double-stranded DNA at the beginning of the library construction process in order to allow the samples to be pooled and then individually identified during downstream, analysis. Finally, the DNA products are amplified using primers to produce a sequence-ready library. Each library was quantified using the Agilent Bioanalyser and a DNA 1000 chip. The cDNA fragments were then blunt-ended through an end-repair reaction and ligated to platform-specific double-stranded bar-coded adapters (four samples per lane).

6.3.3 Sequencing

RNA sequences were acquired from GenBank Remaining reads were mapped to the genome using TopHat v.1.1.3. Only uniquely mapped reads were recorded and used for downstream analysis in both paired and unpaired data.

For $DDAH2^{flox/flox}$ LysM-Cre samples, the exons deleted (exon 2-5) were used to mask all reads to account for this deletion. This region is the functional region of DDAH2. Exons 1, 6 and 7 are non-functional and remain in the genetic make-up of the mice. Read that uniquely map to these remaining exons were used in the analysis for differential expression. The number of aligned reads was counted across all samples. Transcript abundance was determined from the TopHat alignment using a custom perl script and annotated transcripts from RefSeq. RefSeq exons were considered to be detected if at least one read mapped within annotated exon boundaries.

Differential expression was assessed using transcript abundances as inputs to Differential Expression Sequencing (DESeq). The transcripts with an adjusted $p>0.05$ were considered to be differentially expressed.

6.3.4 Analysis of RNA-Seq results

cDNA was prepared from mRNA enriched either by TruSeq™ poly-A selection. From these reads, a group average of 43 millionTruSeq™ poly-A reads were mapped to the mouse genome. The RNASeq reads were aligned against mm9 version of Mouse genome using the TopHat (Version 1.4.0) [http://tophat.cbcb.umd.edu/] software, part of the Tuxedo package of computational pipelines. This aligns RNA-Seq reads to the genome, determines and aligns reads to splice junctions and calculates FPKM/RPKM (fragments/reads per kilo base of exon per million fragments/reads mapped) - a normalized value representing gene expression.

Post alignment RNA-Seq specific quality assessment was then performed usingRNASEQC[https://confluence.broadinstitute.org/display/CGATools/RNA-SeQC] tool. Read counts to ambiguous regions were removed from the counts table. Differential expression analysis was performed using DESeq Bioconductor package [http://bioconductor.org/packages/2.10/bioc/html/DESeq.html] with multi factor design. One factor comparisons were also performed to find the differentially expressed genes due to treatment and due to genotype.

False discovery rate was set at 0.05 and lists of DE genes were obtained. Cuffdiff [http://cufflinks.cbcb.umd.edu/manual.html] was also used to test for differential expression. Gene Oncology (GO) and Pathway enrichment analysis was also performed to see the categories enriched in the differentially expressed genes. GOseqpackage [http://www.bioconductor.org/packages/2.10/bioc/html/goseq.html] was used to test the GO category enrichment in differentially expressed genes. In the above analysis, alignments were done so that only uniquely mapping reads were considered. So, the reads were mapped again and all alignments including non-unique were considered. This was done in response to low reads mapping to DDHA2 gene in both $DDAH2^{flox/flox}$ and $DDAH2^{flox/flox}$ LysM-Cre samples. These aligned data was used with Cuff-diff to test for differential expression. The gene knocked out in

the samples is DDAH2. Here, only exons 2-5 were deleted, leaving exons 1, 6 and 7.

These exons (1, 6 and 7) were masked in the annotation file (GTF) as follows. In order to use the exon masking strategy, the analysis was repeated from alignment stage to differential expression analysis. First, raw reads were aligned with TopHat using annotation file where specific DDAH2 exons were masked. All other parameters were same as above. Differential expression testing was done with DESeq. The count files were then merged as described above. Also, ambiguous counts were removed. The count files were then merged as described above. Also, ambiguous counts were removed.

GO enrichment analysis was also done to test the over representation of GO categories in differentially expressed genes. The false discover rate (FDR) was set at 0.05.

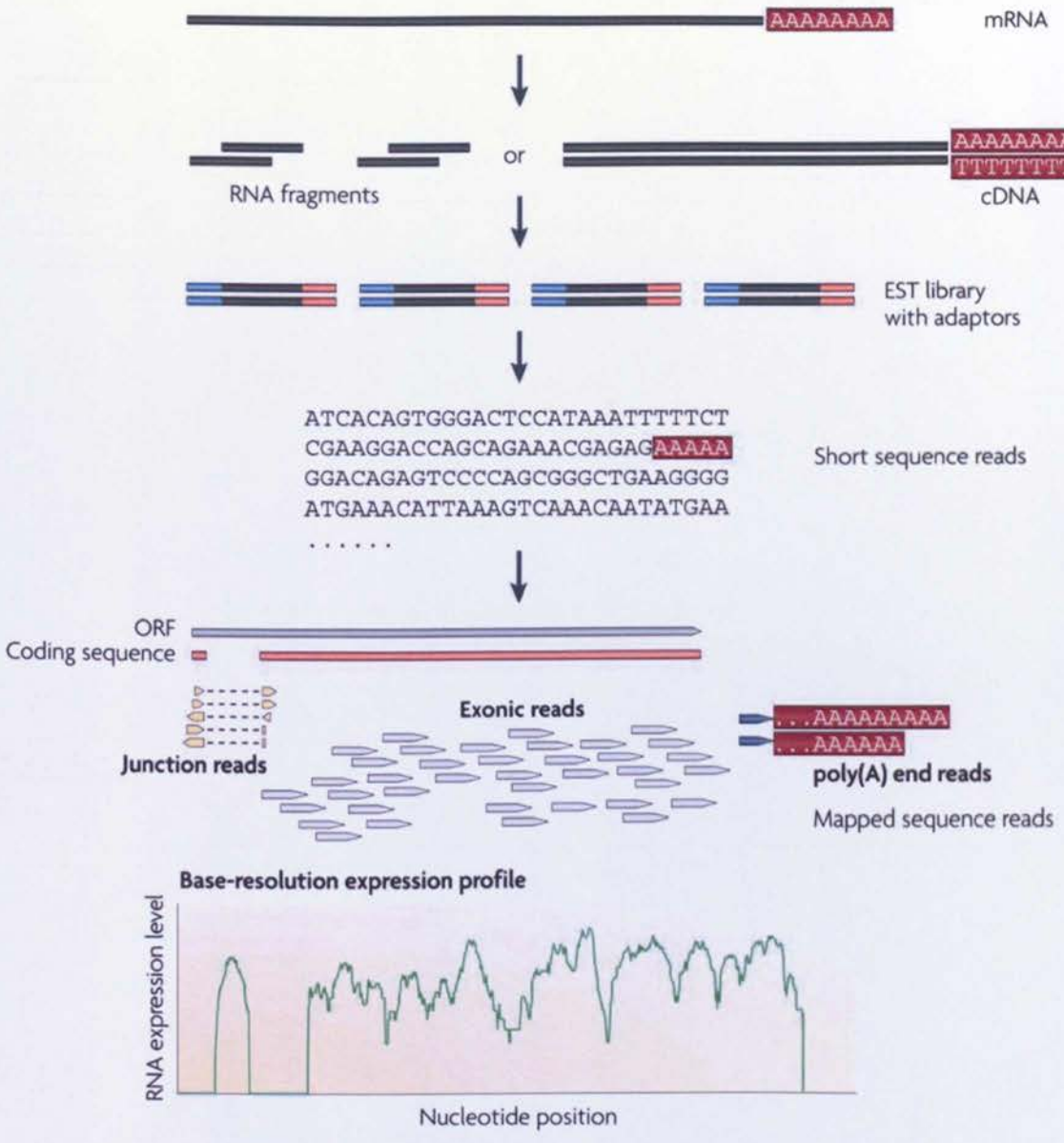

Fig. 6.1: The processes involved in RNA-Seq experiments

Long RNAs are converted into a library of cDNA fragments via RNA or DNA fragmentation. Adapters are joined to each cDNA fragment to produce a short sequence from each cDNA using high-throughput sequencing technology. This sequence is then aligned with a reference genome/ transcriptome and an expression profile is created based on each gene by classifying data into three types: junction reads, poly (A) end-reads and exonic reads.

Sample Information				TopHat Result				Total Reads After trimming		
Lane	Sample ID	Total reads passing QC	Paired in sequencing	Read1	Read 2	Properly Paired	Itself and mate mapped	Singleton	Read1+ Read2	Percentage Aligned
1	W1A	70035326	70035326	35085957	34949369	67691820 (96.65%)	69092306	943020 (1.35%)	73497258	95.29
1	W2A	38276204	38276204	19182231	19093973	37196508 (97.18%)	37798180	478024 (1.25%)	40440576	94.65
1	W3A	52489509	52489509	26302478	26187031	50927210 (97.02%)	51849792	639717 (1.22%)	55261596	94.98
1	W4A	52933012	52933012	26523442	26409570	51230282 (96.78%)	52252950	680062 (1.28%)	55718612	95.00
2	M1A	31819576	31819576	15952068	15867508	30742586 (96.62%)	30958070	861506 (2.71%)	34804654	91.42
2	M2A	25894817	25894817	12993822	12900995	24678392 (95.30%)	25458308	436509 (1.69%)	27548050	94.00
2	M3A	34317721	34317721	17223973	17093748	33243268 (96.87%)	33749948	567773 (1.65%)	36731908	93.43
3	W1B	22899328	22899328	11501482	11397846	21812558 (95.25%)	22438216	461112 (2.01%)	24709176	92.68
3	W2B	26458374	26458374	13291089	13167285	25239342 (95.39%)	25957048	501326 (1.89%)	28376644	93.24
3	W3B	15355842	15355842	7713859	7641983	14575256 (94.92%)	15018536	337306 (2.02%)	16594892	92.53
3	W4B	10653349	10653349	5348585	5304764	10262932 (96.34%)	10439886	213463 (2.0%)	11971418	88.99
4	M1B	28343558	28343558	14207414	14136144	27006822 (95.28%)	27830074	513484 (1.81%)	30573030	92.71
4	M2B	19942010	19942010	9994996	9947014	19202668 (96.29%)	19576906	365104 (1.83%)	21669326	92.03
4	M3B	19684554	19684554	9861513	9823041	18932820 (96.18%)	19325574	358980 (1.82%)	21297718	92.43

Table. 6.1: Quality control statistics for run

Raw data from the sequencing machine regarding quality of the run – number of reads. Only four mice were used in the WT pools as one sample was discarded due to double peaks in the Bioanalyser QC step. Results show approximately ≥90% alignment.

A

Sample	Total reads	Mapped reads	% Mapped reads
WT untreated 1	73,497,258	70,035,326	95
WT untreated 2	40,440,576	38,276,204	95
WT untreated 3	55,261,596	52,489,509	95
WT untreated 4	55,718,612	52,933,012	95
Mac KO Untreated 1	34,804,654	31,819,576	96
Mac KO Untreated 2	27,548,050	25,894,817	94
Mac KO Untreated 3	36,731,908	34,317,721	93
WT Treated 1	57,941,990	48,823,020	84
WT Treated 2	70,762,308	57,398,492	81
WT Treated 3	36,423,756	32,591,461	89
WT Treated 4	32,465,390	23,222,061	72
Mac KO Treated 1	64,459,272	60,627,623	94
Mac KO Treated 2	58,925,240	38,434,971	65
Mac KO Treated 3	47,548,596	43,807,621	92

B

Comparison	Differentially expressed Genes
WT untreated samples vs. KO untreated samples	3696
WT untreated vs. WT treated	7740
KO untreated vs. KO treated	3349
WT treated vs. KO treated	2582

Table. 6.2: Differential analysis and expression results

The total reads obtained (A) and the differentially expressed genes (B) between the different genotypes and treatments. There were >2500 differentially expressed genes per treatment and/or genotype. WT and Mac KO refer to $DDAH2^{flox/flox}$ and $DDAH2^{flox/flox}$ LysM-Cre respectively.

6.4 Pathways affected by DDAH2$^{flox/flox}$ LysM-Cre deletion

The data generated from the RNA-Seq provided us with over 10,000 different genes which showed both significant and non-significant changes compared to controls. Based on this information, GO term was conducted to determine macrophage pathways which were significantly altered either following the deletion of DDAH2 or the addition of LPS. To calculate this false discovery rate (FDR) was determined by determining the adjusted p-values for each test. Because of this, it is less conservative than the Bonferroni approach and has a greater power in finding to find truly significant results.

First and foremost the data obtained was used to confirm the deletion of the DDAH2 gene in macrophages. The results showed that DDAH2 was completely deleted from DDAH2$^{flox/flox}$ LysM-Cre whilst in DDAH2$^{flox/flox}$ it was present. This, along with the previous data, confirms the successful deletion of DDAH2 in this novel knock-out model. Similarly DDAH1 was not present in the samples again confirming that macrophages contain only DDAH2.

Following this, we wanted to investigate the key pathways altered by the deletion of DDAH2. The results from the GO terms showed that the most significant changes were seen in pathways associated with the immune system response and activation (5.397405 $x10^{-50}$ FDR), activation of cells (8.931668 $x10^{-32}$), regulation of cytokine production (5.957076 $x10^{-15}$), the recruitment of other cell types such as B cells and T cells (7.459397 $x10^{-13}$) and the regulation and stimulation of cell motility (4.241194 $x10^{-12}$) (Table 6.3), Consequently, genes related to these pathways were selected and the fold difference between the DDAH2$^{flox/flox}$ LysM-Cre and DDAH2$^{flox/flox}$ in untreated and LPS treated conditions were determined.

Pathway	FDR
Immune system processes	5.397405×10^{-50}
Cell activation (a change in morphology or behaviour)	8.931668×10^{-32}
Leukocyte activation	4.101069×10^{-30}
Defence Response	1.752888×10^{-19}
Response to wounding	3.181437×10^{-18}
Regulation of cytokine production	5.957076×10^{-15}
Inflammatory response	2.557091×10^{-14}
Regulation of T cell activation	7.459397×10^{-13}
Cell motility	4.241194×10^{-12}
Leukocyte migration	1.008012×10^{-12}

Table 6.3: Pathways associated with DDAH2 deletion in macrophages.

The immune response, cell activation, response to wound healing, cell migration, cell apoptosis and the regulation of cytokine productions are some of the several important macrophage functions associated with the deletion of DDAH2. This analysis was carried out on $DDAH2^{flox/flox}$ treated versus $DDAH2^{flox/flox}$ LysM-Cre treated.

6.5 DDAH2 significantly regulates Arginase 1 expression

Initial analysis was carried out in genes which are known to be directly associated with the NOS/ADMA pathway (Table 6.4). Although there were trend in NOS expression between $DDAH2^{flox/flox}$ and $DDAH2^{flox/flox}$ LysM-Cre, the results did not reach statistical significance therefore are inconclusive.

The AGXT2 receptor, which catalyses the conversion of glyoxylate to glycine using L-alanine as the amino donor, was significantly reduced by 0.816-fold. Interestingly arginase (Arg1), which catalyses the hydrolysis of arginine to ornithine, was significantly increased by 12.0-fold. Argininosuccinate synthase 1 (ASS1), which aids the conversion of arginine to ornithine and urea, was reduced by 0.485-fold. Similarly NO and COX are known to be related. COX-2, the inducible isoform involved in prostaglandin synthesis, is elevated by 2.17-fold.

Data obtained following activation of pMacs with LPS for 6 hours shows that there are significant differences between the cells prior to activation and after activation. Upon LPS activation the AGXT2 receptor and Arg1 were both reduced compared to the previous fold change seen in untreated conditions (AGXT2 expression reduced from 0.816 to 0.534-fold whereas Arg1 also reduced from 12.0 to 7.72-fold). COX-1 expression was now elevated 1.81-fold whereas COX-2 expression went from being increased in untreated conditions by 2.17-fold to being reduced following inflammatory stimulus by 0.642-fold.

Gene	Important in	F.C (Untreated)	F.C (LPS)
ADMA/NO associated pathways			
Agxt2l2	Catalyses conversion of glyoxylate to glycine using L-alanine as an amino donor	-0.816	-0.534
Arg1	Catalyses hydrolysis of arginine to ornithine and urea; Expressed predominantly in liver	+12.0	+7.72
ASS1	Aids conversion of arginine to ornithine and urea	-0.485	-0.751
COX-1	Mediates formation of prostaglandins from arachidonate; Important in promoting cell proliferation	N/A	+1.851
COX-2	Mediates formation of prostaglandins from arachidonate; Important for inflammation	+2.170	-0.642

Table. 6.4: ADMA/NO associated genes altered by DDAH2.

RNA-sequencing was used to investigated the gene profiling of different genes associated with the ADMA/NO pathway from pMacs in untreated and LPS treated (6 hours) from DDAH2$^{flox/flox}$ LysM-Cre and DDAH2$^{flox/flox}$ LysM-Cre. F.C represents fold change and highlighted in grey are the genes which show the biggest significant fold change.

6.6 Macrophage cytokine production is regulated by DDAH2

One of the main pathways affected by DDAH2 was shown to be the regulation of cytokine production (GO analysis revealed FDR of 5.957076×10^{-15}). Since cytokine production and the immune system response are closely linked (as described previously), the significant fold changes in macrophages extracted from $DDAH2^{flox/flox}$ LysM-Cre compared to $DDAH2^{flox/flox}$ mice and in both untreated and LPS treated conditions were determined (Table 6.5). These genes were selected based on prior research indicating them to be an important factor related to the NO pathway and/or macrophage function.

In untreated conditions, there was a significant down-regulation in the TNF superfamily of genes. TNFaip2 and TNFrsf10b, important mediators of inflammation and regulation of intracellular apoptosis in the immune system respectively, were significantly reduced 0.652 and 0.264-fold in $DDAH2^{flox/flox}$ LysM-Cre pMacs. Similarly RANTES, which is a chemo-attractant for monocytes, memory T-helper cells and eosinophil's which causes releases of histamines from basophils, was significantly reduced by 0.198-fold. IL-3, which induces macrophages and mast cells, was also reduced by 0.320-fold. Interestingly both pro-inflammatory and inflammatory genes- were shown to be up-regulated in $DDAH2^{flox/flox}$ LysM-Cre pMacs cultured under resting conditions. VEGF-α, IL-1β, IL-6 and TGF-β significantly increased 1.24, 2.39, 5.76 and 1.69-fold respectively. IL-9 and IL-10 were shown to increase significantly higher than this to 35.0 and 8.98-fold.

Upon LPS treatment, all fold changes in cytokines were significantly reduced in DDAH2 deleted animals apart from IL-9 which went from 35.0-fold higher in untreated conditions to 43.6-fold higher in inflammatory conditions, IL-10 which went from 8.98-fold higher to 1.09-fold higher in inflammatory conditions and RANTES which went from 0.198-fold in untreated conditions to an 0.425-fold increase in inflammatory conditions. The TNF receptors were highly reduced in $DDAH2^{flox/flox}$ LysM-Cre mice compared to control: TNF, TNFaip3, TNFaip2 and TNFrsf10b levels were 0.130, 0.751, 0.533 and 0.286-

fold less respectively. Interestingly TNFRSF18 increased by 10.13-fold in inflammatory conditions. VEGF, IL-1β and IL-6 levels were significantly lower in DDAH2$^{flox/flox}$ LysM-Cre mice by 0.519, 0.711 and 0.498-fold in inflammatory stimulated conditions. IL-1α, IL-12b, IL18 were also significantly lower (0.667, 1.47, 0.637 less respectively).

Gene	Important in	F.C (Untreated)	F.C (LPS)
	Cytokines		
TNF	Involved in proliferation, apoptosis and differentiation.	N/S	-0.130
TNFaip2	Mediator of inflammation and angiogenesis	- 0.652	-0.533
TNFaip3	Inflammatory response; Inhibits NFkβ activity	N/S	-0.751
TNFrsf10b	Promotes activation of NFkβ; Mediates apoptosis	- 0.264	-0.286
TNFRSF18	Member of TNF receptor family; Important in interaction between T cells and endothelial cells.	+4.08	+10.13
VEGF-α	Regulates angiogenesis, proliferation and permeability	+1.24	-0.519
IL-1α	Inflammatory response; Stimulates prostaglandin release	N/S	-0.667
IL-1β	Inflammatory response; Stimulates proliferation	+2.39	-0.711
IL-3	Induces macrophages, mast cells	-0.320	
IL-6	Induces acute phase response; Acts on B/T cells	+5.76	-0.498
IL-9	Supports growth of helper T cells; Linked to asthma	+35.0	+43.6
IL-10	Inhibits cytokines (IFN-γ, IL-2, IL-3 and TNF)	+8.98	+1.09
IL-12b	Growth factor for activated T/NK cells; Important for innate and adaptive immunity	N/A	-1.47
IL-18	Stimulates IFN-γ in T-helper cells; Increases NK cell activity in spleen cells	N/S	-0.637
TGF-β	Regulates cell division, differentiation and death	+1.69	N/S
RANTES	Chemo-attractant; Causes release of histamine and activates eosinophils	-0.198	+0.425

Table. 6.5: Cytokine genes altered by DDAH2

RNA-sequencing was used to investigated the gene profiling of different cytokines from pMacs in untreated and LPS treated (6 hours) from $DDAH2^{flox/flox}$ LysM-Cre and $DDAH2^{flox/flox}$ LysM-Cre. F.C represents fold change and highlighted in grey are the genes which show the biggest significant fold change.

6.7 Macrophage motility is regulated by DDAH2

Other factors shown to be affected by DDAH2 deletion in macrophages were genes associates with cell motility (GO analysis revealed a FDR of 4.241194 $x10^{-12}$). Significantly altered genes were selected based on previous research showing them to be key regulator of motility or associating them to NO (Table 6.6).

RhoA leads to the activation of stress fibres via the enzyme ROCK1. The deletion of DDAH2 caused an increase in ROCK1 by 1.42-fold. Furthermore it caused an increase in the small Ras family proteins - RhoB and its associated receptor Rhobtb1 and Rhobtb2 (0.321, 1.82 and 1.92 respectively). These are important for mediating apoptosis and affect cell adhesion. GTPases are highly involved in cell motility and Rhoq has been shown to cause the formation of actin filaments and filipodia. Rhoq was significantly increased by 1.84-fold. Significant increases in this can lead to high levels of actin being produced, eventual stress fiber formation, therefore causing the inability of the cells to move.

Similarly the adhesion molecules ICAM1 and PECAM1, important for the adhesion of monocytes to the endothelial monolayer displayed contrasting results. ICAM1 expression was significantly lower in $DDAH2^{flox/flox}$ LysM-Cre mice (0.521-fold) whereas PECAM1 expression massively increased by 71.30-fold. MIF levels were 0.445-fold lower in $DDAH2^{flox/flox}$ LysM-Cre pMacs than in control pMacs.

Upon LPS activation, RhoB, Rhobtb1 and Rhobtb2 had expression levels of -0.271, 1.14 and 2.69-fold respectively. PECAM1 expression was now up by 28.9-fold compared to 71.3-fold in untreated conditions. The expression profile of the important macrophage/monocyte chemo-attractant protein MIF increased by 1.59-fold. All fold changes shown were significantly different to $DDAH2^{flox/flox}$.

Gene	Important in	F.C (Untreated)	F.C (LPS)
Motility factors			
ROCK1	Regulator of actin cytoskeleton, focal adhesions and polarity	+1.42	N/S
RHOB	Affects cell adhesion and mediates apoptosis	+0.321	-0.271
Rhobtb1	Involved in organisation of actin filament	+1.82	+1.14
Rhobtb2	Inhibits growth and spread of breast cancers	+1.92	+2.69
Rhoq	Causes formation of fillopodia	+1.843	N/S
ICAM1	Ligand for leukocyte adhesion protein LFA-1. Important in trans-endothelial migration.	-0.521	N/S
PECAM1	Involved in leukocyte migration, angiogenesis and integrins activation	+71.3	+28.9
MIP-1α	Increases intracellular calcium levels	N/S	-0.787
MIP-2α	Produced by activated monocytes at sites of inflammation; Supresses progenitor cell proliferation	N/S	-0.550
LIF	Induces terminal differentiation in leukaemic cells	N/S	-0.519
MIF	Pro-inflammatory cytokine; Innate immune response	-0.445	+1.59

Table. 6.6: Motility genes altered by DDAH2

RNA-sequencing was used to investigated the gene profiling of different motility genes from pMacs in untreated and LPS treated (6 hours) from $DDAH2^{flox/flox}$ LysM-Cre and $DDAH2^{flox/flox}$ LysM-Cre. F.C represents fold change and highlighted in grey are the genes which show the biggest significant fold change.

6.8 Cell activation and the immune system responses are regulated by DDAH2

Some of the major genes affected by DDAH2 deletion were apoptosis markers and markers which lead to the activation of other cell types such as B and T cells and platelets and genes associated with immune system responses (GO analysis revealed FDR of 8.931668 $x10^{-32}$, 4.101069 $x10^{-30}$, 5.397405 $x10^{-50}$, 7.459397 $x10^{-13}$ for cell activation, leukocyte activation, immune system processes and regulation of T cell activation respectively) (Table 6.7).

The results show that in untreated conditions, there was no significant difference in TLR expression between the different genotypes in untreated conditions. Following inflammatory stimulus, however, TLR expression tended to decrease (0.5-fold, 0.78-fold, 0.57-fold and 0.62-fold for TLR1, 4, 6 and 13 respectively). TLR8 and TLR9 increased singificantly by 1.9-fold and 58-fold respectively.

Binding of pathogen ligands to most TLRs results in the activation of downstream NF-κB. NF-κB (1 and 2) was significantly reduced by 0.700-fold and 0.680-fold respectively in untreated conditions and was also significantly reduced in inflammatory conditions by 0.720 and 0.537-fold.

Similarly, the BCl family of genes (which are important for regulating and suppressing cell death) were all reduced in $DDAH2^{flox/flox}$ LysM-Cre pMacs by 0.545, 0.446 and 0.737-fold in BCl-2, BCl-3 and BCl-6 respectively. Caspase 7, which is involved in apoptosis and programmed cell death, was significantly reduced by 0.544-fold in untreated conditions. On the other hand, caspase 8 which is also associated with cell death and has been shown to be associated with neurodegenerative diseases was increased by 1.65-fold. The heat-shock protein, HSP90, is a molecular chaperone which aids protein folding and is critical in signal transduction and structural maintenance. It has been shown to be an intermediate in the signalling cascades leading to the activation of eNOS (Shah *et al.*, 1999). HSP90 was increased by 1.34-fold.

Similarly CD69 is involved in lymphocyte proliferation and functions as a signal transmitting receptor in lymphocytes, natural killer cells and platelets and was increased by 3.70-fold. CD25 and CD121b, two important receptor molecules for interleukin and associated with cell activation, were found to be increased by 86.0 and 9.21-fold respectively. CD74 is associated with the MHC II complex and is an important chaperone that regulates antigen presentation for immune response. Similarly it is involved in NOS binding and is also a cell surface receptor for macrophage migration inhibitory factor (MIF) which initiates survival pathways and proliferation. CD74 was increased by 4.97-fold in $DDAH2^{flox/flox}$ LysM-Cre pMacs.

Endoglin (CD105) is a glycoprotein of the vascular endothelium and is critical to the binding of the endothelium to other integrins. This was shown to be reduced by 0.547-fold. Another mediator of NK cell adhesion and effect function, CD155, was shown to be reduced 0.813-fold in $DDAH2^{flox/flox}$ LysM-Cre mice. Interestingly the macrophage scavenger receptor (CD204) which is a membrane glycoprotein implicated in the pathologic deposition of cholesterol in arterial walls during atherogenesis was shown to be elevated by 1.45-fold. Also CD206, a mannose receptor which mediates the endocytosis of glycoproteins was shown to be elevated by 1.32-fold.

The majority of the apoptosis regulating genes (BCl and caspases) which were significantly reduced prior to activation increased following the addition of LPS. BCl-6 increased by 2.57-fold as did caspases 2, 6, 8 and 9 by; 1.49, 1.53, 1.28 and 1.40-fold respectively. Only caspase 1 and 7 (which were already reduced prior to activation) were shown to be reduced by; 0.524 and 0.337-fold respectively. HSP90, which has been shown to help stimulate eNOS and prior to activation had increased expression in knock-out animals, was significantly reduced in expression by 5.38-fold following stimulation. LXR-β which is critical for cholesterol homeostasis and activation of the innate immune response was significantly reduced by 0.789-fold in knock-out animals. MAPK-8 and MAPK-9 are significantly reduced by 0.584 and 0.734-fold upon inflammation in $DDAH2^{flox/flox}$ LysM-Cre compared to $DDAH2^{flox/flox}$ animals.

There was no real statistically significant variation in data between the different CD markers in untreated conditions compared to LPS-treated conditions, only that the change fold was attenuated. Only CD105, whose expression was previously reduced by 0.547-fold in untreated conditions, now increased in expression by 1.24-fold. In untreated conditions, the fold change of the markers CD74, CD121b, CD204, CD206, CD25 and CD69 was reduced by; 5.38, 6.31, 1.37, 1.64, 19.3 and 23.9-fold respectively and for the CD155 marker was reduced 1.24-fold in $DDAH2^{flox/flox}$ LysM-Cre. Following inflammatory stimuli, the fold change of the markers was attenuated; 5.38, 6.31, 1.37, 1.64, 19.3 and 23.9-fold in CD74, CD121b, CD204, CD206, CD25 and CD69 respectively. In inflammatory conditions, CD155 levels were further reduced by a fold change of 0.742.

Gene	Important in	F.C (Untreated)	F.C (LPS)
Cell activation, cell death and inflammatory responses			
TLR1	Receptor for bacterial lipoproteins; Activates NF-κB	NS	-0.5
TLR4	Receptor for LPS, viral envelope protein; Activates NF-κB and IRF3	NS	-0.78
TLR6	Receptor for LTA, diacyl lipoproteins, zymosan; Activates NF-κB	NS	-0.57
TLR8	Receptor for ssRNA; Activates NF-κB	NS	+1.9
TLR9	Receptor for unmethylated CpG DNA; Activates IRF7	NS	+58.0
TLR13	Receptor for bacterial RNA; Activates NF-κB	NS	-0.62
NF-κB1	Stimulates cytokines; Regulates immune response	-0.700	-0.720
NF-κB2	Stimulates cytokines; Regulates immune response	-0.680	-0.537
MAPK8	Involved in proliferation, migration and differentiation	NS	-0.584
MAPK9	Involved in proliferation, migration and differentiation	NS	-0.734
BCL-2	Suppresses apoptosis and regulates cell death	-0.545	NS
BCL-3	Regulates NF-kB gene activation	-0.446	NS
BCL-6	Important for antibody affinity maturation	-0.737	+2.57
Caspase-1	Important for the defence against pathogens	NS	-0.524
Caspase-2	Involved in the activation of caspases	NS	+1.49
Caspase-6	Involved in the activation of caspases	NS	+1.53

Caspase-7	Executioner caspase- has an important role in cell apoptosis; implicated in pathogenesis of stroke, Alzheimer's disease, cancer and inflammatory diseases	-0.544	-0.337
Caspase-8	Initiator caspase- starts the apoptosis cycle	+1.653	+1.28
Caspase-9	Involved in the activation cascade of caspases	NS	+1.40
HSP90	Promotes cell maturation; linked to ATPase activity	+1.34	-0.856
CD25	Involved in immune system and a receptor for IL-2	+86.0	+19.3
CD74	MHC II; chaperone that regulates antigen presentation in immune response	+4.97	+5.38
CD69	Lymphocyte proliferation; transmits signals in platelets and NK cells	+3.70	+23.9
CD121b	Binds to IL-1α	+9.21	+6.31
CD155	Mediates NK adhesion	-0.813	-0.742
CD204	Mediates deposition of cholesterol in arterial wall	+1.45	+1.37
CD206	Acts as a phagocytotic receptor for pathogens	+1.32	+1.64
LXR-β	Cholesterol homeostasis; Inhibition of pro-inflammatory gene expression in atherosclerosis	NS	-0.874

Table. 6.7: Genes associated with cell activation, cell death and immune system responses are altered by DDAH2

RNA-sequencing was used to investigated the gene profiling of different genes associated with cell, activation, cell death and the immune response from pMacs in untreated and LPS treated (6 hours) from DDAH2$^{flox/flox}$ LysM-Cre and DDAH2$^{flox/flox}$ LysM-Cre. F.C represent fold change and highlighted in grey are the genes which show the biggest significant fold change.

6.9 Discussion

The data from previous chapters has shown DDAH2 to be an important regulator of macrophage function and TNF-α production. The main aim of the chapter was to simultaneously determine the effect of DDAH2 on a variety of immunological pathways using high-throughput RNA-seq. This was carried out to investigate the hypothesis that DDAH2 can mediate important macrophage inflammatory responses and is critical in immune cell functions.

First and foremost, the RNA-Seq data confirmed the successful deletion of DDAH2 in $DDAH2^{flox/flox}$ LysM-Cre pMacs compared to $DDAH2^{flox/flox}$ pMacs and showed that it was the only DDAH isoform present in pMacs. Although there were trends in NOS expression, there was no significant difference between the results.

The RNA-Seq results were also used to investigate any genes that appeared to be regulated by DDAH2. Besides, iNOS, Arg1 is the major L-arginine consuming enzyme and has a high activity in stimulated macrophages. Arg1 is induced with iNOS during macrophage activation and has a higher Km value for arginine (~10mmol/ L and ~5μmol/ L for arginase and iNOS respectively) (Mori, 2007). It hydrolyses L-arginine into urea and ornithine, a precursor to L-proline and polyamines, which are implicated in tissue repair and wound healing (Munder, 2009). We found Arg1 levels to be significantly elevated in both untreated and inflammatory treated conditions (12-fold and 7.72-fold in untreated and LPS treated conditions respectively) suggesting a strong correlation between DDAH2 and Arg1. In accordance with our finding that DDAH2 knock-outs have reduced NO production, Chang *et al* showed that Arg1 is capable of reducing NO production in activated macrophages by lowering L-arginine availability to NOS (Chang *et al.*, 1998).

This increased expression of Arg1 is interesting in terms of the ADMA NO pathway. Increasing Arg1 expression results in reduced L-arginine levels and therefore less substrate for NOS. This may be one indirect ADMA mechanism which can regulate NO levels in macrophages and may therefore also be important in macrophage function,

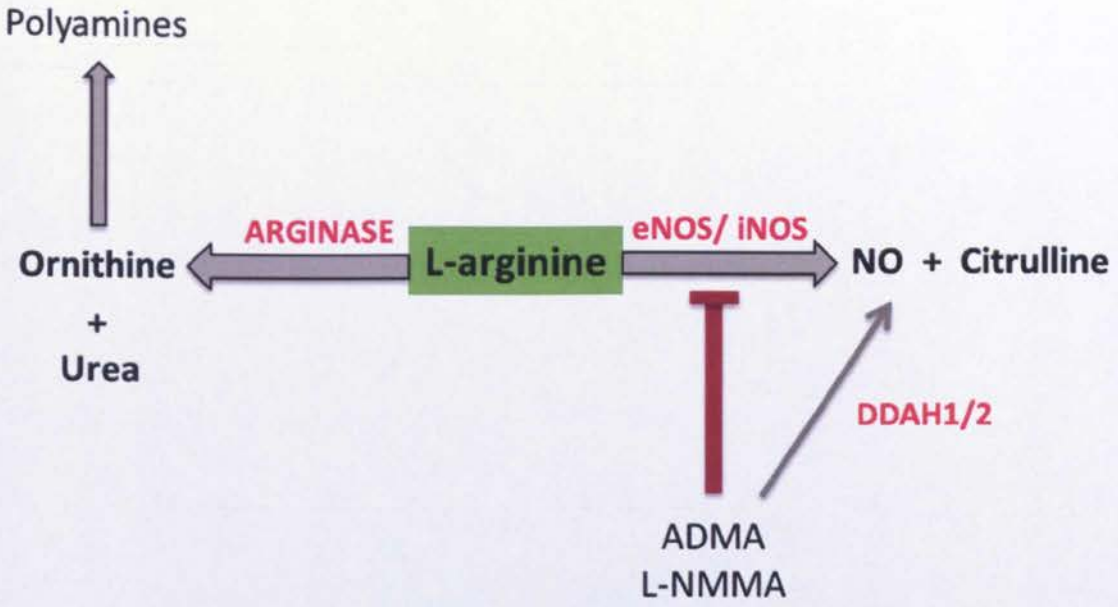

Fig. 6.2: Role of Arginase in the ADMA/NO pathway

Arginine converts L-arginine into ornithine and urea which goes on to form polyamines. ADMA and L-NMMA are competitive inhibitors of all NOS isoforms. These inhibitors are metabolized by the enzyme DDAH of which there are two isoforms. NO production can be controlled by modulating the synthesis of NOS inhibitors via PRMTS or their metabolism by DDAH. NO is critical to cGMP production, peroxynitrite formation and various metabolic pathways.

In terms of clinical importance, studies in human and mice (Khallou-Laschet *et al.*, 2010; Pourcet *et al.*, 2011; Teupser *et al.*, 2006) have shown that an increase in macrophage Arg1 is associated with enhanced vascular smooth muscle cell proliferation (Khallou-Laschet *et al.*, 2010), which may contribute to the remodelling of the fibrous cap surrounding the atherosclerotic lesion thus promoting plaque stabilization. Elevated levels of macrophage Arg1 are also associated with atherosclerotic plaques of smaller size and less lipid and macrophage content, thus its expression is inversely associated with the degree of atherosclerosis. For instance, high macrophage Arg1 levels correlate with resistance to atherogenesis in rabbits (Teupser *et al.*, 2006).

TLRs were also shown to be regulated by DDAH2. Cole *et al.* demonstrated that NO production by iNOS induced TLR signals and therefore increased the cell-spreading required during macrophage phagocytosis (Cole *et al.*, 2012). Hence, the decrease in cell surface TLR expression in DDAH2 KO's compared to WT's may explain the reduced phagocytosis levels seen in these pMacs. Interestingly, TLR8 and TLR9, which are localised in intracellular vesicles such as the endosome or lysosome, were significantly increased in DDAH2 KO's suggesting that DDAH2 may have varying effects on intracellular and extracellular surface receptors.

One potential way to target atherosclerosis in disease is to encourage macrophage death in plaques in addition to anti-inflammatory drugs (De Meyer *et al.*, 2012). LPS activation resulted in an increase in the key apoptotic genes involved in modulating apoptosis, including; BCl-6, and caspase 2, 6, 8, and 9. The increase in these genes suggests that DDAH2 deletion may lead to a reduction in macrophage recruitment but also increased apoptosis may lead to the disruption of the plaque. In macrophages, NO has been shown to activate the caspase cascade and induce apoptosis suggesting that the apoptosis pathway in macrophage is NO dependent (Gotoh *et al.*, 2002).

Overall this chapter identifies DDAH2 as a key regulator of pathways associated with the immune response, B and T cell activation and motility. These findings corroborate the previous data in previous chapters but also highlight novel genes which are significantly modulated by DDAH2. The deletion of DDAH2 was found to reduce many key cytokine genes and pathways associated with the inflammatory response such as NF-κB and MAPK pathway whilst Arg1 was found to be significantly increased.

Conclusion

In this chapter we set out to investigate and discover known genes as well as novel genes and their associated pathways which may be regulated by DDAH2. To do this we used RNA-Seq – a cutting-edge and novel method used to simultaneously determine 1000's of genes altered between different genotypes and treatments. Based on the results from this chapter we can reject our null hypothesis and conclude that:

1. *DDAH2 is a critical regulator of the immune response, cell activation and migration.*

2. *Arg1, an important mediator of NO levels and signalling as well as a modulator of collagen content and cellular proliferation, is regulated by DDAH2 in macrophages. This may provide novel insight into the link between the involvements of Arg1-DDAH in atherosclerosis.*

CHAPTER 7

General Discussion

7.1 General discussion

Endogenous methylarginines can be degraded by the DDAH enzymes. There are two isoforms of the gene that makes these enzymes; DDAH1 and DDAH2, which are found to be ubiquitously expressed in cells containing NOS but also cells that don't contain NOS (Ogawa *et al.*, 1987, Ogawa *et al*,. 1989, Leiper *et al.*, 1999). In the 1990's levels of ADMA were found to be elevated in patients with chronic renal failure and further research showed that this was also the case in various cardiovascular diseases. This led to the hypothesis that ADMA blocks NOS activity and that DDAH, the enzyme involved in its metabolism, may be modulated therapeutically in various diseases (Leiper and Nandi, 2011). These observations sparked interest in this enzymatic pathway and over the years NO has been shown to be involved in many cell regulatory pathways. More importantly interest in DDAH itself has increased in the last few years. DDAH1 knock-out *in vivo* has been shown to cause an increase in ADMA concentrations and led to increased blood pressure, endothelial dysfunction and a reduced cardiac performance (Leiper *et al.*, 2007).

Despite this knowledge regarding DDAH1, little is known about DDAH2 and in particular its role in iNOS regulation and association with cardiovascular disease and inflammation. To understand more fully the role of DDAH2, we have used the human monocytic cell line U937 which can be differentiated into macrophages and are easily grown. Furthermore, we have used global DDAH2$^{-/-}$ mice as well as generating a novel DDAH2 macrophage-specific mouse knock-out model (DDAH2$^{flox/flox}$ LysM-Cre) – from both of which macrophages were extracted. Using primary macrophages allows us to investigate the effect of intracellular changes of ADMA on macrophage function. Macrophages are important coordinators of the innate immune response that are capable of producing high levels of NO following inflammation (Assreuy *et al.*, 1994; Billack, 2006; Mosser, 2003; Hibbs, 2002). They are necessary for the destruction of pathogens and recruitment of other immune cells through production of pro-inflammatory cytokines but in inflammatory diseases such as

atherosclerosis they may increase pathogenesis. Any potential to regulate macrophage function can thus be clinically beneficial.

The main aim of the thesis was to determine the effects of DDAH2 on macrophage NO production, motility, phagocytosis, proliferation and cytokine production and investigate the effect of DDAH2 deletion on the regulation of important macrophage-related genes. This was led by the hypothesis that DDAH2 is a critical regulator of macrophage function and therefore may play a significant role in inflammatory related diseases.

7.2 DDAH2 as a regulator of endogenous methylarginine concentrations

The role of DDAH, in particular DDAH2, in methylarginine degradation has been very controversial. Over the last two decades there has been significant information regarding the involvement of DDAH1 in ADMA metabolism and NO synthesis (Dayoub *et al.*, 2003; Hu *et al.*, 2011; Konishi *et al.*, 2007; Jacobi *et al.*, 2005), which has led to the development of specific DDAH1 inhibitors for therapeutic use (Rossiter *et al.*, 2005; Leiper *et al.*, 2007). It was initially suggested that DDAH2, like DDAH1, metabolises ADMA and L-NMMA (Leiper *et al.*, 1999) and this was shown by using a model of DDAH2-overexpression (Wang *et al.*, 2007), gene transfer (Feng *et al.*, 2010), cell culture (Achan *et al.*, 2002) and DDAH2 transgenic mice (Feng *et al.*, 2010; Hasegawa *et al.*, 2007) to relate changes in ADMA and DDAH2 activity to DDAH2 expression. However, a major drawback to elucidating the role of DDAH2 in methylarginine metabolism has been the inability to produce active purified, native or recombinant DDAH2 although Leiper *et al.* has expressed His_6- tagged human DDAH2 (Leiper *et al.*, 1999).

More recent *in vitro* and *in vivo* studies have raised concerns about the involvement of DDAH2 in ADMA metabolism (Hu *et al.*, 2011; Wang *et al.*, 2007; Pope *et al.*, 2009; Zhang *et al.*, 2011; Altmann *et al.*, 2012). Hu *et al.*,

found no metabolism of stable-isotope-labelled ADMA and L-NMMA in tissue from DDAH1$^{-/-}$ mice despite unaltered DDAH2 expression (Hu *et al.*, 2011). Knipp found methylarginine metabolism in purified DDAH1, but not DDAH2, from porcine and bovine kidney and liver. siRNA studies targeting DDAH1 or DDAH2 in rat have shown increased ADMA levels by knockdown of DDAH1, without changes in NO-mediated relaxation of mesenteric arteries but no effect on DDAH2 (Wang *et al.*, 2007). Most recently, Altmann *et al* failed to show any degradation of L-NMMA and ADMA by DDAH2 in porcine tissue and suggested that 'analysis of methylarginine metabolism by DDAH2 is unsuitable for investigations on isoform selectivity of DDAH2 inhibitors' (Altmann *et al.*, 2012). A homology model of human DDAH2 created by Knipp showed differences in the substrate binding of DDAH2 in comparison with DDAH1 although the relevant catalytic amino acids in the structure were the same. This implied that binding of methylarginine might be hindered yet in principle their conversion is possible (Knipp *et al.*, 2001).

First and foremost our data confirmed what was initially thought (Tran *et al.*, 2000) – that DDAH2 is the only isoform present in macrophages. More importantly, we found that at least in macrophages, DDAH2 is a regulator of endogenous methylarginine concentrations. Both the global disruption and macrophage-specific deletion of DDAH2 resulted in significant increase in endogenous ADMA and L-NMMA levels respectively and a 2-fold reduction in nitrite production following inflammatory stimulation. Although DDAH2 activity was not measured, these two mouse models independently highlight DDAH2 to be a key regulator of endogenous methylarginine concentrations and NO production. These findings contradict those of others who show that DDAH2, despite having a 50% sequence identity with DDAH1, does not metabolise methylarginines (Altmann *et al.*, 2012; Hu *et al.*, 2011; Wang *et al.*, 2007). Moreover, the fact that DDAH1 is seen to have greater effects *in vivo* than DDAH2 may suggest that DDAH2 metabolises lower concentrations of ADMA whereas DDAH1 metabolises higher ADMA concentrations.

7.3 AGXT2 as an alternative mechanism for methylarginine metabolism

DDAH is recognised as the primary target for methylarginine metabolism; however, AGXT2 has also been shown to modulate ADMA and SDMA levels. In rats, 16% of ADMA is metabolised by AGXT2 (Ogawa *et al.*, 1987) whilst in mice overexpression of AGXT2 reduces ADMA levels (Rodionov *et al.*, 2010). AGXT2 may also control blood pressure in mice alongside mediating plasma ADMA and NO levels (Caplin *et al.*, 2012; Kittel *et al.*, 2013). It has been postulated that a downregulation of DDAH could result in an increased contribution of AGXT2 to the metabolism of ADMA in pathological conditions such as chronic kidney disease amongst others (Matsuguma *et al* 2006; Rodionov *et al.*, 2010). The kidney, which is important in regulating metabolites in plasma, is the only site of AGXT2 (as well as DDAH1 and DDAH2) expression. Whilst AGXT2 may affect ADMA metabolism in the kidney, it can be accepted that it is not involved in methylarginine metabolism in macrophages. This reinforces the previous findings – that DDAH2 is the primary source of methylarginine metabolism in macrophages.

7.4 The association between VEGF and DDAH2

DDAH expression can also moderate the production of growth factors, such as VEGF. VEGF is involved in angiogenesis whilst DDAH1 can enhance angiogenesis by reducing ADMA and increasing the synthesis of the pro-angiogenic factor NO. Increased DDAH expression has been shown to increase tumour and endothelial cell VEGF production (Kostourou *et al.*, 2002; Smith *et al.*, 2003). A possible mechanism was not elucidated until later by Hasegawa *et al* who found that DDAH2 overexpression increased endothelial VEGF production, proliferation and migration via the transcription factor SP-1 and thus would be an NO/ADMA-independent mechanism of DDAH2 activity (Hasegawa *et al.*, 2006).

The activation of macrophages with LPS produces high levels of VEGF through a NF-κB dependent pathway. Subsequently high levels of VEGF are seen in chronic inflammatory diseases such as RA (Itaya *et al.*, 2001; Perez-Ruiz *et al.*, 1999). Our RNA-Seq data shows only VEGF-α to be significantly increased in $DDAH2^{flox/flox}$ LysM-Cre compared to $DDAH2^{flox/flox}$ by 1.24-fold, yet reduced during inflammation, by 0.52-fold. These values, although significant, are low and unlikely to significantly affect protein expression. Similarly, VEGF expression in media from inflammatory treated macrophages increased significantly with time, however, was not significantly different between both DDAH2 knock-outs compared to controls (see Appendix). This confirms that DDAH2 deletion does not regulate macrophage exogenous VEGF production as was initially postulated and demonstrates that any downstream effects of DDAH2 in macrophages are not VEGF, but NO, mediated. However, this does not exclude the possibility that DDAH2 can locally regulate VEGF expression in certain cell types *in vivo*.

7.5 The difference between NOS inhibition and DDAH deletion on macrophage function

The biological significance of NOS in comparison to DDAH has become a key discussion topic. DDAH2 and NOS both play an important role in macrophage inflammatory-induced NO release; however, based on our results the effect of NOS on NO production appears to be greater. NO levels were significantly reduced following DDAH2 disruption but its production was not completely abolished and in fact increased significantly over time. Total NO inhibition was only obtained following the genetic and pharmacological inhibition of eNOS confirming previous findings that eNOS activity may be critical for macrophage iNOS stimulation and subsequent NO production (Connelly *et al.*, 2003) and that iNOS is important for macrophage activation (Aktan, 2004).Co-inciding with this, our data found that phagocytosis levels were signifcantly reduced by DDAH2 deletion/ disruption.Tumer *et al.* found iNOS inhibition to completely

abolish the phagocytic action of macrophages and total nitrite levels when treated with LPS and LPS with L-arginine (Tumer *et al.* 2006). This again suggests eNOS/iNOS inhibition to be more effective than DDAH2 deletion in disrupting macrophage function.

7.6 The role of DDAH2 on macrophage function

We have shown that DDAH2 metabolises methylarginines and is a regulator of NO production. Key macrophage functions, which include; cytokine production, transmigration, macrophage motility and phagocytosis are therefore DDAH2 dependent. Activation of the innate response is dependent on pro-inflammatory cytokines, however, DDAH2 was shown to reduce the important pro-inflammatory cytokine TNF-α and increase anti-inflammatory IL-9. More specifically, TNF-α is actively involved in the development of both chronic inflammation and autoimmune disease and promotes macrophage transmigration through chemokine (C-C motif) receptor 1 (CCR1) (Wang *et al.*, 2013). We also found that DDAH2 deletion also significantly down-regulated TLR1, 4, 6 and 13 in macrophages. TLRs bind microbial factors to the cell surface or endosome and subsequently activate cytoplasmic signal transduction pathways. This may explain the lack of phagocytosis by DDAH2 of an E-coli bio-particle in DDAH2 knock-out mice compared to WTs.

Macrophage gradient sensing and polarisation is controlled by Rho, rac and cdc42 (and more specifically filopodia) (Jones *et al.*, 1998). During inflammation, increases in macrophage motility and nitrite production coincide with increased filamentous actin production (Fukushima *et al.*, 1994), however, overexpression of stress fibres results in the inability of cells to retract and move (Wojciak-Stothard *et al.*, 2007). DDAH2 was found to affect actin remodelling in inflamed macrophages (see Appendix), which affects their motility and phagocytosis (as phagocytosis has been shown to be reliant on sufficient actin remodelling)(Allen and Aderem, 1996).

It has been postulated that NO mediates HIF-1α through cdc42 and Rac1 and this promotes motility (Zhou *et al.*, 2009). Although HIF-1α was significantly increased in DDAH2$^{flox/flox}$ LysM-Cre compared to DDAH2$^{flox/flox}$ in basal conditions and increased signifcantly in both genotypes following inflammatory stimulation, there was no significant difference between the two genotypes in inflammatory conditions. This implies that at least in inflammatory conditions HIF-1α is not DDAH2 mediated.

Despite there being no significant differences in the intracellular expression of macrophage RhoA, Rac1 and cdc42, ROCK1, the enzyme involved in the activation of RhoA and formation of stress fibres, was increased following DDAH2 disruption. This suggests that DDAH2 inhibition potentially increases RhoA which in turn inhibits Rac1 associated motility (Tang *et al.*, 2012). Despite the increase in RhoA, there was no significant difference in Rac1 expression between the different genotypes, although Rac1 has been shown to be regulated by ADMA/DDAH in endothelial cells (Wojciak-Stothard *et al.*, 2009). Instead, RhoB and Rhoq, which mediate cell adhesion and cause the formation of actin filaments and filipodia, were significantly increased suggesting that DDAH2 may facilitate motility via these genes.

7.7 Clinical relevance of DDAH2 manipulation

NO is responsible for macrophage endotoxin and anti-microbial actions, however, impaired and elevated NO levels are implicated in the pathogenesis of several inflammatory diseases such as atherosclerosis, sepsis and arthritis (Mosser *et al.*, 2003).This suggests that this enzymatic pathway may offer a potential endogenous mechanism for the tissue-specific regulation of NO production by competitive inhibition.

In cardiovascular disease, the constant recruitment of macrophages to the endothelium is a major contributor to atheroma formation and progression. NO helps maintain a healthy endothelium, however, its overproduction results in;

endothelial shear stress, increased macrophage recruitment to the area and increased smooth muscle cell proliferation (Ross, 1999). Methods of reducing atheroma formation include reducing inflammatory stimuli by lowering circulating lipids and promoting cholesterol efflux from the plaque, targeting the adhesion molecules and cytokines associated with monocyte adhesion and transmigration, and inducing macrophage death in atherosclerotic plaques (De Meyer *et al.*, 2012).

In accordance with this, several genes associated with atherosclerosis were regulated by DDAH2. These genes included TNF-α, CD204 and Arg1. DDAH2 reduced TNF-α expression which was associated with, a significant reduction of atheroma in mice (Branen *et al.*, 2004) and reduced risk for cardiovascular events in several clinical trials (Ridker *et al.*, 1997). The proposed mechanism of action is thought to be through promoting matrix degradation thus facilitating the influx of inflammatory cells to the vessel wall during shear stress (Rajavashisth *et al.*, 1999; Galis *et al.*, 1995). Similarly, deletion of DDAH2 increased the expression of the membrane glycoprotein CD204, which is implicated in the pathologic deposition of cholesterol in arterial walls during atherogenesis. DDAH2 reduced Arg1 expression, which is associated with atherosclerotic plaques of smaller size and less lipid and macrophage content (Teupser *et al.*, 2006). An increase in Arg1 is associated with enhanced vascular smooth muscle cell proliferation, which may contribute to the remodelling of the fibrous cap surrounding the atherosclerotic lesion thus promoting plaque stabilization (Khallou-Laschet *et al.*, 2010; Pourcet *et al.*, 2011; Teupser *et al.*, 2006).

Sepsis could also benefit from potential DDAH therapy. iNOS activation results in markedly increased vascular NO levels and both animal and clinical studies have demonstrated significant increases in NO in septic shock (Julou-Schaeffer *et al.*, 1990; Lorente *et al.*, 1993; Sharshar *et al.*, 2003). Despite this apparent detrimental effect of iNOS activation in vascular smooth muscle, the induction of iNOS and concomitant high NO concentrations produced in macrophages are a critical part of the host defence response to an infection. This is seen in

septic iNOS$^{-/-}$ animals which have increased mortality due to their inability to generate NO from iNOS and control bacterial infection (MacMicking *et al.* 1995; Wei *et al.* 1995).

Our DDAH2$^{-/-}$ model showed that, like the model employing direct iNOS$^{-/-}$ inhibition, DDAH2$^{-/-}$ mice had significantly increased mortality over time following CLP. They also displayed increased bacterial titres in the blood and peritoneal cavity compared to control mice. This effect can be attributed to reduced macrophage function such as the loss of motility and phagocytic ability. Interestingly, the specific DDAH1 inhibitor, L-257 has been shown to be effective in reducing NO levels by increasing circulating ADMA levels and maintaining hemodynamic pressures in sepsis (Nandi *et al.*, 2012), however, this is through a macrophage independent mechanism since macrophages do not express DDAH1.

7.8 Future work

$ONOO^-$ is the short-lived oxidant and inducer of cell death that is potentially responsible for the progress of vascular disease and inflammation. It has been previously demonstrated that the second phase of macrophage activation (8-24 hours) is driven predominantly by uncoupled iNOS (Pekarova *et al.*, 2011) which leads to increased production of $ONOO^-$. Since DDAH2 already regulates NO production, and high levels of NO and O_2^- drive $ONOO^-$ production, it would be ideal to measure O_2^- and $ONOO^-$ production from DDAH2$^{flox/flox}$ LysM-Cre and DDAH2$^{flox/flox}$ pMacs.

Moreover, if DDAH2 is associated with inflammatory-mediated diseases, then it could be predicted that predisposing DDAH2$^{flox/flox}$ LysM-Cre mice to disease would result in reduced severity or progression of the disease. For instance, to investigate the effect of DDAH2 on atherosclerosis, DDAH2$^{flox/flox}$ LysM-Cre and DDAH2$^{flox/flox}$ mice could be placed on a high-fat diet to allow plaque formation. The following can then be measured; circulating levels of ADMA and NO in blood, urine and tissues, aorta contractile and relaxation responses, blood

pressure, glucose tolerance, macrophage infiltration into adipose tissue, and the number of macrophages and extent of plaque formation along the aortic arch. These parameters could be modified to suit other inflammatory associated diseases such as arthritis and would further confirm the effect of DDAH2 on inflammatory mediated diseases.

7.9 Conclusion

This work has confirmed that DDAH2 metabolises endogenous ADMA and L-NMMA in macrophages and is a critical regulator of primary macrophage function via an NO, but not a VEGF, dependent pathway. The data from the macrophage specific knock-out and DDAH2 global knock-out were complimentary and both mouse models independently show the same characteristics. The biochemical changes in macrophage function and the spectrum of genes altered by DDAH2 that appear to be correlated with the onset or progression of various inflammatory diseases reinforces the potential benefit of developing a specific DDAH2 inhibitor.

REFERENCES

Achan, V., Tran, C. T., Arrigoni, F., Whitley, G. S., Leiper, J. M. & Vallance, P. 2002. all-trans-Retinoic acid increases nitric oxide synthesis by endothelial cells: a role for the induction of dimethylarginine dimethylaminohydrolase. *Circ Res,* 90, 764-9.

Adams, D. O. & Hamilton, T. A. 1987. Molecular transductional mechanisms by which IFN gamma and other signals regulate macrophage development. *Immunol Rev,* 97, 5-27.

Aderem, A. & Underhill, D. M. 1999. Mechanisms of phagocytosis in macrophages. *Annu Rev Immunol,* 17, 593-623.

Aktan, F. 2004. iNOS-mediated nitric oxide production and its regulation. *Life Sci,* 75, 639-53.

Alexopoulou, L., Holt, A. C., Medzhitov, R. & Flavell, R. A. 2001. Recognition of double-stranded RNA and activation of NF-kappaB by Toll-like receptor 3. *Nature,* 413, 732-8.

Allen, W. E., Zicha, D., Ridley, A. J. & Jones, G. E. 1998. A role for Cdc42 in macrophage chemotaxis. *J Cell Biol,* 141, 1147-57.

Allen, W. E., Zicha, D., Ridley, A. J. & Jones, G. E. 1998. A role for Cdc42 in macrophage chemotaxis. *J Cell Biol,* 141, 1147-57.

Altinova, A. E., Arslan, M., Sepici-Dincel, A., Akturk, M., Altan, N. & Toruner, F. B. 2007. Uncomplicated type 1 diabetes is associated with increased asymmetric dimethylarginine concentrations. *J Clin Endocrinol Metab,* 92, 1881-5.

Altmann, K. S., Havemeyer, A., Beitz, E. & Clement, B. 2012. Dimethylarginine-dimethylaminohydrolase-2 (DDAH-2) does not metabolize methylarginines. *Chembiochem,* 13, 2599-604.

Ananthakrishnan, R. & Ehrlicher, A. 2007. The forces behind cell movement. *Int J Biol Sci,* 3, 303-17.

Anderson, T. J., Gerhard, M. D., Meredith, I. T., Charbonneau, F., Delagrange, D., Creager, M. A., Selwyn, A. P. & Ganz, P. 1995. Systemic nature of endothelial dysfunction in atherosclerosis. *Am J Cardiol,* 75, 71B-74B.

Arrigoni, F., Ahmetaj, B. & Leiper, J. 2010. The biology and therapeutic potential of the DDAH/ADMA pathway. *Curr Pharm Des,* 16, 4089-102.

Assreuy, J., Cunha, F. Q., Epperlein, M., Noronha-Dutra, A., O'Donnell, C. A., Liew, F. Y. & Moncada, S. 1994. Production of nitric oxide and superoxide by activated macrophages and killing of Leishmania major. *Eur J Immunol,* 24, 672-6.

Assreuy, J., Cunha, F. Q., Liew, F. Y. & Moncada, S. 1993. Feedback inhibition of nitric oxide synthase activity by nitric oxide. *Br J Pharmacol,* 108, 833-7.

Aucella, F., Maas, R., Vigilante, M., Tripepi, G., Schwedhelm, E., Margaglione, M., Gesualdo, L., Boeger, R. & Zoccali, C. 2009. Methylarginines and mortality in patients with end stage renal disease: a prospective cohort study. *Atherosclerosis,* 207, 541-5.

Ayling, L. J., Whitley, G. S., Aplin, J. D. & Cartwright, J. E. 2006. Dimethylarginine dimethylaminohydrolase (DDAH) regulates trophoblast invasion and motility through effects on nitric oxide. *Hum Reprod,* 21, 2530-7.

Babaev, V. R., Yancey, P. G., Ryzhov, S. V., Kon, V., Breyer, M. D., Magnuson, M. A., Fazio, S. & Linton, M. F. 2005. Conditional knockout of macrophage PPARgamma increases atherosclerosis in C57BL/6 and low-density lipoprotein receptor-deficient mice. *Arterioscler Thromb Vasc Biol,* 25, 1647-53.

Baigent, C., Burbury, K. & Wheeler, D. 2000. Premature cardiovascular disease in chronic renal failure. *Lancet,* 356, 147-52.

Barnes, P. J. & Liew, F. Y. 1995. Nitric oxide and asthmatic inflammation. *Immunol Today,* 16, 128-30.

Baylis, C. 2006. Arginine, arginine analogs and nitric oxide production in chronic kidney disease. *Nat Clin Pract Nephrol,* 2, 209-20.

Bedford, M. T. & Clarke, S. G. 2009. Protein arginine methylation in mammals: who, what, and why. *Mol Cell,* 33, 1-13.

Bedford, M. T. & Richard, S. 2005. *Arginine methylation an* emerging regulator of protein function. *Mol Cell,* 18, 263-72.

Berse, B., Brown, L. F., Van de Water, L., Dvorak, H. F. & Senger, D. R. 1992. Vascular permeability factor (vascular endothelial growth factor) gene is expressed differentially in normal tissues, macrophages, and tumors. *Mol Biol Cell,* 3, 211-20.

Bertholet, S., Tzeng, E., Felley-Bosco, E. & Mauel, J. 1999. Expression of the inducible NO synthase in human monocytic U937 cells allows high output nitric oxide production. *J Leukoc Biol,* 65, 50-8.

Bianchi, M. E. 2007. DAMPs, PAMPs and alarmins: all we need to know about danger. *J Leukoc Biol,* 81, 1-5.

Billack, B. 2006. Macrophage activation: role of toll-like receptors, nitric oxide, and nuclear factor kappa B. *Am J Pharm Educ,* 70, 102.

Birdsey, G. M., Leiper, J. M. & Vallance, P. 2000. Intracellular localization of dimethylarginine dimethylaminohydrolase overexpressed in an endothelial cell line. *Acta Physiol Scand,* 168, 73-9.

Boger, R. H., Bode-Boger, S. M., Thiele, W., Junker, W., Alexander, K. & Frolich, J. C. 1997. Biochemical evidence for impaired nitric oxide synthesis in patients with peripheral arterial occlusive disease. *Circulation,* 95, 2068-74.

Bogle, R. G., MacAllister, R. J., Whitley, G. S. & Vallance, P. 1995. Induction of NG-monomethyl-L-arginine uptake: a mechanism for differential inhibition of NO synthases? *Am J Physiol,* 269, C750-6.

Bondeson, J. 1997. The mechanisms of action of disease-modifying antirheumatic drugs: a review with emphasis on macrophage signal

transduction and the induction of proinflammatory cytokines. *Gen Pharmacol,* 29, 127-50.

Bonizzi, G. & Karin, M. 2004. The two NF-kappaB activation pathways and their role in innate and adaptive immunity. *Trends Immunol,* 25, 280-8.

Branen, L., Hovgaard, L., Nitulescu, M., Bengtsson, E., Nilsson, J. & Jovinge, S. 2004. Inhibition of tumor necrosis factor-alpha reduces atherosclerosis in apolipoprotein E knockout mice. *Arterioscler Thromb Vasc Biol,* 24, 2137-42.

Brodsky, I. E. & Monack, D. 2009. NLR-mediated control of inflammasome assembly in the host response against bacterial pathogens. *Semin Immunol,* 21, 199-207.

Broer, A., Wagner, C. A., Lang, F. & Broer, S. 2000. The heterodimeric amino acid transporter 4F2hc/y+LAT2 mediates arginine efflux in exchange with glutamine. *Biochem J,* 349 Pt 3, 787-95.

Bruewer, M., Luegering, A., Kucharzik, T., Parkos, C. A., Madara, J. L., Hopkins, A. M. & Nusrat, A. 2003. Proinflammatory cytokines disrupt epithelial barrier function by apoptosis-independent mechanisms. *J Immunol,* 171, 6164-72.

Brunner, H., Cockcroft, J. R., Deanfield, J., Donald, A., Ferrannini, E., Halcox, J., Kiowski, W., Luscher, T. F., Mancia, G., Natali, A., Oliver, J. J., Pessina, A. C., Rizzoni, D., Rossi, G. P., Salvetti, A., Spieker, L. E., Taddei, S. & Webb, D. J. 2005. Endothelial function and dysfunction. Part II: Association with cardiovascular risk factors and diseases. A statement by the Working Group on Endothelins and Endothelial Factors of the European Society of Hypertension. *J Hypertens,* 23, 233-46.

Burmester, G. R., Stuhlmuller, B., Keyszer, G. & Kinne, R. W. 1997. Mononuclear phagocytes and rheumatoid synovitis. Mastermind or workhorse in arthritis? *Arthritis Rheum,* 40, 5-18.

Campbell, J. J., Bowman, E. P., Murphy, K., Youngman, K. R., Siani, M. A., Thompson, D. A., Wu, L., Zlotnik, A. & Butcher, E. C. 1998. 6-C-kine (SLC), a

lymphocyte adhesion-triggering chemokine expressed by high endothelium, is an agonist for the MIP-3beta receptor CCR7. *J Cell Biol,* 141, 1053-9.

Caplin, B. & Leiper, J. 2012. Endogenous nitric oxide synthase inhibitors in the biology of disease: markers, mediators, and regulators? *Arterioscler Thromb Vasc Biol,* 32, 1343-53.

Caplin, B., Wang, Z., Slaviero, A., Tomlinson, J., Dowsett, L., Delahaye, M., Salama, A., Wheeler, D. C. & Leiper, J. 2012. Alanine-glyoxylate aminotransferase-2 metabolizes endogenous methylarginines, regulates NO, and controls blood pressure. *Arterioscler Thromb Vasc Biol,* 32, 2892-900.

Cardounel, A. J., Cui, H., Samouilov, A., Johnson, W., Kearns, P., Tsai, A. L., Berka, V. & Zweier, J. L. 2007. Evidence for the pathophysiological role of endogenous methylarginines in regulation of endothelial NO production and vascular function. *J Biol Chem,* 282, 879-87.

Cardounel, A. J., Xia, Y. & Zweier, J. L. 2005. Endogenous methylarginines modulate superoxide as well as nitric oxide generation from neuronal nitric-oxide synthase: differences in the effects of monomethyl- and dimethylarginines in the presence and absence of tetrahydrobiopterin. *J Biol Chem,* 280, 7540-9.

Cardounel, A. J. & Zweier, J. L. 2002. Endogenous methylarginines regulate neuronal nitric-oxide synthase and prevent excitotoxic injury. *J Biol Chem,* 277, 33995-4002.

Carlos, T. M. & Harlan, J. M. 1994. Leukocyte-endothelial adhesion molecules. *Blood,* 84, 2068-101.

Cavaillon, J. M., Adib-Conquy, M., Fitting, C., Adrie, C. & Payen, D. 2003. Cytokine cascade in sepsis. *Scand J Infect Dis,* 35, 535-44.

Chang, C. I., Liao, J. C. & Kuo, L. 1998. Arginase modulates nitric oxide production in activated macrophages. *Am J Physiol,* 274, H342-8.

Charo, I. F. 2007. Macrophage polarization and insulin resistance: PPARgamma in control. *Cell Metab,* 6, 96-8.

Chawla, A., Boisvert, W. A., Lee, C. H., Laffitte, B. A., Barak, Y., Joseph, S. B., Liao, D., Nagy, L., Edwards, P. A., Curtiss, L. K., Evans, R. M. & Tontonoz, P. 2001. A PPAR gamma-LXR-ABCA1 pathway in macrophages is involved in cholesterol efflux and atherogenesis. *Mol Cell,* 7, 161-71.

Chen, X. L., Grey, J. Y., Thomas, S., Qiu, F. H., Medford, R. M., Wasserman, M. A. & Kunsch, C. 2004. Sphingosine kinase-1 mediates TNF-alpha-induced MCP-1 gene expression in endothelial cells: upregulation by oscillatory flow. *Am J Physiol Heart Circ Physiol,* 287, H1452-8.

Chen, Y., Xu, X., Sheng, M., Zhang, X., Gu, Q. & Zheng, Z. 2009. PRMT-1 and DDAHs-induced ADMA upregulation is involved in ROS- and RAS-mediated diabetic retinopathy. *Exp Eye Res,* 89, 1028-34.

Chong, M. M., Thomas, H. E. & Kay, T. W. 2002. Suppressor of cytokine signaling-1 regulates the sensitivity of pancreatic beta cells to tumor necrosis factor. *J Biol Chem,* 277, 27945-52.

Clarke, S. 1993. Protein methylation. *Curr Opin Cell Biol,* 5, 977-83.

Clausen, B. E., Burkhardt, C., Reith, W., Renkawitz, R. & Forster, I. 1999. Conditional gene targeting in macrophages and granulocytes using LysMcre mice. *Transgenic Res,* 8, 265-77.

Clementi, E., Brown, G. C., Feelisch, M. & Moncada, S. 1998. Persistent inhibition of cell respiration by nitric oxide: crucial role of S-nitrosylation of mitochondrial complex I and protective action of glutathione. *Proc Natl Acad Sci U S A,* 95, 7631-6.

Cloonan, N. & Grimmond, S. M. 2008. Transcriptome content and dynamics at single-nucleotide resolution. *Genome Biol,* 9, 234.

Closs, E. I., Basha, F. Z., Habermeier, A. & Forstermann, U. 1997. Interference of L-arginine analogues with L-arginine transport mediated by the y+ carrier hCAT-2B. *Nitric Oxide,* 1, 65-73.

Cole, C., Thomas, S., Filak, H., Henson, P. M. & Lenz, L. L. 2012. Nitric oxide increases susceptibility of Toll-like receptor-activated macrophages to spreading Listeria monocytogenes. *Immunity,* 36, 807-20.

Cole, J. E., Mitra, A. T. & Monaco, C. 2010. Treating atherosclerosis: the potential of Toll-like receptors as therapeutic targets. *Expert Rev Cardiovasc Ther,* 8, 1619-35.

Connelly, L., Jacobs, A. T., Palacios-Callender, M., Moncada, S. & Hobbs, A. J. 2003. Macrophage endothelial nitric-oxide synthase autoregulates cellular activation and pro-inflammatory protein expression. *J Biol Chem,* 278, 26480-7.

Cooke, J. P. 2003. Flow, NO, and atherogenesis. *Proc Natl Acad Sci U S A,* 100, 768-70.

Cox, D., Chang, P., Zhang, Q., Reddy, P. G., Bokoch, G. M. & Greenberg, S. 1997. Requirements for both Rac1 and Cdc42 in membrane ruffling and phagocytosis in leukocytes. *J Exp Med,* 186, 1487-94.

Cox, G. W., Mathieson, B. J., Giardina, S. L. & Varesio, L. 1990. Characterization of IL-2 receptor expression and function on murine macrophages. *J Immunol,* 145, 1719-26.

Daems, W. T., Koerten, H. K. & Soranzo, M. R. 1976. Differences between monocyte-derived and tissue macrophages. *Adv Exp Med Biol,* 73 PT-A, 27-40.

Daeron, M. 1997. Structural bases of Fc gamma R functions. *Int Rev Immunol,* 16, 1-27.

Daigneault, M., Preston, J. A., Marriott, H. M., Whyte, M. K. & Dockrell, D. H. 2010. The identification of markers of macrophage differentiation in PMA-stimulated THP-1 cells and monocyte-derived macrophages. *PLoS One,* 5, e8668.

Dalton, D. K., Pitts-Meek, S., Keshav, S., Figari, I. S., Bradley, A. & Stewart, T. A. 1993. Multiple defects of immune cell function in mice with disrupted interferon-gamma genes. *Science,* 259, 1739-42.

Dayal, S., Rodionov, R. N., Arning, E., Bottiglieri, T., Kimoto, M., Murry, D. J., Cooke, J. P., Faraci, F. M. & Lentz, S. R. 2008. Tissue-specific downregulation of dimethylarginine dimethylaminohydrolase in hyperhomocysteinemia. *Am J Physiol Heart Circ Physiol,* 295, H816-25.

Dayoub, H., Achan, V., Adimoolam, S., Jacobi, J., Stuehlinger, M. C., Wang, B. Y., Tsao, P. S., Kimoto, M., Vallance, P., Patterson, A. J. & Cooke, J. P. 2003. Dimethylarginine dimethylaminohydrolase regulates nitric oxide synthesis: genetic and physiological evidence. *Circulation,* 108, 3042-7.

De Meyer, I., Martinet, W. & De Meyer, G. R. 2012. Therapeutic strategies to deplete macrophages in atherosclerotic plaques. *Br J Clin Pharmacol,* 74, 246-63.

Denis, M. 1991. Tumor necrosis factor and granulocyte macrophage-colony stimulating factor stimulate human macrophages to restrict growth of virulent Mycobacterium avium and to kill avirulent M. avium: killing effector mechanism depends on the generation of reactive nitrogen intermediates. *J Leukoc Biol,* 49, 380-7.

Denis, M. 1994. Human monocytes/macrophages: NO or no NO? *J Leukoc Biol,* 55, 682-4.

Donnelly, E. T., Lewis, S. E., Thompson, W. & Chakravarthy, U. 1997. Sperm nitric oxide and motility: the effects of nitric oxide synthase stimulation and inhibition. *Mol Hum Reprod,* 3, 755-62.

Dranoff, G. 2004. Cytokines in cancer pathogenesis and cancer therapy. *Nat Rev Cancer,* 4, 11-22.

Duncan, C., Dougall, H., Johnston, P., Green, S., Brogan, R., Leifert, C., Smith, L., Golden, M., Benjamin, N. 1995. Chemical generation of nitric oxide in the mouth from the enterosalivary circulation of dietary nitrate. *Nature Med,* 6, 515-7.

Eardley, I. 1997. The role of phosphodiesterase inhibitors in impotence. *Expert Opin Investig Drugs,* 6, 1803-10.

Eid, H. M., Eritsland, J., Larsen, J., Arnesen, H. & Seljeflot, I. 2003. Increased levels of asymmetric dimethylarginine in populations at risk *for atherosclerotic* disease. Effects of pravastatin. *Atherosclerosis,* 166, 279-84.

Etienne-Manneville, S. & Hall, A. 2002. Rho GTPases in cell biology. *Nature,* 420, 629-35.

Feldmann, M. & Maini, R. N. 1999. The role of cytokines in the pathogenesis of rheumatoid arthritis. *Rheumatology (Oxford),* 38 Suppl 2, 3-7.

Feng, M., He, Z. M., Zhu, Y. X., Liu, L. H., Lu, C. W. & Xiong, Y. 2010. Improvement of endothelial dysfunction in atherosclerotic rabbit aortas by ex vivo gene transferring of dimethylarginine dimethylaminohydrolase-2. *Int J Cardiol,* 144, 180-6.

Fickling, S. A., Holden, D. P., Cartwright, J. E., Nussey, S. S., Vallance, P. & Whitley, G. S. 1999. Regulation of macrophage nitric oxide synthesis by endothelial cells: a role for NG,NG-dimethylarginine. *Acta Physiol Scand,* 167, 145-50.

Fliser, D., Kronenberg, F., Kielstein, J. T., Morath, C., Bode-Boger, S. M., Haller, H. & Ritz, E. 2005. Asymmetric dimethylarginine and progression of chronic kidney disease: the mild to moderate kidney disease study. *J Am Soc Nephrol,* 16, 2456-61.

Fukushima, T., Sekizawa, K., Jin, Y. & Sasaki, H. 1994. Interferon-gamma increases cytoplasmic motility of alveolar macrophages via nitric oxide-dependent signaling pathways. *Am J Respir Cell Mol Biol,* 10, 65-71.

Furchgott, R. F. & Zawadzki, J. V. 1980. The obligatory role of endothelial cells in the relaxation of arterial smooth muscle by acetylcholine. *Nature,* 288, 373-6.

Galis, Z. S., Sukhova, G. K., Kranzhofer, R., Clark, S. & Libby, P. 1995. Macrophage foam cells from experimental atheroma constitutively produce matrix-degrading proteinases. *Proc Natl Acad Sci U S A,* 92, 402-6.

Goligorsky, M. S., Abedi, H., Noiri, E., Takhtajan, A., Lense, S., Romanov, V. & Zachary, I. 1999. Nitric oxide modulation of focal adhesions in endothelial cells. *Am J Physiol,* 276, C1271-81.

Gordon, S. 2003. Alternative activation of macrophages. *Nat Rev Immunol,* 3, 23-35.

Gordon, S. & Taylor, P. R. 2005. Monocyte and macrophage heterogeneity. *Nat Rev Immunol,* 5, 953-64.

Gotoh, T., Oyadomari, S., Mori, K. & Mori, M. 2002. Nitric oxide-induced apoptosis in RAW 264.7 macrophages is mediated by endoplasmic reticulum stress pathway involving ATF6 and CHOP. *J Biol Chem,* 277, 12343-50.

Gray, G. A., Patrizio, M., Sherry, L., Miller, A. A., Malaki, M., Wallace, A. F., Leiper, J. M. & Vallance, P. 2010. Immunolocalisation and activity of DDAH I and II in the heart and modification post-myocardial infarction. *Acta Histochem,* 112, 413-23.

Green, S. J., Crawford, R. M., Hockmeyer, J. T., Meltzer, M. S. & Nacy, C. A. 1990. Leishmania major amastigotes initiate the L-arginine-dependent killing mechanism in IFN-gamma-stimulated macrophages by induction of tumor necrosis factor-alpha. *J Immunol,* 145, 4290-7.

Griendling, K. K. & Ushio-Fukai, M. 2000. Reactive oxygen species as mediators of angiotensin II signaling. *Regul Pept,* 91, 21-7.

Hackam, D. J., Rotstein, O. D., Schreiber, A., Zhang, W. & Grinstein, S. 1997. Rho is required for the initiation of calcium signaling and phagocytosis by Fcgamma receptors in macrophages. *J Exp Med,* 186, 955-66.

Hahn, G., Stuhlmuller, B., Hain, N., Kalden, J. R., Pfizenmaier, K. & Burmester, G. R. 1993. Modulation of monocyte activation in patients with rheumatoid arthritis by leukapheresis therapy. *J Clin Invest,* 91, 862-70.

Hasegawa, K., Wakino, S., Tanaka, T., Kimoto, M., Tatematsu, S., Kanda, T., Yoshioka, K., Homma, K., Sugano, N., Kurabayashi, M., Saruta, T. & Hayashi,

K. 2006. Dimethylarginine dimethylaminohydrolase 2 increases vascular endothelial growth factor expression through Sp1 transcription factor in endothelial cells. *Arterioscler Thromb Vasc Biol,* 26, 1488-94.

Hasegawa, K., Wakino, S., Tatematsu, S., Yoshioka, K., Homma, K., Sugano, N., Kimoto, M., Hayashi, K. & Itoh, H. 2007. Role of asymmetric dimethylarginine in vascular injury in transgenic mice overexpressing dimethylarginie dimethylaminohydrolase 2. *Circ Res,* 101, e2-10.

Hashimoto, S., Morohoshi, K., Suzuki, T. & Matsushima, K. 2003. Lipopolysaccharide-inducible gene expression profile in human monocytes. *Scand J Infect Dis,* 35, 619-27.

He, H., Xu, J., Warren, C. M., Duan, D., Li, X., Wu, L. & Iruela-Arispe, M. L. 2012. Endothelial cells provide an instructive niche for the differentiation and functional polarization of M2-like macrophages. *Blood,* 120, 3152-62.

Hibbs, J. B., Jr. 2002. Infection and nitric oxide. *J Infect Dis,* 185 Suppl 1, S9-17.

Hibbs, J. B., Jr., Taintor, R. R. & Vavrin, Z. 1987. Macrophage cytotoxicity: role for L-arginine deiminase and imino nitrogen oxidation to nitrite. *Science,* 235, 473-6.

Hibbs, J. B., Jr., Taintor, R. R., Vavrin, Z. & Rachlin, E. M. 1988. Nitric oxide: a cytotoxic activated macrophage effector molecule. *Biochem Biophys Res Commun,* 157, 87-94.

Hibbs, J. B., Jr., Vavrin, Z. & Taintor, R. R. 1987. L-arginine is required for expression of the activated macrophage effector mechanism causing selective metabolic inhibition in target cells. *J Immunol,* 138, 550-65.

Hirsch, J. G. 1956. Phagocytin: a bactericidal substance from polymorphonuclear leucocytes. *J Exp Med,* 103, 589-611.

Hosokawa, Y., Hosokawa, I., Ozaki, K., Nakae, H. & Matsuo, T. 2006. Cytokines differentially regulate ICAM-1 and VCAM-1 expression on human gingival fibroblasts. *Clin Exp Immunol,* 144, 494-502.

Hu, X., Atzler, D., Xu, X., Zhang, P., Guo, H., Lu, Z., Fassett, J., Schwedhelm, E., Boger, R. H., Bache, R. J. & Chen, Y. 2011. Dimethylarginine dimethylaminohydrolase-1 is the critical enzyme for degrading the cardiovascular risk factor asymmetrical dimethylarginine. *Arterioscler Thromb Vasc Biol,* 31, 1540-6.

Hu, X., Xu, X., Zhu, G., Atzler, D., Kimoto, M., Chen, J., Schwedhelm, E., Luneburg, N., Boger, R. H., Zhang, P. & Chen, Y. 2009. Vascular endothelial-specific dimethylarginine dimethylaminohydrolase-1-deficient mice reveal that vascular endothelium plays an important role in removing asymmetric dimethylarginine. *Circulation,* 120, 2222-9.

Huang, K. T., Kuo, L. & Liao, J. C. 1998. Lipopolysaccharide activates endothelial nitric oxide synthase through protein tyrosine kinase. *Biochem Biophys Res Commun,* 245, 33-7.

Ignarro, L. J., Harbison, R. G., Wood, K. S. & Kadowitz, P. J. 1986. Activation of purified soluble guanylate cyclase by endothelium-derived relaxing factor from intrapulmonary artery and vein: stimulation by acetylcholine, bradykinin and arachidonic acid. *J Pharmacol Exp Ther,* 237, 893-900.

Ignarro, L. J., Buga, G. M., Wood, K. S., Byrns, R. E., Chaudhuri, G. 1987. Endothelium-derived relaxing factor produced and released from artery and vein is nitric oxide. *Proc Natl Acad Sci USA*, 84, 9265-9.

Itaya, H., Imaizumi, T., Yoshida, H., Koyama, M., Suzuki, S. & Satoh, K. 2001. Expression of vascular endothelial growth factor in human monocyte/macrophages stimulated with lipopolysaccharide. *Thromb Haemost,* 85, 171-6.

Jacobi, J., Sydow, K., von Degenfeld, G., Zhang, Y., Dayoub, H., Wang, B., Patterson, A. J., Kimoto, M., Blau, H. M. & Cooke, J. P. 2005. Overexpression

of dimethylarginine dimethylaminohydrolase reduces tissue asymmetric dimethylarginine levels and enhances angiogenesis. *Circulation,* 111, 1431-8.

Jain, B., Rubinstein, I., Robbins, R. A. & Sisson, J. H. 1995. TNF-alpha and IL-1 beta upregulate nitric oxide-dependent ciliary motility in bovine airway epithelium. *Am J Physiol,* 268, L911-7.

Janeway, C. A., Jr. & Medzhitov, R. 2002. Innate immune recognition. *Annu Rev Immunol,* 20, 197-216.

Jones, G. E., Allen, W. E. & Ridley, A. J. 1998. The Rho GTPases in macrophage motility and chemotaxis. *Cell Adhes Commun,* 6, 237-45.

Julou-Schaeffer, G., Gray, G. A., Fleming, I., Schott, C., Parratt, J. R. & Stoclet, J. C. 1990. Loss of vascular responsiveness induced by endotoxin involves L-arginine pathway. *Am J Physiol,* 259, H1038-43.

Karin, M. & Ben-Neriah, Y. 2000. Phosphorylation meets ubiquitination: the control of NF-[kappa]B activity. *Annu Rev Immunol,* 18, 621-63.

Kawai, T. & Akira, S. 2010. The role of pattern-recognition receptors in innate immunity: update on Toll-like receptors. *Nat Immunol,* 11, 373-84.

Khallou-Laschet, J., Varthaman, A., Fornasa, G., Compain, C., Gaston, A. T., Clement, M., Dussiot, M., Levillain, O., Graff-Dubois, S., Nicoletti, A. & Caligiuri, G. 2010. Macrophage plasticity in experimental atherosclerosis. *PLoS One,* 5, e8852.

Kielstein, J. T., Salpeter, S. R., Bode-Boeger, S. M., Cooke, J. P. & Fliser, D. 2006. Symmetric dimethylarginine (SDMA) as endogenous marker of renal function--a meta-analysis. *Nephrol Dial Transplant,* 21, 2446-51.

Kiley, S. C., Adams, P. D. & Parker, P. J. 1997. Cloning and characterization of phorbol ester differentiation-resistant U937 cell variants. *Cell Growth Differ,* 8, 221-30.

Kim, Y. R., Abraham, N. G. & Lutton, J. D. 1991. Mechanisms of differentiation of U937 leukemic cells induced by GM-CSF and 1,25(OH)2 vitamin D3. *Leuk Res,* 15, 409-18.

Kimoto, M., Whitley, G. S., Tsuji, H. & Ogawa, T. 1995. Detection of NG,NG-dimethylarginine dimethylaminohydrolase in human tissues using a monoclonal antibody. *J Biochem,* 117, 237-8.

Kittel, A., Maas, R., Konig, J., Mieth, M., Weiss, N., Jarzebska, N., Hohenstein, B., Martens-Lobenhoffer, J., Bode-Boger, S. M. & Rodionov, R. N. 2013. *In vivo* evidence that Agxt2 can regulate plasma levels of dimethylarginines in mice. *Biochem Biophys Res Commun,* 430, 84-9.

Klockars, M. 1974. Concentration and immunohistochemical localization of lysozyme in germ-free and conventionally reared rats. *Acta Pathol Microbiol Scand A,* 82, 675-82.

Knipp, M., Charnock, J. M., Garner, C. D. & Vasak, M. 2001. Structural and functional characterization of the Zn(II) site in dimethylargininase-1 (DDAH-1) from bovine brain. Zn(II) release activates DDAH-1. *J Biol Chem,* 276, 40449-56.

Konishi, H., Sydow, K. & Cooke, J. P. 2007. Dimethylarginine dimethylaminohydrolase promotes endothelial repair after vascular injury. *J Am Coll Cardiol,* 49, 1099-105.

Kostourou, V., Robinson, S. P., Cartwright, J. E. & Whitley, G. S. 2002. Dimethylarginine dimethylaminohydrolase I enhances tumour growth and angiogenesis. *Br J Cancer,* 87, 673-80.

Leiper, J., Murray-Rust, J., McDonald, N. & Vallance, P. 2002. S-nitrosylation of dimethylarginine dimethylaminohydrolase regulates enzyme activity: further interactions between nitric oxide synthase and dimethylarginine dimethylaminohydrolase. *Proc Natl Acad Sci U S A,* 99, 13527-32.

Leiper, J. & Nandi, M. 2011. The therapeutic potential of targeting endogenous *inhibitors of nitric oxide synthesis. Nat Rev Drug Discov,* 10, 277-91.

Leiper, J., Nandi, M., Torondel, B., Murray-Rust, J., Malaki, M., O'Hara, B., Rossiter, S., Anthony, S., Madhani, M., Selwood, D., Smith, C., Wojciak-Stothard, B., Rudiger, A., Stidwill, R., McDonald, N. Q. & Vallance, P. 2007. Disruption of methylarginine metabolism impairs vascular homeostasis. *Nat Med,* 13, 198-203.

Leiper, J. & Vallance, P. 1999. Biological significance of endogenous methylarginines that inhibit nitric oxide synthases. *Cardiovasc Res,* 43, 542-8.

Leiper, J. & Vallance, P. 2006. New tricks from an old dog: nitric oxide-independent effects of dimethylarginine dimethylaminohydrolase. *Arterioscler Thromb Vasc Biol,* 26, 1419-20.

Leiper, J. M. 2005. The DDAH-ADMA-NOS pathway. *Ther Drug Monit,* 27, 744-6.

Leiper, J. M., Santa Maria, J., Chubb, A., MacAllister, R. J., Charles, I. G., Whitley, G. S. & Vallance, P. 1999. Identification of two human dimethylarginine dimethylaminohydrolases with distinct tissue distributions and homology with microbial arginine deiminases. *Biochem J,* 343 Pt 1, 209-14.

Lewis, S. E., Donnelly, E. T., Sterling, E. S., Kennedy, M. S., Thompson, W. & Chakravarthy, U. 1996. Nitric oxide synthase and nitrite production in human spermatozoa: evidence that endogenous nitric oxide is beneficial to sperm motility. *Mol Hum Reprod,* 2, 873-8.

Li, C. Q. & Wogan, G. N. 2005. Nitric oxide as a modulator of apoptosis. *Cancer Lett,* 226, 1-15.

Liew, F. Y. 1995. Nitric oxide in infectious and autoimmune diseases. *Ciba Found Symp,* 195, 234-9; discussion 239-44.

Lorente, J. A., Landin, L., De Pablo, R., Renes, E. & Liste, D. 1993. L-arginine pathway in the sepsis syndrome. *Crit Care Med,* 21, 1287-95.

Lorsbach, R. B. & Russell, S. W. 1992. A specific sequence of stimulation is required to induce synthesis of the antimicrobial molecule nitric oxide by mouse macrophages. *Infect Immun,* 60, 2133-5.

Lowenstein, C. J., Glatt, C. S., Bredt, D. S. & Snyder, S. H. 1992. Cloned and expressed macrophage nitric oxide synthase contrasts with the brain enzyme. *Proc Natl Acad Sci U S A,* 89, 6711-5.

Luzio, J. P., Pryor, P. R. & Bright, N. A. 2007. Lysosomes: fusion and function. *Nat Rev Mol Cell Biol,* 8, 622-32.

Maa, M. C., Chang, M. Y., Chen, Y. J., Lin, C. H., Yu, C. J., Yang, Y. L., Li, J., Chen, P. R., Tang, C. H., Lei, H. Y. & Leu, T. H. 2008. Requirement of inducible nitric-oxide synthase in lipopolysaccharide-mediated Src induction and macrophage migration. *J Biol Chem,* 283, 31408-16.

MacAllister, R. J., Parry, H., Kimoto, M., Ogawa, T., Russell, R. J., Hodson, H., Whitley, G. S. & Vallance, P. 1996. Regulation of nitric oxide synthesis by dimethylarginine dimethylaminohydrolase. *Br J Pharmacol,* 119, 1533-40.

MacMicking, J., Xie, Q. W. & Nathan, C. 1997. Nitric oxide and macrophage function. *Annu Rev Immunol,* 15, 323-50.

MacMicking, J. D., Nathan, C., Hom, G., Chartrain, N., Fletcher, D. S., Trumbauer, M., Stevens, K., Xie, Q. W., Sokol, K., Hutchinson, N. & *et al.* 1995. Altered responses to bacterial infection and endotoxic shock in mice lacking inducible nitric oxide synthase. *Cell,* 81, 641-50.

Madara, J. L. & Stafford, J. 1989. Interferon-gamma directly affects barrier function of cultured intestinal epithelial monolayers. *J Clin Invest,* 83, 724-7.

Maini, R. N., Elliott, M. J., Brennan, F. M., Williams, R. O., Chu, C. Q., Paleolog, E., Charles, P. J., Taylor, P. C. & Feldmann, M. 1995. Monoclonal anti-TNF alpha antibody as a probe of pathogenesis and therapy of rheumatoid disease. *Immunol Rev,* 144, 195-223.

Malandro, M. S. & Kilberg, M. S. 1996. Molecular biology of mammalian amino acid transporters. *Annu Rev Biochem,* 65, 305-36.

Marioni, J. C., Mason, C. E., Mane, S. M., Stephens, M. & Gilad, Y. 2008. RNA-seq: an assessment of technical reproducibility and comparison with gene expression arrays. *Genome Res,* 18, 1509-17.

Markart, P., Korfhagen, T. R., Weaver, T. E. & Akinbi, H. T. 2004. Mouse lysozyme M is important in pulmonary host defense against Klebsiella pneumoniae infection. *Am J Respir Crit Care Med,* 169, 454-8.

Marks-Konczalik, J., Chu, S. C. & Moss, J. 1998. Cytokine-mediated transcriptional induction of the human inducible nitric oxide synthase gene requires both activator protein 1 and nuclear factor kappaB-binding sites. *J Biol Chem,* 273, 22201-8.

Marletta, M. A., Yoon, P. S., Iyengar, R., Leaf, C. D. & Wishnok, J. S. 1988. Macrophage oxidation of L-arginine to nitrite and nitrate: nitric oxide is an intermediate. *Biochemistry,* 27, 8706-11.

Marx, N., Kehrle, B., Kohlhammer, K., Grub, M., Koenig, W., Hombach, V., Libby, P. & Plutzky, J. 2002. PPAR activators as antiinflammatory mediators in human T lymphocytes: implications for atherosclerosis and transplantation-associated arteriosclerosis. *Circ Res,* 90, 703-10.

Matsuguma, K., Ueda, S., Yamagishi, S., Matsumoto, Y., Kaneyuki, U., Shibata, R., Fujimura, T., Matsuoka, H., Kimoto, M., Kato, S., Imaizumi, T. & Okuda, S. 2006. Molecular mechanism for elevation of asymmetric dimethylarginine and its role for hypertension in chronic kidney disease. *J Am Soc Nephrol,* 17, 2176-83.

McBride, A. E. & Silver, P. A. 2001. State of the arg: protein methylation at arginine comes of age. *Cell,* 106, 5-8.

McDermott, J. R. 1976. Studies on the catabolism of Ng-methylarginine, Ng, Ng-dimethylarginine and Ng, Ng-dimethylarginine in the rabbit. *Biochem J,* 154, 179-84.

McLaughlin, T., Stuhlinger, M., Lamendola, C., Abbasi, F., Bialek, J.,Reaven, G. M., Tsao, P. S. 2006. Plasma asymmetric dimethylarginine concentrations are elevated in obese insulin-resistant women and fall with weight loss. *J Clin Endocrinol Metab*, 91, 1896-900.

Medzhitov, R. & Janeway, C. A., Jr. 1997. Innate immunity: the virtues of a nonclonal system of recognition. *Cell,* 91, 295-8.

Miller, D. K. 1999. Activation of apoptosis and its inhibition. *Ann N Y Acad Sci,* 886, 132-57.

Moncada, S. & Higgs, A. 1993. The L-arginine-nitric oxide pathway. *N Engl J Med,* 329, 2002-12.

Moncada, S., Palmer, R. M. & Higgs, E. A. 1989. Biosynthesis of nitric oxide from L-arginine. A pathway for the regulation of cell function and communication. *Biochem Pharmacol,* 38, 1709-15.

Moncada, S., Rees, D. D., Schulz, R. & Palmer, R. M. 1991. Development and mechanism of a specific supersensitivity to nitrovasodilators after inhibition of vascular nitric oxide synthesis *in vivo*. *Proc Natl Acad Sci U S A,* 88, 2166-70.

Mookerjee, R. P., Malaki, M., Davies, N. A., Hodges, S. J., Dalton, R. N., Turner, C., Sen, S., Williams, R., Leiper, J., Vallance, P. & Jalan, R. 2007. Increasing dimethylarginine levels are associated with adverse clinical outcome in severe alcoholic hepatitis. *Hepatology,* 45, 62-71.

Mori, M. 2007. Regulation of nitric oxide synthesis and apoptosis by arginase and arginine recycling. *J Nutr,* 137, 1616S-1620S.

Mortazavi, A., Williams, B. A., McCue, K., Schaeffer, L. & Wold, B. 2008. Mapping and quantifying mammalian transcriptomes by RNA-Seq. *Nat Methods,* 5, 621-8.

Mosmann, T. 1983. Rapid colorimetric assay for cellular growth and survival: application to proliferation and cytotoxicity assays. *J Immunol Methods,* 65, 55-63.

Mosser, D. M. 2003. The many faces of macrophage activation. *J Leukoc Biol,* 73, 209-12.

Mueller, C. F., Laude, K., McNally, J. S. & Harrison, D. G. 2005. ATVB in focus: redox mechanisms in blood vessels. *Arterioscler Thromb Vasc Biol,* 25, 274-8.

Mulherin, D., Fitzgerald, O. & Bresnihan, B. 1996. Synovial tissue macrophage populations and articular damage in rheumatoid arthritis. *Arthritis Rheum,* 39, 115-24.

Munder, M., Choi, B. S., Rogers, M. & Kropf, P. 2009. L-arginine deprivation impairs Leishmania major-specific T-cell responses. *Eur J Immunol,* 39, 2161-72.

Murohara, T. & Asahara, T. 2002. Nitric oxide and angiogenesis in cardiovascular disease. *Antioxid Redox Signal,* 4, 825-31.

Murray-Rust, J., Leiper, J., McAlister, M., Phelan, J., Tilley, S., Santa Maria, J., Vallance, P. & McDonald, N. 2001. Structural insights into the hydrolysis of cellular nitric oxide synthase inhibitors by dimethylarginine dimethylaminohydrolase. *Nat Struct Biol,* 8, 679-83.

Muzio, M., Stockwell, B. R., Stennicke, H. R., Salvesen, G. S. & Dixit, V. M. 1998. An induced proximity model for caspase-8 activation. *J Biol Chem,* 273, 2926-30.

Nagalakshmi, U., Wang, Z., Waern, K., Shou, C., Raha, D., Gerstein, M. & Snyder, M. 2008. The transcriptional landscape of the yeast genome defined by RNA sequencing. *Science,* 320, 1344-9.

Nagase, S., Takemura, K., Ueda, A., Hirayama, A., Aoyagi, K., Kondoh, M., Koyama, A. 1997. A novel nonenzymatic pathway for the generation of nitric oxide by the reaction of hydrogen peroxide and D- or L- Arginine. *Biochem. Biophys. Res. Commun,* 233, 150-3.

Nagy, L., Tontonoz, P., Alvarez, J. G., Chen, H. & Evans, R. M. 1998. Oxidized LDL regulates macrophage gene expression through ligand activation of PPARgamma. *Cell,* 93, 229-40.

Naha, P. C., Davoren, M., Lyng, F. M. & Byrne, H. J. 2010. Reactive oxygen species (ROS) induced cytokine production and cytotoxicity of PAMAM dendrimers in J774A.1 cells. *Toxicol Appl Pharmacol,* 246, 91-9.

Nandi, M., Kelly, P., Torondel, B., Wang, Z., Starr, A., Ma, Y., Cunningham, P., Stidwill, R. & Leiper, J. 2012. Genetic and pharmacological inhibition of dimethylarginine dimethylaminohydrolase 1 is protective in endotoxic shock. *Arterioscler Thromb Vasc Biol,* 32, 2589-97.

Nijveldt, R. J., Teerlink, T., Van Der Hoven, B., Siroen, M. P., Kuik, D. J., Rauwerda, J. A. & van Leeuwen, P. A. 2003. Asymmetrical dimethylarginine (ADMA) in critically ill patients: high plasma ADMA concentration is an independent risk factor of ICU mortality. *Clin Nutr,* 22, 23-30.

Niks, M., Otto, M., Busova, B. & Stefanovic, J. 1990. Quantification of proliferative and suppressive responses of human T lymphocytes following ConA stimulation. *J Immunol Methods,* 126, 263-71.

Nobes, C. D. & Hall, A. 1995. Rho, rac, and cdc42 GTPases regulate the assembly of multimolecular focal complexes associated with actin stress fibers, lamellipodia, and filopodia. *Cell,* 81, 53-62.

Nwariaku, F. E., Rothenbach, P., Liu, Z., Zhu, X., Turnage, R. H. & Terada, L. S. 2003. Rho inhibition decreases TNF-induced endothelial MAPK activation and monolayer permeability. *J Appl Physiol,* 95, 1889-95.

Oberg, F., Botling, J. & Nilsson, K. 1993. Functional antagonism between vitamin D3 and retinoic acid in the regulation of CD14 and CD23 expression during monocytic differentiation of U-937 cells. *J Immunol,* 150, 3487-95.

O'Dwyer, M. J., Dempsey, F., Crowley, V., Kelleher, D. P., McManus, R. & Ryan, T. 2006. Septic shock is correlated with asymmetrical dimethyl arginine levels, which may be influenced by a polymorphism in the dimethylarginine

dimethylaminohydrolase II gene: a prospective observational study. *Crit Care,* 10, R139.

Ogawa, T., Kimoto, M. & Sasaoka, K. 1989. Purification and properties of a new enzyme, NG,NG-dimethylarginine dimethylaminohydrolase, from rat kidney. *J Biol Chem,* 264, 10205-9.

Ogawa, T., Kimoto, M. & Sasaoka, K. 1990. Dimethylarginine:pyruvate aminotransferase in rats. Purification, properties, and identity with alanine:glyoxylate aminotransferase 2. *J Biol Chem,* 265, 20938-45.

Ogawa, T., Kimoto, M., Watanabe, H. & Sasaoka, K. 1987. Metabolism of NG,NG-and NG,N'G-dimethylarginine in rats. *Arch Biochem Biophys,* 252, 526-37.

Olsson, A. K., Dimberg, A., Kreuger, J. & Claesson-Welsh, L. 2006. VEGF receptor signalling - in control of vascular function. *Nat Rev Mol Cell Biol,* 7, 359-71.

Osanai, T., Saitoh, M., Sasaki, S., Tomita, H., Matsunaga, T. & Okumura, K. 2003. Effect of shear stress on asymmetric dimethylarginine release from vascular endothelial cells. *Hypertension,* 42, 985-90.

Ozaki, H., Ishii, K., Horiuchi, H., Arai, H., Kawamoto, T., Okawa, K., Iwamatsu, A. & Kita, T. 1999. Cutting edge: combined treatment of TNF-alpha and IFN-gamma causes redistribution of junctional adhesion molecule in human endothelial cells. *J Immunol,* 163, 553-7.

Ozaki, K. & Leonard, W. J. 2002. Cytokine and cytokine receptor pleiotropy and redundancy. *J Biol Chem,* 277, 29355-8.

Pace, J. L., Russell, S. W., Torres, B. A., Johnson, H. M. & Gray, P. W. 1983. Recombinant mouse gamma interferon induces the priming step in macrophage activation for tumor cell killing. *J Immunol,* 130, 2011-3.

Paik, W. K. & Kim, S. 1968. Protein methylase I. Purification and properties of the enzyme. *J Biol Chem,* 243, 2108-14.

Paik, W. K., Paik, D. C. & Kim, S. 2007. Historical review: the field of protein methylation. *Trends Biochem Sci,* 32, 146-52.

Palm, F., Onozato, M. L., Luo, Z. & Wilcox, C. S. 2007. Dimethylarginine dimethylaminohydrolase (DDAH): expression, regulation, and function in the cardiovascular and renal systems. *Am J Physiol Heart Circ Physiol,* 293, H3227-45.

Palmer, R. M., Ashton, D. S. & Moncada, S. 1988. Vascular endothelial cells synthesize nitric oxide from L-arginine. *Nature,* 333, 664-6.

Palmer, R. M., Ferrige, A. G. & Moncada, S. 1987. Nitric oxide release accounts for the biological activity of endothelium-derived relaxing factor. *Nature,* 327, 524-6.

Palmer, R. M. & Moncada, S. 1989. A novel *citrulline-forming enzyme* implicated in the formation of nitric oxide by vascular endothelial cells. *Biochem Biophys Res Commun,* 158, 348-52.

Payne, W. J., Liu, M. Y., Bursakov, S. A., Gall, Jle. 1997. Microbial and plant metabolism of NO. *BioFactors*, 9, 1-6.

Pekarova, M., Kubala, L., Martiskova, H., Bino, L., Twarogova, M., Klinke, A., Rudolph, T. K., Kuchtova, Z., Kolarova, H., Ambrozova, G., Kuchta, R., Kadlec, J. & Lojek, A. 2013. Asymmetric dimethylarginine regulates the lipopolysaccharide-induced nitric oxide production in macrophages by suppressing the activation of NF-kappaB and iNOS expression. *Eur J Pharmacol,* 713, 68-77.

Perez-Ruiz, M., Ros, J., Morales-Ruiz, M., Navasa, M., Colmenero, J., Ruiz-del-Arbol, L., Cejudo, P., Claria, J., Rivera, F., Arroyo, V., Rodes, J. & Jimenez, W. 1999. Vascular endothelial growth factor production in peritoneal macrophages of cirrhotic patients: regulation by cytokines and bacterial lipopolysaccharide. *Hepatology,* 29, 1057-63.

Petrache, I., Crow, M. T., Neuss, M. & Garcia, J. G. 2003. Central involvement of Rho family GTPases in TNF-alpha-mediated bovine pulmonary endothelial cell apoptosis. *Biochem Biophys Res Commun,* 306, 244-9.

Petrache, I., Verin, A. D., Crow, M. T., Birukova, A., Liu, F. & Garcia, J. G. 2001. Differential effect of MLC kinase in TNF-alpha-induced endothelial cell apoptosis and barrier dysfunction. *Am J Physiol Lung Cell Mol Physiol,* 280, L1168-78.

Pettersson, A., Hedner, T. & Milsom, I. 1998. Increased circulating concentrations of asymmetric dimethyl arginine (ADMA), an endogenous inhibitor of nitric oxide synthesis, in preeclampsia. *Acta Obstet Gynecol Scand,* 77, 808-13.

Pope, A. J., Karrupiah, K., Kearns, P. N., Xia, Y. & Cardounel, A. J. 2009. Role of dimethylarginine dimethylaminohydrolases in the regulation of endothelial nitric oxide production. *J Biol Chem,* 284, 35338-47.

Pourcet, B., Feig, J. E., Vengrenyuk, Y., Hobbs, A. J., Kepka-Lenhart, D., Garabedian, M. J., Morris, S. M., Jr., Fisher, E. A. & Pineda-Torra, I. 2011. LXRalpha regulates macrophage arginase 1 through PU.1 and interferon regulatory factor 8. *Circ Res,* 109, 492-501.

Price, P. & McMillan, T. J. 1990. Use of the tetrazolium assay in measuring the response of human tumor cells to ionizing radiation. *Cancer Res,* 50, 1392-6.

Pullamsetti, S., Kiss, L., Ghofrani, H. A., Voswinckel, R., Haredza, P., Klepetko, W., Aigner, C., Fink, L., Muyal, J. P., Weissmann, N., Grimminger, F., Seeger, W. & Schermuly, R. T. 2005. Increased levels and reduced catabolism of asymmetric and symmetric dimethylarginines in pulmonary hypertension. *FASEB J,* 19, 1175-7.

Rajavashisth, T. B., Xu, X. P., Jovinge, S., Meisel, S., Xu, X. O., Chai, N. N., Fishbein, M. C., Kaul, S., Cercek, B., Sharifi, B. & Shah, P. K. 1999. Membrane type 1 matrix metalloproteinase expression in human atherosclerotic plaques: evidence for activation by proinflammatory mediators. *Circulation,* 99, 3103-9.

Rao, K. M. 2001. MAP kinase activation in macrophages. *J Leukoc Biol,* 69, 3-10.

Ribas, G., Neville, M., Wixon, J. L., Cheng, J. & Campbell, R. D. 1999. Genes encoding three new members of the leukocyte antigen 6 superfamily and a novel member of Ig superfamily, together with genes encoding the regulatory nuclear chloride ion channel protein (hRNCC) and an N omega-N omega-dimethylarginine dimethylaminohydrolase homologue, are found in a 30-kb segment of the MHC class III region. *J Immunol,* 163, 278-87.

Ricote, M., Li, A. C., Willson, T. M., Kelly, C. J. & Glass, C. K. 1998. The peroxisome proliferator-activated receptor-gamma is a negative regulator of macrophage activation. *Nature,* 391, 79-82.

Ridker, P. M., Cushman, M., Stampfer, M. J., Tracy, R. P. & Hennekens, C. H. 1997. Inflammation, aspirin, and the risk of cardiovascular disease in apparently healthy men. *N Engl J Med,* 336, 973-9.

Ridley, A. J. 2001. Rho proteins, PI 3-kinases, and monocyte/macrophage motility. *FEBS Lett,* 498, 168-71.

Rodionov, R. N., Murry, D. J., Vaulman, S. F., Stevens, J. W. & Lentz, S. R. 2010. Human alanine-glyoxylate aminotransferase 2 lowers asymmetric dimethylarginine and protects from inhibition of nitric oxide production. *J Biol Chem,* 285, 5385-91.

Romijn, J. C., Verkoelen, C. F. & Schroeder, F. H. 1988. Application of the MTT assay to human prostate cancer cell lines *in vitro*: establishment of test conditions and assessment of hormone-stimulated growth and drug-induced cytostatic and cytotoxic effects. *Prostate,* 12, 99-110.

Ross, R. 1980. Platelets, smooth muscle proliferation and atherosclerosis. *Acta Med Scand Suppl,* 642, 49-54.

Ross, R. 1993. The pathogenesis of atherosclerosis: a perspective for the 1990s. *Nature,* 362, 801-9.

Ross, R. 1999. Atherosclerosis--an inflammatory disease. *N Engl J Med,* 340, 115-26.

Rossiter, S., Smith, C. L., Malaki, M., Nandi, M., Gill, H., Leiper, J. M., Vallance, P. & Selwood, D. L. 2005. Selective substrate-based inhibitors of mammalian dimethylarginine dimethylaminohydrolase. *J Med Chem,* 48, 4670-8.

Russell, D. G., Vanderven, B. C., Glennie, S., Mwandumba, H. & Heyderman, R. S. 2009. The macrophage marches on its phagosome: dynamic assays of phagosome function. *Nat Rev Immunol,* 9, 594-600.

Santa Maria, J., Vallance, P., Charles, I. G. & Leiper, J. M. 1999. Identification of microbial dimethylarginine dimethylaminohydrolase enzymes. *Mol Microbiol,* 33, 1278-9.

Sarih, M., Souvannavong, V. & Adam, A. 1993. Nitric oxide synthase induces macrophage death by apoptosis. *Biochem Biophys Res Commun,* 191, 503-8.

Sasser, J. M., Moningka, N. C., Cunningham, M. W., Jr., Croker, B. & Baylis, C. 2010. Asymmetric dimethylarginine in angiotensin II-induced hypertension. *Am J Physiol Regul Integr Comp Physiol,* 298, R740-6.

Schmidt, H. H. & Walter, U. 1994. NO at work. *Cell,* 78, 919-25.

Schnabel, R., Blankenberg, S., Lubos, E., Lackner, K. J., Rupprecht, H. J., Espinola-Klein, C., Jachmann, N., Post, F., Peetz, D., Bickel, C., Cambien, F., Tiret, L. & Munzel, T. 2005. Asymmetric dimethylarginine and the risk of cardiovascular events and death in patients with coronary artery disease: results from the AtheroGene Study. *Circ Res,* 97, e53-9.

Schnog, J. B., Teerlink, T., van der Dijs, F. P., Duits, A. J. & Muskiet, F. A. 2005. Plasma levels of asymmetric dimethylarginine (ADMA), an endogenous nitric oxide synthase inhibitor, are elevated in sickle cell disease. *Ann Hematol,* 84, 282-6.

Schoedon, G., Schneemann, M. & Schaffner, A. 1995. Tetrahydrobiopterin and dysfunction of endothelial nitric oxide synthase. *Circulation,* 92, 1060-1.

Schoedon, G., Troppmair, J., Fontana, A., Huber, C., Curtius, H. C. & Niederwieser, A. 1987. Biosynthesis and metabolism of pterins in peripheral blood mononuclear cells and leukemia lines of man and mouse. *Eur J Biochem,* 166, 303-10.

Schulze, F., Lenzen, H., Hanefeld, C., Bartling, A., Osterziel, K. J., Goudeva, L., Schmidt-Lucke, C., Kusus, M., Maas, R., Schwedhelm, E., Strodter, D., Simon, B. C., Mugge, A., Daniel, W. G., Tillmanns, H., Maisch, B., Streichert, T. & Boger, R. H. 2006. Asymmetric dimethylarginine is an independent risk factor for coronary heart disease: results from the multicenter Coronary Artery Risk Determination investigating the Influence of ADMA Concentration (CARDIAC) study. *Am Heart J,* 152, 493 e1-8.

Selley, M. L. 2003. Increased concentrations of homocysteine and asymmetric dimethylarginine and decreased concentrations of nitric oxide in the plasma of patients with Alzheimer's disease. *Neurobiol Aging,* 24, 903-7.

Seneviratne, A. N., Sivagurunathan, B. & Monaco, C. 2012. Toll-like receptors and macrophage activation in atherosclerosis. *Clin Chim Acta,* 413, 3-14.

Sharshar, T., Gray, F., Lorin de la Grandmaison, G., Hopkinson, N. S., Ross, E., Dorandeu, A., Orlikowski, D., Raphael, J. C., Gajdos, P. & Annane, D. 2003. Apoptosis of neurons in cardiovascular autonomic centres triggered by inducible nitric oxide synthase after death from septic shock. *Lancet,* 362, 1799-805.

Sibal, L., Agarwal, S. C., Schwedhelm, E., Luneburg, N., Boger, R. H. & Home, P. D. 2009. A study of endothelial function and circulating asymmetric dimethylarginine levels in people with Type 1 diabetes without macrovascular disease or microalbuminuria. *Cardiovasc Diabetol,* 8, 27.

Sladowski, D., Steer, S. J., Clothier, R. H. & Balls, M. 1993. An improved MTT assay. *J Immunol Methods,* 157, 203-7.

Smith, C. L., Birdsey, G. M., Anthony, S., Arrigoni, F. I., Leiper, J. M. & Vallance, P. 2003. Dimethylarginine dimethylaminohydrolase activity modulates

ADMA levels, VEGF expression, and cell phenotype. *Biochem Biophys Res Commun,* 308, 984-9.

Sprague, A. H. & Khalil, R. A. 2009. Inflammatory cytokines in vascular dysfunction and vascular disease. *Biochem Pharmacol,* 78, 539-52.

Stahl, P. D. & Ezekowitz, R. A. 1998. The mannose receptor is a pattern recognition receptor involved in host defense. *Curr Opin Immunol,* 10, 50-5.

Stamler, J. S. 1994. Redox signaling: nitrosylation and related target interactions of nitric oxide. *Cell,* 78, 931-6.

Stamler, J. S., Singel, D. J. & Loscalzo, J. 1992. Biochemistry of nitric oxide and its redox-activated forms. *Science,* 258, 1898-902.

Stearns-Kurosawa, D. J., Osuchowski, M. F., Valentine, C., Kurosawa, S. & Remick, D. G. 2011. The pathogenesis of sepsis. *Annu Rev Pathol,* 6, 19-48.

Svedersky, L. P., Benton, C. V., Berger, W. H., Rinderknecht, E., Harkins, R. N. & Palladino, M. A. 1984. Biological and antigenic similarities of murine interferon-gamma and macrophage-activating factor. *J Exp Med,* 159, 812-27.

Takada, Y. & Noguchi, T. 1982. Subcellular distribution, and physical and immunological properties of hepatic alanine: glyoxylate aminotransferase isoenzymes in different mammalian species. *Comp Biochem Physiol B,* 72, 597-604.

Takeuchi, O. & Akira, S. 2010. Pattern recognition receptors and inflammation. *Cell,* 140, 805-20.

Tanaka, M., Sydow, K., Gunawan, F., Jacobi, J., Tsao, P. S., Robbins, R. C. & Cooke, J. P. 2005. Dimethylarginine dimethylaminohydrolase overexpression suppresses graft coronary artery disease. *Circulation, 112, 1549-56.*

Tang, A. T., Campbell, W. B. & Nithipatikom, K. 2012. ROCK1 feedback regulation of the upstream small GTPase RhoA. *Cell Signal,* 24, 1375-80.

Taylor, A. E., Finney-Hayward, T. K., Quint, J. K., Thomas, C. M., Tudhope, S. J., Wedzicha, J. A., Barnes, P. J. & Donnelly, L. E. 2010. Defective *macrophage phagocytosis of bacteria* in COPD. *Eur Respir J,* 35, 1039-47.

Teerlink, T., Luo, Z., Palm, F. & Wilcox, C. S. 2009. Cellular ADMA: regulation and action. *Pharmacol Res,* 60, 448-60.

Teupser, D., Burkhardt, R., Wilfert, W., Haffner, I., Nebendahl, K. & Thiery, J. 2006. Identification of macrophage arginase I as a new candidate gene of atherosclerosis resistance. *Arterioscler Thromb Vasc Biol,* 26, 365-71.

Tojo, A., Welch, W. J., Bremer, V., Kimoto, M., Kimura, K., Omata, M., Ogawa, T., Vallance, P. & Wilcox, C. S. 1997. Colocalization of demethylating enzymes and NOS and functional effects of methylarginines in rat kidney. *Kidney Int,* 52, 1593-601.

Towbin, H., Staehelin, T. & Gordon, J. 1979. Electrophoretic transfer of proteins from polyacrylamide gels to nitrocellulose sheets: procedure and some applications. *Proc Natl Acad Sci U S A,* 76, 4350-4.

Tran, C. T., Fox, M. F., Vallance, P. & Leiper, J. M. 2000. Chromosomal localization, gene structure, and expression pattern of DDAH1: comparison with DDAH2 and implications for evolutionary origins. *Genomics,* 68, 101-5.

Tran, C. T., Leiper, J. M. & Vallance, P. 2003. The DDAH/ADMA/NOS pathway. *Atheroscler Suppl,* 4, 33-40.

Tumer, C., Bilgin, H. M., Obay, B. D., Diken, H., Atmaca, M. & Kelle, M. 2007. Effect of nitric oxide on phagocytic activity of lipopolysaccharide-induced macrophages: possible role of exogenous L-arginine. *Cell Biol Int,* 31, 565-9.

Tzeng, E., Billiar, T. R., Robbins, P. D., Loftus, M. & Stuehr, D. J. 1995. Expression of human inducible nitric oxide synthase in a tetrahydrobiopterin (H4B)-deficient cell line: H4B promotes assembly of enzyme subunits into an active dimer. *Proc Natl Acad Sci U S A,* 92, 11771-5.

Usui, M., Matsuoka, H., Miyazaki, H., Ueda, S., Okuda, S., Imaizumi, T. 1998. Increased endogenous nitric oxide synthase inhibitor in patients with congestive heart failure. *Life Sci*, 62, 2425-30.

Vallance, P., Collier, J. & Moncada, S. 1989. Effects of endothelium-derived nitric oxide on peripheral arteriolar tone in man. *Lancet,* 2, 997-1000.

Vallance, P., Collier, J. & Moncada, S. 1989. Nitric oxide synthesised from L-arginine mediates endothelium dependent dilatation in human veins *in vivo*. *Cardiovasc Res,* 23, 1053-7.

Vallance, P. & Leiper, J. 2004. Cardiovascular biology of the asymmetric dimethylarginine:dimethylarginine dimethylaminohydrolase pathway. *Arterioscler Thromb Vasc Biol,* 24, 1023-30.

Vallance, P., Leone, A., Calver, A., Collier, J. & Moncada, S. 1992. Accumulation of an endogenous inhibitor of nitric oxide synthesis in chronic renal failure. *Lancet,* 339, 572-5.

Van Dervort, A. L., Yan, L., Madara, P. J., Cobb, J. P., Wesley, R. A., Corriveau, C. C., Tropea, M. M. & Danner, R. L. 1994. Nitric oxide regulates endotoxin-induced TNF-alpha production by human neutrophils. *J Immunol,* 152, 4102-9.

Vanhoutte, P. M. 1997. Endothelial dysfunction and atherosclerosis. *Eur Heart J,* 18 Suppl E, E19-29.

Wang, D., Gill, P. S., Chabrashvili, T., Onozato, M. L., Raggio, J., Mendonca, M., Dennehy, K., Li, M., Modlinger, P., Leiper, J., Vallance, P., Adler, O., Leone, A., Tojo, A., Welch, W. J. & Wilcox, C. S. 2007. Isoform-specific regulation by N(G),N(G)-dimethylarginine dimethylaminohydrolase of rat serum asymmetric dimethylarginine and vascular endothelium-derived relaxing factor/NO. *Circ Res,* 101, 627-35.

Wang, J., Tian, Y., Phillips, K. L., Chiverton, N., Haddock, G., Bunning, R. A., Cross, A. K., Shapiro, I. M., Le Maitre, C. L. & Risbud, M. V. 2013. Tumor necrosis factor alpha- and interleukin-1beta-dependent induction of CCL3

expression by nucleus pulposus cells promotes macrophage migration through CCR1. *Arthritis Rheum,* 65, 832-42.

Wang, Z., Gerstein, M. & Snyder, M. 2009. RNA-Seq: a revolutionary tool for transcriptomics. *Nat Rev Genet,* 10, 57-63.

Wei, X. Q., Charles, I. G., Smith, A., Ure, J., Feng, G. J., Huang, F. P., Xu, D., Muller, W., Moncada, S. & Liew, F. Y. 1995. Altered immune responses in mice lacking inducible nitric oxide synthase. *Nature,* 375, 408-11.

Weinberg, J. B., Misukonis, M. A., Shami, P. J., Mason, S. N., Sauls, D. L., Dittman, W. A., Wood, E. R., Smith, G. K., McDonald, B., Bachus, K. E. & *et al.* 1995. Human mononuclear phagocyte inducible nitric oxide synthase (iNOS): analysis of iNOS mRNA, iNOS protein, biopterin, and nitric oxide production by blood monocytes and peritoneal macrophages. *Blood,* 86, 1184-95.

Wheeler, A. P., Wells, C. M., Smith, S. D., *Vega, F. M., Henderson, R. B.,* Tybulewicz, V. L. & Ridley, A. J. 2006. Rac1 and Rac2 regulate macrophage morphology but are not essential for migration. *J Cell Sci,* 119, 2749-57.

Wheeler, D. S., Lahni, P. M., Denenberg, A. G., Poynter, S. E., Wong, H. R., Cook, J. A. & Zingarelli, B. 2008. Induction of endotoxin tolerance enhances bacterial clearance and survival in murine polymicrobial sepsis. *Shock,* 30, 267-73.

Wojciak-Stothard, B., Torondel, B., Tsang, L. Y., Fleming, I., Fisslthaler, B., Leiper, J. M. & Vallance, P. 2007. The ADMA/DDAH pathway is a critical regulator of endothelial cell motility. *J Cell Sci,* 120, 929-42.

Wojciak-Stothard, B., Torondel, B., Zhao, L., Renne, T. & Leiper, J. M. 2009. Modulation of Rac1 activity by ADMA/DDAH regulates pulmonary endothelial barrier function. *Mol Biol Cell,* 20, 33-42.

Woollard, K. J. & Geissmann, F. 2010. Monocytes in atherosclerosis: subsets and functions. *Nat Rev Cardiol,* 7, 77-86.

Xia, Y. & Zweier, J. L. 1997. Superoxide and peroxynitrite generation from inducible nitric oxide synthase in macrophages. *Proc Natl Acad Sci U S A,* 94, 6954-8.

Xia, Y. F., Liu, L. P., Zhong, C. P. & Geng, J. G. 2001. NF-kappaB activation for constitutive expression of VCAM-1 and ICAM-1 on B lymphocytes and plasma cells. *Biochem Biophys Res Commun,* 289, 851-6.

Yanni, G., Whelan, A., Feighery, C. & Bresnihan, B. 1994. Synovial tissue macrophages and joint erosion in rheumatoid arthritis. *Ann Rheum Dis,* 53, 39-44.

Yasinska, I. M., Kozhukhar, A. V. & Sumbayev, V. V. 2004. S-nitrosation of thioredoxin in the nitrogen monoxide/superoxide system activates apoptosis signal-regulating kinase 1. *Arch Biochem Biophys,* 428, 198-203.

Yoo, J. H. & Lee, S. C. 2001. Elevated levels of plasma homocyst(e)ine and asymmetric dimethylarginine in elderly patients with stroke. *Atherosclerosis,* 158, 425-30.

Yoshizumi, M., Perrella, M. A., Burnett, J. C., Jr. & Lee, M. E. 1993. Tumor necrosis factor downregulates an endothelial nitric oxide synthase mRNA by shortening its half-life. *Circ Res,* 73, 205-9.

Zakrzewicz, D. & Eickelberg, O. 2009. From arginine methylation to ADMA: a novel mechanism with therapeutic potential in chronic lung diseases. *BMC Pulm Med,* 9, 5.

Zambrowicz, B. P., Abuin, A., Ramirez-Solis, R., Richter, L. J., Piggott, J., BeltrandelRio, H., Buxton, E. C., Edwards, J., Finch, R. A., Friddle, C. J., Gupta, A., Hansen, G., Hu, Y., Huang, W., Jaing, C., Key, B. W., Jr., Kipp, P., Kohlhauff, B., Ma, Z. Q., Markesich, D., Payne, R., Potter, D. G., Qian, N., Shaw, J., Schrick, J., Shi, Z. Z., Sparks, M. J., Van Sligtenhorst, I., Vogel, P., Walke, W., Xu, N., Zhu, Q., Person, C. & Sands, A. T. 2003. Wnk1 kinase deficiency lowers blood pressure in mice: a gene-trap screen to identify

potential targets for therapeutic intervention. *Proc Natl Acad Sci U S A,* 100, 14109-14.

Zambrowicz, B. P., Friedrich, G. A., Buxton, E. C., Lilleberg, S. L., Person, C. & Sands, A. T. 1998. Disruption and sequence identification of 2,000 genes in mouse embryonic stem cells. *Nature,* 392, 608-11.

Zatz, R. & Baylis, C. 1998. Chronic nitric oxide inhibition model six years on. *Hypertension,* 32, 958-64.

Zhang, P., Hu, X., Xu, X., Chen, Y. & Bache, R. J. 2011. Dimethylarginine dimethylaminohydrolase 1 modulates endothelial cell growth through nitric oxide and Akt. *Arterioscler Thromb Vasc Biol,* 31, 890-7.

Zhang, Z., Naughton, D., Winyard, P. G., Benjamin, N., Blake, D. R., Symons, M. C. 1998. Generation of nitric oxide by a nitric reductase activity of xanthine oxidase: a potential pathway for nitric oxide formation in the absence of nitric oxide synthase activity. *Biochem Biophys Res Commun*, 249, 767-72.

Zhang, X., Goncalves, R. & Mosser, D. M. 2008. The isolation and characterization of murine macrophages. *Curr Protoc Immunol,* Chapter 14, Unit 14 1.

Zhou, J., Dehne, N. & Brune, B. 2009. Nitric oxide causes macrophage migration via the HIF-1-stimulated small GTPases Cdc42 and Rac1. *Free Radic Biol Med,* 47, 741-9.

Zweier, J. L., Wang, P., Samouilov, A., Kuppusamy, P. 1995. Enzyme-independent formation of nitric oxide in biological tissues. *Nature Med*, 8, 804-809.

APPENDIX

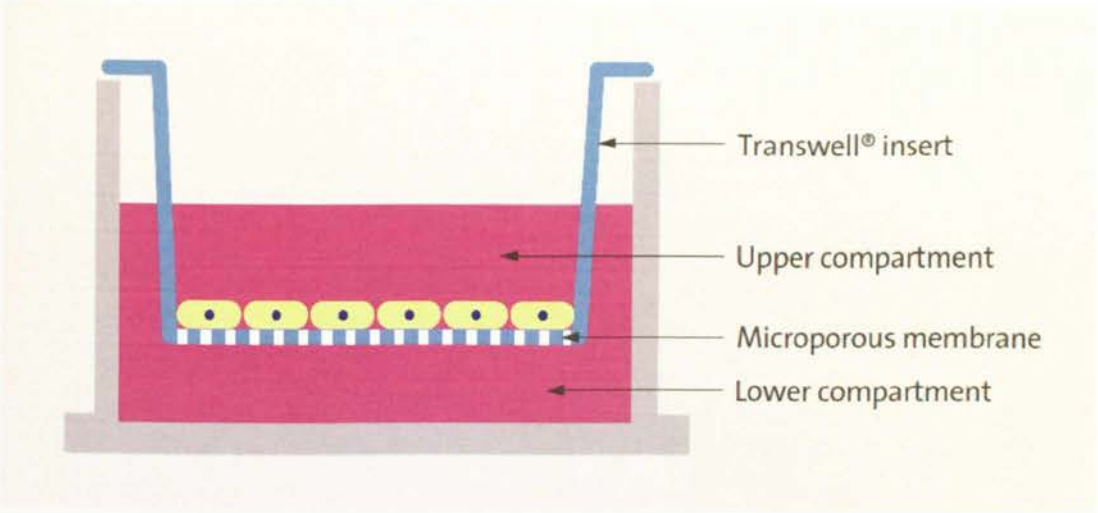

Fig. 1: Transwell insert used for chemotaxis experiments (Corning, UK)

Transwell with monocytes in the upper compartment inserted were inserted into 24 well plates and allowed to migrate through the microporous membrane to the lower compartment.

Optical properties	Clear	Translucent	Clear when wet
Cell visibility	Good	Poor	Cell outlines
Tissue culture treated	Yes	Yes	No
Membrane thickness	10µm	10µm	50µm
Matrix/ECM coat-able	Yes	Yes	Yes
Collagen treated	No	No	Yes
Available Pore Sizes (µm)	0.4, 1.0, 3.0, 8.0	0.4, 3.0, 5.0, 8.0	0.4, 3.0

Table 1: Characteristics of transwell membranes (Corning, UK).

3.0µm polycarbonate transwell inserts were selected for the chemotaxis experiments.

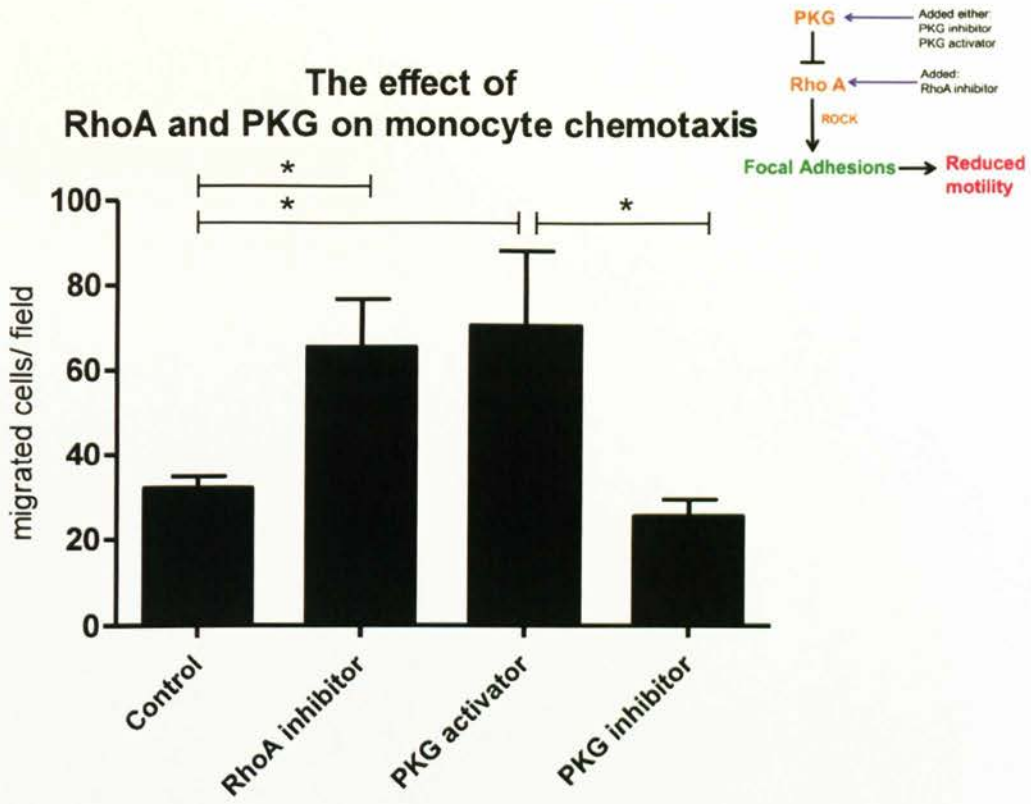

Fig. 2: Effect of RhoA and PKG on monocyte migration after 4 hours.

To determine the effect of GTPases on monocyte motility, selective inhibitor of the Rho-associated protein kinase p160ROCK, Y-27632 (10μM; Calbiochem) was added to the bottom chamber. Alternatively, to determine the effect of protein kinase G (PKG) on monocyte motility, the PKG activator guanosine 3',5'-cyclic monophosphate, 8-bromo-, sodium salt (BrcGMP, Na; 500μM; Calbiochem) or the PKG inhibitor guanosine, 3',5'-cyclicmonophosphorothioate, 8-(4-chlorophenylthio)-, Rp-isomer, triethylammonium (Rp-8-pCPT-cGMPS,TEA; 100nM; Calbiochem). U937 cells ($5x10^4$) were added to the upper compartment of a transwell insert and allowed to migrate through for 4 hours after which the number of cells migrated was counted. One way ANOVA comparing all means using a Bonferroni post-test was carried out and significance was accepted when $P<0.05$. Data is representative of 3 individual experiments (bars are representative of mean ± SEM).

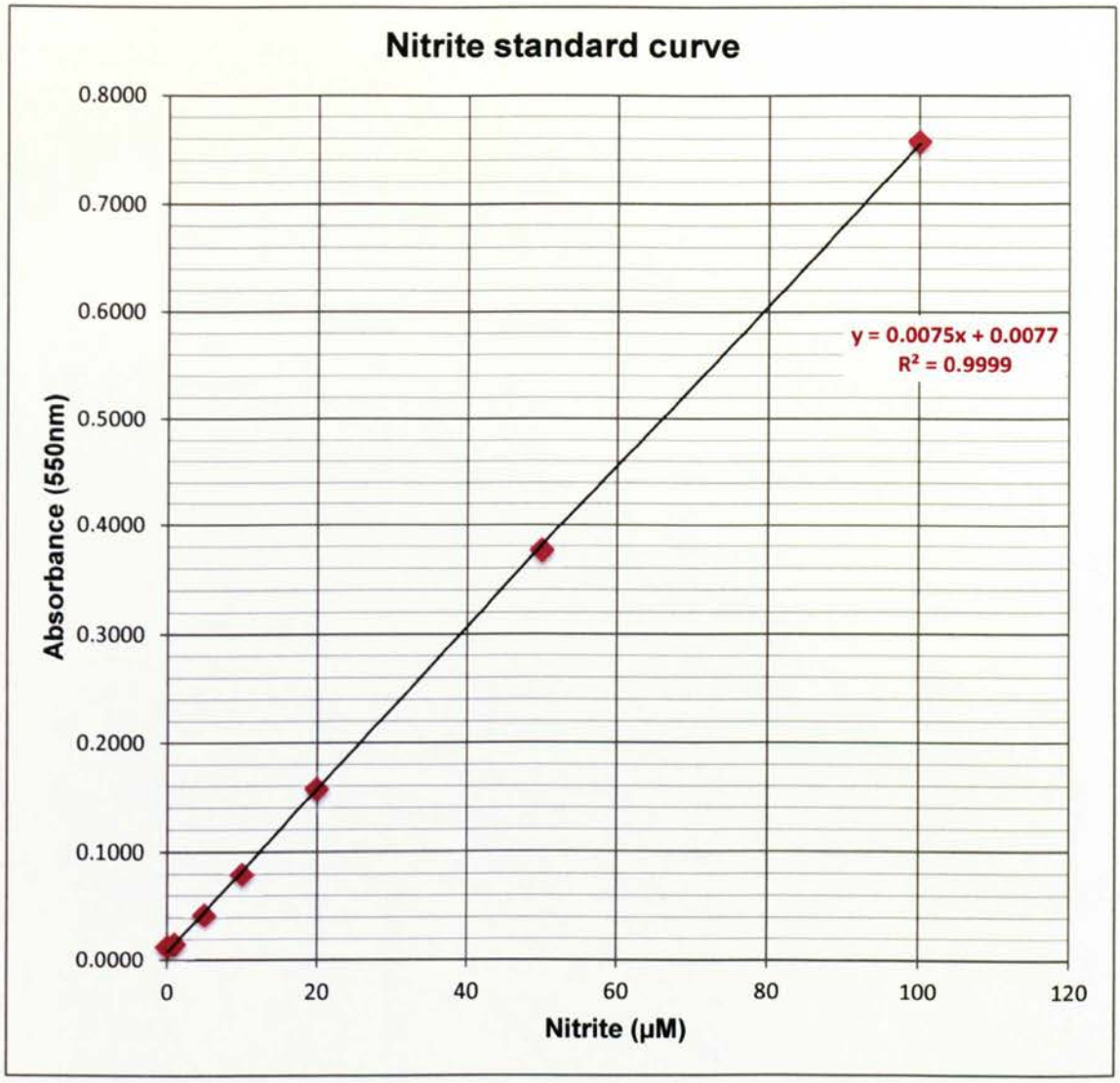

Fig. 3: Nitrite standard curve comparing the absorbance with the nitrite concentration.

The standard curve of macrophage media spiked with increased concentrations of sodium nitrite (Sigma Aldrich) was conducted. The absorbance was measured at 550nm. The graph gives a clear and accurate relationship between nitrite levels and absorbance; absorbance increases with increasing concentrations of nitrite.

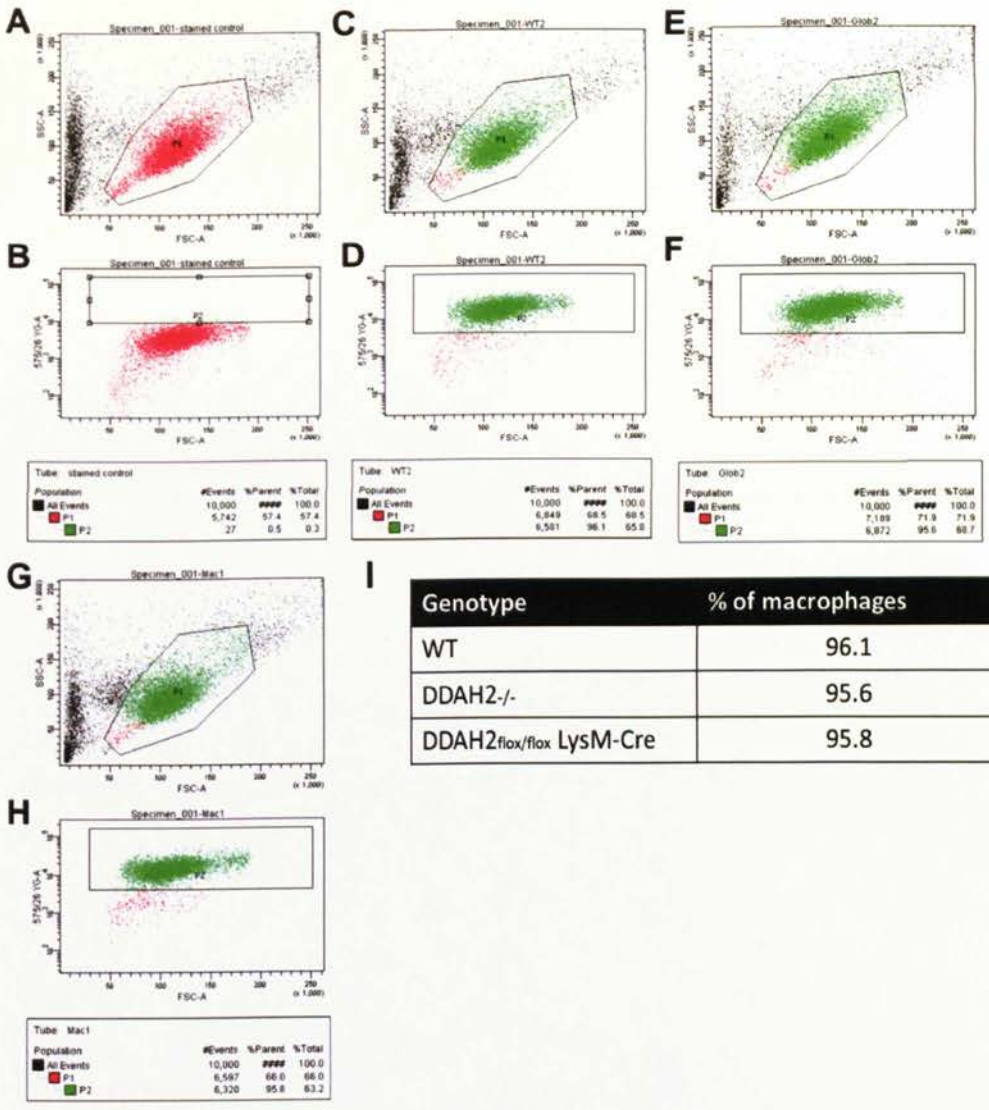

I

Genotype	% of macrophages
WT	96.1
DDAH2-/-	95.6
DDAH2$_{flox/flox}$ LysM-Cre	95.8

Fig. 4: Conformation of primary macrophage extracted from DDAH2$^{+/+}$, DDAH2$^{-/-}$ and DDAH2$^{flox/flox}$ LysM-Cre mice.

Flow cytometry was used to analyse pMacs stained with F4/80 (1:20,000) (A) IgG control (without F4/80), (B) DDAH2$^{+/+}$ and (C) global DDAH2$^{-/-}$. FACS data shows that ≥95% of peritoneal cells cultured are macrophages. An average of approximately 95% of cells obtained from the washout and cultured were macrophages.

β-actin	Cell Signalling	Rabbit anti-mouse	1:1000	47
α-tubulin	Cell Signalling	Rabbit anti-mouse	1:500	50
DDAH1	Privately manufactured, James Leiper/Sigma Aldrich	Goat anti-mouse	1:1000	37
DDAH2	Privately manufactured, James Leiper/Sigma Aldrich	Goat anti-mouse	1:500	37
eNOS	Cell Signalling	Rabbit anti-mouse	1:500	140
iNOS	Cell Signalling	Rabbit anti-mouse	1:500	130
2°	Licor	Donkey anti-goat	1:20,000	N/A
2°	Licor	Donkey anti-rabbit	1:20,000	N/A

Table 2: Antibodies used for western blotting

The antibodies used and/or associated with the NO signalling pathway are as follows β actin, α-tubulin, DDAH1, DDAH2, eNOS and iNOS. The secondary antibodies (2°) used included the following Licor antibodies raised in the same species; donkey anti-goat and donkey anti-rabbit.

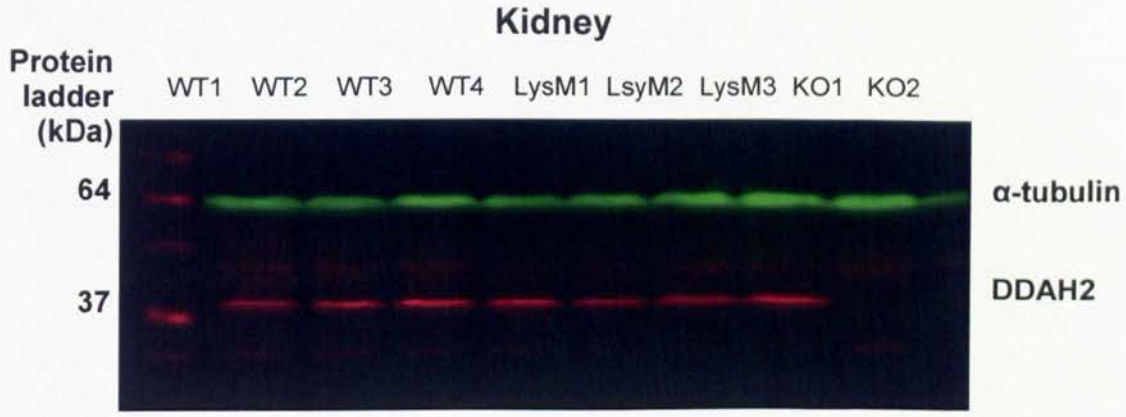

Fig. 5: Example of fluorescent western blot.

The new Odyssey CLx Licor machine allows dual staining of proteins in different colours (green and red in this case) if the primary species are different. Image is of kidney protein from wild type (WT), DDAH2$^{flox/flox}$ LysM-Cre (LysM) and DDAH2$^{-/-}$ (KO) stained for α-tubulin (green, 64kDa) and DDAH2 (red, 37kDa).

β-actin	CCAGGGTGTGATGGTGGGAATG	CGCACGATTTCCCTCTCAGCTG
Pol-2	CCGCTCATGAAATGCTCCTT	CGGGTCACTCTCCCCATGT,
DDAH1	CACAGAAGGCCCTCAAGATCA	TCTCATAGACCTTTGCGCTTTC
DDAH2	CCTGGTGCCACACCTTTCC	AGGGTGACATCAGAGAGCTTCTG
eNOS	AAGACAAGGCAGCGGTGG	GCAGGGGACAGGAAATAGTT
iNOS	CAGCTGGGCTGTACAAACCTT	ATGTGATGTTTGCTTCGGACA
Il-1β	GCTGCTTCCAAACCTTTGAC	TGTCCTCATCCTGGAAGGTC
Il-6	CCGGAGAGGAGACTTCACAG	TTCTGCAAGTGCATCATCGT
TNF-α	CAAACCACCAAGTGGAGGAG	GTGGGTGAGGAGCACGTAGT
LysM-Cre	TCAACGGTACCGGTCTCAG	CATCTGGGAGGGTCAGAGAG

Table 3: Primers used in RT-qPCR reactions

The table highlights the forward and reverse primers used in RT-qPCR reactions and includes β-actin, Pol-2, DDAH1, DDAH2, eNOS, iNOS, Il-1β, Il-6 and TNF-α. All of the primers mentioned were obtained from Sigma Aldrich, UK and are to be used again mice only (not human) samples.

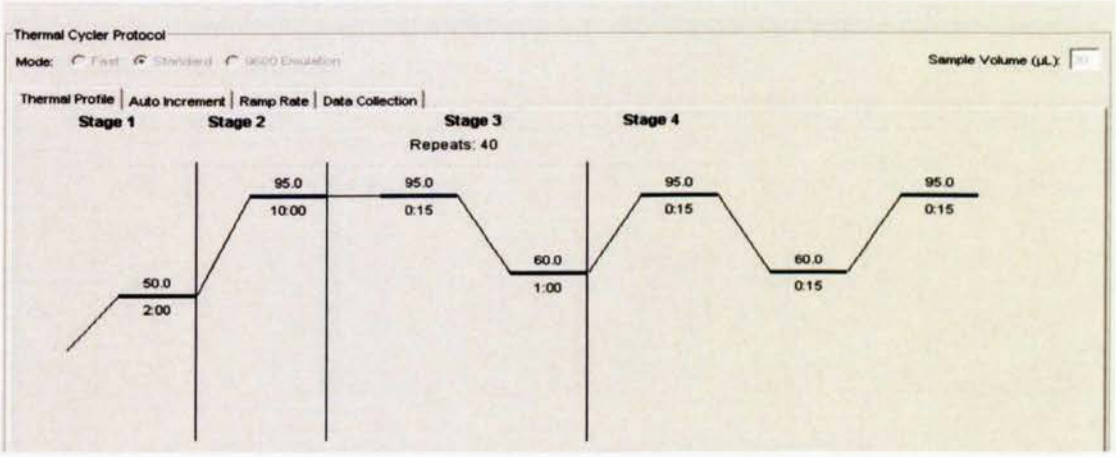

Fig. 6: Thermal profile for the qPCR program.

The thermocycler protocol goes through 4 stages as follows: temperature at 50°C for 2 minutes, 95°C for 10 minutes, 40 repeats of RNA amplification at 95°C (15 seconds), 60°C (1 minute), 95°C (15 seconds), 60°C (15 seconds) and 95°C (15 seconds).

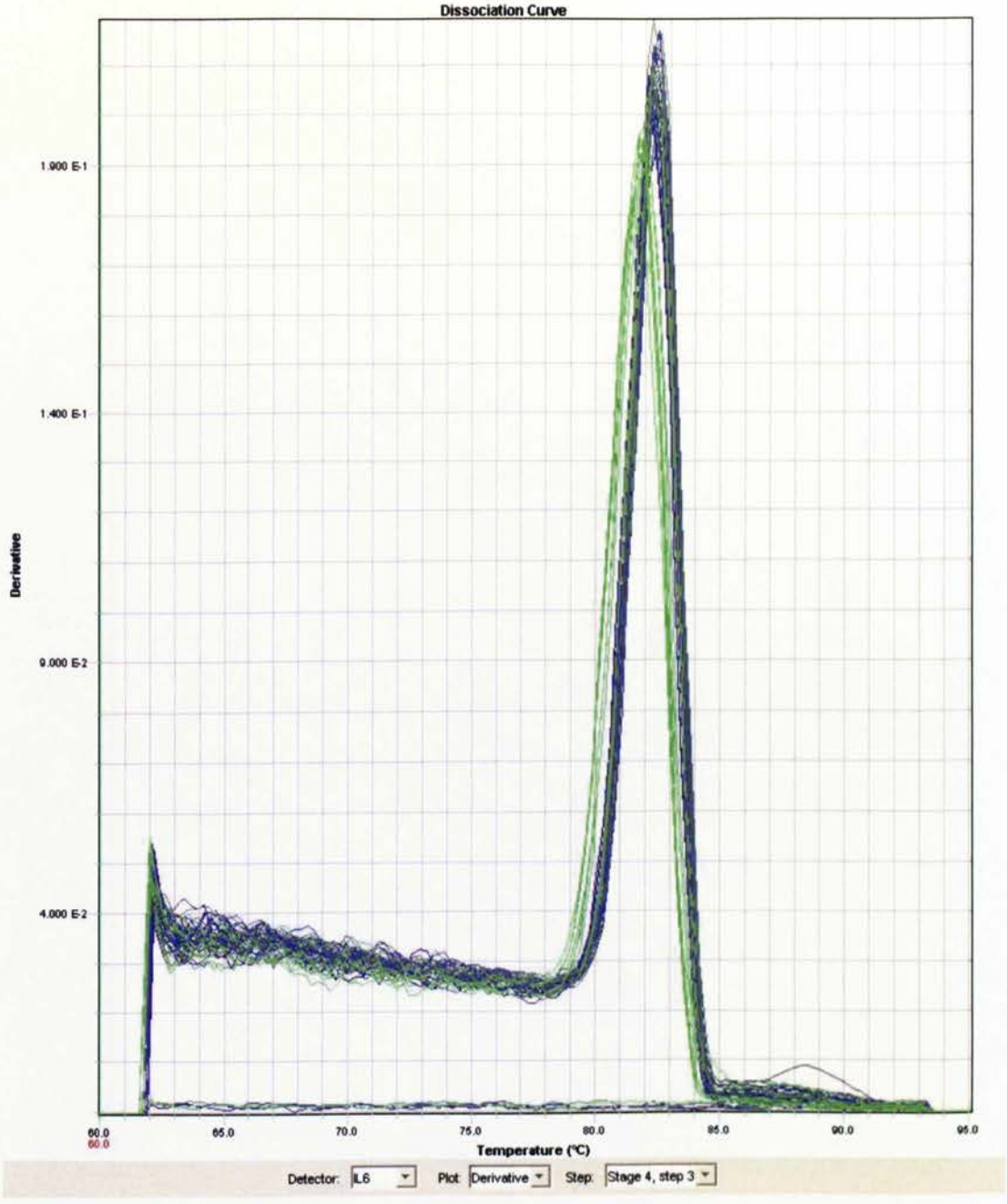

Fig. 7: **Dissociation curves of IL-6 following qPCR.**

Dissociation curve of IL-6 following completion of PCR program. It is clear that the samples have run well by the compactness of the lines. The dissociation of IL-6 primers and all other primers used in our experiments were at 82°C.

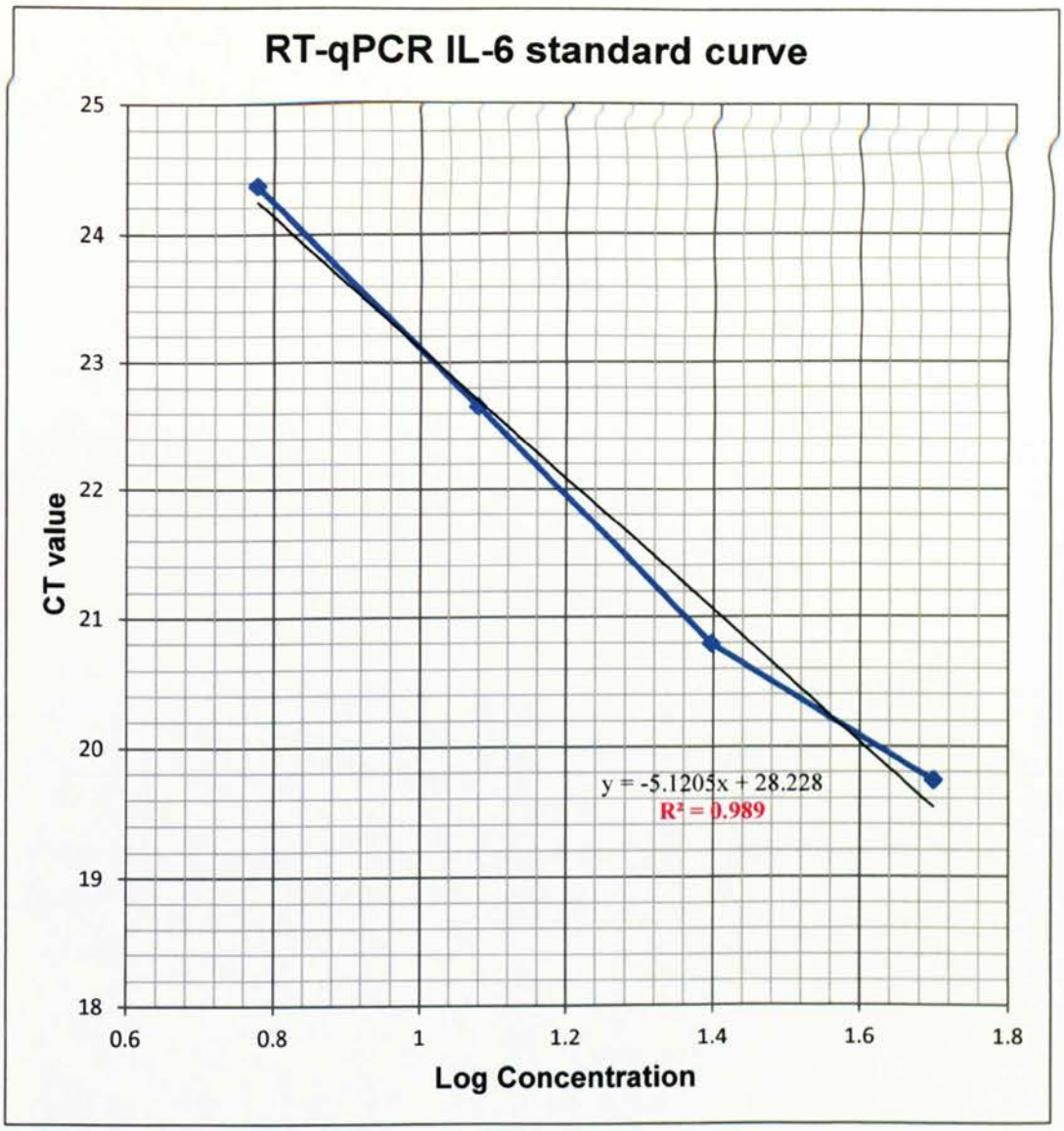

Fig. 8: Standard curve of IL-6 for RT-qPCR

Standard curve reveals the accuracy of the primers in response to PCR. Different concentrations of samples were added to the PCR plate and amplified. The R^2 value is 0.989 which suggests that this experiments as well as the method behind it is highly accurate. This was repeated for all cytokine primers and any results which did not show an R^2 of ≥0.95 were rejected and the data was not used. Polymerase-2 was selected as a housekeeper control in all following experiments as it showed less variation between samples when compared to other standard housekeepers such as β-actin.

WT-untreated	IL-6	28.81	29.11	**28.96**	-1.70	0.019	85.01	0.00023
	IL-6	27.59	27.95	**27.77**	-1.36	0.043	58.99	0.00073
	IL-6	29.39	29.67	**29.53**	-1.86	0.013	21.91	0.00062
	IL-6	28.91	29.45	**29.18**	-1.76	0.017	98.31	0.00017
LysM-Cre *untreated*	IL-6	26.70	26.91	**26.80**	-1.08	0.081	79.88	0.0010
	IL-6	26.75	27.09	**26.92**	-1.12	0.075	132.87	0.00056
	IL-6	27.92	27.93	**27.93**	-1.40	0.038	74.00	0.00052
	IL-6	28.04	28.16	**28.10**	-1.45	0.034	36.89	0.00094
	IL-6	26.56	26.46	**26.51**	-1.00	0.098	113.78	0.00086
WT LPS treated	IL-6	17.38	17.11	**17.25**	1.62	42.04	57.96	0.72
	IL-6	15.56	16.04	**15.80**	2.03	108.30	91.86	1.17
	IL-6	15.83	15.88	**15.85**	2.01	104.55	94.20	1.10
	IL-6	15.85	15.95	**15.90**	2.00	101.38	43.78	2.31
LysM-Cre LPS treated	IL-6	16.37	16.25	**16.31**	1.88	77.47	44.53	1.73
	IL-6	16.64	16.76	**16.70**	1.77	60.12	83.56	0.71
	IL-6	13.20	13.53	**13.37**	2.72	532.62	134.52	3.95
	IL-6	16.04	15.94	**15.99**	1.98	95.55	75.67	1.26
	IL-6	13.85	16.27	**15.06**	2.24	175.83	100.36	1.75
Standard curve	IL-6	16.90	17.80	**17.35**	1.69			
	IL-6	17.33	17.54	**17.43**	1.39			
	IL-6	19.362	19.27	**19.31**	1.07			
	IL-6	20.33	NA	**20.33**	0.77			

Table 4: Example of Excel spread sheet of analysis of RT-qPCR data

RNA extracted from DDAH2flox/flox and DDAH2flox/flox LysM-Cre pMacs in untreated and LPS treated conditions were plated in duplicate on a 96 well plate. Two individual readings were obtained and averaged. A standard curve of the gene (in this case IL-6) was also plated in duplicate and the readings averaged. The equation for the standard curve was obtained and placed back into the individual sample readings. In order to determine the expression levels, the values were Logged and the samples corrected for the housekeeper (Pol2a). Results are indicative of n=4 for $DDAH2^{flox/flox}$ (WT) and n=5 for $DDAH2^{flox/flox}$ LysM-Cre (LysM-Cre). Statistical significance was determined using a two-tailed t-test where mean ± SEM and $*p<0.05$.

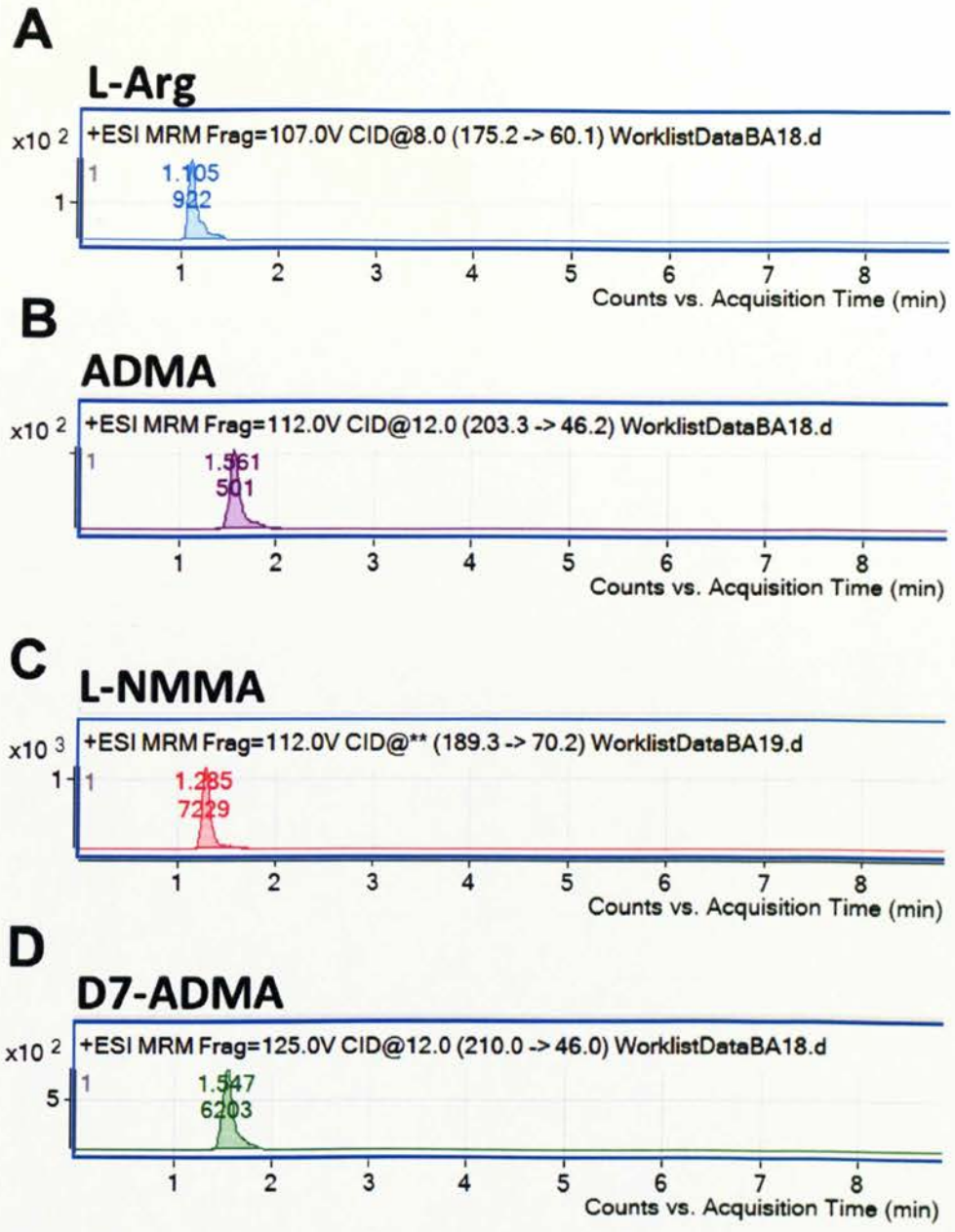

Fig. 9: Arginine and methylarginine peaks observed using LC-MS/MS

The methylarginines ADMA, L-NMMA and SDMA were measured using LC-MS/MS. (A) L-arg eluted at 175.2 and 60.1 (at 1.1mins), (B) ADMA eluted at 203.3 and 46.2 (at 1.5mins), (C) L-NMMA eluted at 189.3 and 70.2 (at 1.2 mins and (D) the internal standard D7-ADMA eluted at 210.0 and 46.0 (at 1.5mins). SDMA typically elutes at 203 and 172 (at 1.8mins) but was present in undetectable concentrations in our samples.

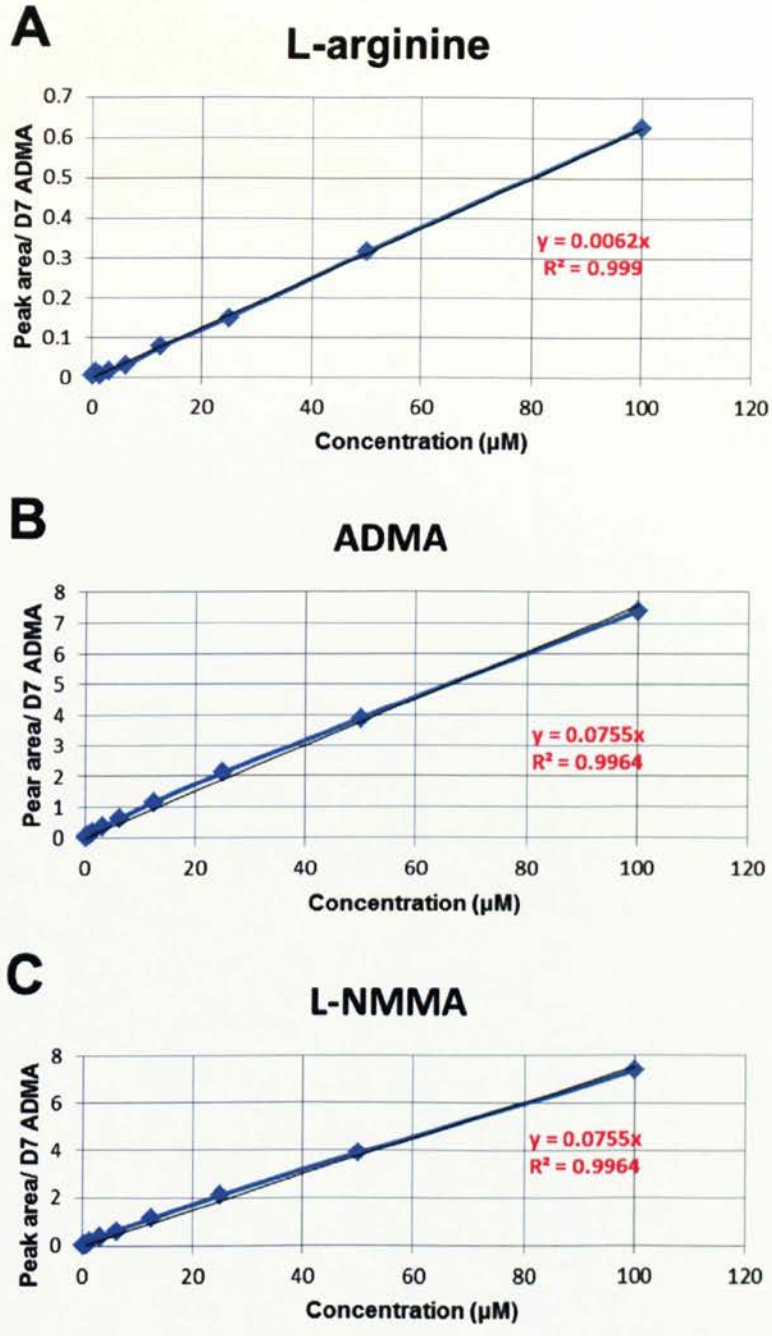

Fig. 10: L-arginine, ADMA and L-NMMA standard curves for LC-MS/MS

Standards of concentrations varying from 0-1000µM of (A) L-arg, (B) ADMA and (C) L-NMMA were run on the LC-MS/MS simultaneously with samples to be analysed. The equation calculated was used to determine the actual concentrations of our samples.

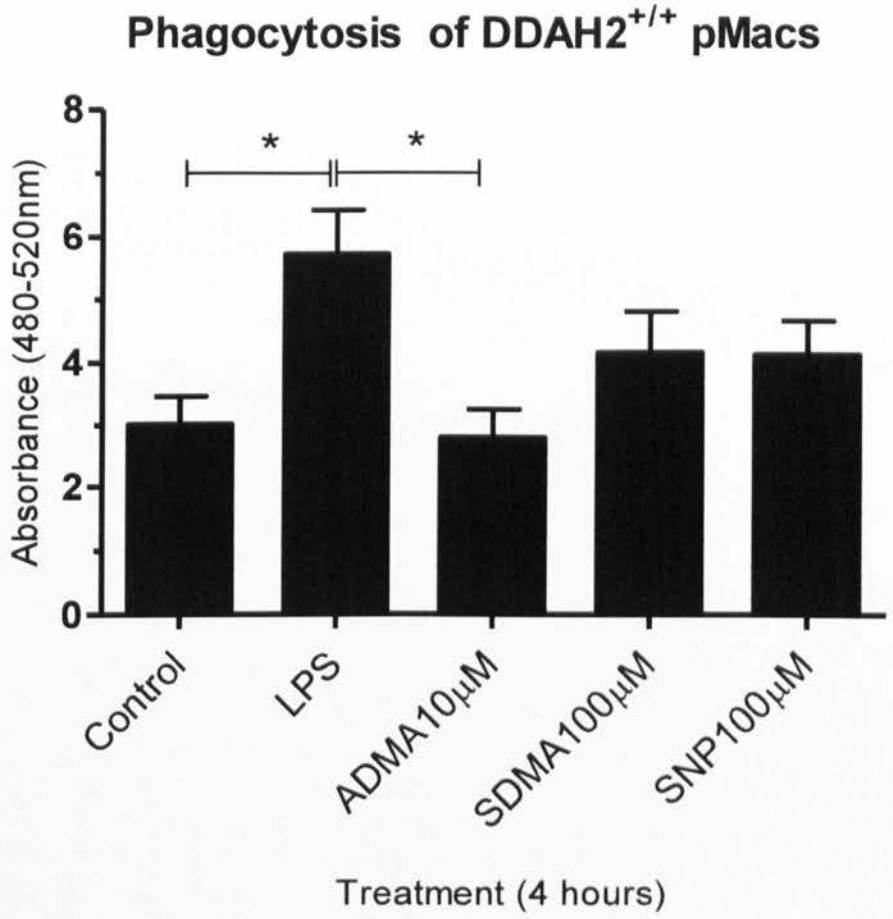

Fig. 11: Phagocytosis levels of DDAH2$^{+/+}$ mice.

pMacs ($2x10^5$) were cultured in triplicate in a 96 well plate and treated with either an inflammatory cocktail, ADMA (10μM), SDMA (100μM) or SNP (100μM) for 4 hours. Following treatment, the media was removed and cells were incubated with a fluorescent E-coli bio-particle for 2 hours. Trypan blue was added for 1 minute and the absorbance at 480-520nm measured using a spectrophotometer. Data is presented in response to a reference sample of media only (blank). Results correspond to n=3 experiments and statistical analysis was carried out using a one-way ANOVA and Bonferroni post-hoc test; significance was accepted where $*p<0.05$.

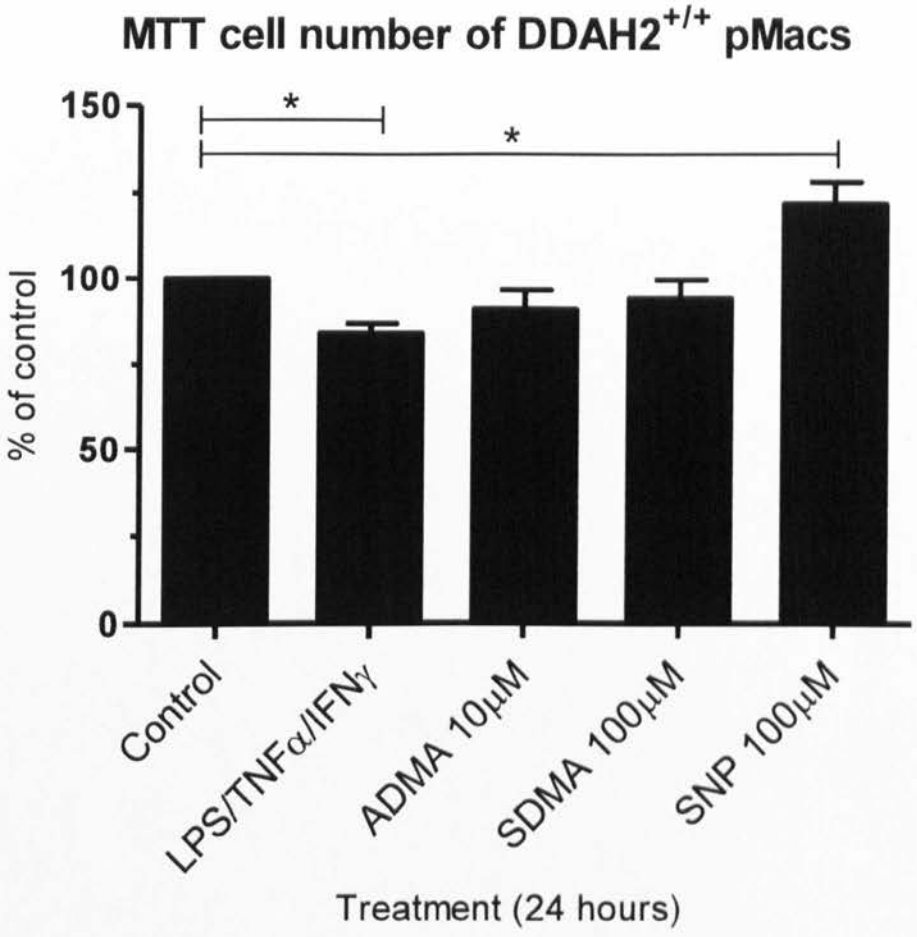

Fig. 12: Cell proliferation of macrophages from DDAH2$^{+/+}$ mice.

pMacs ($1x10^5$ cells/well) were cultured in triplicate a 96 well plate and treated with inflammatory cocktail, ADMA (10μM), SDMA (100μM) or SNP (100μM) for 24 hours. Cell proliferation was determined using the MTT assay using a reference sample of media only (blank). Results show that the addition of an inflammatory cocktail significantly reduces proliferation whereas SNP significantly increases proliferation. ADMA (10μM) and SDMA (100μM) have no significant effect on macrophage proliferation. Data is based on n=4 experiments using a one way ANOVA and Bonferroni post-hoc test; significance was accepted where $*p<0.05$.

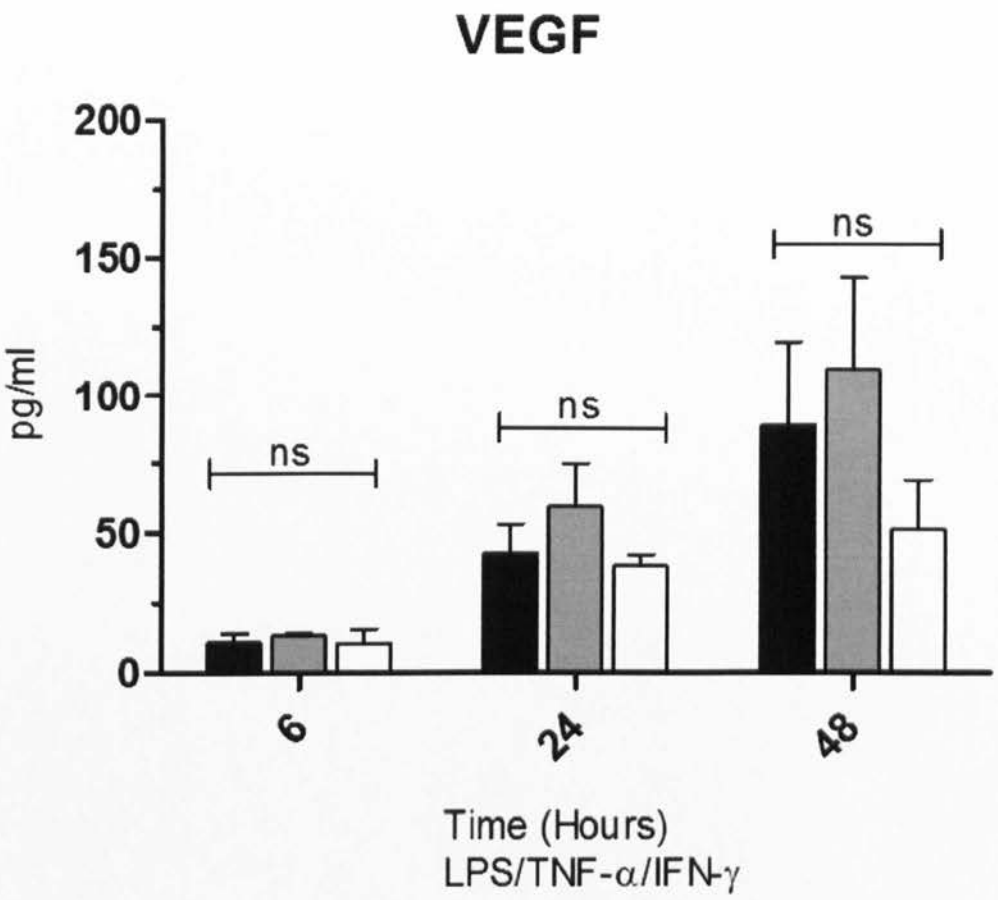

Fig. 13: VEGF concentrations in media from DDAH2$^{+/+}$, DDAH2$^{-/-}$ and DDAH2$^{flox/flox}$ LysM-Cre macrophages

Media extracted from DDAH2$^{+/+}$, DDAH2$^{-/-}$ and DDAH2$^{flox/flox}$ LysM-Cre pMacs plated for the Griess assay was used to determine VEGF concentrations. VEGF concentrations (in pg/ml) were measured using the Millipore Milliplex Kit (Millipore, UK). There was no significant difference between genotypes following 6, 24 and 48 hours LPS/TNF-α/IFN-γ treatment confirming that VEGF expression is not effected by DDAH2 deletion/disruption. Results are indicative of n=5 mice for each genotype, where mean ± SEM. Statistical significance was carried out using a one-way ANOVA and Bonferroni post-hoc test; significance was accepted were *p<0.05.

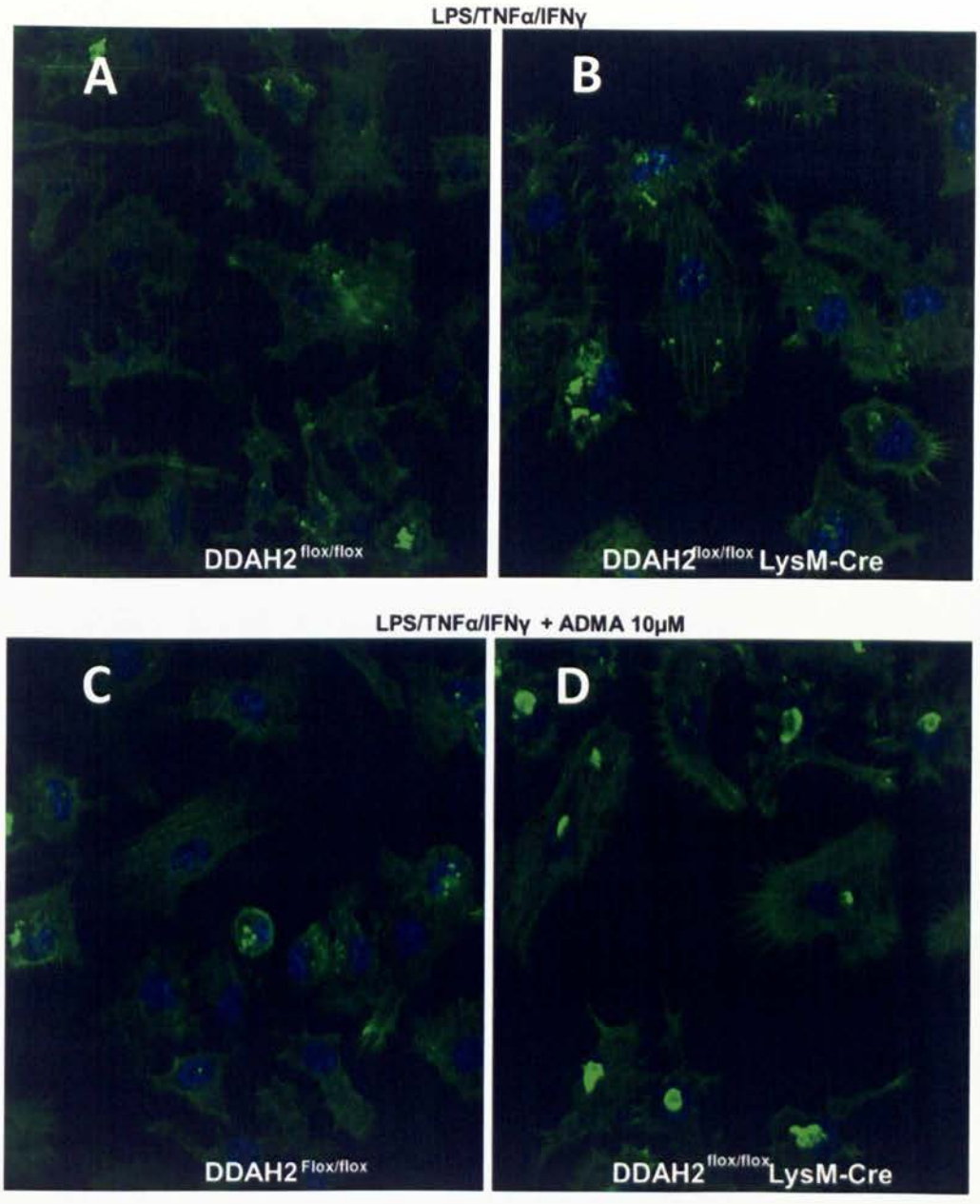

Fig. 14: F-actin staining of DDAH2$^{flox/flox}$ and DDAH2$^{flox/flox}$ LysM-Cre pMacs

DDAH2$^{flox/flox}$ and DDAH2$^{flox/flox}$ LysM-Cre treated with (A) LPS/TNF-α/IFN-γ and (B) LPS/TNF-α/IFN-γ with ADMA (100μM). pMacs were stained with F-actin phalloidin (green) (Invitrogen, UK) and the nucleus stained with dapi (blue). Images taken using a confocol microscope. DDAH2$^{flox/flox}$ LysM-Cre have more F-actin stress fibres in both conditions thus limiting motility.

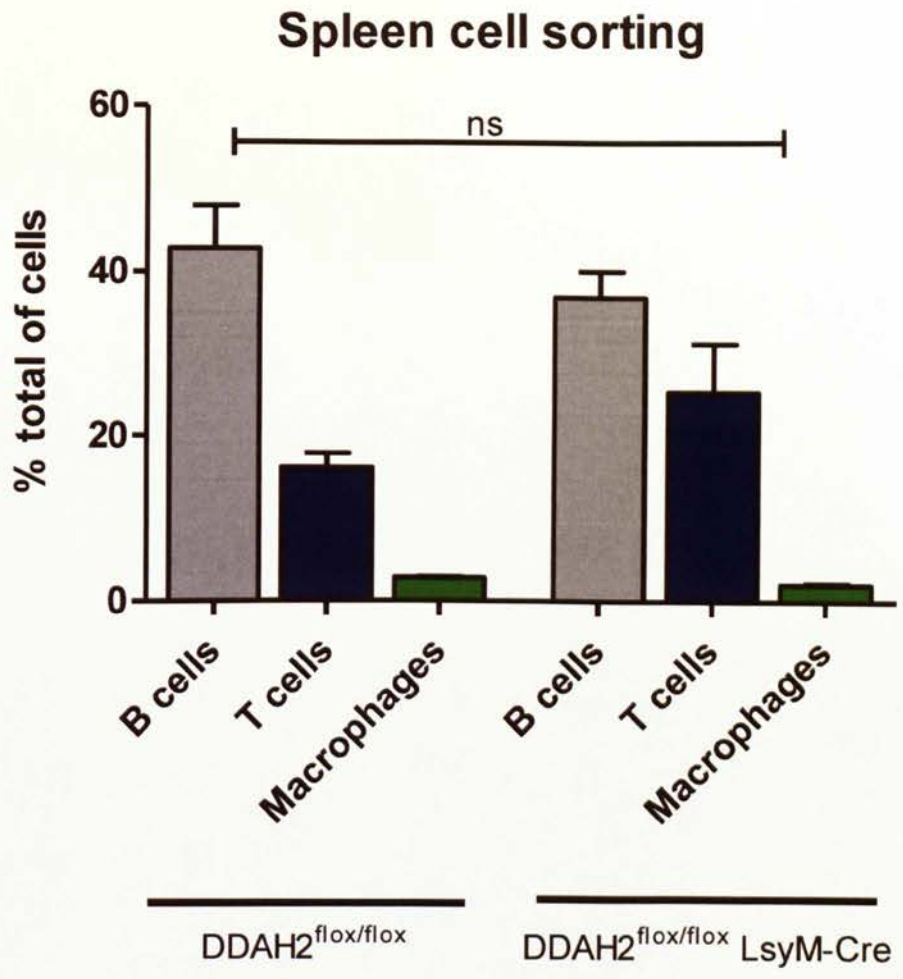

Fig. 15: Difference between macrophages, B and T cells in DDAH2$^{flox/flox}$ and DDAH2$^{flox/flox}$ LysM-Cre peritoneal washout

The spleen was homogenised and the expression of B-cells, T-cells and macrophages using flow cytometry. Cells were stained using specific markers; F4-80 for macrophages (1:20,000; Cell Signalling), CD-3 for T cells (1:20,000; BD BioSciences), CD19 for B cells (1:20,000; BD Biosciences). DDAH2 deletion did not have any significant effect on the number of B cells, T cells and macrophages in the spleen although the spleen did appear to be enlarged in DDAH2 knock-outs. Data shown is of n=3 for both genotypes where mean ± SEM. Statistical significance was determined using a one-way ANOVA and Bonferroni post-hoc test; significance was accepted where *p<0.05.

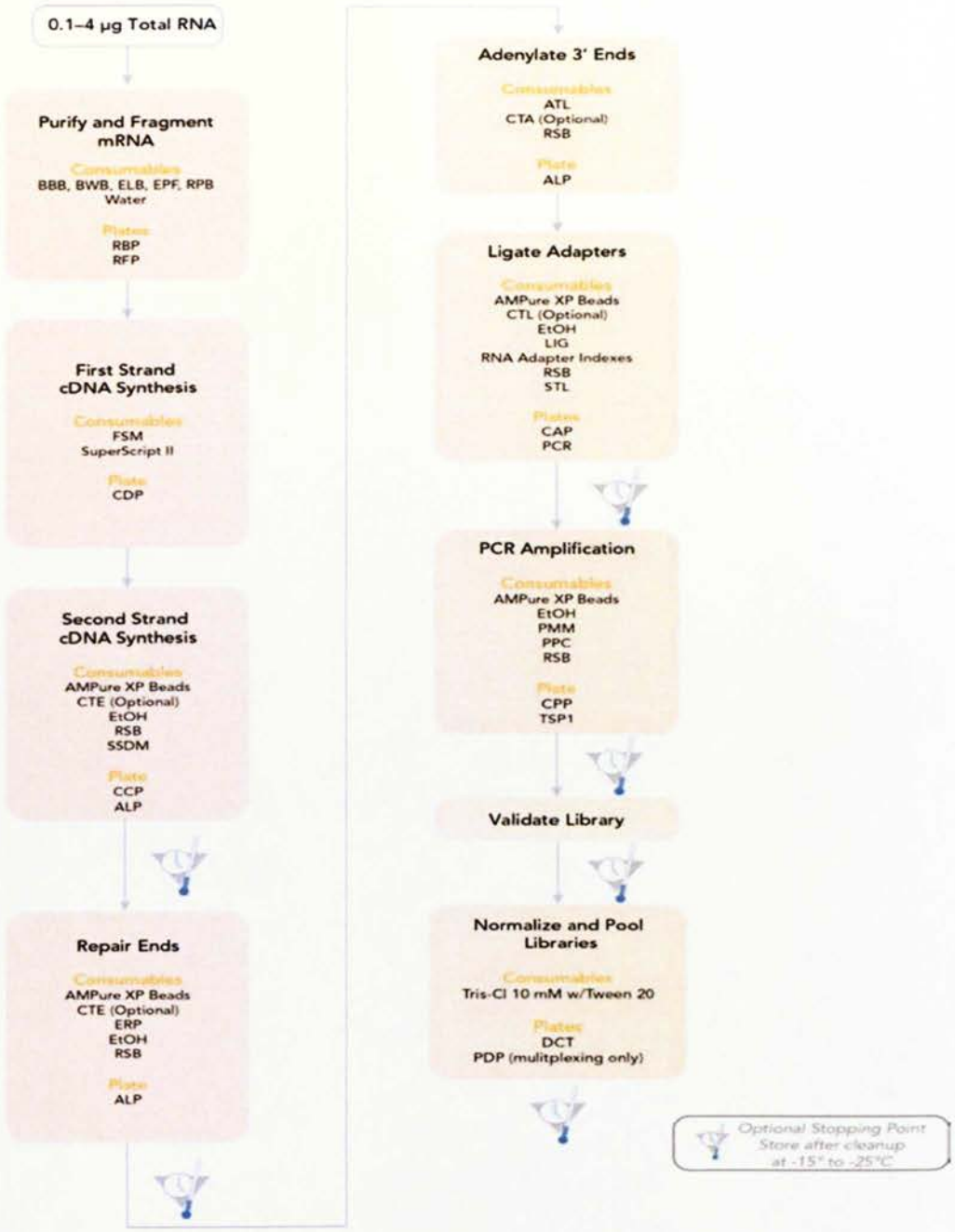

Fig. 16: TruSeq RNA Sample Preparation v2 high samples work flow

Illustration of the processes of the TruSeq RNA Sample Preparation v2 high samples (HS) protocol to prepare templates using 24 indexed adapters. Image taken from Illumina TruSeq RNA Sample Preparation v2 Guide (http://supportres.illumina.com/documents/myillumina/b386d5c9-c919-48db-bdc1-8a687ba2a101/truseq_rna_sampleprep_v2_guide_15026495_d.pdf).

ID	Symbol	Base Mean	Base Mean WT	Base Mean KO	Fold Change	log2 Fold Change	pval
ENSMUSG0000002	Thbs4	28.0586855	0.166320719	55.95105029	336.404571	8.394053499	3.54E-46
ENSMUSG0000005	Krt16	17.36299194	0.120741689	34.60524219	286.6055839	8.162922908	9.44E-29
ENSMUSG0000001	Il10	258.1795879	2.202501605	514.1566742	233.4421338	7.866921165	1.13E-228
ENSMUSG0000007	4930579C12F	12.92767647	0.120741689	25.73461125	213.137745	7.735642295	2.93E-17
ENSMUSG0000001	Slamf1	253.1999959	2.580690319	503.8193016	195.2265632	7.609005554	2.39E-227
ENSMUSG0000006	BC023105	16.27444691	0.166320719	32.3825731	194.6995732	7.605105912	2.48E-27
ENSMUSG0000002	Edn1	85.64558961	0.914242861	170.3769364	186.3585089	7.541936882	4.77E-107
ENSMUSG0000001	Il19	101.5494449	1.090879785	202.00801	185.1789837	7.532776564	4.94E-115
ENSMUSG0000002	Tslp	8.539706843	0.117384008	16.96202968	144.5003451	7.174929128	5.82E-12
ENSMUSG0000004	Kctd4	69.05759669	0.94974885	137.1654445	144.4228593	7.174155301	2.89E-91
ENSMUSG0000002	Nos2	1068.110191	15.99094126	2120.229441	132.5894084	7.050821723	0.00E+00
ENSMUSG0000007	Gm14047	153.4272938	2.55138161	304.3032059	119.2699692	6.898087024	2.06E-156
ENSMUSG0000003	Tpbpa	275.1388629	4.607158743	545.670567	118.4397147	6.88800911	6.93E-221
ENSMUSG0000005	Gja1	316.6556074	5.456870153	627.8543446	115.0575929	6.846212383	2.58E-235
ENSMUSG0000005	Ppp1r3g	75.42134967	1.304654811	149.5380445	114.618858	6.840700617	6.47E-88
ENSMUSG0000000	Ccnd2	552.5158326	9.616944832	1095.41472	113.9046485	6.831682815	6.89E-282
ENSMUSG0000008	Gm13822	43.15429195	0.832882923	85.47570098	102.6263099	6.681256826	3.38E-56
ENSMUSG0000002	Upp1	417.5349342	8.124332484	826.9455359	101.7862745	6.669399222	1.30E-259
ENSMUSG0000002	Nr4a3	581.6611976	11.57192152	1151.750474	99.52975157	6.637055937	3.17E-298
ENSMUSG0000002	Mx2	586.5628221	12.35825276	1160.767391	93.92649708	6.553460301	1.21E-291
ENSMUSG0000008	Gm5970	141.4919459	3.142938657	279.840953	89.03799393	6.476349183	1.59E-131
ENSMUSG0000008	Gm11547	7.686660471	0.176636924	15.19668402	86.03345007	6.426825788	3.22E-11
ENSMUSG0000003	2310014L17R	205.3997131	4.814736489	405.9846898	84.32126882	6.397824671	1.97E-177
ENSMUSG0000002	Fst	503.1232991	12.21925585	994.0273424	81.34925358	6.346057203	1.66E-270
ENSMUSG0000002	Pamr1	14.83094487	0.362225066	29.29966468	80.88800976	6.337853959	4.99E-23
ENSMUSG0000003	Dbn1	4.917708024	0.120741689	9.714674359	80.45832772	6.330169848	3.53E-08
ENSMUSG0000003	Cish	506.269506	12.8384572	999.7005549	77.86765492	6.282952273	1.53E-270
ENSMUSG0000007	Adam25	107.795891	2.812618736	212.7791633	75.65161981	6.241299068	5.79E-114
ENSMUSG0000000	Has1	288.2658593	7.959133589	568.5725851	71.43649227	6.158589337	2.02E-212
ENSMUSG0000003	Ccl7	40.81108192	1.156573145	80.4655907	69.57241837	6.120443565	7.73E-54
ENSMUSG0000000	Itih1	41.00317167	1.228378122	80.77796521	65.75985339	6.039135177	4.51E-52
ENSMUSG0000001	Dusp14	5.773866577	0.176636924	11.37109623	64.3755334	6.008440576	7.23E-09
ENSMUSG0000002	Ptx3	28.18492906	0.870985348	55.49887276	63.71963992	5.993666209	6.34E-39
ENSMUSG0000004	Gpr82	2.848714495	0.088318462	5.609110529	63.51005654	5.988913149	0.000174668
ENSMUSG0000004	Trem1	506.4827543	15.81979231	997.1457163	63.03153017	5.978001781	1.35E-245
ENSMUSG0000005	Robo2	110.3718511	3.461991872	217.2817104	62.76205098	5.971820593	6.63E-107
ENSMUSG0000000	Abca13	44.03294831	1.385143881	86.68075274	62.57888002	5.967603934	6.00E-55
ENSMUSG0000001	Gm11435	43.03134192	1.380664376	84.68201946	61.33425396	5.93862111	1.26E-53
ENSMUSG0000003	Piwil4	3.638198869	0.117384008	7.159013731	60.98798165	5.930453067	1.48E-06
ENSMUSG0000006	2010002M12F	41.20725312	1.362275615	81.05223063	59.49767414	5.894761367	7.54E-48
ENSMUSG0000002	Cacng4	6.838249164	0.234768016	13.44173031	57.25537291	5.839339179	6.21E-12
ENSMUSG0000008	Gm3513	12.94439557	0.470657857	25.41813329	54.00554334	5.755035594	8.09E-18
ENSMUSG0000007	Ifit3	1056.830187	39.6007363	2074.059637	52.37426955	5.710786313	4.73E-302
ENSMUSG0000005	Prdx6b	3.11765711	0.117384008	6.117930213	52.11894118	5.70373587	4.77E-06
ENSMUSG0000007	Gm10654	2.340410119	0.088318462	4.592501775	51.99934034	5.700421416	0.000415599
ENSMUSG0000004	Penk	119.9920007	4.592613989	235.3913875	51.25433752	5.679602196	3.22E-111
ENSMUSG0000000	Il12b	289.6057844	11.87627424	567.3352946	47.77047777	5.578047401	4.39E-193
ENSMUSG0000008	1500002O10F	2.923177908	0.120741689	5.725614128	47.4203582	5.567434655	4.86E-05
ENSMUSG0000002	Ifi44	94.45972326	4.017124185	184.9023223	46.02853032	5.524456473	4.65E-95

Table 5: Top 50 genes with the biggest significant fold changes in DDAH2$^{flox/flox}$ in untreated and LPS treated conditions

RNA-sequencing was carried out on untreated and LPS treated pMacs extracted from DDAH2$^{flox/flox}$. These data shows the top 50 genes significantly altered by DDAH2. Results are from n=4 mice and significance was accepted where *p<0.05.

ID	Symbol	Base Mean	Base Mean	Base Mean LPS	Fold Change	log2 Fold Change	pval
ENSMUSG0000002	U90926	718.1174145	1.654849935	1434.579979	866.894302	9.75971229	4.93E-88
ENSMUSG0000003	Csf3	5114.355712	20.27210406	10208.43932	503.5707833	8.976050771	6.91E-106
ENSMUSG0000003	Ccl7	338.8570512	1.392913992	676.3211883	485.5441127	8.923458563	1.54E-70
ENSMUSG0000001	Csf2	1244.140938	6.261883449	2482.019992	396.3695608	8.630702365	3.29E-88
ENSMUSG0000001	Il19	133.3490345	0.798309914	265.8997591	333.0783627	8.379717827	8.31E-49
ENSMUSG0000004	Inhba	2786.643496	22.68578693	5550.601205	244.6730731	7.934711528	3.53E-89
ENSMUSG0000004	1110032A04F	30.6694257	0.266103305	61.0727481	229.507665	7.842398527	5.11E-21
ENSMUSG0000002	Il6	16871.21745	146.5488108	33595.88608	229.2470741	7.84075951	3.55E-93
ENSMUSG0000002	Areg	811.7228169	7.22233854	1616.223295	223.7811598	7.80594477	5.77E-76
ENSMUSG0000005	Ppp1r3g	27.60764027	0.266103305	54.94917724	206.4956589	7.689967642	1.50E-18
ENSMUSG0000002	Hdc	2711.408135	26.4112332	5396.405037	204.3223426	7.674703161	9.67E-86
ENSMUSG0000007	Gm5483	24.66028895	0.266103305	49.0544746	184.3437257	7.526254504	8.71E-18
ENSMUSG0000003	Ccl2	695.707686	7.80027317	1383.615099	177.3803389	7.470702298	1.08E-73
ENSMUSG0000002	Nos2	925.7992552	10.48835101	1841.110159	175.538572	7.455644266	5.55E-77
ENSMUSG0000000	Slc1a2	316.3814732	4.979135571	627.7838108	126.0828917	6.978228718	5.51E-58
ENSMUSG0000008	Gm16292	36.35031753	0.588353035	72.11228202	122.5663466	6.937419099	2.49E-22
ENSMUSG0000007	Adam25	51.95169122	0.856540021	103.0468424	120.3059284	6.910563927	2.79E-27
ENSMUSG0000007	4933404M02F	64.49399027	1.064413219	127.9235673	120.1822422	6.909079933	4.15E-31
ENSMUSG0000003	Ptgs2	87774.40723	1553.97892	173994.8355	111.9673074	6.806933741	8.21E-79
ENSMUSG0000004	Lad1	32.56820487	0.590436716	64.54597303	109.3190367	6.772400842	1.03E-19
ENSMUSG0000002	Edn1	71.05970128	1.386662949	140.7327396	101.4902286	6.665197022	1.03E-32
ENSMUSG0000005	Gja1	700.0741546	14.40098969	1385.747319	96.22583931	6.588352445	2.32E-63
ENSMUSG0000002	Il23a	213.2309902	4.588237329	421.873743	91.94680063	6.522727471	1.84E-47
ENSMUSG0000004	Mmp3	817.5243432	17.64445296	1617.404233	91.66644251	6.51832178	4.87E-64
ENSMUSG0000004	Kctd4	79.10425066	1.715163722	156.4933376	91.24104922	6.511611132	3.95E-33
ENSMUSG0000000	Timp1	342.0256412	7.598651015	676.4526314	89.02272654	6.476101782	8.39E-57
ENSMUSG0000002	Ereg	3418.586036	76.24884424	6760.923227	88.66918961	6.470360985	1.24E-70
ENSMUSG0000002	Il1f6	84.80435152	1.929287963	167.6794151	86.91259069	6.441493285	1.71E-34
ENSMUSG0000001	Ccl4	3430.274176	79.85142323	6780.696928	84.91641919	6.407971631	1.07E-70
ENSMUSG0000004	Armcx4	378.2976467	8.991565007	747.6037283	83.14500621	6.377557711	8.84E-55
ENSMUSG0000004	Oasl1	5163.83269	129.3828299	10198.28255	78.82253431	6.300536231	6.96E-70
ENSMUSG0000003	Lif	2087.251558	52.31329324	4122.189823	78.79813272	6.300089537	1.06E-66
ENSMUSG0000004	Mmp1b	10.65233412	0.268186986	21.03648126	78.43960513	6.293510368	1.60E-08
ENSMUSG0000004	Penk	34.00221785	0.856540021	67.14789569	78.39434711	6.292677723	1.71E-19
ENSMUSG0000000	Has1	88.77949798	2.245286651	175.3137093	78.08076945	6.286895365	1.46E-33
ENSMUSG0000002	Fst	1935.113172	49.868382	3820.357961	76.60882122	6.259438618	1.48E-65
ENSMUSG0000000	Ncan	10.1774209	0.266103305	20.0887385	75.49225489	6.238256734	2.71E-08
ENSMUSG0000004	Olfr56	39.36861876	1.064413219	77.6728243	72.97243488	6.189279688	4.60E-22
ENSMUSG0000007	Fjx1	9.614894432	0.266103305	18.96368556	71.26437449	6.155109139	1.12E-07
ENSMUSG0000002	Rsad2	5021.931066	139.2828385	9904.579293	71.11126824	6.152006281	7.18E-68
ENSMUSG0000002	Hnf1b	9.511759144	0.268186986	18.7553313	69.93378614	6.127917708	2.67E-07
ENSMUSG0000003	Cxcl10	836.3302678	23.65453369	1649.006002	69.71204858	6.123336119	2.20E-61
ENSMUSG0000002	Gng4	124.3349809	3.530075153	245.1398866	69.44324864	6.117762535	1.25E-37
ENSMUSG0000003	Scube3	9.400914916	0.268186986	18.53364285	69.10716715	6.110763436	3.86E-07
ENSMUSG0000003	Ifit1	3406.944058	98.35652432	6715.531591	68.27743902	6.093337041	8.00E-67
ENSMUSG0000000	Abca13	73.87604494	2.139244843	145.612845	68.06740497	6.088892204	3.80E-29
ENSMUSG0000008	Gm13822	29.2965972	0.85445634	57.73873805	67.57365517	6.07838899	3.18E-18
ENSMUSG0000003	Ccl5	10990.40013	336.8031248	21643.99713	64.26305322	6.005917622	1.31E-64
ENSMUSG0000002	Il1b	107725.9285	3350.436879	212101.4202	63.305601	5.984261243	3.92E-66

Table 6: Top 50 genes with the biggest significant fold changes in DDAH2$^{flox/flox}$ LysM-Cre in untreated and LPS treated conditions

RNA-sequencing was carried out on untreated and LPS treated pMacs extracted from DDAH2$^{flox/flox}$ LysM-Cre mice. These data shows the top 50 genes significantly altered by DDAH2. Results are from n=4 mice and significance was accepted where *p<0.05.

ID	Symbol	Base Mean	Base Mean WT	Base Mean KO	Fold Change	log2 Fold Change	pval
ENSMUSG00000027377	Mall	35.71417054	0.202406728	106.7376982	527.3426381	9.04259684	2.39E-29
ENSMUSG00000076613	Ighg2b	62.02619328	0.435650967	185.2072779	425.1276636	8.73175233	8.59E-49
ENSMUSG00000076613	Ighg	62.02619328	0.435650967	185.2072779	425.1276636	8.73175233	8.59E-49
ENSMUSG00000076619	Ighj3	21.50863417	0.151241167	64.22342017	424.6424531	8.7301048	3.76E-18
ENSMUSG00000076677	Ighv6-3	45.49194094	0.404813457	135.6661959	335.1326236	8.388588323	2.56E-36
ENSMUSG00000076606	Igkj3	22.40470955	0.202406728	66.80931521	330.0745766	8.366648212	1.10E-18
ENSMUSG00000074259	Gramd2	43.87197334	0.413405837	130.7891083	316.3697668	8.305467928	5.29E-35
ENSMUSG00000021749	Oit1	39.71100451	0.404813457	118.3233866	292.2911395	8.191262286	8.10E-33
ENSMUSG00000076605	Igkj2	29.01745199	0.302482334	86.44739129	285.7931904	8.158827732	1.30E-23
ENSMUSG00000085417	Gm13919	36.32250686	0.413405837	108.1407089	261.584862	8.031135244	9.25E-29
ENSMUSG00000076508	Igkv17-127	22.99123237	0.2844098	68.40487752	240.5151912	7.909984209	3.99E-19
ENSMUSG00000039457	Ppl	63.15525959	0.822515484	187.8207478	228.3491939	7.835097887	1.16E-47
ENSMUSG00000025127	Gcgr	44.8290976	0.607220185	133.2728524	219.4802736	7.777947469	1.06E-34
ENSMUSG00000076695	Ighv1-18	12.96256753	0.206702919	38.47429674	186.1333019	7.540192387	8.47E-11
ENSMUSG00000022696	Sidt1	16.72032569	0.2844098	49.59215746	174.3686659	7.445997001	6.18E-14
ENSMUSG00000076607	Igkj4	16.0561871	0.2844098	47.5997417	167.3632261	7.386838756	4.14E-14
ENSMUSG00000003309	Ap1m2	11.36414109	0.202406728	33.68760981	166.4352271	7.378817011	1.64E-09
ENSMUSG00000062007	Hsh2d	24.19900996	0.435650967	71.72572794	164.6403505	7.363174148	2.10E-19
ENSMUSG00000084773	Gm12159	11.08118888	0.202406728	32.83875319	162.2414108	7.341998293	2.00E-09
ENSMUSG00000076518	Igkv2-112	10.45501737	0.202406728	30.96023867	152.9605211	7.257015533	5.75E-09
ENSMUSG00000027863	Cd2	199.1310574	3.945588602	589.5019951	149.4078716	7.223112348	1.02E-113
ENSMUSG00000076501	Igkv2-137	28.22561936	0.568819601	83.53921888	146.8641706	7.198338665	7.07E-23
ENSMUSG00000076676	Ighv12-3	84.65355824	1.76598396	250.4287068	141.8068977	7.147783899	3.65E-54
ENSMUSG00000057098	Ebf1	314.7586416	6.793324271	930.6892763	137.0005669	7.098038053	5.44E-155
ENSMUSG00000076580	Igkv8-27	25.10259536	0.568819601	74.17014688	130.3930926	7.026723637	6.29E-20
ENSMUSG00000043931	Gimap7	17.71891013	0.404813457	52.34710347	129.3116683	7.014708651	2.81E-14
ENSMUSG00000022416	Cacna1i	266.1795321	6.110067095	786.318462	128.6922794	7.007781695	2.65E-139
ENSMUSG00000038630	Zkscan16	8.657711869	0.202406728	25.56832215	126.321503	6.980956431	2.34E-07
ENSMUSG00000076563	Igkv5-48	12.07511486	0.2844098	35.65652497	125.3702401	6.970051118	3.97E-10
ENSMUSG00000043592	Unc5cl	17.15692248	0.404813457	50.66114052	125.1468785	6.967478497	1.00E-13
ENSMUSG00000033060	Lmo7	71.54825858	1.747911426	211.1489529	120.8007166	6.916485203	8.36E-48
ENSMUSG00000087406	E130215H24Rik	11.51312721	0.2844098	33.97056202	119.4423047	6.900170098	1.48E-09
ENSMUSG00000076620	Ighj2	8.001406817	0.202406728	23.59940699	116.5939847	6.865349548	9.24E-07
ENSMUSG00000026080	Chst10	30.56073268	0.809626914	90.06294422	111.2400572	6.797532582	7.64E-23
ENSMUSG00000059336	Slc14a1	20.08403169	0.568819601	59.11445586	103.924787	6.699395981	9.41E-16
ENSMUSG00000030468	Siglecg	828.6821523	23.59545281	2438.855551	103.3612523	6.691551645	7.70E-253
ENSMUSG00000044867	Gm3345	6.950806999	0.202406728	20.44760754	101.0223706	6.658530992	3.56E-06
ENSMUSG00000076618	Ighj4	33.77545257	1.012033642	99.30229042	98.12153101	6.61649784	1.40E-24
ENSMUSG00000035000	Dpp4	161.6428118	4.91187343	475.1046884	96.72575958	6.595828248	2.69E-92
ENSMUSG00000076583	Igkv8-24	58.00817083	1.871599906	170.2813127	90.98168476	6.507504245	3.08E-39
ENSMUSG00000014030	Pax5	89.8423908	3.015558031	263.4960564	87.37887104	6.449212561	4.80E-55
ENSMUSG00000026581	Sell	201.8665495	6.844242644	591.9111631	86.48307692	6.434345948	5.55E-107
ENSMUSG00000026770	Il2ra	89.96945813	3.06468292	263.7790086	86.0705709	6.427448133	1.05E-55
ENSMUSG00000076522	Igkv16-104	14.19885711	0.491112719	41.6143459	84.73481605	6.404882964	4.77E-11
ENSMUSG00000076530	Igkv19-93	21.42701794	0.775522519	62.73000879	80.88741105	6.33784328	7.09E-16
ENSMUSG00000076577	Igkv8-30	27.29738224	1.009778125	79.87259047	79.09914911	6.30559027	2.98E-19
ENSMUSG00000023963	Cyp39a1	46.88761653	1.79682147	137.0692066	76.2842658	6.253313616	4.70E-30
ENSMUSG00000051590	Ysk4	19.4559203	0.758461352	56.85083819	74.95548457	6.22796214	3.72E-14
ENSMUSG00000061723	Tnnt3	3.789755859	0.151241167	11.06678524	73.17310136	6.193241502	0.001539139

Table 7: Top 50 genes with the biggest significant fold changes in DDAH2$^{flox/flox}$ versus DDAH2$^{flox/flox}$ LysM-Cre in untreated conditions

RNA-sequencing was carried out on untreated pMacs extracted from DDAH2$^{flox/flox}$ and DDAH2$^{flox/flox}$ LysM-Cre mice. These data shows the top 50 genes significantly altered by DDAH2. Results are from n=4 mice and significance was accepted where *p<0.05.

ID	Symbol	Base Mean	Base Mean WT	Base Mean KO	Fold Change	log2 Fold Change	pval
ENSMUSG0000002	Hcn3	6.832207893	0.12848779	20.2396481	157.5219569	7.299409129	2.95E-09
ENSMUSG0000008	Gm15232	5.123763001	0.12848779	15.11431342	117.6322936	6.878140368	5.28E-06
ENSMUSG0000007	Igkv8-27	13.14509978	0.331755098	38.77178915	116.8687063	6.868744864	3.02E-17
ENSMUSG0000009	Gm8810	37.41925952	1.330386493	109.5970056	82.37982429	6.364219144	2.84E-38
ENSMUSG0000002	Il17a	26.66713897	0.948753101	78.10391071	82.32269345	6.36321828	4.68E-26
ENSMUSG0000007	Ighg2b	34.4708426	1.236582184	100.9393634	81.62770311	6.350986957	1.17E-35
ENSMUSG0000007	Ighg	34.4708426	1.236582184	100.9393634	81.62770311	6.350986957	1.17E-35
ENSMUSG0000005	Gm10020	21.88265688	0.795364087	64.05724247	80.53826362	6.331602463	5.90E-21
ENSMUSG0000006	Hemt1	4.031075273	0.156495141	11.78023554	75.27540775	6.234106713	4.05E-05
ENSMUSG0000007	Ighv8-12	3.046650392	0.12848779	8.882975597	69.13478398	6.111339855	0.000703
ENSMUSG0000008	Gm14230	2.996642297	0.12848779	8.732951312	67.96716888	6.086766125	0.000902
ENSMUSG0000007	Igkj3	10.67518735	0.460242888	31.10507626	67.58404542	6.078610804	3.41E-12
ENSMUSG0000002	Wnt10b	10.55708954	0.488250239	30.69476813	62.86687782	5.974228211	8.46E-13
ENSMUSG0000007	Igkv2-137	15.24678826	0.710542338	44.3192801	62.37387658	5.962870021	4.44E-17
ENSMUSG0000004	Tlr9	156.7360658	7.750129502	454.7079383	58.67101165	5.874575963	1.91E-90
ENSMUSG0000004	Pacsin1	6.617193848	0.331755098	19.18807135	57.83806019	5.853947262	2.30E-08
ENSMUSG0000007	Igkv4-91	55.26605541	2.969074563	159.8600171	53.84169839	5.750652014	6.91E-40
ENSMUSG0000004	Gm14492	8.525037286	0.460242888	24.65462608	53.56872797	5.743319134	1.65E-09
ENSMUSG0000000	Fcer2a	104.3403225	5.838711544	301.3435445	51.6113088	5.689615311	7.44E-67
ENSMUSG0000003	Lmo7	28.89554306	1.621245858	83.44413745	51.46914456	5.685635899	3.70E-27
ENSMUSG0000007	Igkv6-32	5.751456724	0.331755098	16.59085997	50.00935949	5.644126222	1.91E-06
ENSMUSG0000008	4933421A08F	3.496465368	0.222292099	10.04481191	45.18744462	5.497850069	0.000145
ENSMUSG0000002	Il9r	117.8662012	7.746819472	338.1049645	43.64435827	5.447723269	1.53E-71
ENSMUSG0000004	Fcrl5	200.615085	13.32037257	575.2045097	43.18231391	5.432368647	2.57E-95
ENSMUSG0000008	Gm14290	6.206936405	0.413470721	17.79386777	43.03537563	5.427451156	8.48E-06
ENSMUSG0000003	Ppp1r16b	173.1090327	11.59786635	496.1313653	42.77781362	5.418790843	2.38E-89
ENSMUSG0000002	Tpsab1	82.80688068	5.611342707	237.1979566	42.27115844	5.401601745	1.53E-57
ENSMUSG0000002	Ephb4	1.880395779	0.12848779	5.384211756	41.90446237	5.389031978	0.024452
ENSMUSG0000000	Vpreb3	1.830387684	0.12848779	5.234187472	40.73684727	5.348262425	0.017126
ENSMUSG0000003	Ly6d	657.7384445	46.19959924	1880.816135	40.7106591	5.347334674	1.43E-144
ENSMUSG0000005	Gpr183	97.39289232	6.931890874	278.3148952	40.1499245	5.32732537	1.36E-61
ENSMUSG0000002	Selp	51.15419582	3.650086003	146.1624155	40.04355386	5.323498114	8.31E-45
ENSMUSG0000007	E130208F15F	1.766655759	0.12848779	5.042991698	39.24880102	5.294576678	0.021124
ENSMUSG0000000	Bcl11a	258.5230134	19.33222859	736.904583	38.11793242	5.252397962	1.65E-106
ENSMUSG0000008	4930538E20R	2.96799892	0.222292099	8.459412562	38.0553902	5.250028908	0.0006437
ENSMUSG0000003	Dyrk4	11.95989056	0.904827086	34.07001751	37.65362248	5.234716762	2.47E-11
ENSMUSG0000007	Igkv17-121	10.90311275	0.830047567	31.0492431	37.40658285	5.225220274	2.49E-09
ENSMUSG0000002	Kcnq5	19.02108272	1.459134257	54.14497965	37.10760637	5.213643038	6.84E-17
ENSMUSG0000004	Clspn	2.886124863	0.222292099	8.21379039	36.95043788	5.207519556	0.000181
ENSMUSG0000007	Igkv8-24	36.15102017	2.834710339	102.7836398	36.25895685	5.180265515	3.81E-27
ENSMUSG0000007	Ighj1	1.625468081	0.12848779	4.619428663	35.95227739	5.168011256	0.037097
ENSMUSG0000002	Ptprd	1.949544361	0.156495141	5.535642802	35.37261778	5.144561086	0.004972
ENSMUSG0000002	Lrrc16b	25.2413326	2.11901838	71.48596105	33.7354134	5.076191936	9.09E-23
ENSMUSG0000006	Hsh2d	26.0953359	2.270620911	73.74476589	32.47779738	5.021381888	7.47E-20
ENSMUSG0000004	Myzap	1.456832743	0.12848779	4.11352265	32.01489148	5.000671215	0.081854679
ENSMUSG0000002	Plac8	194.945139	17.30534254	550.224732	31.79507894	4.990731586	6.44E-92
ENSMUSG0000003	Zcchc18	3.525064861	0.312990282	9.949214021	31.78761323	4.990392791	0.000257512
ENSMUSG0000000	Spib	329.2539262	29.46906206	928.8236544	31.51860254	4.978131665	9.11E-108
ENSMUSG0000007	Nrarp	1.712289876	0.156495141	4.823879345	30.82446726	4.946004055	0.025321351

Table 8: Top 50 genes with the biggest fold change between DDAH2$^{flox/flox}$ and DDAH2$^{flox/flox}$ LysM-Cre in LPS treated conditions

RNA-sequencing was carried out on LPS treated (6 hours) pMacs extracted from DDAH2$^{flox/flox}$ and DDAH2$^{flox/flox}$ LysM-Cre mice. These data shows the top 50 genes significantly altered by DDAH2. Results are from n=4 mice and significance was accepted where *p<0.05.